Rutherford Laboratory
CHILTON, DIDCOT, OXON OX11 0QX

RL-77-064/C

Copy

A pulsed neutron facility for condensed matter research

EDITED BY

L C W HOBBS, G H REES AND G C STIRLING

JUNE 1977

A PULSED NEUTRON FACILITY FOR CONDENSED MATTER RESEARCH

CONTENTS

F O R E W O R D

The Science Research Council has recently been given Government approval to proceed with the construction of a new high intensity pulsed neutron source at the Rutherford Laboratory. The scientific and technical basis of the project was given in the proposal documentation submitted in its original form to the Council in December 1976 and largely reproduced here.

The team to be responsible for the design and construction of the new facility has been formed with Dr G Manning as Project Leader. Dr L Hobbis has particular responsibility for utilisation. Where appropriate the Rutherford Laboratory will be advised by a Science Planning Group (a Sub-Committee of the Neutron Beam Research Committee) representing user interest and chaired initially by Dr B E F Fender (Oxford University). Planning for the new source has progressed since initial plans were formulated and this work will now accelerate rapidly. Wide user participation is welcomed; any potential user not already involved is invited to contact Dr Manning, Dr Fender or Dr Hobbis.

G H Stafford

Rutherford Laboratory
June 1977

Reader's Guide

This report follows closely the text of the documentation on the Spallation Neutron Source (SNS) Proposal prepared for the SRCs Neutron Beam Research Committee in the summer of 1976. Details of cost estimates, and financial and manpower projections are not included. The report is issued in the present form to enable wider dissemination of the background to the project. The scientific and technical specifications given here represent the initial reference design which will be subject to review and refinement as the project proceeds.

There are three main parts to the report, namely

(a) Proposal for a Spallation Neutron Facility
(b) Appendix 1 of the Proposal - Utilization
(c) Appendix 2 of the Proposal - Project Description

It was felt that readers of part (a) would come to it with varying degrees of familiarity with the tools and techniques of neutron scattering and of their widely ranging applications in scientific research. The presentation of information in the Proposal sought to take account of this situation and inevitably this led to some repetition and overlap of material between chapters. The following guide to part (a) may therefore be helpful.

Chapter 1 gives a broad synopsis of the whole proposal.

Chapter 2 is essentially a layman's guide to neutron scattering concluding with brief surveys of the main application areas and their relationship to the SNS.

Chapter 3 summarises the conclusions of the scientific working groups. These are rather specialised but a summary of the important scientific gains which would accrue from the SNS is given in the opening paragraphs.

Chapter 4 is an account of the thinking on neutron sources which has led to the conclusion that the provision of the SNS is the best possible step forward to realise high effective neutron intensities.

Chapter 5 contains an outline description of the SNS and its neutron performance parameters.

Appendix 1 gives a fuller account of aspects of utilisation and includes the complete Working Group reports.

Appendix 2 gives details of the project.

PROPOSAL FOR A SPALLATION NEUTRON FACILITY

CONTENTS

APPENDICES

APPENDIX I - Utilization

1. SNS neutron beam intensities
2. SNS Science Panel : Reports of Working Groups

   Working Group A : Solid State Physics
   Working Group B : Fluids and Amorphous Solids
   Working Group C : Structure Determination
   Working Group D : Molecular and Biological Sciences
3. Instrumentation
4. Other (non thermal neutron) uses

APPENDIX II - Project description

1. 800 MeV synchrotron
2. Target station
3. Shielding, radioactivity and radiation damage
4. Utilization
5. Overall programme

P R E F A C E

This proposal for a new neutron source for thermal neutron scattering studies has been prepared by a Coordinating Group under the auspices of the Neutron Beam Research Committee, and represents the culmination of several years' study by the NBRC of the long term needs of the field and of the options for their realization. The scientific case was formulated by a Science Panel on the basis of the conclusions of four Working Groups appointed to examine specific areas of science to be served by the proposed facility. The proposals for implementation have been prepared by the Rutherford Laboratory.

The various working parties have demonstrated their enthusiasm for the proposal in a practical way by meeting demanding deadlines and I thank all who participated for their co-operation. We are all grateful to the many scientists in the UK and abroad whose work we have drawn upon without reference in reviewing the progress and prospects of neutron beam science.

The day to day burden of preparing the proposal has fallen on members of the Rutherford Laboratory staff and I should like to record how much their excellent work has been appreciated by everyone else involved.

B E F Fender

Chairman,
Neutron Beam Research Committee

October 1976

SPALLATION NEUTRON SOURCE COORDINATING GROUP

Dr B E F Fender (Chairman)	University of Oxford
Dr M Carpenter	SRC London Office
Professor J E Enderby	University of Leicester
Dr J A Fendley	SRC London Office
Dr L C W Hobbis	SRC Rutherford Laboratory
Professor E W J Mitchell	University of Reading
Dr G H Stafford	SRC Rutherford Laboratory
Dr G C Stirling	SRC Rutherford Laboratory
Mrs E J Hawkins (Secretary)	SRC London Office

SPALLATION NEUTRON SOURCE SCIENCE PANEL AND WORKING GROUPS

SPALLATION NEUTRON SOURCE SCIENCE PANEL

Dr B E F Fender (Chairman)	University of Oxford
Dr E M Bradbury	Portsmouth Polytechnic
Professor J E Enderby	University of Leicester
Dr L C W Hobbis	SRC Rutherford Laboratory
Professor A J Leadbetter	University of Exeter
Professor E W J Mitchell	University of Reading
Professor J G Powles	University of Kent
Dr G C Stirling	SRC Rutherford Laboratory
Professor J J Turner	University of Newcastle
Dr C G Windsor	AERE Harwell
Mrs E J Hawkins	SRC London Office
Dr A D Taylor (Secretaries)	SRC Rutherford Laboratory

SOLID STATE PHYSICS

Dr P H Borcherds	University of Birmingham
Professor L J Challis	University of Nottingham
Dr J R Chamberlain	University of Salford
Professor R J Elliott	University of Oxford
Dr N W Grimes	Aston University
Dr M T Hutchings	AERE Harwell
Professor E W Lee	University of Southampton
Dr R D Lowde	AERE Harwell
Professor E W J Mitchell (Convener)	University of Reading
Dr B D Rainford	Imperial College, London
Dr G L Squires	University of Cambridge
Dr R J Stewart	University of Reading
Dr W G Williams (Secretary)	SRC Rutherford Laboratory
Dr C G Windsor	AERE Harwell

FLUIDS AND AMORPHOUS SOLIDS

Dr J H Clarke	University of Kent
Dr G J Coombs	University of Edinburgh
Dr J C Dore	University of Kent
Professor J E Enderby (Convener)	University of Leicester
Dr M W Johnson	SRC Rutherford Laboratory
Dr B H Meardon (Secretary)	SRC Rutherford Laboratory
Dr G W Neilson	University of Leicester
Dr V T Nguyen	University of Leicester
Dr B R Orton	Brunel University
Dr D I Page	AERE Harwell
Professor J G Powles	University of Kent
Mr P Schofield	AERE Harwell
Dr A C Wright	University of Reading

STRUCTURE DETERMINATION

Professor G E Bacon	University of Sheffield
Dr P H Borcherds	University of Birmingham
Dr A K Cheetham	University of Oxford
Dr B E F Fender (Convener)	University of Oxford
Dr R H Fenn	Portsmouth Polytechnic
Dr J B Forsyth (Secretary)	SRC Rutherford Laboratory
Dr A M Glazer	University of Cambridge
Dr A J Jacobson	University of Oxford
Dr D W Jones	University of Bradford
Dr D F R Mildner	SRC Rutherford Laboratory
Dr O S Mills	University of Manchester
Dr R J Nelmes	University of Edinburgh
Dr E Sándor	Queen Mary College, London
Dr M W Thomas	AERE Harwell
Dr P J Webster	University of Salford
Dr C Wilkinson	Queen Elizabeth College, London

MOLECULAR AND BIOLOGICAL SCIENCES

Dr M R Anderson	University of Oxford
Dr J P Baldwin	Portsmouth Polytechnic
Dr C J Carlile	SRC Rutherford Laboratory
Dr P G Hall	University of Exeter
Dr J S Higgins	Imperial College, London
Professor A J Leadbetter (Convener)	University of Exeter
Dr G S Pawley	University of Edinburgh
Professor Sir John Randall	University of Edinburgh
Dr D K Ross	University of Birmingham
Dr G C Stirling	SRC Rutherford Laboratory
Dr A D Taylor (Secretary)	SRC Rutherford Laboratory
Dr R K Thomas	University of Oxford
Professor J J Turner	University of Newcastle
Professor T C Waddington	University of Durham
Dr C J Wright	AERE Harwell
Dr D L Worcester	AERE Harwell

CHAPTER 1. SYNOPSIS OF THE PROPOSAL

1.1 The proposal presents the case for a high intensity neutron facility designed for thermal neutron scattering. The facility is based on the use of a proton synchrotron to generate very intense neutron pulses from a spallation target. By making use of existing plant and buildings it could be built at the Rutherford Laboratory for a capital cost of £10M compared with an estimated £30M if built on a green field site.

1.2 Why is this new source needed? The question is best answered by considering the scientific successes which have been achieved in thermal neutron scattering to date, the restricted availability of high flux instruments currently accessible to UK scientists, and especially the exciting new science that would follow construction of a high intensity pulsed source with its emphasis on the higher energy region of the neutron spectrum. All the major areas of science at present making use of neutron scattering, involving physicists, chemists and biologists, would benefit from the spallation neutron source (SNS) and we would expect immediate advances in, for example, the liquid and amorphous state, chemical applications of neutron spectroscopy, high energy excitations in crystalline solids, relaxation phenomena in polymers, and kinetic aspects of biological processes. Moreover the enormously enhanced flux of hot neutrons is bound to lead to new and unexpected experiments in a manner analogous to the advances stimulated by the availability of cold neutrons at ILL.

1.3 In Chapter 2 of this proposal, the history of the SRC-supported programme is traced through to today's partnership in the Institut Laue-Langevin (ILL) in Grenoble. Although it has long been appreciated that neutrons play a crucial role in furthering our understanding of fields as diverse as magnetism and the dynamical properties of crystals and liquids, the advent of the ILL reactor has provided striking proof that the special properties of the neutron can be employed to provide unique contributions to our knowledge in almost all fields of condensed matter research. Thus it is possible to point to significant advances over the last year or two in areas as varied as the structure of aqueous solutions, alloy precipitation phenomena, the properties of quantum liquids, the structure and dynamics of polymers, and molecular biology.

1.4 This widening of the scope of neutron beam studies has inevitably led to constraints in the availability of ILL facilities. The new research which has developed round the use of the ILL can in no sense be described as a single 'programme', bearing in mind that it supports and extends a scientifically diverse set of projects for scientists from France, the UK and West Germany. The number and range of users increases yearly, and it is already difficult to accommodate the pressure of good experiments. As far as the UK is concerned this pressure is not surprising, given that the facilities represent only one third of those judged to be necessary when in 1971 the Council accepted the case for a UK high flux reactor.

1.5 The exploitation of the higher neutron intensities available at ILL, despite successes achieved, has already exposed limitations arising from currently available intensities. At every stage in the exploitation of neutrons, higher intensities have revealed new science, for example through the possibilities of improving experimental resolution, of examining systems which are relatively weak scatterers, or of investigating phenomena over wider ranges of experimental conditions. Experiments at the ILL have also demonstrated the value of marked increases in intensity outside the neutron wavelength range of 1-2 $\mathring{A}$ most frequently employed. It is possible now to see areas of science which will benefit from the increase in intensity associated with the proposed new source, and these are indicated in Chapter 2.

1.6 Useful neutron beam intensities can only be obtained through the provision of expensive central facilities; even at ILL the intensity of an average beam is only 10^8 neutron per second compared with around 10^{11} photons

per second from a laboratory x-ray generator. Yet it is apparent from the comments above, and especially from the range of science discussed in Chapters 2 and 3 that the use of neutron beams - unlike high energy physics where a big machine serves a relatively small number of 'big' experiments - affects many scientists in many disciplines and contributes to the solutions of a large number of 'small science' problems. The concept is more like the use of a large computer processing many different jobs.

1.7 Because of the restraint of the potential scientific programme imposed by the limitation in flux, the Neutron Beam Research Committee (NBRC), through a study programme carried out by the Neutron Beam Research Unit (NBRU), has maintained a continuing review of possible new neutron sources. Recently it has concentrated on the types of source which might give gains in intensity approaching 100 times today's highest fluxes and which would represent an improvement of neutron beam facilities in the 1980's which could serve at least to the year 2000. Chapter 4 summarises the general consideration of new sources which has led to the present proposal.

1.8 It has become apparent that conventional reactors are nearing their limits in terms of flux although it is possible to envisage, after a considerable development programme, gains of $\sim$ 10 using a fluid fuelled reactor. The cost however could hardly be less than £100M and a pulsed reactor of comparable performance - even if judged safe to operate in the UK - would also be prohibitively expensive.

1.9 The advantages of accelerator-based pulsed neutron sources for many experimental regimes have recently been clarified through assessments in this country and abroad. Experience on continuous reactors has shown that instruments based on continuous beams with energy selection by monochromating devices are roughly equivalent in performance with those based on chopped beams in which energy selection is carried out by time-of-flight methods. Instrument design studies confirm this rough equivalence in many circumstances, and so it may be considered that the intrinsic instantaneous brightness of a source is the vital factor, and that a pulsed source with favourable pulse characteristics may for many experiments be equivalent to a continuous reactor of mean brightness equal to the peak brightness of the pulsed source. There will also be a range of experiments where the time-averaged flux is the important variable, and the pulsed source then suffers a disadvantage.

1.10 Consideration of pulsed sources in the UK goes back to 1965 when a detailed technical and scientific examination by the UKAEA favoured the known technology of a high flux reactor over the uncertain technology of the then most promising alternative - an electron linac producing neutrons which are multiplied in a variable reactivity plutonium booster assembly. Since those early considerations of proton and electron accelerators, and in the light of subsequent developments, thinking on such sources has crystallised to a point where we can state that the SNS is the optimum facility which can be built at present irrespective of the favourable siting at the Rutherford Laboratory. The site and availability of plant and buildings at the Rutherford Laboratory must be considered a bonus, and do not of themselves determine the decision.

1.11 In pulsed sources, the primary source neutrons are only partially moderated in order to maintain suitably short pulse lengths. This gives, as well as a roughly Maxwellian distribution of energies corresponding approximately to the moderator temperature (cf a steady-state reactor), neutrons whose intensity at higher energies is inversely proportional to energy. This difference in approach precludes a straightforward comparison with reactor-based facilities. In broad terms however the assessments which have been made in Appendix I show that although the time-averaged intensity of the SNS falls below that of the highest flux reactors, except at relatively high energies, there are, for the reasons alluded to in paragraph 1.9, some remarkably large gains in *effective* flux. This arises from the necessity with continuous sources to discard most of the neutron flux to achieve appropriate energy selection; in pulsed sources the incident beam is inherently 'tailored' for time-of-flight measurement. For those instruments - the majority at present - which can make use of a broad band of incident wavelengths around 1 Å, there are order of magnitude gains over comparable instruments now operating at the ILL. At shorter wavelengths (higher energies) the advantage over ILL instruments is even more marked allowing for the first time the use of a high flux of neutrons with wavelengths less than 0.3 Å. As the wavelength increases beyond 1 Å the gains diminish steadily but we still envisage instruments with distinct advantages in performance even at 6-10 Å.

1.12 The scientific programme which could be carried out at the SNS has been examined by about 60 UK scientists, including representatives from over 20 different university departments, contributing to four main working groups.

In addition two general discussion meetings with a wider audience have been held at the Rutherford Laboratory. The reports of the working groups are summarised in Chapter 3 of this Proposal; the full reports are available in Appendix I.

1.13 The NBRU in collaboration with the Working Groups has compiled a list of 26 instruments (Appendix I) with specifications precise enough to proceed to the design stage. Fourteen basic types of instrument (close to the maximum number which can be accommodated at a single target station) are listed in Table 3.1 and these could cover almost all the scientific developments so far proposed. The precise determination of the instruments to be built and their priority will be determined after an up to date reassessment of the scientific programme and in the light of experience gained on the new Harwell linac. During the planning stage instruments of advanced conception to match novel applications are also likely to emerge.

1.14 Part of our confidence in the new source stems from the experience of UK scientists at the Harwell linac, the only pulsed accelerator in Europe used for neutron scattering studies. Even though the flux is more than 1000 times less than that of the SNS and only a minor share of the facility is available, useful scientific results have been obtained and several different types of instrument have been tested. The new Harwell linac will be an important intermediate step in the development of the Rutherford Laboratory facility, but its intensity (100 times less than the SNS) precludes most of the scientific programme proposed for the SNS.

1.15 The proposal demonstrates that the SNS achieves the features demanded of a next generation source, with gains in performance over a large part of the scientific programme which are larger - often considerably larger - than the differences between medium flux reactors built in the 1950's and 60's and the present generation of high flux reactors. It is recognised however that not all types of experiment benefit. Indeed, some which require high resolution simultaneously in both energy and direction, as in certain phonon and magnon studies, or experiments which make ingenious use of a continuous beam, as in the ultra high resolution spin echo technique, will continue to be best done at the ILL. It is the different time and energy distribution of the neutrons from the two sources which ensures a complementarity between the ILL reactor and the SNS. This is also illustrated by the new fields, such

as ultra cold neutron ($\lambda > 200$ Å) studies and neutron interferometry which are being developed at the ILL but which are not part of the programme proposed for the SNS.

1.16 The SNS and ILL together would provide unrivalled neutron beam facilities and the NBRC's Spallation Neutron Source Coordinating Group recommends that the SNS project begin at the Rutherford Laboratory early in 1977 with a view to starting the first experiments in 1982.

CHAPTER 2. NEUTRON SCATTERING IN THE UK

INTRODUCTION

2.1 Like many other particles and radiations the neutron, although discovered in the search for the ultimate nature of matter, has been utilized as a probe in a wide range of scientific activity. In this sense the properties of the neutron are being exploited as in their turn have been x-rays in crystallography, electrons in diffraction for all disciplines, microwaves in ESR, radio waves in NMR etc. The major difference between the exploitation of neutrons in this way and the other cases, is that to obtain a useful flux of neutrons a large investment is required in the source.

2.2 The characteristics of the neutron which make it so useful for studying condensed matter are:

- it is uncharged
- it is scattered primarily by nuclei
- it has mass
- it has a magnetic moment
- it may be polarized
- it usually suffers low absorption (capture) and has a relatively large penetration of condensed matter such that large samples and a wide range of wavelengths may be utilized

2.3 It is this unique combination of characteristics which makes neutron beams such crucial probes for the study of condensed matter. Neutrons should

only be used when their special characteristics permit measurements that cannot be made more cheaply, and they are frequently used in conjunction with other experimental techniques. In order to give some general feel for the continuing and developing applicability of neutrons it is no exaggeration to say that their versatility in the study of matter is much greater than that of the generally more familiar x-rays. The scientific case that we are presenting, however, is no longer a justification in comparison with x-rays; that has been amply demonstrated in experiments using UKAEA medium flux reactors and the high flux reactor at the ILL.

THE PRINCIPLES OF THE NEUTRON SCATTERING METHOD

2.4 The basic nature of a typical neutron scattering experiment is simple, although the hardware may be complicated. The basic experiment may be illustrated in a block diagram as follows:

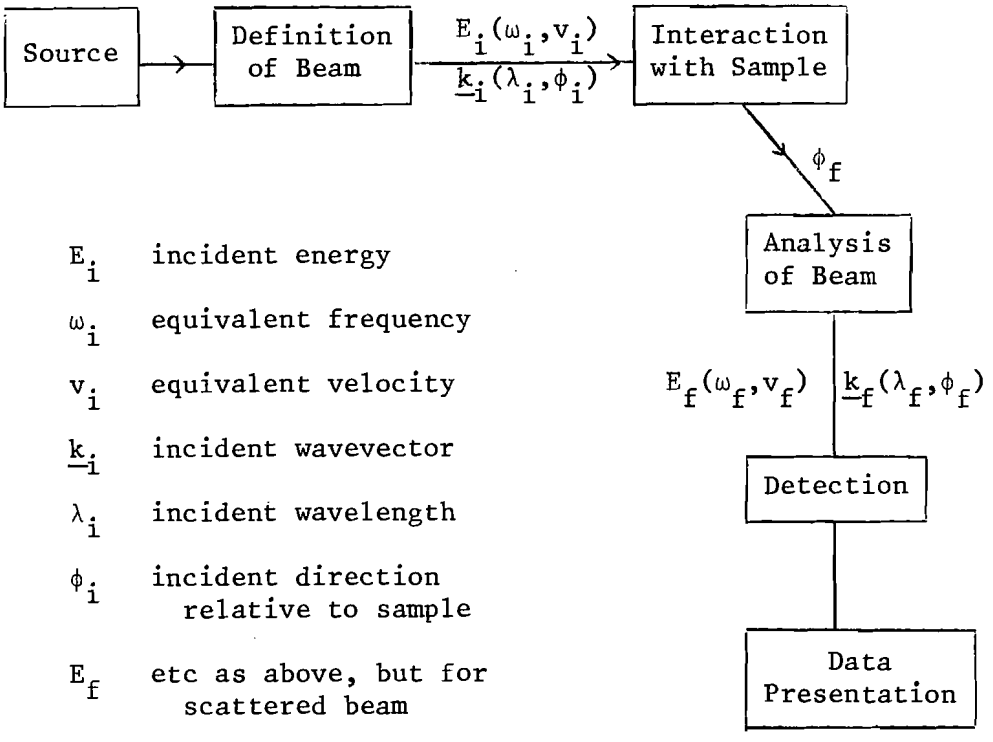

E_i incident energy

ω_i equivalent frequency

v_i equivalent velocity

$\underline{k}_i$ incident wavevector

λ_i incident wavelength

ϕ_i incident direction relative to sample

E_f etc as above, but for scattered beam

$$\epsilon = E_f - E_i$$

$$\underline{Q} = \underline{k}_f - \underline{k}_i$$

In such an experiment the intensity scattered per incident neutron per unit solid angle per unit of energy change may be written as

$$\frac{d^2\sigma}{d\Omega d\varepsilon} = \frac{k_f}{k_i} \sum_{\substack{mn \\ if}} P_i\, b_m\, b_n \left| M_{if}(mn) \right|^2 \delta(\varepsilon - \hbar\omega) \qquad (1)$$

where $M_{if}(mn)$ is the matrix element for scattering involving atoms m (scattering length b_m) and n (b_n) between initial and final states i and f, P_i is the thermodynamic probability of finding the system in the initial state and the sum is over all pairs of atoms and all initial and final states. The δ-function is zero except when $\varepsilon = \hbar\omega$ when $\delta = 1$. For crystalline systems we describe the crystal by reciprocal lattice vectors $\underline{\tau}$ and the excitations by wavevector $\underline{q}$ and energy $\hbar\omega_q$ and (1) becomes of the form

$$\frac{d^2\sigma}{d\Omega d\varepsilon} = \frac{k_f}{k_i} \left| M(\underline{Q},\underline{\tau},\underline{q},\hbar\omega_{\underline{q}}) \right|^2 \delta(\underline{Q} - \underline{q} + \tau)\ \delta(\varepsilon - \hbar\omega_{\underline{q}}) \qquad (2)$$

In non-crystalline systems it is more convenient to express (1) by expressions of the type

$$\frac{d^2\sigma}{d\Omega d\varepsilon} = N \frac{b^2}{\hbar} \frac{k_f}{k_i} S(\underline{Q},\omega) \qquad (3)$$

where $S(\underline{Q},\omega)$ transforms to $G(\underline{r},t)$, the space-time correlation function, which is a composite function including the motion of the same particle and the motion of pairs of particles.

2.5 Experiments may be *elastic* for which:

$$E_i = E_f, \quad \omega_i = \omega_f, \quad v_i = v_f;$$

$$\underline{k}_f - \underline{k}_i = Q, \quad |k_i| = |k_f|$$

and for $\phi_i = 0$ the scattering angle $\phi = \phi_f$ and $Q = \frac{4\pi \sin\phi/2}{\lambda}$.

Elastic experiments represent the structural mode and include all conventional crystallography, general structural diffuse scattering (including small angle scattering - better called small Q scattering) and the determination of atomic positions in disordered systems such as liquids, glasses, amorphous materials, polymers, biological membranes etc. A notable feature in the development of

elastic neutron scattering has been the progress from relatively simple structures to systems of considerable structural complexity. The structural mode also includes all the corresponding magnetic structural information ranging from the magnetic structure of ferro-, antiferro- and ferri-magnetic structures to the diffuse magnetic scattering associated with the distribution of magnetic moments surrounding magnetic ions in non-magnetic hosts and the associated ability to study covalency effects of general chemical - not specifically magnetic - relevance. The intensity scattered elastically into unit solid angle per incident neutron is measured and for the purposes of this discussion will be written as

$$\frac{d\sigma}{d\Omega} = \sum_{\substack{mn \\ if}} P_i b_m b_n \left| M_{if}(mn) \right|^2 .$$

Whatever the system, the information about the structure on atomic positions is contained in $|M_{if}(mn)|^2$ - ie, $|M(\underline{Q},\tau)|^2$ or $G(\underline{r},\infty)$ - and various procedures have been developed for unravelling this information. The analysis makes substantial use of modern computers and is usually performed at the scientist's home base rather than at the reactor centre.

2.6 Experiments may be *inelastic* for which:

$$E_i \neq E_f \text{ etc and } \varepsilon = E_f - E_i = E_{exc} = \hbar\omega_{\underline{q}}$$

where E_{exc} is an excitational energy of the system;

$$\underline{k}_i \neq \underline{k}_f \text{ and } |k_i| \neq |k_f|$$

and

$$\underline{Q} = \underline{k}_f - \underline{k}_i = \underline{q}$$

where $\underline{q}$ is the corresponding wavevector of the excitation. Furthermore selection rules exist such that from the intensities the nature of the mode of n collective excitations (phonons, magnons) may be deduced. The scattered intensity is measured per unit solid angle per unit of transferred energy per incident neutron and is given by equation (1) - or its alternatives (2) and (3). The excitation may be dynamical or magnetic - ie

motion of atoms or fluctuations in the directions of atomic magnetic moments - or, indeed, mixed. The information about the excitation is contained in $|M_{if}(mn)|^2$ - ie, $|M(\underline{k},\underline{\tau},\underline{q},\hbar\omega_{\underline{q}}|^2$ or $G(\underline{r},t)$ - and again various procedures for unravelling the information have been developed. The underlying physics of this unravelling process is relatively straightforward although in practice computer support is usually required.

2.7 In addition to the elastic/inelastic division, it is convenient to consider the *coherent* and *incoherent* parts of the cross-section. When the scattering is coherent, many-particle information is contained in the scattered beam allowing collective phenomena to be studied. When the scattering is incoherent, then information is obtained on the self correlation function, which describes the dynamical behaviour of individual molecules. The latter is particularly important in the molecular sciences, since the cross-section of hydrogen is both large and almost completely incoherent.

2.8 In inelastic experiments the information obtained is essentially spectroscopic and the spectroscopic mode includes:

- lattice vibrations in crystals (coherent scattering)
- instabilities of vibrational modes associated with the onset of phase changes (coherent)
- magnetic excitations (coherent)
- instabilities of magnetic modes associated with the onset of magnetic phase changes (coherent)
- motions of atoms in liquids and solutions (coherent and incoherent)
- general diffusion in matter (incoherent)
- molecular excitations (coherent and incoherent)
- polymer chain motion (coherent and incoherent)

2.9 In many neutron experiments where there is a magnetic interaction between the neutron moment and either an atomic or nuclear moment density, an increase in the sensitivity of the measurement of the interaction cross-section can be achieved by selecting the neutron spin state in the incident beam. When the polarized beam technique was first introduced it played an

important role in the determination of magnetic structures, but more recently it has been increasingly applied to the measurement of electron spin density distributions and is revealing more and more about the microscopic nature of magnetism. An extension of the technique to a spin analysis of the scattered beam (polarization analysis) enables spin-dependent cross-sections to be determined often in the presence of several other scattering processes; this type of experiment is, however, still in its infancy, and will benefit greatly from an increase in neutron intensity.

GENERAL CONSIDERATION OF INTENSITIES

2.10 The maximum thermal neutron flux Φ in nuclear reactors varies from $\sim 10^{12}$ n cm^{-2} sec^{-1} in small university based reactors to $1 - 2 \times 10^{15}$ in installations such as the ILL. This flux maximum in the reactor moderator is not available for neutron scattering experiments, since definition of the beam in terms of energy and direction reduces the intensity by factors of 10^{-6} to 10^{-11} depending on resolution requirements. The feasibility of an individual experiment further depends on factors such as the magnitude of the scattering from the sample (conceivably a factor of 10^{-1} but generally much less), and the need to match the energy/spatial resolution of the scattered and incident beams, which involves further losses in the range 10^{-4} - 10^{-6}. For acceptable accuracy one usually needs to collect $\sim 10^{4}$ counts per counting element (more if the background is quite large) so that even with multidetectors (spatial) and time channelling (energy) to allow simultaneous counting in many resolution elements data collection rates are slow.

2.11 In practice reactors of $\Phi = 10^{12}$ are now quite unsuited for condensed matter research. With $\Phi = 10^{13}$ in the early days, some reasonably accurate structural work on simple structures could be pursued as well as simple phonon curves and diffuse scattering from samples with high impurity or defect concentrations. Most of the experiments currently carried out at the ILL would be impossible with $\Phi = 10^{13}$ and not realistically possible for $\Phi = 10^{14}$. At the ILL typical individual experiments range in time from $\sim$ 10 secs (small angle scattering with a 4×10^{3} multielement counter) enabling simple time dependences to be followed in favourable cases (eg alloys and polymers) to $\sim$ 10 weeks for high resolution, inelastic studies on relatively weakly scattering samples or complex crystal structures. In the latter studies the demand for the high flux facilities is such that to complete one phase of a major experimental programme may take several years even for proposals given the highest priority. In addition there is now also increasing interest in

examining *in situ* time dependent processes (in alloys, polymers, glasses, defect crystals etc) and the greatly enlarged scientific scope afforded by high resolution studies from weak scatterers (surfaces, diffusion studies, excitations in phase changes, studies involving polarization analysis etc). The implications are that the next generation source should have an effective $\Phi > 10^{16}$. The SNS is just such a source.

THE PROVISION OF NEUTRON SCATTERING FACILITIES FOR UK UNIVERSITY SCIENTISTS

2.12 The way in which neutron beams have been made available to a growing number of UK University scientists (see the table below) and the impact that neutron scattering studies have made first in physics, more recently in chemistry and biology, can be seen as one of the most successful developments in post-war science.

YEAR	UNIVERSITY STAFF	RES. FELLOWS AND ASSOCIATES	RESEARCH STUDENTS	TOTALS
1967	38	16	62	116
1968	44	24	63	131
1969	39	20	68	127
1970	47	25	76	148
1971	52	41	75	168
1972	59	46	68	173
1973	61	51	72	184
1974	94	52	70	216
1975	103	61	83	247

The important developments were:

1951 - 1965 Limited but growing *ad hoc* use by university scientists of UKAEA reactors, principally DIDO and PLUTO at Harwell with $\Phi = 7 \times 10^{13}$ (now $\sim 10^{14}$) and Herald at Aldermaston with $\Phi = 2 \times 10^{13}$.

1966 SRC sets up NBRC. 25% of the Harwell instruments available to university users, and three instruments at Aldermaston.

1967 France and Germany begin construction of the ILL reactor.

1968 Rental of Harwell instruments increased to 50%.

1971 SRC recommends construction of a high flux beam reactor ($\Phi = 2 \times 10^{15}$) in UK.

1971 Neutron Beam Research Unit created at the Rutherford Laboratory. The unit works in close collaboration with users both at Harwell and the ILL and is a centre for research and development covering a variety of aspects of neutron scattering. It has been the focus of the continuing discussion about the next generation source.

1971 Significant use by university scientists of Harwell linac commences.

1972 ILL reactor operational and the first instruments commissioned.

1973 SRC becomes a *de facto* associate of the ILL giving UK scientists access to about one third of the facilities which earlier, and conservatively, had been predicted as necessary for a wide exploitation of the use of neutron beams.

1975 Most of the ILL instruments working routinely, with a total of over 500 experiments performed (∿ 200 involving UK scientists). Demand on several instruments substantially exceeding availability.

SCIENTIFIC DEVELOPMENTS

2.13 We conclude this general survey of the scope of the neutron scattering technique and its development in the UK by summarising the status in some of the important areas of application and indicating how these would benefit from the provision of the SNS. Such a summary must inevitably be subjective to some extent; the reader can find a full account of the programmes supported since 1967 by consulting the annual reports of the NBRC. The more specific conclusions of the Working Groups on the scientific gains which would accrue from using the SNS follow in Chapter 3.

Magnetism

2.14 Neutron scattering studies have revolutionized the subject of magnetism. After early success with the determination of the simpler magnetic structures quite complicated arrangements of atomic magnetic moments are now determined. The dynamics of these structures can be studied and the motions described in terms of the magnetic excitations or magnons of the structure (cf phonons in lattice dynamics). Measurement of these excitations by inelastic magnetic scattering has been one of the major successes of neutron scattering. Diffuse

magnetic scattering has been able to demonstrate the spread of magnetic influence around a magnetic impurity and this has important applications in probing electronic wave functions in non-magnetic hosts (eg, covalency). The spin glass systems are also being examined by diffuse scattering.

2.15 The future of this field is extremely promising both in relation to the present types of experiment and to the extensions, difficult at present, to higher energies and, by combining polarization and energy analysis, to the separation of magnetic and vibrational effects, especially above critical points. Whereas few phonon excitations occur above 0.1 eV, there exists a large number of magnetic materials exhibiting magnetism due to itinerant rather than localised electrons, whose collective excitations in the ordered state range into the 0.1 - 0.3 eV region. This region extends beyond the upper limit of energy-transfer currently observable using a hot-moderated steady-state source, but should be readily attainable with the SNS. Experiments of immediate interest include investigation of itinerant ferromagnets (eg Fe, Ni), where interaction with Stoner modes has been suggested by conventional experiments, and itinerant antiferromagnets (eg γ-Mn, Cr, NiS) whose steep energy dispersion has limited observations using conventional sources to excitations up to 0.14 eV and 2/3 q_{max}. Investigation of the generalised susceptibility $\chi(\underline{q},\omega)$ in transition metals is another area limited by current sources, the experiments requiring wide ranges of energy transfers without large momentum transfers. The exciting possibility of observing electronic band excitations in magnetic materials should also be mentioned. Cross-sections of only a few millibarns have been predicted, and experiments would need to be carried out with high energy neutrons, of a few eV, at relatively low Q, conditions only attainable on a source like the SNS.

2.16 Another type of experiment which presently suffers from a lack of neutron flux is that of polarization analysis in the measurement of diffuse and inelastic scattering cross-sections. The technique has potentially wide applications in the separation of nuclear spin-incoherent from coherent scattering. In magnetism, in addition to separating pure phonons and magnons, it can be used to identify magneto-vibrational scattering, where the phonons are excited through the magnetic interaction.

Liquids

2.17 The structure of liquids has to be represented by a probability distribution. At any instant the overall distribution will be the same but individual atoms will have moved in a given interval of time. They will diffuse and execute molecular motions (vibrations etc...). All these aspects may be determined by neutron scattering experiments. There is a profitable interaction between theory and experiment in this field and the ability comprehensively to determine probability distributions and the atomic dynamics from the 'microscopic' approach provided by neutron scattering has transformed the experimental study of liquids. Isotopes can be used to study structural and dynamic effects in binary (or higher) systems so that for example in a system AB the distributions r_{AB}, r_{AA} and r_{BB} may be separately determined. Such measurements require high intensities and many natural extensions of the present work, for example, AB, AA and BB motional correlations are barely possible. The work completed has shown the existence of molecular orientation in molecular liquids, structure in aqueous solutions and has allowed atomic distributions in metals and molten salts to be compared directly with the fundamental atom-atom interaction potentials. The structural aspect of this discussion applies also to glasses and the solid amorphous state generally.

2.18 The SNS will clearly serve wide areas of research in the field of fluids and amorphous materials. The case rests on the long-term, continuing programmes of investigation of the structure and dynamics of various classes of materials and their relevance to poorly understood properties. The scientific advantages arise through the ability to study wider ranges of composition of materials, and of materials over a wider range of the thermodynamic phase diagram, than is possible with existing sources. The extended Q range available with the SNS is particularly important for structural studies, providing new information on intramolecular properties. A wide selection of experiments can be immediately identified, for example, the study of aqueous solutions, and liquid alloys, aimed at understanding the correlation of the microscopic behaviour with macroscopic properties. The structure and dynamics of ^{3}He, ^{4}He and their mixtures should be studied to test the theoretical basis of our understanding of quantum fluids; this is particularly topical in the light of the recent discoveries of superfluid ^{3}He phases. The provision of the new source raises the possibility of carrying out kinetic experiments during phase separation and crystallisation processes, giving a new dimension to neutron beam studies.

Phase Changes

2.19 In the last decade there has been considerable interest in both the general formulation and in specific applications of the statistical mechanical and atomic theory of phase changes. The subject is all embracing and manifests itself for example in the helium λ-point, in ferroelectricity, in magnetism and in the classical first order change of melting. Neutron scattering has contributed substantially on the structural side. Many ferroelectric structures, for example, depend on hydrogen (or deuterium) displacements or displacements between ions of similar x-ray scattering power; in both these cases structural information from neutron scattering has been essential. However, in all cases one is interested in the way the instability occurs as the transition temperature is reached and the dynamics, whether motional or magnetic, are also studied by neutron scattering. A related problem is the persistence of order characteristic of temperatures below the transition temperature in local regions at temperatures above the transition temperature. This field is so large that experimentally it is only beginning to be explored. The addition of special perturbations and the separation of magnetic and atomic local ordering effects using polarized neutrons will need higher fluxes; the pulsed nature of the SNS is particularly important for high pressure investigations.

Polymers

2.20 Both structural and dynamic aspects of polymers have now been extensively studied by neutron scattering techniques. Structural work has been concerned primarily with determinations of the chain conformation in concentrated solution and in bulk samples (glassy, crystalline and rubber). Neutron scattering provides a quite unique tool for these studies because of the different coherent scattering cross-sections of H and D. Use of a small concentration of deuterated polymer in a matrix of protonated polymer (or vice versa) gives a scattering contrast which permits the coherent scattering from the individual molecules to be isolated (as for a true dilute solution) and hence enables molecular conformations to be determined. Such experiments established the validity of Flory's hypothesis that polymer chains in their own matrix have unperturbed dimensions. Experiments on crystalline polyethylene have shown that the dimensions of the chains in the crystal are not very different from those in the melt, implying that an individual molecule may form part of several folded crystalline regions in different layers.

2.21 The study of the dynamics of polymers is concerned with side-group motions and with the low frequency long range conformational motions of chains in solution and in the melt. Another important aspect of the study of polymer dynamics concerns the study of phonons. Where single crystals can be grown the information obtained in such work is like that for similar studies of any single crystal, the $\omega(\underline{q})$ relations across the Brillouin zone for modes of various symmetries propagating in specified crystal directions. This gives directly the elastic stiffnesses, for example along the perpendicular to the chains, and provides a very good probe for both intramolecular and intermolecular forces.

2.22 The enormous backlog of experiments and pressure of time available at ILL mean that a small angle scattering instrument of only comparable performance to those at ILL on the SNS would be important, especially in extending polymer work from scientific problems to those of a technological, and relatively more time-consuming, nature. With count rates improved by an order of magnitude however, entirely new experiments on the time dependence of chain conformation (relaxation phenomena) will be possible, opening up a whole new area of polymer science and technology. For inelastic scattering, the pulsed nature of the source will make possible the study of rotational isomerison in relaxing systems, which is especially important because the rotational isomeric model of the polymer chain underpins all accepted models concerning the influence of chemical structure.

Alloys and Materials

2.23 There are many systems showing structural disorder, although a lattice basis exists. For example, precipitation in alloys, defect arrangements in non-stoichiometric compounds and materials disordered by extensive radiation damage. These invariably exhibit diffuse scattering either at large or small angles, or indeed at both. Neutrons can penetrate reasonably sized samples compared with x-rays or electrons and moreover the much longer wavelengths which may be used have enabled much better information to be obtained. In many cases the ability to discriminate between elements of similar x-ray scattering power (eg, Al, Mg, Si) has also been exploited. A number of cases has now been observed in which there are significant anisotropies in the small angle scattering obtained from single crystal samples. These

effects are being related to the shape of the structural fluctuation producing the scattering and experiments are in progress on systems of technological importance. Another important aspect of the present work is the fact that in a few favourable cases the time dependence of ageing or dissolution can be followed so that the growth and decay of the precipitates (say) can be followed atomically.

2.24 An important consequence of the SNS will be the possibility of extending the range of materials, and conditions, under which experiments can be carried out. This is particularly important because of the technological implications of much of materials science. An important area of application is the study of voids and point defects caused by irradiation, where it should be possible with sufficiently high flux to follow annealing processes *in situ* as a function of temperature. It should also be possible to follow the effects of stress on the damage, and the pulsed nature of the beam may be used to investigate the microscopic nature of fatigue by synchronous loading of a sample.

Biophysics

2.25 The impact of neutrons in this field is in its infancy having effectively become possible with the fluxes available at the ILL and even there requiring in many cases long counting times. Information on structures characterized by large repeat distances is being obtained by small angle neutron diffraction from membranes, muscle and collagen. The use of different H_2O/D_2O mixtures to vary the contrast between a particle (or a particular component of a particle) and its surrounding medium allows the size, shape and internal structure of various biological units to be determined by small angle neutron scattering. Applications have been made to the study of viruses, ribosomal subunits, chromatin and such proteins as catalase and tubulin. The interest is such that a wide-ranging international meeting 'Neutron Scattering for the Analysis of Biological Structures' has recently been held at Brookhaven.

2.26 The immediate effect of a new source 'tomorrow' would be to provide facilities additional to those presently available, thus relieving the chronic bottlenecks in beam time and enabling a greater variety of experiments to be covered. Of particular importance will be the development of

studies involving selective deuteration, to give the distribution of proteins in mixed biological systems (eg ribosomes). Among the more ambitious experiments to be attempted with increased fluxes, one can foresee detailed inelastic measurements on biological systems, whereby rapid dynamical processes such as diffusional motions can be studied, while the pulsed nature of the source will be exploited to follow kinetic processes in 'real-time' experiments such as activation and relaxation of muscle, and activation by light of retinal membranes.

General Spectroscopy

2.27 There are large numbers of inelastic experiments carried out to determine energy levels of localized systems not obtainable by other types of spectroscopy. This may be because the selection rules for neutron induced transitions are allowed - where those for transitions induced by electromagnetic radiation are forbidden - as in chemical neutron spectroscopy; or because with rare earth metals or alloys the neutrons can penetrate the sample where electromagnetic radiation cannot. These fields are vast and neutron inelastic spectroscopy is part of the general spectroscopic armoury available to the chemist and physicist, although at present the energy range available is restricted to relatively low energy excitations in comparison with the range of infra-red and Raman spectroscopy. The SNS should enable neutron scattering to fully complement the range covered by the optical methods.

2.28 Closely related to many of these studies are the observations of the very small energy changes associated with diffusive motions, both translational and rotational, manifested by quasi-elastic scattering. Experiments of this type have led to major advances in the understanding of liquid and plastic crystalline phases and the behaviour of hydrogen in metals. A combination of quasi-elastic scattering and neutron spectroscopic techniques has been employed in studies of the vibrations and diffusional motions of adsorbed and intercalated molecules. Such investigations hold the promise of important contributions to surface chemistry but present-day fluxes have so far limited experiments to systems of relatively large surface area. A major function of the SNS will be to provide the possibility of high flux experiments with good resolution for such experiments.

CHAPTER 3. SCIENTIFIC APPLICATIONS OF THE SPALLATION NEUTRON SOURCE

INTRODUCTION

3.1 The general features of the SNS in relation to a high flux reactor have been described in Chapter 1, paragraph 1.11, and the estimated performance of the source is given in Chapter 5, paragraphs 5.12-5.19. The four Working Groups (Chapter 1, paragraph 1.12) have used the latter data in assessing the impact of the new source in the scientific areas of interest to the Science Board, and this chapter presents their conclusions. A group of instruments which might be used for the suggested science programme is summarised (paragraph 3.87) and the chapter also includes some possible other uses of the facility (paragraph 3.88). Appendix I contains the full reports of the Working Groups and preliminary specifications of possible instruments.

3.2 The practical advantages of the SNS can be summarised as follows:

- Wide regions of momentum and energy transfer become accessible to the experimenter. The available domain of $(Q,\hbar\omega)$ is expected to be between $(0.3\ \text{Å}^{-1}, 0\ \text{eV})$ and $(100\ \text{Å}^{-1}, \sim 0.5\ \text{eV})$
- Measurements can be made at higher rates of data collection
- Improved resolution will be available, particularly at higher energy transfers

- The use of smaller crystals or samples than hitherto becomes feasible

- Experimentation will also be possible on samples which are 'small' in the geometrical sense (eg surfaces or thin films) or in the chemical sense (eg dilute solution where the behaviour of the solute is of particular interest)

- The use of fixed scattering angle enables studies of samples to be undertaken under extreme conditions of temperature and pressure which are otherwise difficult or impossible

- The use of higher energies up to and beyond 1 eV enables studies to be made of highly absorbing samples and promotes the employment of anomalous scattering techniques

- Kinematic corrections at high incident energies, particularly for fluid systems, are smaller and better controlled.

3.3 In each of the scientific areas solid state physics, liquids and amorphous solids, structure determination, and chemistry, it is possible to identify experiments which depend on the SNS for their successful execution, and those which though feasible today would benefit markedly from the increased intensity. The latter are not necessarily inferior to the former, and particularly in chemistry or biology the ability to be able to complete a planned series of experiments may lead to scientific advances of greater significance than a single 'difficult' experiment. Examples of each type of experiment are headlined in the following paragraphs.

3.4 New experiments, or experiments that are barely possible at present, which can be performed with the SNS include:

- magnon studies in itinerant ferromagnets and antiferromagnets

- residual spin wave structure in ferromagnets above T_c

- the study of Kondo or spin fluctuating systems

- dispersion curves for electronic excitations in semiconductors

- magnon creation and annihilation studies

- the influence of fluid flow on liquid structure factors

- collision mechanisms from dynamical studies of dense gases
- the transition between binary collisions and collective mode coupling effects in simple fluids
- separation of coherent and self motions in liquid metals
- anomalous scattering techniques in the study of liquid alloys
- the structure of dilute electrolyte solutions
- molecular configurational changes in collisions between flexible molecules
- the structure of amorphous thin films
- phonon lifetimes in glasses
- structural, vibrational and rotational studies of molecules adsorbed on surfaces of area $\sim 1\ m^2$ or less
- high energy transfer vibrational spectroscopy - the energy range and the ease of data collection becomes comparable with infra-red techniques
- relaxation of chain conformations in polymers
- mechanical deformation - structure relationships in polymers
- very high pressure studies of crystal structure

3.5 Experiments currently feasible but given new scope by the higher intensity of the SNS:

- crystal and spin orbit splitting in metals and metallic compounds
- pair potentials and triplet distribution functions in simple fluids and their mixtures
- magnetism in liquid transition and rare-earth metals
- isotopic substitution techniques in aqueous solutions, molten salts and liquid alloys
- structural studies of water
- the structure of molecular liquids

- structural and dynamical studies of ^3He and ^3He-^4He mixtures

- kinetics of glass transitions

- collective motions in liquid crystals and intercalates

- mechanisms involving diffusion of non-hydrogenous atoms

- the spectroscopy of dilute and small samples, lipid bilayers, biological membranes, matrix isolated molecules etc

- kinetics of H-D exchange in biological systems

- the determination of the position of labelled sites in biological macromolecules in solution

- complex structure refinements by very high resolution powder diffraction

- simultaneous studies of the structural change and diffusion kinetics of host-molecule systems

- single crystal structure determination of polymers, and other small crystals

SOLID STATE PHYSICS

3.6 In discussing the impact of the SNS on solid state physics experiments it is convenient to classify these into (a) those which benefit from increased intensity, (b) experiments at the limits of feasibility at the ILL but which could be best carried out on SNS instruments on grounds of the spectral characterisation of the beam as well as flux, and (c) experiments which at present cannot be carried out at any neutron source in the world.

3.7 We have identified experiments in various areas of physics according to this classification, as follows:

'class (a)'

- phonon and magnon dispersion

- crystal field and spin-orbit splittings in paramagnets

- inhomogeneities in solids

'class (b)'

- generalised susceptibility $\chi(\underline{q},\omega)$
- magnon excitations in itinerant ferromagnets and antiferromagnetics
- separation of coherent/spin-incoherent and nuclear/magnetic scattering

'class (c)'

- high energy transitions
- inelastic polarization analysis

3.8 For 'class (b)' experiments, two instruments are suggested for the SNS which would extend the scope of experiments at present attempted only with difficulty. These are (a) a high energy (0.1 to 0.3 eV) inelastic instrument and (b) a total scattering polarization analysis instrument. The former instrument would contribute very significantly to magnon and crystal field studies and it would in addition open up the study of two other important problems in magnetism, viz measurements of the generalised susceptibility $\chi(\underline{Q},\omega)$ and the study of itinerant magnetism. Some experiments in this class are described in paragraphs 3.13 - 3.15 below.

3.9 With the high effective intensities available from the SNS, the use of inelastic polarization analysis techniques becomes possible, essentially for the first time. In addition, a favourable feature of the energy spectrum of the SNS is the intensity gains it provides at the higher neutron energies (1 to 10 eV), and these can be employed to carry out totally new high-energy low-Q inelastic experiments with energy transfers $\sim$ 0.3 to 1 eV. These experiments fall in 'class (c)' and are described in paragraphs 3.16 - 3.19.

Phonon and Magnon Dispersion

3.10 The unique property of thermal neutrons, that both their wavevector and energy match closely those of elementary excitations in solids, has been exploited extensively during the past 15 years to determine the energy dispersion throughout the Brillouin zone of magnons and phonons in many elements and compounds. These measurements have generally involved neutron

energy transfers (excitation energies) of 0-0.1 eV, and have mainly been performed on continuous or chopped beams from steady state reactors. They have yielded important and unique information on the interactions between the magnetic electrons, or between atoms or ions, in materials, and they have been extended to investigate details of the dynamical behaviour of spins and lattices near phase transitions. Information on excitation lifetimes, and the interactions between different kinds of excitations (such as external and internal modes, or magnon-phonon coupling) has also been obtained.

Crystal Field and Spin-Orbit Splittings in Paramagnets

3.11 Crystalline electric field levels in rare earth ions can be measured directly by neutron inelastic scattering. The method has played a key role in the study of metals, since photon spectroscopy is not applicable here, due to the interaction with conducting electrons. Although the lanthanide metals have received considerable attention, there has so far been little success in observing transitions in actinide materials, since here the 5f shell is on the outside of the atom, and the crystal field splittings are somewhat larger ($\sim$ 0.1 eV). Spin orbit splittings in the rare earths fall in the range 0.04 to 0.3 eV. These may be studied in the insulating compounds by optical spectroscopy, but again in the metals and in metallic compounds optical techniques are no longer appropriate. In one particular field, that of intermediate valence compounds (which are usually metallic), the measurement of transitions between spin orbit levels would be an extremely useful tool. Though the splittings are relatively small in SmS, in other rare earths showing intermediate valence behaviour eg, Ce, Tm and Yb, the splittings are much larger.

Inhomogeneities in Solids

3.12 Any deviation from order in a crystal lattice gives rise to scattering which is additional to Bragg scattering and is termed as diffuse. In many instances where this deviation is due to dislocations, point clusters, alloy precipitates, magnetic moment fluctuations, density changes etc, the inhomogeneity gives rise to a $\underline{Q}$-dependent scattering, which is generally best-observed at neutron wavelengths greater than that of the material being studied, so as to avoid multiple Bragg scattering, and at small

scattering angles. Some examples of areas now under study are radiation induced defects, alloy decomposition, non-stoichiometric defects, covalency, flux-line lattices in superconductors, polymers in solution and magnetic impurities. The study of magnetic defects is considerably enhanced by using spin polarized beams. Two major advantages of diffuse scattering experiments with a pulsed neutron beam are the possibility of separating elastic and inelastic scattering if the wavelength spread is limited, and the possibility of synchronising a perturbation of a sample with the neutron pulse and then studying the response of the sample by collecting the scattered neutrons from many such cycles. Possible areas of application are the study of voids, point defects and point defect clusters caused by irradiation, where it becomes possible to follow the annealing of the damage as a function of temperature. It should also be possible to follow the effects of stress on the damage and to investigate the microscopic nature of fatigue by synchronous loading of a sample.

Generalised Susceptibility $\chi(\underline{q},\omega)$

3.13 The investigations of the generalised susceptibility $\chi(\underline{q},\omega)$ in transition metals are of two broad types, (a) nearly magnetic materials like Pd, and (b) ferromagnets like Ni and Fe and antiferromagnets like Cr and Mn, above their ordering temperature. In category (a) calculations have been made of the neutron cross-sections for the case of Pd. These showed that the total response is spread over a wide energy range, of the order of the bandwidth of the d bands. However, many fascinating many-body effects (eg "the paramagnon peak") appear at energies below 0.1 eV at low temperatures. Attempts to study the magnetic scattering have not succeeded with present techniques since the 4d form factor of Pd drops rather rapidly, and with present sources wide ranges of energy transfers cannot be studied without large momentum transfers, though scattering has been observed from the narrow 4f band of αCe. Similar considerations apply to category (b) above. Recent measurements on Ni and Fe above T_c have shown a surprising amount of structure in the paramagnetic response. This has been interpreted as a residual spin wave branch which extends up to 0.1 eV, where the spin waves disappear below T_c. The origin of this scattering is not understood at present.

Magnon Excitations in Itinerant Ferromagnets and Antiferromagnets

3.14 Whereas few phonon excitations occur above 0.1 eV, there exists a large number of magnetic materials, mainly metallic or semi-metallic and exhibiting magnetism due to itinerant rather than localised electrons, whose collective excitations (magnons) in the ordered magnetic state range into the 0.1 - 0.3 eV region. This region extends beyond the upper limit of energy-transfer observable using a conventional triple-axis spectrometer on a beam from a hot-moderated steady-state source, and a number of recent experiments performed on such an instrument has indicated that it contains, tantalizingly, important and fundamental physical effects. Examples of possible experiments include the investigation of the itinerant ferromagnets nickel and iron, where sudden decreases in scattered intensity have suggested the possibility of the magnon interacting with the continuum band of Stoner modes near 0.1 eV, and the study of itinerant antiferromagnets such as γ-manganese, chromium and nickel sulphide, whose steep energy-dispersion (200, 450 and $\sim$ 450 meV Å respectively) has limited observation using conventional sources.

Separation of Coherent/Spin-Incoherent and Nuclear/Magnetic Scattering

3.15 Probably the most important application of a total scattering polarization analysis instrument would be in the study of paramagnetic or magnetic defect scattering. One of the main problems in the usual determination of paramagnetic cross-sections is to separate this from the other scattering processes viz, nuclear disorder, multiple Bragg, thermal diffuse, Bragg, and nuclear spin incoherent scattering. A measurement of the spin-flip scattering cross-section provides a powerful method for separating the paramagnetic scattering. One of the fields of study where an accurate evaluation of the paramagnetic cross-section would make a large impact is dilute magnetic alloys, where it can reveal the existence of the onset of long range magnetic order, interacting impurities and Kondo or spin fluctuating systems.

Inelastic Polarization Analysis

3.16 Many useful polarization analysis experiments such as those mentioned above can be adequately performed without energy analysis. When some

energy-analyser is included in a polarization analysis instrument, the accompanying decrease in flux is sufficient at present to make inelastic experiments effectively impossible. The provision of an inelastic polarization analysis instrument on the SNS will, however, enable a significant number of spin dynamics experiments, both in magnetic as well as non-magnetic materials to be carried out. Inelastic polarization analysis provides the most effective way of separating magnon and phonon scattering, since the latter is nuclear and coherent, hence always non-spin-flip. By selecting both the incident and scattering neutron spin states the observation of magnon creation and annihilation has been clearly demonstrated in the saturated ferromagnet $Fe_{2.5}Li_{0.5}O_4$, though it has not been possible to carry out experiments routinely. In addition to separating pure phonons and magnons, it is also possible to use the technique to identify magnetovibrational scattering, where the phonons are excited through the magnetic interaction, and which exhibits the same polarization-dependent effects as magnetic Bragg scattering.

High Energy Transitions

3.17 The role of neutrons in determining the frequency/wavevector dispersion curves for phonons (see previous section on phonon and magnon dispersion) derives from the ability in neutron experiments to measure, with sufficient accuracy, excitations in the range $0.02 < \hbar\omega < 0.1$ eV over a wavevector range $0 < \underline{q} < 5$ Å^{-1}; this enables energy dispersion information to be obtained within the first Brillouin zone. No other probe eg, x-rays, infra-red, visible light Raman scattering, allows such comprehensive data to be obtained; these other techniques yield information only for restricted regions of the Brillouin zone, especially near $\underline{q} = 0$ and the zone boundaries, and then not with unique assignment.

3.18 The same general problem occurs in the experimental determination of the dispersion curves for electronic excitations. An important class of such materials is the large group of semiconductors having band excitation energies $0.1 < \hbar\omega < 5$ eV throughout the Brillouin zone of $0 < \underline{q} < 5$ Å^{-1}. Methods currently available for studying these excitations include optical absorption, optical reflectivity, photo-emission, electron scattering, and cyclotron resonance, and these provide accurate information for specific parts of the Brillouin zone. However, no complete experimental determination of frequency/wavevector dispersion curves has been possible.

3.19 As occurred with the studies of vibrational excitations, major computing projects have been developed to interpolate between points, and a further recent initiative has been taken by a number of theoretical physicists in the UK using the Rutherford Laboratory IBM 360/195 computer. It is clear that the ability to measure experimentally more complete dispersion curves would be a major advance both in the study of the electronic states of semiconductors and in the growing possibilities of 'electronic design' of materials.

GASES, LIQUIDS AND AMORPHOUS SOLIDS

3.20 The study of fluids and amorphous solids by neutron scattering provides information on the structure and dynamics of the materials. The SNS will have a major impact on all aspects of this work; some of the main features are described below.

Structural and Dynamical Studies of Simple Fluids

3.21 The study of the structure of pure noble-gas fluids is at present heavily influenced by computer simulation which gives an unambiguous description of kinetics and structures of fluids interacting with realistic and hypothetical pair potentials. There is, however, a lack of very accurate measurements of the structure factor, S(Q), to compare with the computed models. Three regions of the p,V,T diagram of particular interest are:

- the dense fluid region, far from the triple point
- the liquid region, near to the triple point, and
- the region of the critical point.

Such information allows pair potentials to be calculated, as well as data related to the triplet distribution function and so provides an opportunity to test various theories of the fluid state. By the use of isotopic substitution the studies can be extended to include mixtures of the noble gases. Attempts to investigate distortion of the structure factor resulting from fluid flow, which would have an impact on the theory of transport properties, should also be worthwhile.

3.22 The SNS will make possible the accurate study of the dynamical structure factor of dense gases of atoms or molecules as a function of density. The scattering from non-interacting rigid molecules can be calculated exactly. Therefore by studying departures from ideal behaviour as a function of collision rate (by increasing pressure or temperature) it becomes possible to learn about the collision mechanisms themselves.

3.23 A fundamental problem in the theory of fluids is the treatment of the competition between simple binary collisions, which dominate at low densities, and collective mode-coupling effects which become increasingly important at high densities. These effects most strongly influence the transition region between hydrodynamic and kinetic behaviour. This transition region has been investigated at liquid densities using both neutrons and computer simulation, but the neutron data are at present limited. Light scattering has been used to investigate this transition in the low density region, but it is not useful for more dense systems. The intermediate density region has not yet been investigated thoroughly by any technique and there is a pressing need therefore to follow a system like ^{36}Ar through the whole density range.

3.24 The gains described above by using the SNS to study gases are equally applicable to studies of dynamics of liquids which are at present poorly understood. From constant low Q measurements with high energy resolution, information on translational (and rotational for molecular systems) diffusion is obtained while at higher Q the nature of the single particle motion is obtained. The validity of measurements possible with the SNS will enable studies on both natural and induced relaxation processes. Such studies are of particular value also for liquid metals, molten salts, aqueous solutions and molecular liquids.

Liquid Metals and Alloys

3.25 The outstanding problem in the physics of liquid metals is to determine the extent to which the distribution of the ions reflects and is influenced by the electron gas. In the simplest case, an effective pair potential, p(r), can be thought of as representing the interactions between the ions, appropriately screened by the electron gas. Self-consistent methods which relate p(r) to S(Q) require an accurate knowledge of S(Q), particularly in the region for $Q < 2\ \text{Å}^{-1}$, over ranges of temperature and pressure. The need to compare x-rays and neutron scattering to a high degree of accuracy has also recently been emphasised. This enables infor-

mation about electron-ion correlations to be obtained, knowledge of which is basic to our understanding of electronic properties, including under extreme conditions, those liquid metals which are known to undergo a metal-insulator transition. In alloys three broad types of behaviour have been observed:

- metallic behaviour with a statistical distribution of ions
- metallic behaviour with clustering of ions
- semi-conducting behaviour implying the existence of ionic, covalent or mixed bonds.

The occurrence of such diverse behaviour is not understood and arises from that area of science common to physicists, metallurgists and chemists. Again research programmes depend heavily on accurate data using isotopic substitution techniques although with the SNS it also becomes feasible to consider anomalous scattering close to resonance absorption edges as a method of extracting partial structure factors. This is a relatively new technique, but it opens up new and exciting possibilities for liquid alloy work, particularly for systems involving heavy elements and those for which no suitable stable isotopes exist.

3.26 A further application of either isotopic substitution or anomalous scattering is in the domain of alloy critical scattering. With more highly developed polarization techniques and an intense neutron beam, the nature of magnetism in liquid transition and rare-earth metals will be investigated. This subject is still in its infancy but is already beginning to reveal interesting new concepts.

3.27 The enhanced flux also enables one to consider, for a single element, the separate measurements of $S(Q,\omega)$ and $S_s(Q,\omega)$ (related to the coherent and self motions respectively) by inelastic polarization analysis. This technique could be applied in particular to a variety of liquid metals including sodium about which considerable theoretical and experimental knowledge has been built up over the last decade or so.

Molten Salts

3.28 The structure of molten salts (ie. disordered systems in which there is a strong interaction through Coulomb forces) is a topic of long standing interest. Fundamental problems in these types of liquid are:

- the short range repulsive part of the ion-ion interaction
- the role of polarization
- the mechanism of ion transport.

A programme to investigate the partial structure factors of molten salts is already under way in the UK and experiments yielding new information have already been carried out on the salts CuCl, NaCl and RbCl. Extension of this programme to other elements, and later, tertiary and more complicated systems, lies to a large extent outside the capabilities of present sources and requires the SNS.

Aqueous Solutions

3.29 Our knowledge of the structure of aqueous solutions has advanced following a series of experiments using the high flux reactor at Grenoble. From these experiments it has proved possible to determine the ion-solvent and ion-ion arrangement respectively but at present the investigations are limited to a small number of favourable isotopes where the degree of statistical uncertainty is minimised, eg saturated sodium chloride and nickel chloride solutions. The new source will enable a study to be undertaken on a wider variety of solutions and a greater range of dilutions, thus leading to a general picture of electrolyte structure including tests of the validity of a variety of computer simulated models. Because of the wider range of solute-solvent correlations, it will be possible to assess the degree to which various ions enhance or reduce the bulk water structure, a fundamental problem in electro-chemistry.

3.30 The new source is also ideally suited to the examination of the effects of pressure while the boost it should give polarisation analysis techniques - which in principle can give new insights in to the proton distribution in hydrogenous liquids - will have immediate importance for the structural study of water.

Molecular Fluids

3.31 Even the simplest molecular fluids, homonuclear diatomic molecules, are structually an order of magnitude more complicated than the noble-gas fluids, because of the additional degrees of freedom associated with the relative orientations of the particles. Neutron structure factor measurements are one means of studying orientational correlations in molecular

fluids. It has been possible with the present facilities to determine favourable configurations for pairs of molecules in liquid nitrogen, oxygen and bromine. However a thorough study of even such simple molecular systems over the thermodynamic phase diagram, combined with an extensive programme of computer simulation would increase our understanding of the liquid state. For more complex small molecules, studies of the structure of the dense gas phase, not possible with present intensities are desirable; modifications in molecular configuration due to collisions should be detectable, and information obtainable on the rigidity of the molecules.

3.32 Dynamical studies on simple molecular gases will prove rewarding both for the study of collision processes themselves and their effect on the internal motion of the molecules. It is also possible to envisage the study of the dynamical behaviour of metal dimers or other more highly associated groups of atoms or ions in the vapour phase.

Quantum Fluids

3.33 The study of liquid ^{3}He and liquid ^{4}He by neutron scattering shares with other liquids the general advantages to be gained from the use of the new source. Some of the relevant aspects are discussed in the following paragraphs.

3.34 As far as the static structure factor S(Q) is concerned, ^{4}He may, to a good approximation, be regarded as a dense classical fluid, but for a stringent test of theory accurate results over a wide Q range are required. As these theoretical approaches also give the population of the Bose Condensate - a quantity of central importance to the understanding of superfluidity - their critical appraisal is essential. The recently discovered superfluid phases of ^{3}He also creates an interest in the ^{3}He-^{4}He interaction which will stimulate structural studies on ^{3}He-^{4}He mixtures for several years.

3.35 Existing studies of the collective excitations in superfluid ^{4}He using neutrons, though extensive, have been significantly limited with present sources. For example, the behaviour of the one-phonon branch at scattering vectors beyond the roton minimum has long been of theoretical interest and recently of experimental interest, but it is highly desirable to improve both the statistics and resolution of existing measurements as well as extending them to higher wave vectors. The inelastic scattering behaviour is dominated by roton-roton interactions and accurate knowledge of lineshapes would allow a critical test of existing theories.

3.36 Although the interaction potential for ^3He is similar to that of ^4He, its collective excitation spectrum is fundamentally different. Unfortunately the capture cross-section of ^3He for thermal neutrons is extremely large and it is only recently that inelastic scattering has been observed and these results are limited. On the basis of theory the most prominent feature of the scattering from ^3He is the broad distribution of intensity that results from the excitation of particle-hole pairs. This is analogous to the Stoner excitations in itinerant ferromagnets. For large scattering vectors the continuum of excitations becomes independent of the particle scattering. As for ^4He, this region would be accessible with the new source.

Amorphous Solids

3.37 The structures of amorphous solids are again complicated and generally require accurate analysis of data in real space. Since the real space resolution obtained in any experiment is inversely proportional to Q_{max} the new source has a decisive advantage over steady state reactors.

3.38 Most inorganic glass structures are based on covalently bonded networks ranging from the simple one-dimensional chains found in selenium and many phosphates to the fully three-dimensional silicates. The glasses in common use are multicomponent systems (eg. Na_2O-CaO-SiO_2) and the elements present are not amenable to the technique of isotopic substitution. By far the most effective method of studying the structure of these glasses is by systematically varying the composition and a broad programme of structural analysis can be envisaged with the new source which will also allow extremely interesting kinetic studies of the glass transition region.

3.39 A variety of thin films can be made by vapour deposition (eg. Se, As-S, As-Se) and these have structures which are very dependent on preparation conditions. There is considerable interest in the extent to which the network structure of bulk glasses gives way in thin films to a more molecular character. So far the only neutron experiments on thin films have been on As-S and amorphous Ge, the major difficulty being the small amount of sample available. Similar considerations apply to other modes of preparation such as splat cooling and chemical deposition.

3.40 The SNS will encourage studies on the density of vibrational states and it will also be possible to study phonon lifetimes in glasses, which are related to low temperature anomalies.

STRUCTURE DETERMINATION

3.41 Most crystallographic studies form part of a wide investigation of physical, chemical or biological properties and the importance of the neutron part in this acquisition of basic structural data arises from

- the relatively small range of neutron scattering amplitudes which allows the ready detection of light atoms in the presence of atoms of high atomic number
- the irregular variation of scattering amplitudes which often generate significant fluctuations in scattering length between neighbouring atoms in the Periodic Table
- the fact that in many cases absorption is small (compared with x-rays) so that measurements down to liquid helium temperatures or up to 1500°C can be as routine as at room temperature. Experiments at even higher temperatures and at high pressure may also be performed
- the magnetic moment for magnetic structure determinations and magnetic moment distributions.

3.42 The SNS has three distinct advantages which can be employed in opening new areas of structure determination. These are

- the time-of-flight techniques used in conjunction with a white beam which facilitate the study of samples in special environments
- the very high rates of data collection in conjunction with the simultaneous recording of all or a large part of the diffraction pattern, which adds a further dimension to the study of time-dependent processes such as reaction mechanisms and transient phenomena
- the opportunity to examine relaxation processes in the solid state by the synchronisation of an external perturbation with the pulse frequency of the beam. We note that some of these features are also offered by x-ray radiation from a synchrotron source.

However, apart from the general advantages of neutron scattering referred to above, the troublesome preferred orientation effects in powders are much more pronounced for x-rays and the energy dispersive analysis of the synchrotron x-radiation has poor resolution compared with neutron time-of-flight methods.

3.43 Some of the new experiments based on the features in the preceding paragraph which will follow the introduction of the SNS are:

- high pressure experiments up to 100 kbars for studies of phase transitions, geophysical problems, and new phases which exist only under high pressure conditions
- accurate structure determinations at very high temperatures up to 3000°C
- structural changes associated with the application of a small periodic electric field to a piezoelectric crystal (or ceramic) or to a liquid crystal
- the mechanism of dipole switching with ferroelectrics (one such experiment on $NaNO_2$ has already been demonstrated)
- studies of metamagnetic phase transition using small rapid oscillations of a magnetic field
- speculative investigations of muscle contraction effects and structural changes associated with shock waves
- structural studies (complemented by neutron topography and particle size analysis) of reaction mechanisms.

3.44 In conventional crystallography - particularly involving complex chemical or biochemical crystals,the desire to include neutron diffraction (when appropriate) in the attack on the structure is frequently frustrated by the lack of crystals of a suitable size. Moreover, the delicate preparative conditions or the crystal morphology often prevent larger crystals being grown. In some cases involving relatively simple structures the problem can be overcome by using powders and employing profile methods to analyse the diffraction pattern. But either the resolution or the data collection rate is restricted with present fluxes. The improvements possible with the SNS in both single crystal and powder techniques are given below.

Single Crystal Studies

3.45 It is clear that the high intensity of the SNS, coupled with a large area position sensitive detector, would allow single crystal structure

factors to be measured as a function of wavelength and at rates some two orders of magnitude higher than at the most intense reactor source currently available. A feature of the SNS is the extension of data to high values of sin θ/λ. This is vital to many structural problems involving the study of positional parameter changes at phase transitions, electron distributions from x-ray/neutron data, and anisotropic and anharmonic thermal vibrations. The measurement of the wavelength dependence of strong structure factors is the surest way of obtaining the best estimate of their extinction-free values. The same basic instrument can be used for:

- high resolution structural studies of materials with simple structures having cell dimensions of 5 - 10 Å (ambient moderator)
- normal structural studies cell dimensions 10 - 20 Å, wavelengths 0.5 - 1.5 Å (ambient moderator)
- structural studies of complex molecules with large unit cells having dimensions up to 40 Å using wavelengths in the range 1 - 6 Å (cooled moderator).

Studies of magnetisation density distributions in materials with cell dimensions in the range 5-20 Å can also be carried out with the insertion of a polarization filter and Drabkin flipper into the incoming neutron beam with similar improvements in the data collection rate. In both nuclear and magnetic crystallography many experimentalists will need to exchange the possibility of a greatly enhanced data collection rate for a reduction in specimen size.

3.46 One aspect of single crystal structure determinations by time-of-flight methods is that each structure factor is readily obtained at a number of different wavelengths, and when the crystal contains strongly absorbing nuclei and anomalous dispersion effects are present it is possible to solve the well known phase problem. The data collection rate of the SNS will increase the precision with which weak anomalous scattering effects can be measured and encourage the use of the technique as part of the general armoury employed in single crystal structure determination. New techniques like the diffraction of polarised neutrons from dynamically polarised targets will also benefit from the enhanced flux.

Powder Studies

3.47 The recent remarkable profile analysis methods applied to powder

samples now enable refinements to be carried out routinely on structures with 20-30 structural parameters and unit cell volumes up to 1000 $\AA^3$. Apart from large gains in effective flux the SNS provides the possibility of very high resolution at reasonable counting rates by the use of the back scattering mode. Two types of diffractometer are envisaged to exploit the SNS. A high resolution diffractometer would very considerably extend the power of powder methods in structure determination. The resolution could be 2-3 times better than conventional diffractometers and only slowly dependent on $\sin \theta/\lambda$. With such an instrument the refinement of structures with at least 100 structural parameters will be possible, over a very wide range of experimental conditions. Other applications, for single crystals as well as powders, are the observation of phase transitions involving very small changes of symmetry, critical scattering associated with a phase transition or the diffuse scattering associated with point defects in the sample. Particle line broadening effects will be observable and the instrument could be used for the study of small amounts of precipitated phase occluded in the bulk material. A moderate resolution instrument with very rapid data collection would be used to exploit the kinetic processes.

3.48 The applications of conventional crystal structure determination on the SNS will reflect the scientific topics of importance in the 1980's. To a greater extent than some of the other sections the neutron measurements are supplementary though that is not to underestimate their importance. To illustrate the general scope of neutron diffraction studies, some current examples are given in fields which will benefit from the SNS.

Phase Transitions

3.49 The structure of several important ferroelectric (and piezoelectric) materials are being intensively studied. Often the structural behaviour is complex; in the $Na_xK_{1-x}NbO_3$ system for example there are twenty different phases, half of them being ferroelectric with a high spontaneous polarization - and the crystallographic study is a necessary first step before an examination of the lattice dynamics. Marked changes in electrical conductivity may be associated with a phase change, and the structural changes occurring with metallic-semiconductor transitions feature in recent reports. Sometimes the transition of interest is one which confers enhanced ionic conductivity and the structural properties of a number of these superionic conductors are being investigated.

3.50 Most of our accurate information about hydrogen bonded structures has been derived from single crystal neutron diffraction studies. Current examples of this work include the clustering of water molecules about H_3O^+, the study of very short hydrogen bonds and the exploration of less common hydrogen bond interactions for example with acceptor phenyl rings. Attempts are also being made to elucidate the detailed hydrogen bonding scheme for molecular crystals which can serve as a model for the packing of side chains in globular proteins. More investigations of this kind should prove rewarding.

Molecular Crystals

3.51 The relative ease with which accurate neutron diffraction experiments can be carried out at low temperatures, coupled with the rapid development of profile analysis techniques applicable to polycrystalline samples, is stimulating considerable interest in the structures of molecular crystals. Generally there are subtle structural changes with variations in temperature and pressure. We can expect this type of study to extend our understanding of intermolecular forces not only in simple plastic crystals or hydrogen bonded systems but also to the large class of ionic compounds (eg hexafluorides) whose behaviour is intermediate between molecular crystals and simple salts. In selected cases the structural determination will be a necessary prelude to a complete dynamical investigation. The extension to more complex molecular systems, eg organometallic compounds, pharmacologically important organic molecules and simple polymeric compounds is readily envisaged but it is frequently impossible to obtain crystals of sufficient size (for present fluxes) or sufficient instrumental resolution (also limited by flux) for powder experiments.

Defect and Disordered Solids

3.52 The increasing emphasis in recent years on the science of materials has created considerable interest in the structure of inorganic solids including ceramics. Many of the important compounds contain light atoms and frequently the high temperature phases demonstrate broad ranges of non-stoichiometry. Some aspects of the ultra microstructure - short range order and clustering of defects - is revealed by diffuse or small angle neutron scattering and by electron microscopy, but the contents of the average unit cell can often only be accurately determined by neutron Bragg diffraction. The main leads to our

understanding of non-stoichiometry in simple compounds and derived from such investigations and have stimulated considerable theoretical effort. Even so only a small number of structural types has been studied over limited concentration and temperature ranges. Non-stoichiometric compounds represent just one example of the very widespread occurrence of order-disorder phenomena in solids, many of which are profitably studied by neutrons.

Intercalation and Surface Solids

3.53 A feature of recent crystallographic studies has been the exploration of host-guest structures with host lattices such as the transition metal dichalcogenides and the clays. The molecular orientation of pyridine in NbS_2 is one recent determination which gives an unexpected result, but the range of inclusion compounds in this class alone is enormous and we still understand little about the host-guest interaction. In addition these layer hosts allow the examination of the properties of two dimensional monolayers, and could serve as templates for 'tailored' chemical reactions.

3.54 As well as the examination of occluded layers, present fluxes just enable - in favourable cases - direct structural investigation of simple gases on high surface area solids (eg graphite). Microcrystalline clusters are observed and in krypton for instance two solid phases are observed on a layer related to the graphite lattice and a compressed phase with Kr-Kr distances close to those in the pure solid. With the SNS the structure of surface layers of relatively low area will be possible.

Electron Distributions

3.55 It is possible from accurate x-ray and neutron data to derive electron distributions.

Magnetic Structure, Moment Distributions and Covalency

3.56 The interaction of the magnetic moment of the neutron with the magnetization density resulting from unpaired electrons in solids has led to the determination of hundred of magnetic structures over the last twenty years. Such investigations will continue to form part of future programmes in magnetic crystallography particularly in connection with novel materials. Much greater

emphasis however will be placed in future on the more detailed information which is available by the use of polarised neutrons. In the past complete magnetization density distributions have been restricted to a limited number of relatively simple systems where large crystals were available. Now we can envisage charting the moment distribution for a much wider variety of compounds which can include free radicals. In alloys the information obtained can relate the observed macroscopic behaviour to atomic properties; thus in YCo_5 which exhibits abnormally high magnetic anisotropy it has been shown that this is associated with the extended spin density of Co (in one of the two Co sites) in the basal plane containing Y atoms. For inorganic salts the often marked aspherical moment distribution is related to the extent and nature of the covalent interaction and the measurements, apart from being able to demonstrate effects such as spin polarisation, provide illuminating guidelines for theoretical studies. These moment density maps are much more revealing than the simple determination of atomic moments which have been common hitherto. The evidence from the ILL suggests that with additional and more intense polarised beam facilities there would be very little restriction on the type of ligand (including complexes) or on the d and f block elements which could be studied.

3.57 Parallel with the greatly extended exploration of unpaired electron distributions there is bound to be a more sophisticated probing of magnetic interactions though a study of magnetic phase diagrams, the influence of pressure and the temperature dependence of correlation lengths in magnetic chains.

MOLECULAR SCIENCES - CHEMISTRY

3.58 The chemistry programme is already very diverse. Neutron scattering investigations provide information about the diffusive and rotational motions of molecular systems (quasi-elastic scattering), molecular energy levels (inelastic scattering), the conformation of polymer molecules and the shape and internal structure of biological particles (small angle scattering) and in addition a number of chemical applications of neutron scattering has already been considered under other headings (Liquids, Structure Determination, etc). Some examples of the current research and likely future developments are outlined in the following sections.

Atomic Diffusion

3.59 The principal area of study here is the important one of hydrogen in metals and in this case the SNS by extending high resolution measurements beyond the first reciprocal lattice points will provide unique information on the diffusion mechanism. There are obvious gains for the study of very low hydrogen concentrations and measurements at low temperature. An important development will be the extension to nuclei with cross-sections small relative to that of the proton. Preliminary experiments have been carried out at the ILL on diffusion in sodium metal and some superionics, but under difficult conditions. The study of carbon in metals or alkali ions in glasses have been proposed as future experiments.

Molecular Crystals

3.60 The study of phonons by coherent scattering from single crystals can give the most definitive information on intermolecular forces. Detailed studies are likely to continue with triple-axis instruments on a reactor, but the SNS has, with the constant-Q spectrometer, a distinct advantage in searching for phonons. This is especially important for investigations of complex molecular crystals and polymers which may have to be carried out without prior calculation of the expected dispersion surfaces and inelastic structure factors. The biggest problem in this area is the growth of suitable single crystals. Higher fluxes will enable smaller crystals to be used, thus allowing a much wider class of materials to be studied.

3.61 The angular part of the intermolecular potential function is of particular importance in many molecular crystals which undergo transitions to orientationally disordered phases. Intramolecular potentials for the rotation of groups within molecules are also of interest. Both these fields can be very effectively studied using both quasi-elastic and inelastic incoherent scattering. Such investigations have already been made for a wide variety of systems, ranging from simple molecules like NH_3, to polymers. In developing this work further, there is a need for

- resolution good enough to separate elastic and quasi-elastic components of the scattering
- a large Q range to provide a sufficiently detailed description of the motion

- instruments of variable resolution and energy scans to cover the wide range of correlation times expected.

All these requirements can be met by the SNS.

Liquid Crystals

3.62 Considerable progress has already been made in the characterisation of the many liquid crystal phases in terms of the self-correlation functions for translational and rotational motion of the molecules. However, little work has been done on the direct study of phase transitions - a problem of general interest. The investigation of collective molecular motions in such systems has hardly begun and is hampered by low inelastic structure factors and the need for fully deuterated single crystal specimens.

Molecular Spectroscopy

3.63 This area is concerned with incoherent inelastic scattering, which, because of the proton's cross-section is essentially the molecular spectroscopy of vibrations involving proton motions. Its development has been hampered by low neutron intensities resulting in data collection rates which are very low in comparison with infra-red spectroscopy, and also by the necessary use of low resolution spectrometers. Increases in flux by a factor of 100 or more thus imply short run times or much improved resolution. This opens up a whole new range of possible applications, for example, in repeated scanning for kinetic experiments where the ease of data collection should be comparable with current infra-red techniques.

3.64 Some systems (eg NH_4ClO_4) show sharp excitations due to tunnelling modes at very low energies, of the order of a few μeV. The availability of a very high resolution spectrometer with a wide energy window will enable the study of a much greater variety of systems. For the first time also, it will be possible to obtain information on rotational and translational dynamics by analysing inelastic vibrational band shapes (cf infra-red and Raman spectroscopy).

High Energy Transfer Vibrational and Electronic Spectroscopy

3.65 With reactor sources there is an upper limit to measurements in energy transfer (generally < 250 meV). The SNS will open up the possibility

of measurements (eg of electron transitions or vibrational harmonics) involving energies greater than 600 meV, but the principal gain will come from the very large increases in flux up to 600 meV.

3.66 The most important application here is the study of hydrogen stretching frequencies which are largely inaccessible on current instruments. In general this implies a study of X-H bonds, frequently in absorbed or occluded phases. Specific instances include:

- The study of the vibrations of hydrogen chemisorbed on a surface, since for many metals the M-H stretching vibration may lie above 200 meV
- The study of metal-hydrogen stretching vibrations in transition metal hydride compounds. It is frequently difficult to identify the stretching frequency in these compounds by conventional optical techniques
- The study of the hydrogen stretching frequency in hydrogen-bonded systems where detailed measurements of the intensity of inelastic neutron scattering will provide information about the potential well in which the hydrogen is moving
- At higher energies the measurements of the relative intensities of overtone modes derived from hydrogen stretching frequencies should enable a much more precise definition of the potential energy curve in X-H bonds. The study of overtone modes in hydrogen in transition metal lattices is also of considerable importance.

3.67 The measurement of crystal field transitions, which up to now has been confined to the f-block compounds, will be possible on the SNS for d-block systems (see also paragraph 3.11).

Surface Chemistry and Other Dilute Systems

3.68 In the study of dilute systems the high counting rates and low background of the SNS will open up exciting areas. The most important field is surface chemistry. Studies already performed on existing sources include:

- the structure and dynamics of physisorbed species
- excitations of hydrogenous molecules chemisorbed on various substrates
- the dynamics of intercalated molecules.

The high effective intensity will make possible experiments with the same accuracy on samples which are up to a thousand times poorer scatterers than

can be currently examined. In favourable cases such as the study of hydrogenous species absorbed on the surface of a crystal with small incoherent scattering, it will be possible to study monolayers down to substrate areas as small as 1 m^2 or less, improving our understanding of catalysis. It will also be possible to study other systems such as multiple water layers on silver iodide crystals, and non hydrogenous species on graphite or concentrated colloids.

3.69 Examples of other dilute systems which will be open to study are:

- lipid bilayers and biological membranes
- matrix isolated unstable species currently studied almost exclusively by infra-red techniques
- species, eg NH_4^+, isolated at low concentration in simple ionic lattices
- hydrogen in metals at low concentration, including metals such as steel where there is considerable technological interest.

Polarisation Analysis

3.70 The major chemical application of polarisation analysis will be the separation of coherent from spin-incoherent scattering. This may be used in two ways:

- the determination of structures of systems which have a large, incoherent background, eg materials which are very difficult to deuterate completely, and biological materials in *in vivo* conditions, ie in light water
- the reverse application - the study of self-correlation function in the presence of a significant coherent signal.

MOLECULAR SCIENCES - POLYMERS

3.71 The application of neutron scattering techniques to polymerised systems has involved the study of rubbers, glasses, partially crystalline materials and polymer solutions. Apart from the intrinsic interest in relationships between chemical structure and physical property for materials composed of long chain molecules there are very important technological applications.

3.72 Neutron scattering has made a unique contribution to the understanding of the structural conformations of polymer molecules and to their molecular dynamics. This is due to the particular wavelength - energy characteristics of neutron beams, and also to the enormous difference in scattering cross-section of hydrogen and deuterium combined with the fact that these isotopes can be substituted for each other with little effect on the general physical properties of the materials. The phenomena of principle interest are outlined below.

Small Angle Neutron Scattering (SANS)

3.73 Most of the work in this field has so far been carried out using D11A at ILL. The work has extended our knowledge of polymer chain conformation into polymers in bulk. Light scattering and small angle x-ray scattering techniques, which hitherto provided all available information, are only applicable to polymer solutions. Neutron scattering results have in the past three years raised Flory's hypotheses on chain conformation in rubbers and glasses (the basis of all theories of amorphous polymers) to the status of fact. Equally important information on the effects of bulk deformations and also of crystallisation on chain conformations is now beginning to emerge.

3.74 The enormous backlog of experiments and pressure on time available at ILL means that an additional SANS instrument even if only of comparable efficiency would be important especially in extending the polymer work to technological problems. However, with count rates improved by an order of magnitude, entirely new experiments on the time dependence of chain conformations (relaxation phenomena) will be possible. This would enable the asymmetry of scattering to be measured as a function of time in a sample undergoing bulk relaxation on a technological time scale. Thus a whole new area of polymer science and technology could be opened up.

Diffraction at Larger Scattering Angles

3.75 The determination of radial distribution functions in the high Q region will give information on local molecular packing in both crystalline and amorphous states. Even more important might be kinetic studies made in this range using a pulsed source while the sample is subjected to relatively low frequency mechanical deformation. The very high epithermal flux should make such kinetic experiments easily possible.

Quasi-Elastic Scattering

3.76 Some of the conformational reorientational motions of polymer chains associated with the onset of main chain motion at the glass-rubber transition, or occurring in polymers in solution, have been investigated by quasi-elastic scattering. In solution, for example, the results support the Zimm model (with hydrodynamic interactions) rather than the Rouse model. The range of interest is $0.01 < Q < 1.0$ Å^{-1} and $\Delta\hbar\omega \sim 1$ μeV. Extension of this work is seriously hindered by pressure of time on ILL instruments and this entirely prevents extension to technological problems. The quasi-elastic instruments proposed would be invaluable in extending the work on rubbers and gels, which in the current situation, will probably be restricted to model systems only.

Inelastic Scattering

3.77 In amorphous systems inelastic neutron scattering has been used mainly to study side-group motions. Measurements on crystalline polymers have involved essentially powders, stretch oriented specimens and in two or three instances specimens approximating to single crystals having macroscopic dimensions. Phonon frequencies have been measured and using perdeuterated samples dispersion curves have been determined. Generally, cold neutron time-of-flight instruments have been used together with triple axis spectrometers for the single crystal work.

3.78 In the single crystal work advance is limited by crystal growth technology rather than by neutron fluxes, but the much greater effective fluxes available with the SNS would make possible the use of significantly smaller crystals. The new source could provide additional capacity for the remaining inelastic work with the possibility of much improved resolution being especially valuable. The pulsed nature of the source would make possible the study of rotational isomerism in relaxing systems, which is important because the rotational isomeric model of the polymer chain is the one which underpins all accepted models concerning the influence of chemical structure.

MOLECULAR SCIENCES - BIOLOGY

3.79 Broadly, the experiments of interest can be classified as follows:

- Studies of single crystals of macromolecules (eg proteins such as myoglobin, lysozyme etc and nucleotides). Here the wavelength range is 1 to 2 Å
- Studies of semi-crystalline macromolecules where Bragg diffraction peaks are observed even though there is inherent disorder (eg fibre diffraction from proteins and DNA, diffraction from collagen, muscle and membranes). Typically 4 to 12 Å neutrons would be involved with these experiments and small angle scattering equipment (eg D11A or D17 at ILL) used
- Neutron quasi-elastic and inelastic scattering studies of the dynamical properties of biological molecules and macromolecular structure
- Small angle scattering studies of separated macromolecules in solution (λ = 4 to 12 Å)
- Kinetic experiments using the pulsed nature of the source (λ = 1 to 12 Å say).

Small Angle Neutron Scattering from Biological Particles in Solution

3.80 These experiments enable the determination of the spherically averaged Patterson function of the macromolecules in contrast against scattering from the solvent. In the absence of crystals of the macromolecules this information is vital to the determination of the low resolution structure and the technique requires that the solvent scattering-length density (usually water) is changed by choosing different D_2O/H_2O mixtures for the solvent and by choosing different small molecule concentrations. Because of the coherent elastic scattering-length-density difference between D_2O and H_2O a variety of contrast conditions are achieved and one can obtain 'fundamental scattering functions' which are related to:

- the outer profile of the particle
- the internal structure
- a 'cross' term of the inner and outer structures
- the distribution of D/H sites within the particle.

Measurements at low angles, in the so-called Guinier region, yield information on the spherically symmetrical component of the scattering-length

density distribution within the macromolecules, but there is interest developing in higher angle measurements, where the deviations from spherical symmetry can be determined and where the details of the internal structure of the particles can be seen.

3.81 Deuteration of the macromolecules at non-labile sites permits the determination of the position of the deuterated sites within the structure. One technique, the so-called triangulation method, involves accurate measurements of differences of scattered intensity as a function of Q for two solutions. The first solution is a mixture of ribosome subunits with both proteins deuterated and both proteins protonated. The second solution is a mixture of ribosome subunits containing the first protein protonated and the second deuterated and subunits with the first protein deuterated and the second protonated. An interference function in the measured difference of intensities as a function of Q gives information about the distance between the scattering length centres of the proteins and a distribution of length between extreme surfaces of the two proteins. By obtaining information on a large number of proteins in the ribosome subunits it should be possible to determine the shape of the proteins. Very high statistics for the scattered neutrons are necessary and the ribosome experiments will take several years to complete so that the value of the increase in flux is obvious.

3.82 In studying dispersions of biological membranes and membrane components in solution the neutron scattered intensity falls off more rapidly than for globular particles in solution. In this case again therefore, higher neutron fluxes provide an important advantage.

Small Angle Studies of Bragg Diffraction in Semi-Crystalline Biological Specimens

3.83 Neutron studies of small-angle Bragg peaks in specimens such as muscle, collagen, biological membranes, are revealing much information on the intact systems and on changes on activating a given system. For example, differences between contracted and relaxed muscle, and between retinal membranes in the dark and activated by light, may be studied. It is also possible to derive information on how the various parts of a structure contribute to the Fourier harmonic corresponding to the amplitude of a given Bragg peak. Many of these specimens are quite highly oriented and therefore information is available at particular Q values. Clearly

information would be lost on spherically averaging the neutron data from an area detector (in an attempt to improve statistics) so that better count rates are a great help in studying the details of a particular Bragg peak.

Studies of Single Crystals of Macromolecules

3.84 Studies of crystals of biological macromolecules using neutrons are in progress both at the ILL and at Brookhaven, and have already provided useful information about hydrogen bonding and the detailed structures of the macromolecular building blocks of amino acids and nucleotides. If it were possible (by virtue of a very high flux of neutrons of $\sim$ 1.5 Å wavelength) to carry out a complete structure determination in one or two weeks, one could look in fine detail at D/H exchange at highly localised sites in the structure. Work at high pressures with cooled samples will reduce the thermal motion in the crystals and enable the full potential of the high resolution capabilities of neutrons to be obtained. These experiments will clearly gain from the high flux of neutrons at 1.5 Å wavelength which would be available from the SNS. The disadvantage of these experiments is that the measurements are not carried out *in vivo*, but there is the potential for a wealth of information of biological importance.

Neutron Quasi-Elastic and Inelastic Scattering

3.85 In biological studies this work has investigated the normal modes of vibration and force constants of poly-α-amino acids. At present the studies have concentrated on polyglycine (the simplest amino acid). More complex systems are now beginning to be investigated. These neutron studies supplement infra-red and Raman studies because they are most sensitive to displacements of hydrogen atoms in vibrational modes and are not restricted by optical selection rules. In this area the possibility of performing an energy analysis in conjunction with small-angle scattering is very attractive.

Kinetic Experiments Using the Pulsed Nature of the New Source

3.86 There is a developing interest in the dynamical aspects of biological processes, eg the kinetics of enzyme action, the rates of H $\rightleftarrows$ D exchange within a structure, changes of structure with electrical signals, magnetic fields, exposure to light, temperature, pressure etc.. These are all studies which will be stimulated by the availability of the SNS.

3.87 A wide diversity of instruments has been considered for carrying out research at pulsed sources. In Appendix I a comprehensive list of 26 instruments has been compiled, from which it will be possible to select the most suitable instruments for the SNS to satisfy the scientific programme envisaged. Present indications are that 12-15 instruments could provide a balanced inventory within the scope of the project. Fourteen basic types of instrument are illustrated in Table 3.1, and these could cover almost all the scientific developments proposed. The precise definition of the instruments to be built and their priority will be determined after an up to date reassessment of the scientific programme and in the light of experience gained on the new Harwell linac. During the planning stage instruments of advanced conception to match novel applications are also likely to emerge.

TABLE 3.1

INSTRUMENTS FOR THE SNS : AMBIENT TEMPERATURE MODERATOR

Instrument	Specification	Field
I. Single Crystal Diffractometer	$0.3 < \lambda < 1.5$ Å $\frac{\Delta Q}{Q} \sim 0.03$ Polarized incident beam option	Single crystal structure determination. Magnetisation density distributions. Structural investigations as a function of temperature, pressure, etc..
II. (a) High Intensity, Medium Resolution Powder Diffractometer	$Q > 2.5$ Å^{-1} ($\phi = 170^{\circ}$) $\frac{\Delta Q}{Q} \sim 3\ 10^{-3}$ $Q > 0.6$ Å^{-1} ($\phi = 30^{\circ}$)	Structural determination using powder samples. Kinetic processes, eg diffusion of gases into solids.
(b) High Pressure Spectrometer	$0.3 < Q < 100$ Å^{-1} Pressures up to 50 kbar	Pressure dependence of structure factors of fluids and amorphous solids. Triplet correlation functions.
III. (a) Elastic Discrimination Spectrometer	$1 < Q < 25$ Å^{-1} $\frac{\Delta Q}{Q} \sim 0.02$	Simultaneous measurement of elastic and total diffraction patterns to allow separation of elastic and inelastic scattering to study the eccentricity of atomic thermal vibration tensors. Structure factors of fluids and amorphous solids.
(b) Total Scattering Spectrometer	$0.3 < Q < 100$ Å^{-1}	
IV. Very High Energy Transfer Spectrometer	$\hbar\omega \sim 1$ eV $\frac{\Delta\hbar\omega}{\hbar\omega} \sim 0.1$ $Q < 4$ Å^{-1}	Electronic excitations: Band energies in semiconductors. Valence fluctuations. Crystal field levels in optically opaque transition metal compounds.
V. (a) High Energy Transfer Chopper Spectrometer	$100 < \hbar\omega < 600$ meV $\Delta\hbar\omega \sim 5$ meV $\Delta Q \sim 0.1$ Å^{-1} low Q bank	Vibrational spectroscopy, in particular the study of hydrogen modes on surfaces, in H-bonded systems and in metal hydride complexes. Phonons, magnons, crystal fields, vibrational modes and liquid dynamics.
(b) High Energy, High Momentum Transfer Spectrometer	$Q_{max} \sim 30$ Å^{-1} ($\phi = 150^{\circ}$)	Measurements on the dynamics of the helium liquids. High Q dependence of $S(Q,\omega)$ for amorphous materials.

VI. (a) Total Scattering Polarization Analysis Spectrometer	Q up to 20 $\AA^{-1}$, with spin analysis of scattered beam	Determination of elastic spin-dependent cross-sections. Structure factor measurements in presence of spin-incoherent scattering.
(b) Inelastic Polarization Analysis Spectrometer	$0 < \hbar\omega < 200$ meV $\frac{\Delta\hbar\omega}{\hbar\omega} \sim 0.01$ Spin selection of both incident and scattered beams	Spin dynamics. Separation of magnon and phonon scattering. Measurements of the dynamical structure factors $S(\underline{Q},\omega)$ and $S_s(\underline{Q},\omega)$ for spin-incoherent scatterers.
VII. Moderate Energy Transfer Chopper Spectrometer	$\hbar\omega < 100$ meV $\frac{\Delta\hbar\omega}{\hbar\omega} \sim 0.02$ low Q bank required $\Delta Q \sim 0.1$ $\AA^{-1}$	Measurements on the dynamical structure factors of liquids. Conventional inelastic spectroscopy. Very low angle bank required for observing inelastic modes in liquids on the energy gain side - the 'small Q method'. Phonon, magnon and crystal field studies.

INSTRUMENTS FOR THE SNS : COLD MODERATOR

Instrument	Specification	Field
VIII. High Resolution Powder Diffractometer	$Q > 6$ $\AA^{-1}$ ($\phi = 170^\circ$) $Q > 0.8$ $\AA^{-1}$ ($\phi = 15^\circ$) $\frac{\Delta Q}{Q} = 0.001$	Resolution of closely spaced peaks in powder diffraction profiles of complex crystals with large unit cells.
IX. (a) Very low Q Spectrometer (SANS)	$0.005 < Q < 1$ $\AA^{-1}$ $\frac{\Delta Q}{Q} \sim 0.1$ $4 < \lambda < 12$ $\AA$	'Small Angle Neutron Scattering': studies of polymers and biological systems. Defects and structural periodicities on the scale ~ 100 $\AA$.
(b) Elastic Diffuse Spectrometer	Polarised incident beam option	Effects of doping, alloying, heat treating and irradiating condensed systems. Magnetic defects.
X. Total Scattering Spectrometer	$0.3 < Q < 100$ $\AA^{-1}$	Structure factors of fluids and amorphous solids. High resolution at low Q.
XI. Constant Q Spectrometer	$10 < \hbar\omega < 200$ meV $\frac{\Delta\hbar\omega}{\hbar\omega} \sim 0.05$ $3 < Q < 6$ $\AA^{-1}$	Triple axis analogue: scans in energy through $(\underline{Q},\omega)$ space at constant $\underline{Q}$. Coherent excitations.
XII. Time-of-flight MARX Spectrometer	$0 < \hbar\omega < 50$ meV $\frac{\Delta\hbar\omega}{\hbar\omega} \sim 0.02$ $\frac{\Delta Q}{Q} \sim 0.1$	Conventional inelastic scattering. Quasi-elastic scattering at good resolution and high Q, diffusive modes of plastic and liquid crystals, hydrogen in metals, etc.. Intermolecular modes of crystals, magnetic crystal field levels.
XIII. Long Wavelength Chopper Spectrometer	$4 < \lambda < 10$ $\AA$ $\Delta\hbar\omega/E$ comparable to that of IN5	High resolution quasi-elastic studies. Low energy inelastic modes (< 20 meV) observable in neutron energy gain.
XIV. White Beam Backscattering Spectrometer (L = 25 m)	$\Delta\lambda = 3$ $\AA$ Quasi-elastic mode: $\Delta\hbar\omega \sim 15$ μeV $-1000 < \hbar\omega < 1000$ μeV Inelastic mode: scan up to 100 meV with $\frac{\Delta\hbar\omega}{E} < 8\ 10^{-3}$	Very high resolution quasi-elastic studies. Slow diffusive processes. Tunnelling transitions. Inelastic band shapes.

OTHER USES OF THE FACILITY

3.88 The SNS has been designed as a high intensity pulsed neutron source for thermal neutron scattering experiments in condensed matter research. However the 800 MeV proton synchrotron, a machine comparable with the best pion factories of the world, would also be a source for the production of intense fluxes of other elementary particles. The provision of beams of these particles, primarily pions and muons, could find use over a wide range of multi-disciplinary studies which could include:

- studies in solid state physics and chemistry using muon spin rotation techniques
- chemical analysis and structure using μ-mesic atomic x-rays
- elementary particle physics
- nuclear structure studies
- biomedical studies and pion therapy
- isotope production
- radiation damage studies

Further information on these possible applications is given in Appendix I, where consideration is also given to the provision of a storage ring facility which, by creating smooth spill conditions, would considerably enhance the scope of many of these investigations. These possibilities are not part of the present Proposal.

CHAPTER 4. NEUTRON SOURCES

INTRODUCTION

4.1 We now return in this chapter to the subject of neutron sources and review the considerations which have led us to conclude that provision of the spallation neutron source at the Rutherford Laboratory is the best way to realise a significant flux increase. An outline of the proposed facility itself is given in Chapter 5.

4.2 Most neutron scattering applications use neutron beams from steady state nuclear reactors. Starting with the first experiments at Oak Ridge in 1946 research instruments have been installed on many reactors built for other applications such as materials testing, including the UKAEA reactors, DIDO and PLUTO at AERE, Harwell. The most powerful reactors available for condensed matter research today are listed in Table 4.1.

Table 4.1 High Flux Reactors

Reactor	Location	Power MW	Thermal Flux $n\ cm^{-2}\ s^{-1}$	First Operation
HFR	ILL-Grenoble	57	1.5×10^{15}	1972
HFIR	Oak Ridge	100	1.5×10^{15}	1967
HFBR	Brookhaven	40	0.7×10^{15}	1965

4.3 The HFR and HFBR were designed primarily as beam reactors for condensed matter studies; HFIR was designed mainly for isotope production. The standard arrangement allows neutrons from the high flux region of the moderator volume to pass to the experiment by beam tubes piercing the reactor vessel and radiation shielding. The neutron spectrum (white beam) corresponds to the Maxwellian velocity distribution at the moderator temperature and can be enhanced in the low and high velocity regions by the provision of special cold and hot sources.

4.4 The instruments on steady state sources commonly require monochromatic neutrons at the sample under investigation. They are selected from the white beam by monochromating crystals or by mechanical choppers; in either case the selection process must discard nearly all of the incident neutron flux.

4.5 Many neutron scattering experiments can be done in principle using an intrinsically pulsed white beam and the time-of-flight technique, instead of a monochromated continuous beam. Roughly speaking it is then the maximum neutron flux in the pulse which is the relevant criterion rather than the time-averaged flux. An important advantage of the pulsed source when it can be used in this way is the greatly reduced mean power to achieve the same effective flux as a steady state reactor.

4.6 Practical pulsed sources can be either pulsed reactors or accelerator based systems in which the burst of fast (MeV) primary neutrons has first to be moderated in, for example, a block of polyethylene whose surface(s) form the effective source for the scattering experiment. Ideally the pulse lengths of the moderated neutrons should not exceed a few tens of microseconds so that the required energy resolution can readily be obtained.

4.7 Relevant experience with pulsed reactors is limited to the Soviet Union where a small (30 kW) system (IBR-30) has been working since 1969; a much larger system (4 MW, IBR-2) is now under construction there. In the UK considerable experience has been obtained using the condensed matter cell on the AERE Harwell linear electron accelerator (linac) and there is similar experience in North America and Japan; the basic fast neutron production process involved is the $(e\gamma)$, (γn) reaction in a heavy target of, for example, tungsten or uranium. Proton accelerators can produce fast

neutrons by nuclear reactions in heavy elements (spallation reactions) and although not yet in use as 'production' sources, proton synchrotrons of energy around 1 GeV are now generally regarded as the best candidates for the next stage of source development.

POSSIBLE FUTURE SOURCES

4.8 Since 1973 the NBRC has kept the 'next generation source' under review with the NBRU actively considering ways to achieve an effective improvement in flux of at least 10 in comparison with the best available today. In terms of a steady state source this means at least 10^{16} n cm^{-2} s^{-1}; for a pulsed source the criterion is not so easily described and its merits must be examined by careful evaluation of 'typical' experiments, taking account of the neutron output characteristics of the source in question.

4.9 Three candidates have been carefully considered, namely:

- steady state reactors
- pulsed reactors
- accelerator systems, with and without neutron boosters

Fusion neutron sources, employing either magnetically or inertially (laser driven) confined plasmas, are much too far from practical realisation to merit serious consideration today.

Reactors

4.10 Reactor studies at Oak Ridge have suggested that pressing solid fuel technology to the limit might yield a gain of 5 in steady state performance. A flowing liquid fuel system, studied at Los Alamos, is in principle capable of attaining at least 10^{16} n cm^{-2} s^{-1}. However, such systems would require considerable development programmes to establish their design parameters and to estimate costs but the capital cost would be at least £100M and operating costs would be proportionately higher than present day levels, probably greater than £10M per annum. Problems in materials technology, radiation damage and safety would be severe and would inhibit the attainment of high operational efficiency.

4.11 The IBR-2 pulsed reactor under construction at Dubna (completion $\sim$ 1977) is designed to produce a peak thermal flux of at least 10^{16} n cm^{-2}s^{-1} at peak power of 7700 MW when operating at 5 pulses per second with a power pulse halfwidth of 90 μs. It is unlikely that a pulsed reactor like IBR-2 would be much cheaper to build than an advanced steady state reactor of comparable performance, and although there should soon be useful operating experience in the USSR when IBR-2 is working, it is doubtful if the new technology could be readily transferred to Western Europe, implying the need for an independent development programme before such a project could begin. Also, the safety aspects would constitute a formidable obstacle to obtaining a nuclear site licence for such a research installation in an SRC laboratory. Finally, the inherently long power pulse is a distinct disadvantage.

4.12 Thus reactors, either steady state or pulsed, do not provide an acceptable solution. They would be far too costly, the technology is not adequately established, and in any case, they could barely offer the flux gains we are seeking.

Accelerator based systems

4.13 Particle accelerators are well established as neutron sources for many applications and continue to be considered for new requirements. Processes and parameters relevant to our interest are given in Table 4.2.

Table 4.2 Neutron production processes

Process	neutron/incident particle	target energy/neutron
$(e^-\gamma)$, (γn) in heavy element	$\sim 10^{-2}$/electron (30 MeV)	$\sim$ 1500 MeV
(dn) in tritium	$\sim 10^{-4}$/deuteron (400 keV)	$\sim$ 3000 MeV
(dn) in lithium	$\sim 3\times10^{-2}$/deuteron (30 MeV)	$\sim$ 1000 MeV
proton spallation in heavy element	$\sim$ 30/proton (800 MeV, ^{238}U target)	$\sim$ 55 MeV
(fission)	($\sim$ 1/fission)	($\sim$ 200 MeV/fission)

4.14 Amongst the accelerator options, proton spallation is clearly the most prolific and most efficient in terms of target power although to draw overall conclusions it is necessary to examine the details of the various systems

and to compare their costs. For instance, on the basis of a Canadian proposal (the unadopted ING project) a continuously rated proton spallation source producing a thermal neutron flux of 10^{16} n cm^{-2} s^{-1} would cost more than £100M.

4.15 For pulsed neutron sources however accelerators command special attention, for the following reasons. High intensity fast neutron bursts can be generated without excessive target heating; pulsing is straightforward (sometimes inherent); the pulse length and repetition rate can be varied within limits; the pulse length of the fast neutron burst is not significant in determining the moderated neutron pulse lengths; high performance can be realised using state of the art technology; operating costs are much less than those of reactors and there are no special problems of nuclear safety.

4.16 Since 1974 therefore, the Rutherford Laboratory has concentrated study on the use of electron linacs and proton synchrotrons for future neutron sources including the possibility of using a fission fuelled booster to increase the fast neutron production from the accelerator target.

PULSED SOURCES USING ELECTRON AND PROTON ACCELERATORS

4.17 Table 4.3 compares various pulsed sources, present or future, that can be realistically considered at this time. Neutron performances are quoted as the time average of fast neutrons produced, a valid criterion for comparison since in all cases the primary neutron burst length is much less than that of the moderated pulse.

4.18 The present Harwell electron linac (Table 2.3, line 1) has a well established condensed matter facility which is exploited in the SRC/AERE joint programme and has demonstrated the advantages conferred by the special features of such pulsed sources. Even at this very modest level of performance this facility is competitive with a high flux reactor for some limited applications. The new Harwell linac with 10 times the beam power will extend this range of usefulness.

4.19 The performance of an electron linac system must ultimately be determined by target dissipation capability. This is likely to be limited to

Table 4.3 Neutron sources based on electron and proton accelerators

Facility	Beam intensity or average target power; proton/pulse or kW	Pulse rate s^{-1}	Particle, energy	Target	Time averaged intensity at target n s^{-1}	Comments
1.Present Harwell electron linac	5 kW	200	e^-, 30 MeV	^{238}U	2×10^{13}	Closing December 1976
2.New Harwell electron linac	45 kW	150	e^-, 60 MeV	^{238}U	2×10^{14}	Under construction. Operational in 1978
3.Oak Ridge electron linac	65 kW	500	e^-, 140 MeV	Ta	1×10^{14}	In operation. Booster study 1975
4.Purpose built e^- linac	450 kW	150	e^-, 450 MeV	^{238}U	2×10^{15}	Estimated capital cost ∿ £12M including instruments
5.Los Alamos weapons neutron research facility	1×10^{12}	120	p, 800 MeV	W	1×10^{15}	Uses protons from Los Alamos Meson Facility, LAMPF
6.KENS	6×10^{11}	15	p, 500 MeV	^{238}U	2×10^{14}	Japanese project to use injector synchrotron of KEK proton HEP facility
7.Optimised proton synchrotron + spallation target	2.5×10^{13}	50	p, 800 MeV	^{238}U	4×10^{16}	Estimated capital cost of accelerator + instruments on green field site - approx. £30M (Argonne IPNS estimated at $70M) Estimated cost if built at Rutherford Laboratory (SNS) using existing Nimrod plant and buildings and NINA power supply, £10M

the region of 450 kW indicating a maximum time average production rate of $\sim 2 \times 10^{15}$ n s^{-1} from a uranium target. Such an installation with buildings and instrumentation would cost about £12M (Table 4.3, line 4).

4.20 A static booster (operating below criticality at constant reactivity) using uranium fuel can readily provide a gain of 10; such a booster has been in use at AERE for many years, although not on the condensed matter cell. Plutonium boosters could have some advantages including that of a higher gain factor. It may be noted that a plutonium static booster added to the new Harwell linac would raise its output to a level of about 4×10^{15} n s^{-1} for an additional cost including instruments of about £6M.

4.21 Gains of several hundred would be possible with dynamic boosters, in which the reactivity is varied so as to exceed criticality for delayed neutrons, but not for prompt neutrons, with the reactivity peak occurring in phase with the primary neutron burst; the device is very similar to a repetitively pulsed reactor. A superbooster of this type was considered by the UKAEA (in consultation with University representatives) in 1965 but rejected because insufficient was known of the technology and on broad scientific grounds. Outside the Soviet Union dynamic booster technology is still not established and the safety implications remain to be examined fully.

4.22 The much smaller target energy generated by protons means that a target heat production rate similar to that considered as a limit for the electron linac ($\sim$ 400 kW) will allow fast neutron yields more than 10 times larger. This advantage has stimulated a number of proposals. In addition to the present UK proposal (Table 4.3, line 7), there is one from the Argonne National Laboratory for a closely similar design but on a green field site (IPNS, costed at $70M), and a more modest proposal in Japan (Table 4.3, line 6).

4.23 Design data for IPNS have been based partly on studies using an existing injector synchrotron at Argonne and the project has been the subject of two study workshops (1973 and 1975) involving potential users in the United States and invited visitors from Europe and Japan. The Argonne proposals have been widely supported and approval to proceed is being sought.

4.24 The choice of 800 MeV primary proton energy in both the IPNS and the SNS designs arises from the optimisation of neutron intensity at the moderator surfaces and from cost considerations. Neutron yield increases rather linearly with incident proton energy, above about 200 MeV, and increases with increasing target mass number. In target nuclei having a low fission threshold energy such as ^{238}U, a significant contribution comes from fissions. Thus protons of several hundred MeV and heavy-element targets are desirable. Proton energies greater than about 1 GeV are not advantageous because of their longer range and consequent extended neutron source distribution. About 90% of the neutrons are from an evaporation spectrum (similar to that of fission neutrons) of average energy 3 MeV, while the remaining 10% result from the nuclear cascade in a distribution extending upward to the incident proton energy. These high energy neutrons make necessary a heavy shield, as much as 5 m of steel.

4.25 The SNS will be about 100 times more powerful than the new Harwell linac and over 10 times that of the best purpose built electron linac. In cost per neutron it is very considerably cheaper than any alternative and at an estimated cost of £10M for the new components, including instruments, is strikingly economic.

4.26 Although provision of the SNS is clearly the best single step to take now to achieve higher neutron fluxes, the eventual addition of a neutron booster should be recognised as offering important development potential for the longer term.

CHAPTER 5. OUTLINE OF SPALLATION NEUTRON SOURCE PROJECT

DESCRIPTION OF THE FACILITY

5.1 The main features of the proposed facility will be a high repetition rate, high intensity, 800 MeV proton synchrotron, using as injector a 70 MeV H^- RF linear accelerator, and delivering the high energy protons to a uranium spallation target located within a substantial shielding blockhouse round which the neutron scattering experiments are arranged. Table 4.1 lists the main parameters; Fig. 5.1 shows a schematic layout. The installations are described in detail in Appendix II.

Table 5.1 SNS main parameters

Mean radius of synchrotron	26.0 m
Long straight length	9.19 m
Injection energy	70 MeV
Maximum energy	800 MeV
Injection scheme	H^-, charge exchange
Repetition rate	53 Hz
Frequency range of RF system	~~0.67–1.54 MHz~~
Harmonic number of RF system	~~1~~ 2
Design intensity	2.5×10^{13} protons per pulse
Duration of extracted proton pulse	0.22 μs
Neutron production, time average, uranium target	4×10^{16} n s^{-1}
Target power	350 kW

5.2 The machine parameters have been chosen so as to optimise the neutron performance while pressing accelerator technology close to reasonable practical limits. An output energy of 800 MeV is about optimum for neutron

production intensity from the moderators, and a magnet ring for this energy with suitable spaces in which to fit the necessary injection and ejection devices and the RF accelerating cavities, fits conveniently inside the existing Nimrod magnet building. The synchrotron ring will completely replace the existing Nimrod magnet ring.

5.3 A repetition rate near 50 Hz is about the maximum for an economic design of the laminated synchrotron magnets, their power supply and the RF accelerating system; it also enables the existing NINA power supply to be used. Combined with the space charge limited intensity of 2.5×10^{13} protons per pulse, such a repetition rate yields a high time averaged neutron produciton rate and it is compatible with the pulse interval needed to avoid frame overlap in the experiments.

5.4 The injector will be the recently commissioned 70 MeV proton linear accelerator; its pre-injector will need modifying to supply the required current of H^- ions and the modulators supplying the RF circuits will have to be uprated from 1 Hz to 53 Hz operation. H^- injection into the synchrotron using charge exchange stripping will ensure that the accumulated beam before acceleration is limited only by space charge effects.

5.5 To obtain an even higher proton intensity per burst would require a higher injection energy and/or a larger magnet aperture with further consequences for many other parts of the system such as RF cavities and extraction magents. There are strong technical and financial deterrents in this direction.

5.6 Single turn extraction is used to give a proton burst of 0.22 μs duration, so short that the corresponding primary neutron burst is not significant in determining the moderated neutron pulse lengths. Standard beam transport techniques are used to direct the proton beam on to the target in the neutron cell. Fig. 5.1 shows the beam horizontal at the target. A vertical proton beam may facilitate geometrical optimisation of the neutron beams and in principle it could be provided but with some fairly strong cost penalties which need further examination.

5.7 It is proposed to use a target of ^{238}U, which, through the contribution of fission neutrons, has about double the neutron yield of non-

fissionable heavy metals. Target dissipation will be 350 kW. The target itself will be 30cm long and 8x8cm^2 in cross-section and can be conveniently water cooled by arranging it in the form of plates, clad in Zircaloy-2 to provide a corrosion and contamination barrier. Dimensional changes in the uranium plates caused by irradiation effects will limit the lifetime of individual target assemblies. The minimum lifetime is expected to be about 10 weeks and by careful attention to the design, target life might be extended to 25 weeks. In any case the target must be regarded as a consumable item.

5.8 Adjacent to the target will be moderator/reflector assemblies operating at ambient and below ambient temperatures, and arranged geometrically with respect to the target and beam tubes in the shield so that fast neutrons from the target cannot reach a sample directly. A possible arrangement provides for 2 moderators serving 12 beam tubes. This will accommodate the optimised selection of instruments given in Chapter 3, Table 3.1. If required guide tubes up to 75 m long can be arranged conveniently on ground at the level of Hall 3; longer ones could be provided by excavating some of the nearby ground. Optimisation of target, moderator, reflector, shield and experiment geometries is an important activity which will be carried out during the design phase and initial period of machine construction.

5.9 It is proposed to construct only one target station initially, in Hall 3, but a second could be added later in Hall 1, or Hall 1 could be used for the applications other than neutron scattering mentioned in Chapter 3 and Appendix I.

5.10 The SNS beam current is significantly higher than that so far achieved in any cyclic accelerator. While this performance is realisable essentially within state of the art machine technology, attention will be needed to confine beam loss to chosen locations in the synchrotron ring and the target station so as to localise the major incidence of radiation effects. Active handling arrangements will be provided where necessary.

5.11 A sophisticated control system will be provided drawing extensively on experience in the development and operation of the CERN SPS. This will be an important feature for the safe and efficient operation of the facility.

fissionable heavy metals. Target dissipation will be 350 kW. The target itself will be 30cm long and 8x8cm^2 in cross-section and can be conveniently water cooled by arranging it in the form of plates, clad in Zircaloy-2 to provide a corrosion and contamination barrier. Dimensional changes in the uranium plates caused by irradiation effects will limit the lifetime of individual target assemblies. The minimum lifetime is expected to be about 10 weeks and by careful attention to the design, target life might be extended to 25 weeks. In any case the target must be regarded as a consumable item.

5.8 Adjacent to the target will be moderator/reflector assemblies operating at ambient and below ambient temperatures, and arranged geometrically with respect to the target and beam tubes in the shield so that fast neutrons from the target cannot reach a sample directly. A possible arrangement provides for 2 moderators serving 12 beam tubes. This will accommodate the optimised selection of instruments given in Chapter 3, Table 3.1. If required guide tubes up to 75 m long can be arranged conveniently on ground at the level of Hall 3; longer ones could be provided by excavating some of the nearby ground. Optimisation of target, moderator, reflector, shield and experiment geometries is an important activity which will be carried out during the design phase and initial period of machine construction.

5.9 It is proposed to construct only one target station initially, in Hall 3, but a second could be added later in Hall 1, or Hall 1 could be used for the applications other than neutron scattering mentioned in Chapter 3 and Appendix I.

5.10 The SNS beam current is significantly higher than that so far achieved in any cyclic accelerator. While this performance is realisable essentially within state of the art machine technology, attention will be needed to confine beam loss to chosen locations in the synchrotron ring and the target station so as to localise the major incidence of radiation effects. Active handling arrangements will be provided where necessary.

5.11 A sophisticated control system will be provided drawing extensively on experience in the development and operation of the CERN SPS. This will be an important feature for the safe and efficient operation of the facility.

NEUTRON PERFORMANCE PARAMETERS OF SNS

5.12 In order to make meaningful assessments of potential scientific applications of the spallation source, it is necessary to know the spectral and temporal characteristics of the neutron burst as well as the gross features such as mean intensity, repetition rate, moderator dimensions and experiment geometry. The information summarised below in paragraphs 5.13-5.19 is treated in more detail in Appendix I.

5.13 Fast neutrons may be moderated to useful energies (ie to energies around and below 1 eV) by interaction with a few centimetres of a light material of high scattering cross-section, in practice hydrogenous. The moderated spectrum has an approximately 1/E dependence in the neutron slowing-down region, corresponding to E greater than $\sim 5\ k_B T_{eff}$ (where k_B is Boltzmann's constant and T_{eff} is the effective temperature of the moderator); at lower energies the spectrum assumes the form of a Maxwellian distribution characteristic of the effective moderator temperature.

5.14 The neutron yield from the moderator surface for an optimized target/reflector/moderator configuration has been estimated from published experimental data to be

$$\phi(E) = \frac{10^{13}}{E}\ n\ eV^{-1}\ ster^{-1}\ s^{-1}$$

in the slowing-down region of the spectrum. The time-averaged intensity at a specimen distance L from the moderator within an energy window ΔE at E is then given by

$$I(E)\ \Delta E = \frac{10^{13}}{L^2}\ \frac{1}{E}\ \Delta E\ \ n\ cm^{-2}\ s^{-1}$$

5.15 In the slowing-down region the pulse shape is relatively narrow and the full width at half maximum may be approximated by the empirical expression

$$\Delta t(\mu s) = 2/\sqrt{E(eV)}$$

5.16 The slowing-down region of the spectrum may be extended by reducing the moderator temperature, which moves the Maxwellian portion of the spectrum to lower energies and maintains the short slowing-down pulse width. For example:

Moderator	Temperature	kT_{eff}	1/E Range
$(CH_2)_n$, H_2O	300K	$\sim$ 35 meV	> 200 meV
CH_4, NH_3	77K	$\sim$ 11 meV	> 50 meV
CH_4, H_2	20K	$\sim$ 3 meV	> 15 meV

Thus Δt is 2 μs for 1 eV neutrons from an ambient moderator, and only 13 μs at 25 meV if a 20K moderator is used.

5.17 In the Maxwellian region (E less than $\sim 2\ k_B T_{eff}$) the pulse width broadens considerably, and the pulse shape is asymmetric and cannot be expressed in a simple analytic form. The width depends on the neutron energy, the moderator material, temperature and configuration, and may be broadened by some moderation within reflectors.

5.18 Estimates of beam intensities from slab moderators (polyethylene and methane) at different temperatures are illustrated in Figure 5.2. The spectra have been normalised to unity at 1 eV, an energy which is in the slowing-down region; F(E) is the ratio of the flux per unit energy at an energy E to that at 1 eV. The time averaged neutron intensity at a specimen at a distance L from the moderator within an energy window ΔE at an energy E is thus

$$I(E)\ \Delta E = \frac{10^{13}}{L^2}\ F(E)\ \Delta E\ \text{n cm}^{-2}\ \text{s}^{-1}$$

5.19 The above estimates have been based on a diversity of published experimental data, and more experimental work and computations will be needed to define closely the characteristics of SNS, particularly for energies in the Maxwellian region for any moderator.

COSTS

5.20 Striking economies are possible in the overall cost of the proposed facility because of the extent to which use can be made of existing plant and buildings, notably, the new Nimrod injector, Nimrod beam handling magnets and quadrupoles, vacuum and control equipment, the extensive service network, steel and concrete shielding, and also the NINA power supply. No new buildings will be required.

5.21 The estimated capital cost of the new accelerator components, target station and neutron scattering instruments is approximately £10M. The cost would be about three times greater were it not for the economies outlined above.

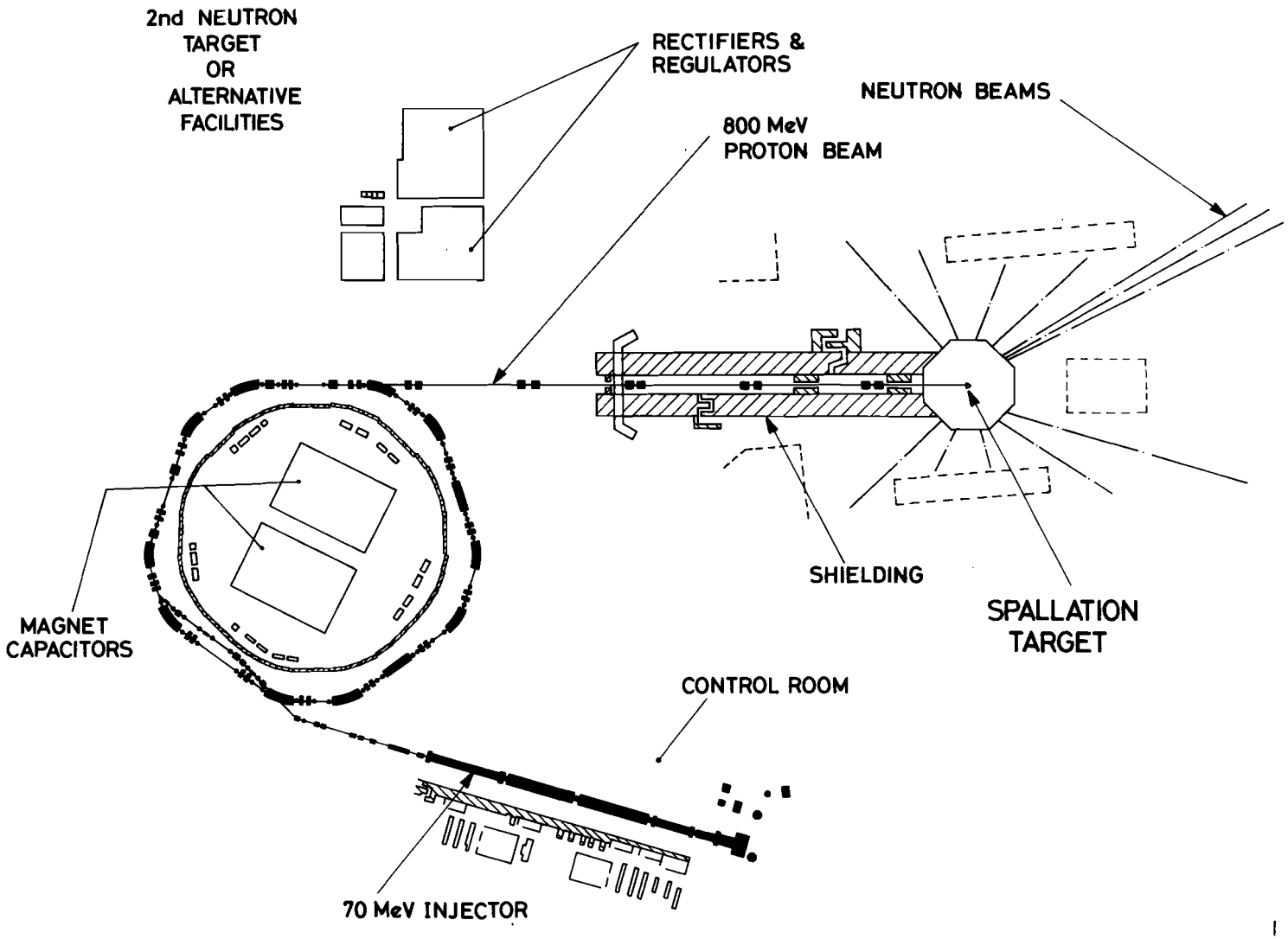

FIG.5.1 LAYOUT OF SNS FACILITY

FIG.2.1 LAYOUT OF SNS FACILITY

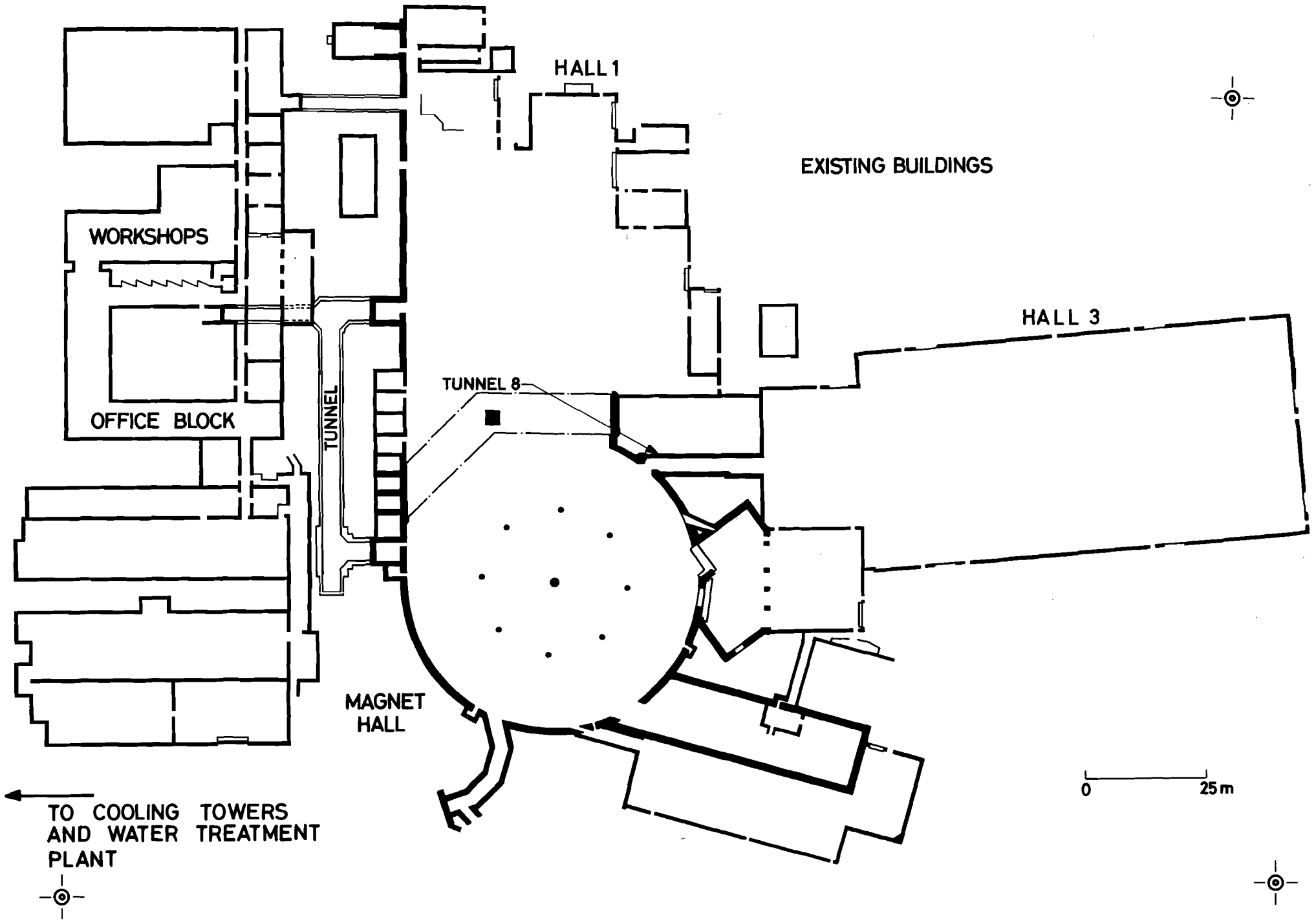
HALL 1
EXISTING BUILDINGS
WORKSHOPS
HALL 3
TUNNEL 8
OFFICE BLOCK
TUNNEL
MAGNET HALL
0
25 m
TO COOLING TOWERS AND WATER TREATMENT PLANT

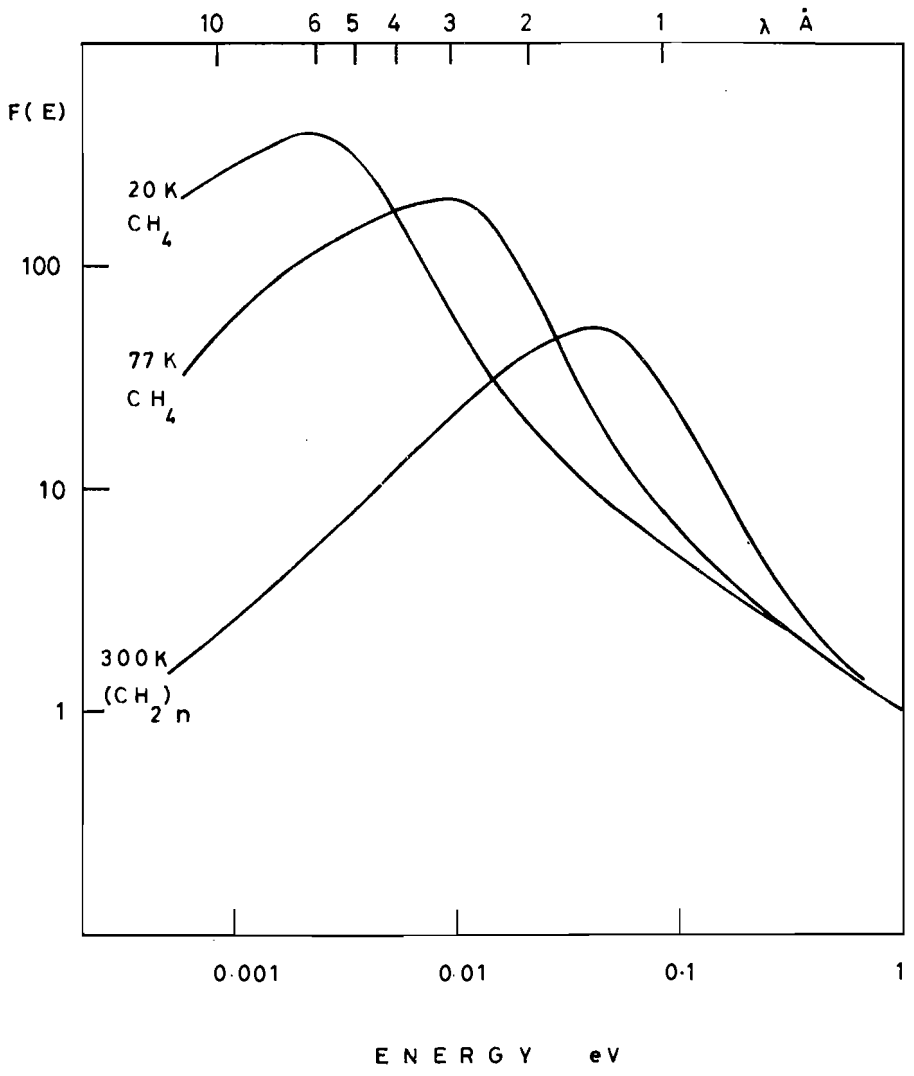

FIGURE 5.2 The spectral distribution of neutrons from various moderators.

PROPOSAL FOR A SPALLATION NEUTRON FACILITY

Appendix I - Utilization

CONTENTS

CHAPTER 1. SNS NEUTRON BEAM INTENSITIES

This chapter reviews the arguments for the moderator-reflector conceptual design and indicates the spectral distribution and pulse widths for the various moderators.

CHAPTER 1. SNS NEUTRON BEAM INTENSITIES

TIME-AVERAGED FAST NEUTRON PRODUCTION RATE

1.1 The proposed synchrotron operates at a frequency of 53 Hz producing $2.5\ 10^{13}$ protons per pulse at an energy of 800 MeV. The reference target is ^{238}U with nominal dimensions of length $\sim$ 30 cm and cross-section 8 x 8 cm^2. Approximately 30 neutrons per incident proton are produced within a length $\sim$ 25 cm along the target axis, giving a neutron production of $4\ 10^{16}$ fast neutrons per second. These neutrons are produced predominantly in the first few centimetres of the target, with about 70% of the neutrons produced in the first 10 centimetres.

MODERATOR EFFICIENCY

1.2 The fast neutrons may be moderated to experimentally useful energies (ie to energies around and below 1 eV) by interaction with a few centimetres of a light material with a high scattering cross-section, in practice some hydrogenous material. The resulting under-moderated spectrum has an approximately 1/E dependence in the slowing-down region, corresponding to E greater than $\sim 5\ k_B T_{eff}$ (where k_B is Boltzmann's constant and T_{eff} is the effective temperature of the moderator). At lower energies, the spectrum assumes the form of a Maxwellian distribution which is characteristic of the effective moderator temperature.

1.3 It is necessary to know the yield of neutrons emanating from the moderator surface as a function of energy. The results of Graham and Carpenter[1] show that the number of neutrons which emerge at 1 eV from a bare polyethylene moderator of dimensions 7.65 cm x 10 cm x 10 cm is of the order of $3.4\ 10^{-4}$ per eV per steradian per fast neutron incident on the moderator. Not all source neutrons, however, are incident on the moderator and we wish to know the number of neutrons emitted from the moderator surface per unit solid angle per unit energy per fast neutron produced in the target. This figure depends on the particular moderator material, geometry and temperature and on the configuration of the moderator.

1.4 A schematic arrangement is illustrated in Figure 1.1. The fraction of neutrons produced in the first 10 cm of the target is ~ 0.7 and the angular acceptance of the moderator further reduces this figure by ~ 0.15. Thus we may expect, at 1 eV, $\sim 0.7 \times 0.15 \times 3.4\ 10^{-4}$ neutrons eV^{-1} $ster^{-1}$ source $neutron^{-1}$. The number of neutrons incident on the moderator may, however, be substantially improved by the use of beryllium as a neutron reflector. The effect of the reflector is two-fold:

(a) to increase the effective solid angle subtended by the moderator by ~ 2 by reflecting into the moderator fast neutrons whose original trajectory would not have crossed the moderator surface;

(b) to increase the yield figure for a given moderator by ~ 5 by reflecting partially thermalised neutrons back into the moderator, thus reducing the overall leakage probability and increasing the emerging slow neutron flux.

Thus we may expect, at 1 eV, for a 10 x 10 cm^2 polyethylene moderator with a beryllium reflector, a source strength of

$0.7 \times 2 \times 0.15 \times 5 \times 3.4\ 10^{-4}$ neutrons eV^{-1} $ster^{-1}$ source $neutron^{-1}$

$= 3.6\ 10^{-4}$ neutrons eV^{-1} $ster^{-1}$ source $neutron^{-1}$

Calculations at Argonne have shown that this is a good average figure for the output of a moderator, and measurements have shown that increases of this magnitude may be expected by the use of reflectors.

---

[1] K F Graham and J M Carpenter, Nucl Sci Eng, 49, 418 (1972)

The beam current at the surface of such a moderator at 1 eV is

$$\phi\ (1\ \text{eV}) = 4\ 10^{16} \times 3.6\ 10^{-4}\ \text{neutrons eV}^{-1}\ \text{ster}^{-1}\ \text{s}^{-1}$$

$$\sim 10^{13}\ \text{neutrons eV}^{-1}\ \text{ster}^{-1}\ \text{s}^{-1}$$

The small angular variation of this current around the normal to the moderator permits the use of multiple beam tubes.

SLOWING DOWN REGION

1.5 The shape of the neutron spectrum emanating from a thin moderator has approximately a 1/E slowing-down form for neutron energies E greater than about $5k_BT_{eff}$. This temperature is a little higher than the physical temperature of the moderator and is defined by the Maxwellian portion of the spectrum.

The neutron angular beam current at the surface of a thin moderator is then

$$\phi(E) = \frac{10^{13}}{E}\ \text{neutrons eV}^{-1}\ \text{ster}^{-1}\ \text{s}^{-1}$$

The slowing-down region of the spectrum may be extended by reducing the moderator temperature, thus shifting the flux build-up corresponding to the Maxwellian part of the spectrum to lower energies.

Moderator	Temperature	kT_{eff}	1/E Range
$(CH_2)_n$, H_2O	300 K	$\sim$ 35 meV	> 200 meV
CH_4, NH_3	77 K	$\sim$ 11 meV	> 50 meV
CH_4, H_2	20 K	$\sim$ 3 meV	> 15 meV

1.6 At reasonable distances from the source, the moderator may be considered as a point-source of neutrons. Consequently the time-averaged intensity at a specimen at a distance L cm from the moderator within an energy window ΔE at E is given by

$$I(E)\ \Delta E = \frac{10^{13}}{L^2}\ \frac{1}{E}\ \Delta E\ \text{neutrons cm}^{-2}\ \text{s}^{-1} \qquad (1.1)$$

1.7 The time associated with moderation depends on the average number of collisions required for neutrons to reach the particular energy. In the slowing-down region, the pulse shape is narrow and the full width at half maximum may be approximated by the empirical expression

$$\Delta t(\mu s) \sim 2/\sqrt{E}(eV) \qquad (1.2)$$

1.8 We can now express the time averaged flux at the sample position for a wavelength resolution

$$R = \frac{\Delta\lambda}{\lambda} = \frac{\Delta E}{2E} \sim \frac{\Delta t}{t} \qquad (1.3)$$

as a function of energy and resolution. Using the velocity-time relationship, the required flight path will be given by

$$L = \sqrt{\frac{2E}{m}}\ t = 1.38\ \sqrt{E}\ t$$

where L is in cm, E in eV and t in μs.

Using equations (1.2) and (1.3) we see that

$$L = \sqrt{\frac{2E}{m}}\ \frac{\Delta t}{R} \sim \frac{2.5}{R}\ \text{cm}$$

The time averaged intensity per eV at the sample is

$$I(E) = \frac{\phi(E)}{L^2} \sim \frac{10^{13}}{E}\ \frac{R^2}{2.5} = 0.16\ 10^{13}\ \frac{R^2}{E}\ \text{neutrons cm}^{-2}\ \text{s}^{-1}\ \text{eV}^{-1}$$

and the time averaged intensity at the sample

$$I(E)\Delta E \sim 0.16\ 10^{13}\ R^2\ \frac{\Delta E}{E} = 0.32\ 10^{13}\ R^3\ \text{neutrons cm}^{-2}\ \text{s}^{-1}$$

THERMAL REGION

1.9 When the neutron energy becomes comparable with thermal motion, both energy gain and energy loss collisions occur. The neutron flux builds up and the pulse width broadens considerably.

In this Maxwellian region (E less than $\sim 2\ k_B T_{eff}$), the intensity depends

on the dynamics of the moderating system and on the leakage and capture of neutrons. The pulse shape is asymmetric and cannot be expressed in a simple analytic form. The width depends on the neutron energy, the moderator material, temperature and configuration, and may be broadened by moderation within the reflector. (A decoupler of $^{10}B_4C$ between the reflector and the moderator is required to restrict this broadening and maintain acceptable pulse widths). At low energies the width is dominated by the fundamental mode decay time of the moderator and consequently tends to approach a constant limit which will vary with moderator dimensions and material.

1.10 Computer calculations of pulse widths in the thermal region are difficult because some model must be assumed for the scattering law and this is not available for many of the moderators which might be envisaged. A number of moderator experiments has been performed in the UK, United States, Japan and Russia, but only a few estimates of the pulse widths for the various low temperature moderators are available from the experimental data.

1.11 Estimates of beam intensities from slab moderators (polyethylene) at ambient and liquid nitrogen temperatures have been made on the basis of the results of Graham and Carpenter, and illustrated in figure 1.2. The spectra are normalized to unity at 1 eV, an energy which is in the slowing down region for both temperatures; F(E) is the ratio of the flux per unit energy at an energy E to that at 1 eV. In addition the values of F(E) for a methane slab moderator at 20 K are shown; these values have been obtained by comparing measured intensities from moderators of solid methane at 77 K and 20 K but of different dimensions[2]. The corresponding pulse widths are given in figure 1.3.

1.12 The ambient temperature moderator intensity curve is also valid for light water, except that the pulse widths are somewhat larger in the Maxwellian region than those for polyethylene. A liquid nitrogen cooled ammonia moderator of similar dimensions to the methane moderator gives narrower pulse widths but a slightly reduced emitted intensity in the thermal region due to its higher neutron absorption cross-sections. Indeed narrow pulse widths can generally be obtained at the expense of some intensity by the use of

---

[2] K Inoue, N Otomo, M Utsuro and Y Fujita, J Nucl Sci Tech 11, 228 (1974)

neutron absorbers, either by homogeneous poisoning (eg small amounts of gadolinium in light water) or by heterogeneous poisoning (eg a cadmium sandwich in two layers of polyethylene).

1.13 The time averaged neutron intensity at a specimen at a distance L cm from the moderator within an energy window ΔE at an energy E is (cf equation 1.1)

$$I(E)\Delta E = \frac{10^{13}}{L^2} F(E)\ \Delta E \quad \text{neutrons cm}^{-2}\ \text{s}^{-1}$$

(In the case of a low temperature moderator the full value of 10^{13} may not be realised due to the spatial demands of the cryogenics).

1.14 From the point of view of intensity alone moderators may be divided into three distinct wavelength regions, viz

Region	Moderator Temperature
$\lambda < 2$ Å	300 K
$2 < \lambda < 4$ Å	77 K
$\lambda > 4$ Å	20 K

Only for spectrometers which require neutrons of predominantly long wavelengths has a cooled moderator an intensity advantage over that at ambient temperature. Cooled moderators, however, will generally give sharper pulse characteristics (see figure 1.3) for those energies which correspond to the thermal region for an ambient temperature moderator.

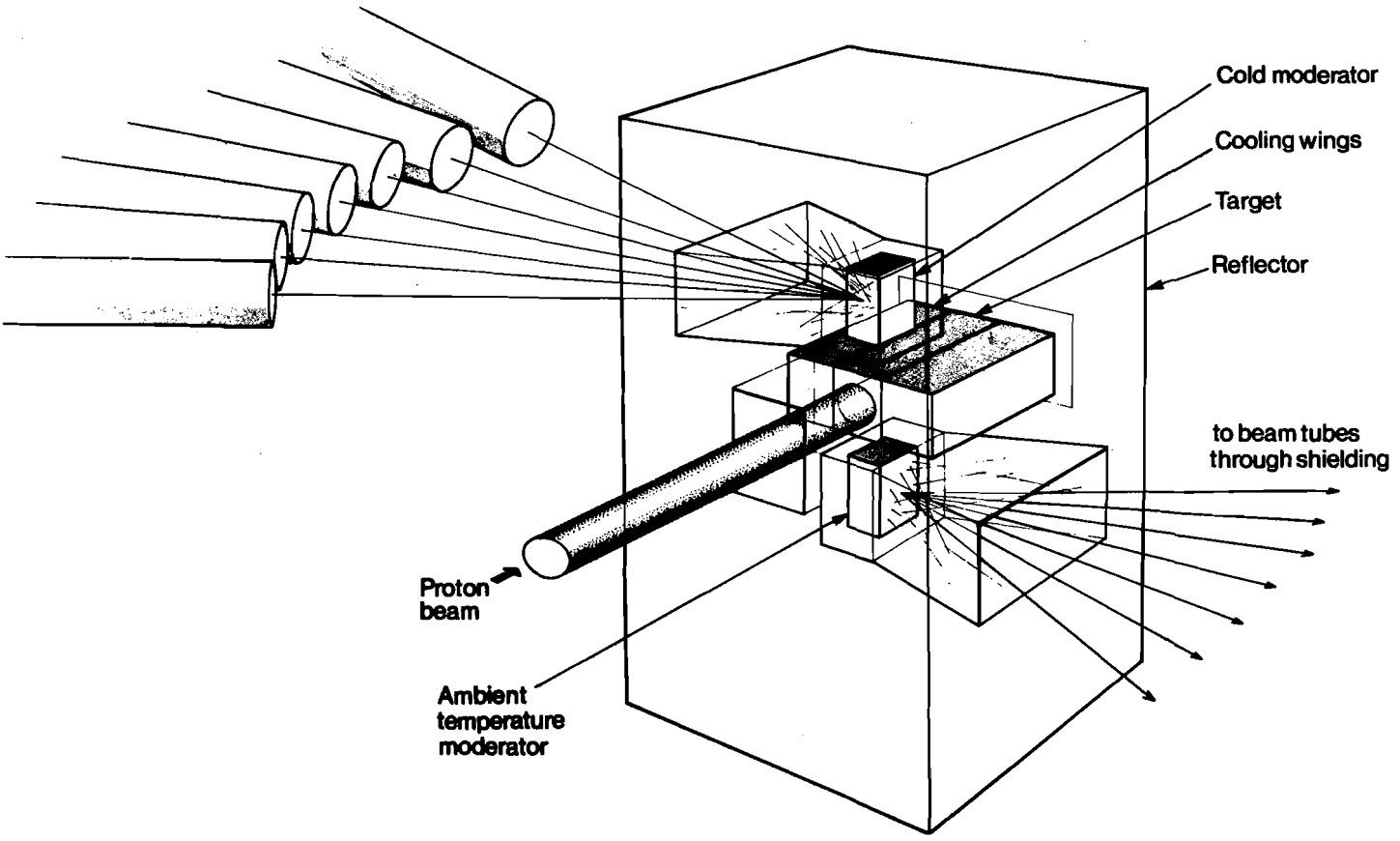

Figure 1.1 Target – Moderator – Reflector Configuration

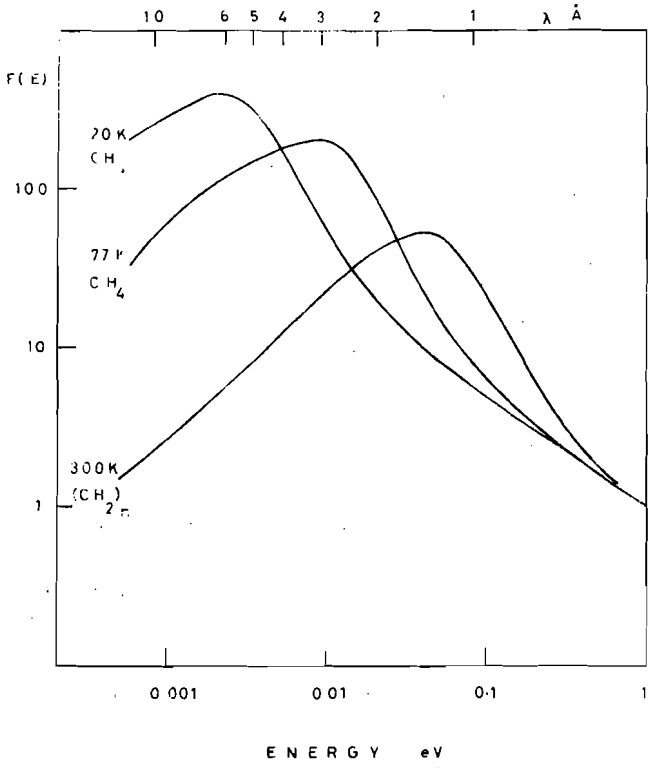

FIGURE 1.2 The spectral distribution of neutrons emanating from various moderators

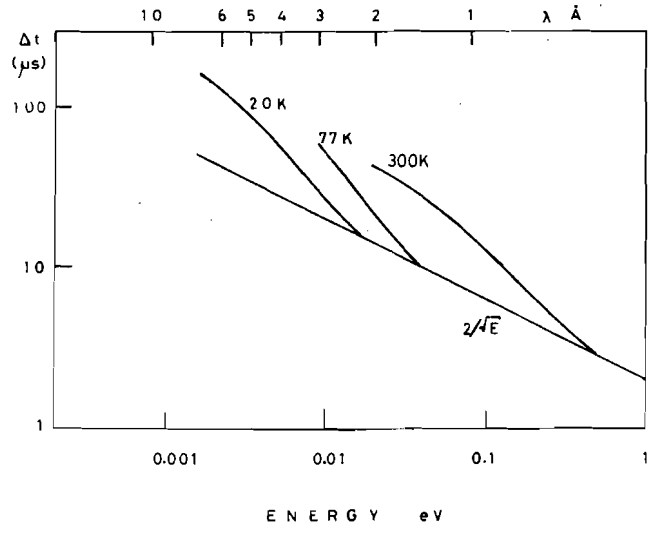

FIGURE 1.3 The FWHM of the neutron pulse as a function of energy for various moderators.

2. SPALLATION NEUTRON SOURCE SCIENCE PANEL : REPORTS OF WORKING GROUPS

This section brings together the individual reports of the Working Groups set up by the Spallation Neutron Source Science Panel, viz

A Solid State Physics

B Fluids and Amorphous Solids

C Structure Determination

D Molecular and Biological Sciences

The reports were originally prepared as 'stand alone' documents, and have been subjected to minimal editing. Instruments identifiable with specific scientific areas in the reports have been tabulated at the end of each report.

SPALLATION NEUTRON SOURCE SCIENCE PANEL

Working Group A : Solid State Physics

Dr P H Borcherds	Physics Department University of Birmingham
Professor L J Challis	Physics Department University of Nottingham
Dr J R Chamberlain	Physics Department University of Salford
Professor R J Elliott	Department of Theoretical Physics University of Oxford
Dr N W Grimes	Physics Department Aston University
Dr M T Hutchings	Materials Physics Division AERE Harwell
Professor E W Lee	Physics Department University of Southampton
Dr R D Lowde	Materials Physics Division AERE Harwell
Professor E W J Mitchell (Convener)	Physics Department University of Reading
Dr B D Rainford	Department of Physics Imperial College London
Dr G L Squires	Cavendish Laboratory University of Cambridge
Dr R J Stewart	Physics Department University of Reading
Dr W G Williams (Secretary)	Neutron Beam Research Unit Rutherford Laboratory
Dr C G Windsor	Materials Physics Division AERE Harwell

SOLID STATE PHYSICS

TABLE OF CONTENTS

4. SPECIAL TECHNIQUES

4.1 POLARIZED NEUTRONS

4.1.1 Polarized Proton Filter

4.1.2 Polarizing Crystals

4.1.3 Polarizing Sollers

4.1.4 ^{149}Sm Polarizing Filter

4.2 TECHNIQUES WITH VERY HIGH ENERGY NEUTRONS

4.2.1 Selection of Neutrons with 10 eV Incident Energies

4.2.2 Detection of 10 eV Energy Neutrons

4.2.3 Simultaneous Energy Selection and Detection at 6 eV

1. INTRODUCTION

The discussions of the Solid State Physics Working Group revealed continuing important scientific interests requiring instruments with parameters similar to some of those now used extensively at the Institut Laue-Langevin (ILL). These are high performance instruments for which there is a heavy and continually increasing demand. Whether the next generation neutron source were a steady state reactor or a pulsed source, further provision for these experiments will be needed. We have therefore first identified a class of instruments which can be constructed on the SNS so as to enable such experiments to be performed efficiently; this is possible primarily because of the increase in flux rather than of any special spectral characteristic.

Following this we have examined those experiments which are now sometimes attempted at the ILL, but which realistically are on the limits of feasibility. These experiments require a more extensive neutron energy range extending into the region now covered by the Harwell linac, but would be best carried out, on grounds of flux and spectral characteristic, on SNS instruments.

In the final category we suggest two types of experiment which, at present, cannot be carried out at any neutron source in the world. The first of these, the measurement of very high energy transitions, becomes possible due to the favourable fast neutron spectral characteristic of the SNS, and the second, inelastic polarization analysis, is due to the higher neutron fluxes of the SNS in the near-thermal region.

2. PHYSICS EXPERIMENTS

2.1 CURRENT STATE OF SOLID STATE PHYSICS RESEARCH PROGRAMMES

The following are examples of the range of experiments which are now carried out at the ILL, and for which we anticipate a need for greater neutron beam time during the next decade.

2.1.1 Phonon and Magnon Dispersion

The unique property of thermal neutrons, that both their wave vector and energy match closely those of elementary excitations in solids, has been exploited extensively during the past 15 years to determine the energy dispersion throughout the Brillouin zone of magnons and phonons in many monatomic and compound crystals. These measurements have generally involved

neutron energy transfers (excitation energies) 0-0.1 eV and have mainly been performed on continuous or chopped beams from steady state reactors. They have yielded important and unique information on the interactions between the magnetic electrons, or between atoms or ions in materials, and they have been extended to investigate details of the dynamical behaviour of spins and atomic dynamics near phase transitions. Information on excitation lifetimes and the interactions between different kinds of excitations (such as external and internal modes, or magnon-phonon coupling) has also been obtained.

2.1.2 Crystal Field and Spin-Orbit Splittings in Paramagnets

Crystalline electric field levels in rare earth ions can be measured directly by neutron inelastic scattering. The method has played a key role in the study of metals, since photon spectroscopy is not applicable here, due to the interaction with conduction electrons; as examples we give the intermetallics HoRh and ErZn which have the CsCl structure, and the superconducting intermetallics $NdSn_3$ and $NdPb_3$. Although the lanthanide metals have received considerable attention, there has so far been little success in observing transitions in actinide materials, since here the 5f shell is on the outside of the atom, and the crystal field splittings are somewhat larger ($\sim$ 0.1 eV).

Spin orbit splittings in the rare earths are of the order of 0.04 to 0.3 eV. These may be studied in the insulating compounds by optical spectroscopy, but again in the metals and in metallic compounds optical techniques are no longer appropriate. In one particular field, that of intermediate valence compounds (which are usually metallic) the measurement of transitions between spin orbit levels would be an extremely useful tool. These transitions have been observed in the semiconducting phase of SmS where the Sm ion is divalent, and it is planned to follow the transition as a function of pressure into the metallic intermediate valence phase of SmS. This is a relatively easy experiment since for Sm^{2+} and Sm^{3+} the spin orbit levels are low, about 0.04 eV above the ground state, but for other rare earths showing intermediate valence behaviour eg, Ce, Tm and Yb, the splittings are much larger and therefore require higher energy neutrons.

2.1.3 Inhomogeneities in Solids

Any deviation from order in a crystal lattice gives rise to scattering which is additional to Bragg scattering and is termed 'diffuse'. In many instances where this deviation is due to dislocations, point clusters, alloy precipitates,

magnetic moment fluctuations, density changes etc, the inhomogeneity gives rise to a $\underline{Q}$-dependent scattering, which is generally observed best at neutron wavelengths greater than the Bragg cut-off of the material being studied (so as to avoid multiple Bragg scattering), and at small scattering angles (small angle neutron scattering, SANS). Some examples of areas now under study are: (a) radiation induced defects; (b) alloy decomposition; (c) non-stoichiometric defects; (d) covalency; (e) flux-line lattices in superconductors; (f) polymers in solution; and (g) magnetic impurities. The study of magnetic defects can be considerably enhanced by using spin polarized neutron beams. It may be readily shown that measurements of the scattering cross-sections for the two spin states separately (this is done by spin-flipping the incident beam) gives a much more sensitive determination of the magnetic interaction than can be obtained by the 'field-switching' technique with unpolarized beams.

Two major advantages of diffuse scattering experiments with a pulsed neutron beam are: (a) the possibility of separating elastic and inelastic scattering if the wavelength spread is limited, and (b) the possibility of synchronising a perturbation of a sample with the neutron pulse and then studying the response of the sample by collecting the scattered neutrons from many such cycles. In cases where the sample response is slower than the pulse repetition rate, the response over several neutron pulses could be studied.

Possible areas of application are the study of voids, point defects and point defect clusters caused by irradiation, where it becomes possible to follow the annealing of the damage as a function of temperature. It is possible, if the flux was sufficiently high, that the annealing could be studied *in situ* using a furnace. It should also be possible to follow the effects of stress on the damage. The pulsed nature of the beam may be used to investigate the microscopic nature of fatigue by synchronous loading of a sample. The response of a sample to shock effects can be observed by collecting data over several pulses of the beam if necessary.

2.2 LIMITATIONS IN THE PRESENT SOLID STATE PHYSICS RESEARCH PROGRAMME

The feasibility of carrying out a neutron scattering experiment often depends on instrumental factors. The Working Group recognised that by the provision of (a) a high energy (0.1 to 0.3 eV) inelastic instrument, and (b) a total scattering polarization analysis instrument on the SNS, many of the Solid State Physics experiments which are on the limits of the existing ILL instruments, would be carried out significantly better. The magnetic inelastic experiments discussed in Sections 2.1.1 and 2.1.2 must be performed at low momentum transfer

$\hbar Q$, and therefore with as high an incident neutron energy E_o as possible. Such experiments are difficult at present but a high energy SNS chopper spectrometer would make it relatively straightforward to obtain good data for many samples of interest. Furthermore such an instrument would open up the study of two other important problems in magnetism viz, measurements of the generalised susceptibility $\chi(\underline{q},\omega)$ and the more extensive study of itinerant magnetism.

Another type of measurement which presently suffers from a lack of neutron flux is that of polarization analysis. Although measurements on samples with well-defined Bragg peaks are reasonably easy to make on the D5 triple-axis polarization analysis instrument at the ILL, much of the scientific interest in the polarization analysis technique centres on the measurement of diffuse and inelastic scattering cross-sections, and these are either very difficult or impossible to obtain at present. A major gain in the possible science will be achieved by the separation of nuclear from magnetic scattering and of nuclear spin-incoherent from coherent scattering. Experiments utilizing this possibility could be carried out using a polarization analysis total-scattering instrument on the SNS. We now give a brief discussion of the areas of science which we believe would benefit from the provision of these two instruments.

2.2.1 Generalised Susceptibility $\chi(\underline{q},\omega)$

The investigations of the generalised susceptibility $\chi(\underline{q},\omega)$ in transition metals (including (a) nearly magnetic materials like Pd and (b) ferromagnets like Ni and Fe and antiferromagnets like Cr and Mn) above their ordering temperature are of considerable current interest. In category (a) calculations have been made of the neutron cross-sections for the case of Pd. These showed that the total response is spread over a wide energy range, of the order of the bandwidth of the d bands. However many fascinating many-body effects (eg 'the paramagnon peak') appear at energies below 0.1 eV at low temperatures. Attempts to study the magnetic scattering have not succeeded with present techniques since the 4d form factor of Pd drops rather rapidly, and with present sources wide ranges of energy transfers cannot be studied without large momentum transfers. In one favourable case, however, magnetic scattering has been recently observed in αCe, where the magnetic response is due to a narrow 4f band and is, therefore, spread out over a much smaller energy range ($\sim$ 0.08 eV).

Similar considerations apply to category (b) above. Recent measurements on Ni and Fe above T_c have shown a surprising amount of structure in the paramagnetic response. This has been interpreted as a residual spin wave branch which extends

up to 0.1 eV, where the spin waves disappear below T_c. The origin of this scattering is not understood at present. There should also be a considerable amount of structure in the single particle excitation spectrum of these metals above 0.1 eV, although there are no reliable intensity estimates at present. Nevertheless the only techniques now available for observing interband transitions in these materials are optical absorption or reflectivity in which one relies on the weak magnetic dipole transitions and these are restricted essentially to zero wave vector transitions. Neutrons, on the other hand, allow transitions at a general wave vector to be investigated and also sample the bulk of the metal rather than a thin surface layer.

2.2.2 Magnon Excitations in Itinerant Ferromagnets and Antiferromagnets

Whereas few phonon excitations occur above 0.1 eV, there exists a large number of magnetic materials, mainly metallic or semi-metallic and exhibiting magnetism due to itinerant rather than localised electrons, whose collective excitations (magnons) in the ordered magnetic state range into the 0.1 - 0.3 eV region. This region extends beyond the upper limit of energy-transfer observable using a conventional triple-axis spectrometer on a beam from a hot-moderated steady-state source (IN1). A number of recent experiments performed on this instrument has indicated that this energy region contains important and fundamental physical effects although the results are tantalizingly on the limits of performance.

Examples of possible experiments are:

(a) investigation of the itinerant ferromagnets nickel and iron, where sudden decreases in scattered intensity have suggested the possibility of the magnon interacting with the continuum band of Stoner modes near 0.1 eV. In the case of nickel evidence of a second magnon mode has been found. Because of their high energies in neither case have the magnons yet been observed right across the Brillouin zone. Pd_3Fe is another case where interaction with Stoner modes is suggested by conventional experiments, and an optic mode is predicted $\sim$ 0.16 eV which could yield more information on this interaction. In a number of Heusler alloys the magnon energies approach 0.1 eV.

(b) investigation of itinerant antiferromagnets such as γ-manganese, chromium, and nickel sulphide, whose steep energy-dispersion (200, 450 and $\sim$ 450 meV Å respectively) has limited observation using conventional sources to excitations up to 0.14 eV and $\frac{2}{3}q_{max}$. In

$Mn_{73}Ni_{27}$ large line widths are observed and these suggest possible interactions with single-particle excitations. A detailed examination of $S(\underline{Q},\omega)$ throughout the zone would help elucidate this problem.

2.2.3 Separation of Coherent/Spin-Incoherent and Nuclear/Magnetic Scattering

One useful application of the polarization analysis technique, which in one mode of operation can be used to distinguish between spin-flip from non spin-flip scattering processes, is the separation of spin-incoherent nuclear scattering from other types of nuclear scattering in non-magnetic materials, especially when hydrogen or deuterium are present. The spin-flip scattering cross-section is equal to two-thirds of the spin-incoherent cross-section, and the non spin-flip scattering is equal to the sum of one-third of the spin-incoherent scattering plus the coherent and isotopic incoherent scattering. The method is particularly helpful in isolating the coherent part of a total scattering cross-section in the presence of a considerable spin-incoherent component.

Probably the most important application of the total scattering polarization analysis instrument would be in the study of paramagnetic or magnetic defect scattering. Only the magnetic spin component perpendicular to the scattering vector can take part in the magnetic scattering of neutrons, therefore, if the polarization direction is parallel to the scattering vector all the magnetic scattering is spin-flip, whereas when the nuclear polarization and scattering vectors are orthogonal, the spin-flip and non spin-flip cross-sections are equal. One of the main problems in the usual determination of paramagnetic cross-sections is to separate this from the other scattering processes, viz nuclear disorder, multiple Bragg, thermal diffuse, Bragg, and nuclear spin incoherent scattering. A measurement of the spin-flip scattering cross-section provides a powerful method for separating the paramagnetic scattering, since the only other source of spin-flip scattering possible is nuclear spin-incoherent scattering.

Some of the fields of study in which a good evaluation of the paramagnetic cross-section would make a large impact are (a) covalency in ionic salts and (b) dilute magnetic alloys, where it can reveal the existence of the onset of long range magnetic order, interacting impurities, and Kondo or spin fluctuating systems.

2.3 NEW AREAS OF SOLID STATE PHYSICS RESEARCH

The Working Group gave careful consideration to the exploitation of the most favourable feature of the energy spectrum of the SNS ie, the intensity gains it provides at the higher neutron energies (1 to 10 eV) compared with a moderated

reactor with a view as to carry out high energy low Q inelastic scattering experiments where the energy transfer $h\omega \sim 0.3$ to 1 eV; this is an energy regime where measurements would not at present be contemplated at any neutron source. We also regarded inelastic polarization analysis as a research area in which only minimal and severely limited work can be done until neutron sources with fluxes higher than those at the ILL reactor become available. The information which would be forthcoming from these types of measurement is now discussed.

2.3.1 Very High Energy Transitions

The role of neutrons in determining the frequency/wave vector dispersion curves for phonons (Section 2.1.1) derives from the ability in neutron experiments to measure, with sufficient accuracy, excitations in the range $0.02 < h\omega < 0.1$ eV over a wave vector range $0 < \underline{q} < 5$ Å^{-1}; this enables energy dispersion information to be obtained within the first Brillouin zone. No other probe eg, x-rays, infra-red, visible light Raman scattering, allows such comprehensive data to be obtained; these other techniques yield information only for restricted regions of the Brillouin zone, especially near $\underline{q} = 0$ and the zone boundaries, and then not with unique assignment.

The same general problem occurs in the experimental determination of the dispersion curves for electronic excitations. An important class of such materials is the large group of semiconductors having band excitation energies $0.1 < \hbar\omega < 5$ eV throughout the Brillouin zone of $0 < \underline{q} < 5$ Å^{-1}. Methods currently available for studying these excitations include (a) optical absorption, both direct and indirect transitions, (b) optical reflectivity, (c) photoemission, (d) electron scattering, and (e) cyclotron resonance, and these provide accurate information for specific parts of the Brillouin zone. However, no complete experimental determination of frequency/wave vector dispersion curves has been possible.

As occurred with the studies of vibrational excitations, major computing projects have been developed to interpolate between these specific points, and a further recent initiative has been taken by a number of theoretical physicists in the UK using the Rutherford Laboratory IBM 360/195 computer. It is clear that the ability to determine experimentally more complete dispersion curves would be a major advance both in the study of the electronic states of semi-conductors and in the growing possibilities of 'electronic design' of materials.

2.3.2 Cross-Sections for Electronic Band Excitations

The cross-section contains the matrix element, modified by: (a) a form factor, and (b) a line shape and width factor.

There are contributions to the matrix element both from the spin and orbital components. The latter will, in practice, be small ($\alpha \frac{1}{Qa}$, where a ∿ atomic radius and $\underline{Q} = \underline{k}_o - \underline{k}_1$) because of the difficulty of working at $Q \to 0$ and simultaneously satisfying the energy conservation. The spin part will give the usual electron magnetic cross-section (∿ 0.4 b/e$^-$) with a possible enhancement in favourable cases of $\left[\frac{m_e}{m_e^*} - g\right]^2$, there m_e and m_e^* are the real and effective electron masses, and g is the electronic splitting factor. Unfortunately when $\left[\frac{m_e}{m_e^*}\right]$ is large, for example as in InSb, g is also large. Thus in general we cannot expect to obtain a contribution greater than 0.4 b/e$^-$ from the matrix element.

For $Q > 0$ the cross-section is reduced by the form factor arising from the extension of the source of the scattering. Thus we are not able to obtain information within a zone utilizing higher zones and $\underline{Q} = \underline{q} + n\,\underline{\tau}$, where $\underline{\tau}$ is a reciprocal lattice vector. In order to maintain reasonable values of cross-section we shall need $0 < Q < 5$ Å^{-1}.

The energy shape factor will mean that for a transition of energy resolution $\Delta\hbar\omega$, when the total cross-section of ∿ 0.4 b/e$^-$ is spread over a band of width $\Delta\varepsilon$, the cross-section will be ∿ 0.4 x $\frac{\Delta\hbar\omega}{\Delta\varepsilon}$ b/e$^-$. The reduction might be typically 10^{-2} (eg, $\Delta\hbar\omega$ ∿ 0.05 eV, $\Delta\varepsilon$ ∿ 5 eV) giving a cross-section of the order of a few millibarns, say 5 mb/e$^-$.

Some of the electronic effects could be studied, in principle, through interactions with excitons. In the case of localised excitons the cross-section will be similar to that for spin-waves and measurable. However, this will apply only to a limited class of materials, eg, the alkali halides. In the extended excitons in narrow gap semiconductors the spread of the exciton, and hence the small probability of finding the electron and hole on adjacent sites, may reduce the cross-section to ∿ 1 mb/e$^-$.

The form factor limitation could be overcome by utilizing an indirect process: neutron-phonon-exciton. The gain in replacing a form factor by a Debye-Waller term is, however, offset by a reduction of order (electron-phonon interaction energy/energy gap) which would typically be ∿ 10^{-2}.

In summary, for band transitions in semiconductors we can expect cross-sections of a few millibarns (say 5 mb) and we require $0 < Q < 5\ \text{Å}^{-1}$. The same general considerations apply to the band effects in magnetic materials, except that the band width $\Delta\varepsilon$ may be considerably less than the 5 eV used here, and hence the process is that more favourable.

2.3.3 Inelastic Polarization Analysis

Many useful polarization analysis experiments such as those discussed in Section 2.2.3, can be adequately performed without energy analysis. When some energy-analyser is included in a polarization analysis instrument, the accompanying decrease in flux is sufficient at present to make inelastic experiments effectively impossible. The Working Group believe that the provision of an inelastic polarization analysis instrument on the SNS will enable a significant number of spin dynamics experiments, both in magnetic as well as non-magnetic materials, to be carried out; an example of its use for separating the dynamical structure factor $S(\underline{Q},\omega)$ and the dynamical self structure factor $S_s(\underline{Q},\omega)$ in liquids which scatter spin incoherently is described by the Fluids and Amorphous Solids Working Group.

Inelastic polarization analysis provides the most effective way of separating magnon and phonon scattering, since the latter is nuclear and coherent, hence always non spin-flip. By selecting both the incident and scattering neutron spin states the observation of magnon creation and annihilation has been clearly demonstrated in the saturated ferromagnet $Fe_{2.5}Li_{0.5}O_4$, though it has not been possible to carry out experiments routinely. In addition to separating pure phonons and magnons, it is also possible to use the technique to identify magneto-vibrational scattering, where the phonons are excited through the magnetic interaction, and which exhibits the same polarization-dependent effects as magnetic Bragg scattering.

3. INSTRUMENTATION FOR SOLID STATE PHYSICS EXPERIMENTS

3.1 SUPPLEMENTARY INSTRUMENTATION TO THAT CURRENTLY AVAILABLE

The Working Group recommend the construction of four instruments at the SNS, which would be either superior or comparable in performance with those which are now used at the ILL, and would thus be used to supplement the existing lines of research, as described in Section 2.1.

3.1.1 Moderate Energy Transfer Spectrometer

Measurements of energy transfers up to $\sim$ 0.05 eV may be carried out with a rotating crystal spectrometer (Figure 2.1) which uses the pulsed nature of the source to eliminate higher order reflections from the rotating crystal in a similar manner to the first crystal on IN4 at the ILL. The final pulse width in time is however determined by the rotating crystal so that the longer pulses from the source at long wavelengths (30 μs at 4 Å) can be shaped up by the crystal to give high overall energy resolution. A very large counter bank is practicable.

General Specification

$|\hbar\omega|$ = 0 to 50 meV, E_o = 5 to 100 meV

$Q \sim 1 - 10$ Å^{-1}, λ_o = 4 to 1 Å

Resolution Specification

We wish high accuracy in locating modes, say 2% of the energy transfer, but wish to study only the general Q variation, say with a resolution of 1/10 of a typical zone dimension or 0.3 Å^{-1},

$$\text{ie } \frac{\Delta\hbar\omega}{\hbar\omega} \sim 0.02, \quad \frac{\Delta Q}{Q} \sim 0.1.$$

Implications for the Incident and Scattered Beam Resolution

Consider a 10 meV energy transfer observed with 20 meV incident energy neutrons at 90° scattering angle to give Q = 3.707 Å^{-1}. The requirement of a resolution of 0.2 meV implies resolutions of $\frac{0.2}{\sqrt{2 \times 20}}$ = 0.7% resolution in E_o, but only $\frac{0.2}{\sqrt{2 \times 10}}$ = 1.4% resolution in E_1. At this incident wavelength of 2.02 Å, the source pulse time is only of order 20 μs and so matches nicely to the typical pulse time from a rotating crystal of order 20 μs. To obtain an incident wavelength resolution of 0.35% ($\frac{1}{2} \times \Delta E_o/E_o$) with graphite 004 planes as the rotating crystal requires a rotating speed of 207 cps. This is easily achieved. The incident flight path need not be longer than necessary for shielding reasons. If possible the rotating crystal should be near the moderator inside the biological shield. The distance between rotating crystal and sample can then help to give the required good collimation (0.3°). The scattered flight path is determined by the 0.7% wavelength resolution (R = 0.007) requirement of the scattered beam and the 20 μs pulse time:

$$L_1 = \frac{0.3956}{\lambda_1} \times \frac{\Delta t}{R} = \frac{0.3956}{2.86} \times \frac{20}{0.007} = 3.95 \text{ m}$$

which leads to a spectrometer of comparable size to IN4.

3.1.2 The Constant Q Spectrometer

The other inelastic spectrometers considered for the SNS are all variants of the fixed incident wavelength time-of-flight method. This has the disadvantage that Q vector and energy transfer both vary non-linearly across the spectrum. In practice many experiments on the excitations in single crystals require data only along high symmetry directions. Unless the excitation spectrum is already known only the constant Q type of scan can ensure that the observed excitation lies at the required high symmetry position. This is the reason for the high demand for reactor triple-axis spectrometers.

The proposed constant Q spectrometer is essentially a MARX analyser on a time-of-flight spectrometer. The constant Q is obtained from picking out the appropriate time-of-flight channel at each counter position. Figure 2.2 shows the principle for an analyser crystal of lattice spacing and set parallel to the incident beam. Setting up axis parallel to $\underline{k}_o$ so that $\underline{Q} = \underline{Q}^{//} + \underline{Q}^{\perp}$

$$Q^{//} = k_o - k_1 \cos \phi$$

$$Q^{\perp} = k_1 \sin \phi$$

For an analyser of spacing d, $\lambda_1 = 2d \sin \theta_a$, so that $\frac{\pi}{d} = k_1 \sin \theta_a$.

In the position with the analyser parallel to k_o, $\theta_a = \phi$ so that $Q^{\perp} = \pi/d$ and so is a constant. The appropriate k_o to make $Q^{//}$ a constant is found by selecting the appropriate k_o from the time-of-flight spectrum. This can be done for each counter position in turn to give an energy scan.

The disadvantages stem from the limited nature of this energy scan. Clearly for the scattering triangle to be real $\pi/d < Q$, and for the scattering angle on the analyser to be real $\phi < \pi/2$. This is seen most stringently in the case of elastic scattering. For this case we have

$$Q = 2k_o \sin \theta/2 \qquad \pi/d = k_o \sin \phi.$$

Eliminating k_o and solving for ϕ we have

$$\cos \phi/2 = (\pi/d)/Q.$$

Since $\phi(= \theta_a)$ must be in general vary from ϕ_{min}, say 20^o, to ϕ_{max}, say 70^o, we have for the allowable range of $(\pi/d)/Q$

$$\cos\left(\frac{20^o}{2}\right) > (\pi/d)/Q > \cos\left(\frac{70^o}{2}\right) \quad \text{or} \quad 1.015 < Q/(\pi/d) < 1.221.$$

Thus the d spacing must be carefully adjusted to give the appropriate scattering angle. In fact for inelastic scans it is much easier to satisfy the required conditions. Figure 2.3 shows the scattering angles as a function of energy transfer for the pyrolytic graphite 002 plane. It is seen that this covers a very useful range of energies for moderate Q vectors of order 4 to 6 Å^{-1}.

Resolution Considerations

We consider a typical scattering configuration with $\hbar\omega$ = 0.05 eV, Q = 4 Å^{-1}, and E_o = 0.1 eV. As with all MARX analysers, which depend on counter and sample dimensions to determine angular collimations, resolution tends to be dominated by the analyser. Taking typical counter and sample dimensions of 12 mm and a 1.4 m scattered flight path we obtain a definition in the analyser scattering angle of order $\sqrt{2} \times \frac{12}{1400} = 0.012$ (0.7^o). This matches nicely with graphite mosaics and implies a time spread Δt_1 of order 8 μs and an energy spread ΔE_1 of order 1.5 meV. The error in the incident beam tuning is then a convolution of the moderation time of ∿ 8 μs and the spread Δt_1 giving a total of 11 μs implying an energy spread of ΔE_o of 2.6 meV. The total energy spread is thus of order 3 meV, so that $\frac{\Delta\hbar\omega}{\hbar\omega} = 0.003/0.05 = 6\%$ comparing favourably with a triple axis spectrometer.

3.1.3 Very Low Q Spectrometer

The construction of this instrument would complement the large and heavily booked programme on D11A at the ILL. For solid state physics applications a wavevector range up to Q ∿ 10^{-2} Å^{-1} is desirable, with a resolution in Q, $\Delta Q/Q$ ∿ 1 or 2%. A detailed discussion of the design of small angle scattering instruments is given later in the Appendix. For the present use we note that time-of-flight can be used to discriminate against both inelastic processes and against double Bragg scattering.

3.1.4 Diffuse Scattering (with polarized beam option)

This instrument complements the ILL instruments D11B (unpolarized beam) and D7 (polarized or unpolarized beam).

General Specification

Q_{max} ∿ 4 Å^{-1} $\quad \Delta Q = 0.03$ Å^{-1}

Implications of Machine Design

The requirement for long wavelengths suggests the use of a curved guide to remove fast neutron and γ background. The incident pulsed white beam can be collected by an array of time-focussed detector banks to give measurements as a function of both incident wavelength and scattering vector.

Consider a white beam centred on 5 Å, with typically $Q = 1$ Å^{-1} and having $\phi = 46.9^{o}$. The incident beam divergence will be of order $0.2\ \lambda \sim 1\%$ for a nickel guide. Matching this to a counter angular resolution of 1^{o} gives an overall angular resolution $\Delta\phi \sim 1.4^{o}$. This gives rise to a contribution to the scattering vector resolution of

$$\Delta Q = Q \cot \phi/2 . \Delta\phi/2$$

$$= 1 \times \cot (23.4^{o}) \times (\frac{1.4/57}{2}) = 0.029.$$

The time contribution to the scattering vector resolution will depend on the total flight path L. If the moderation time for 5 Å neutrons is 50 μs we require a distance L giving a matching contribution to ΔQ.

$$\text{ie } \frac{\Delta\lambda_o}{\lambda_o} = \frac{\Delta t}{t} \simeq 0.029.$$

This will be given by

$$L = \frac{0.3956}{\lambda_o} \times \frac{\Delta t}{0.029} = 136.4 \text{ cm.}$$

This is very small compared with the length of guide required so that the overall scattering vector resolution will be of order 0.03 Å^{-1}.

Polarization beam diffuse scattering can be carried out by installing a polarizing Soller (whose acceptance angle matches the angle divergence of the beam from a nickel guide) and a non-adiabatic spin flipper in front of the sample. Polarizing Sollers at wavelengths $\lambda \sim 5$ Å are reasonably short ($\sim$ 20 cm), and by placing approx 10 of these in front of the detector bank array, this would also enable long wavelength polarization analysis (ie the separation of nuclear and magnetic scattering) experiments to be performed.

3.2 ADVANCED INSTRUMENTATION

The Working Group considered that the construction of an high energy transfer inelastic spectrometer and a total scattering polarization analysis instrument,

as described below, would allow the existing research programme in Solid State Physics to be significantly improved.

3.2.1 High Energy Transfer Inelastic Spectrometer

This instrument to some extent complements IN1 at the ILL, but with improved performance near the high energy transfer limit ($0.1 < \Delta\hbar\omega < 0.3$ eV); it is shown schematically in Figure 2.4.

General Specification

$\hbar\omega$ up to ~ 0.3 eV, but typically $\hbar\omega \sim 0.1$ eV

$$E_o \sim 0.2 \text{ eV}.$$

Resolution Requirements

This depends on the collimators used and is complicated by focussing considerations but is in general of order

$$\Delta\hbar\omega = 0.005 \text{ eV} \quad \Delta Q = 0.1 \text{ Å}^{-1}.$$

Implications for Incident and Scattered Wave Vector Resolutions

Consider first the energy resolution. We assume matched contributions from the incident and scattered beams. Thus

$$\frac{\Delta E_o}{E_o} = \frac{1}{\sqrt{2}} \frac{\Delta\hbar\omega}{E_o} = 0.018 \; ; \; \frac{\Delta\lambda}{\lambda} = 0.009.$$

This is achievable using a time-of-flight spectrometer with time resolution 6.3 μs matching the 6.3 μs moderation time with incident flight path

$$L_o = \sqrt{2}. \frac{h}{m\lambda}. \Delta t_{mod} \times \frac{\lambda}{\Delta\lambda} = \frac{\sqrt{2} \times 0.3956 \times 10}{0.009} \text{ cm} = 6.22 \text{ m}.$$

This flight path matches well with the radius of the expected biological shield.

The scattered beam percentage energy resolution is less stringent because E_1 is only 0.1 eV

$$\frac{\Delta E_1}{E_1} = \frac{1}{\sqrt{2}} \frac{\Delta\hbar\omega}{E_1} = 0.036 \; ; \; \frac{\Delta\lambda_1}{\lambda_1} = 0.018.$$

This could be performed by a 3 m flight path using time-of-flight analysis.

The Q resolution again has components $\Delta Q^{//}$ from the wave vector uncertainty and $\Delta Q^{\perp}$ from angular uncertainties. In the present case $k_o = 9.9$ Å^{-1} and $k_1 = 7.08$ Å^{-1}, so that

$$\Delta k_o^{//} = k_o \times \frac{\Delta\lambda}{\lambda} = 0.089 \text{ Å}^{-1}.$$

If we have a restricted 7.5 cm diameter source block

$$\alpha_o = 7.5/6.22 = 0.0121 \quad (0.7^o)$$

and $$\Delta k_o^{\perp} = k_o \alpha_o = 0.12 \text{ Å}^{-1}.$$

Thus both $\Delta k^{//}$ and $\Delta k^{\perp}$ have the magnitude ~ 0.1 Å^{-1} postulated.

3.2.2 Total Scattering Polarization Analysis Instrument

This instrument would enable polarization analysis measurements to be made under good flux conditions, but with no energy analysis. It is suitable for measuring elastic spin-dependent cross-sections when the inelastic scattering can be either ignored, eliminated, or evaluated separately. The instrument can be designed to operate to high scattering vectors $Q \sim 20$ Å^{-1}, and is shown schematically in Figure 2.5.

A polarized proton white beam polarizing filter is required for the incident beam, as well as a non-adiabatic spin flipper which can operate over a large neutron energy range. The spin analysing filter should contain polarized ^{149}Sm nuclei for scattered neutron energies $E_1 < 0.15$ eV, but for spin analysing at all neutron energies a second polarized proton filter is required.

3.3 INSTRUMENTATION FOR NEW PHYSICS

The two instruments to be described in this section, a very high energy transfer spectrometer and an inelastic polarization analysis spectrometer, would in the opinion of the Working Group enable a completely different type of physics experiment to be carried out than has been possible hitherto.

3.3.1 Very High Energy Transfer Spectrometer

This is required principally for band width investigations where energy transfers up to ~ 1 eV must be measured, naturally with energy loss, and with scattering vectors limited by the form factor to $Q \sim 4$ Å^{-1}. The suggested instrument is illustrated in Figure 2.6.

Resolution

It will at first only be necessary to locate transitions to within say 10% of the energy transfer, ie 100 meV, but this may prove inadequate for later studies. The band dependent effects will change on the scale of the reciprocal lattice and we may specify a resolution of 20% of the zone boundary wave vector, ie, say 0.4 $\mathring{A}^{-1}$.

ie $\Delta\hbar\omega = 0.1$ eV $\quad \Delta Q = 0.4\ \mathring{A}^{-1}$.

Implications for the Incident and Scattered Neutron Energy and Angular Resolutions

To achieve $\hbar\omega = 1$ eV at $Q = 4\ \mathring{A}^{-1}$ will require $E_o \sim 9.1$ eV and a scattering angle $\sim 1.25^o$. With energy loss this implies $k_o = 66.3\ \mathring{A}^{-1}$ and $k_1 \sim 62.5\ \mathring{A}^{-1}$. Thus incident and scattered wave vectors ($\lambda \sim 0.094\ \mathring{A}$) are almost equal and the resolution requirements must be generally divided by $\sqrt{2}$ and applied to incident and scattered wave vector alike.

Thus for the incident beam

$$\frac{\Delta E_o}{E_o} = \frac{1}{\sqrt{2}} \frac{\Delta\hbar\omega}{E_o} = 0.0078$$

and the wavelength resolution is $\Delta\lambda/\lambda = 0.0039$. This gives an intensity at the sample of $I(E)\Delta E \sim 0.32 \times 10^{13} \times (4 \times 10^{-3})^3$

$\sim 2 \times 10^5$ n cm^{-2} s^{-1}.

For a cross-section of 5 mb for a particular event (group) and for a typical valence electron density of 10^{23} cm^{-3} we have for the number of scattered neutrons leaving the sample:

$$(2 \times 10^5) \times (5 \times 10^{-3} \times 10^{-24}) \times 10^{23} = 100\ s^{-1}.$$

For a less stringent case where the transition energy resolution $\Delta\hbar\omega = 0.4$ eV the flux at the scatterer will be greater by a factor ~ 8, and the number of neutrons leaving the sample for a particular event will be $\sim (500 - 1000\ s^{-1})$. Such an experiment would become feasible provided that the detector area allows a sufficient fraction of the neutrons scattered in a particular event to be recorded.

The wavelength resolution $\Delta\lambda/\lambda = 0.0039$ can be achieved for an epithermal moderation time of order 1 μs, coupled with a chopper of matching pulse length with an incident flight path

$$L_o = \sqrt{2}\ \frac{h}{m\lambda}.\ \Delta t_{mod} \times \frac{\lambda}{\Delta\lambda} = \sqrt{2} \times \frac{0.3956 \times 10}{0.0039}\ \text{cm} = 14\ \text{m}.$$

The resolution in Q will have components $\Delta Q''$ from the uncertainty in incident wave vector, and $\Delta Q^{\perp}$ from its finite angular collimation. In this case $k_o = 66.3\ \text{Å}^{-1}$ and $\frac{\Delta k_o}{k_o} = \frac{\Delta\lambda}{\lambda}$ so that $\Delta k_o = 0.26\ \text{Å}^{-1}$.

This nicely matches the assumed wave vector resolution of $0.4/\sqrt{2}\ \text{Å}^{-1}$. The incident angular collimation required for this resolution is

$$\alpha_o = \frac{\Delta Q/\sqrt{2}}{k_o} = \frac{0.283}{66.3} = 0.0043 \qquad (0.4^o).$$

This would be achieved with a 5 cm moderator and sample aperture at the 14 m incident flight path.

Since incident and scattered wave vectors would be roughly equal, similar distances and angular collimations would apply on the scattered wave vector side. With a scattering angle $\phi = 1.25^o$, a 14 m scattered flight path implies counters distant some 30.5 cm from the incident beam. At this size the counter could well be a time-analysed position sensitive detector.

3.3.2 Inelastic Polarization Analysis Spectrometer

Because of intensity problems, it is difficult to specify the instrument parameters with any great confidence at present, however the following parameters give some indication of our requirements:

$Q \sim 5\ \text{Å}^{-1}$, $\Delta Q \sim 0.1\ \text{Å}^{-1}$

$\hbar\omega \sim 0.05$ eV, $\Delta\hbar\omega \sim .005$ eV.

Figure 2.7 shows a possible experimental arrangement for this instrument. The incident beam is polarized and flipped as for the total scattering polarization analysis instrument discussed in Section 3.2.2. The spin and energy analysis can conveniently be carried out simultaneously using conventional Co:Fe polarizing crystals, which in this case would be set to reflect neutrons with scattered energy $E_1 \sim 0.05$ eV. The scattered flight path must be minimised, since the incident energy is evaluated by subtracting the time after the scatter from the total flight time.

4. SPECIAL TECHNIQUES

4.1 POLARIZED NEUTRONS

In the instruments described in Section 3, four different methods for polarizing neutron beams are utilized; these are now discussed in more detail.

4.1.1 Polarized Proton Filter

This is the only polarizing method suitable for a white neutron beam. In a filter containing polarized protons the scattering cross-sectionsfor the two neutron spin states are sufficiently different that one of the states can be preferentially scattered out of the filter with a tolerably small loss of intensity of the transmitted component. The best filter material would seem to be a hydrated double nitrate salt LMN in which the free protons in the water of crystallisation are dynamically polarized using the 'solid effect'. Polarized proton targets have been studied and used in high energy physics work for well over a decade, and the technology required to construct such devices is now routinely available. A 1.5 cm thick LMN filter with proton polarization $\sim$ 80%, would transmit $\sim$ 50% of the neutrons in the required spin state with a polarizing efficiency $\sim$ 75% over most of the energy range up to 1 eV, but with a superior performance towards lower energies (E < 0.1 eV).

4.1.2 Polarizing Crystals

Magnetised ferromagnetic single crystals such as Co:Fe have been used extensively as polarizing monochromators for diffractometry work near wavelengths $\sim$ 1 Å at steady state reactors. These crystals have very low mosaic widths ($\sim$ 5') therefore their reflectivities are in general about 10 times lower than those of the best non-polarizing monochromators. They may however be used to great effect on pulsed source instruments in an inverse geometry configuration where the energy and spin analyses are carried out simultaneously, and an obvious application is in an inelastic polarization analysis instrument with a pulsed white polarized incident beam. One disadvantage of these crystals is that the d-spacings of the useful reflecting planes are higher than ideal; this leads to small reflection angles and often poor energy resolution eg, for Co:Fe where the neutron energy E = 0.05 eV we calculate an energy resolution $\Delta E/E \sim 0.09$ where the crystal acceptance angle $\Delta\theta \sim 1^{o}$.

4.1.3 Polarizing Sollers

Magnetised mirrors have a spin-dependent refractive index for neutrons and the two critical angles for total reflection can be used to polarize cold neutron

beams. The method is particularly useful for mirrors containing cobalt where, under certain conditions, the critical glancing angle for one of the neutron spin states can be arranged to be approximately zero. The polarizing properties of magnetised cobalt-iron thin films evaporated onto plastic substrates have been examined at the Rutherford Laboratory, and mirrors of composition $Co_{75}Fe_{25}$ prepared where the reflection selects essentially 100% neutrons of one spin. A prototype polarizing curved Soller has been constructed by stacking together about 15 of these mirrors to form a series of short conducting channels $\sim$ 20 cm long.

Experimental tests showed the polarizing efficiency of the device to be $\sim$ 95%, with transmittance $\sim$ 40% for the neutrons of the required spin at wavelengths greater than 6.5 Å (the critical cut-off wavelength for the system). We would now expect the technology required to produce these polarizing Sollers to rapidly improve, so that within a few years they could well become the standard polarizers and spin analysers on long wavelength instruments. Great advances in the measurement of magnetic diffuse scattering cross-sections are expected as a result of this development.

4.1.4 ^{149}Sm Polarizing Filter

The spin-dependent capture of neutrons by polarized ^{149}Sm nuclei at neutron energies near the resonance peak at 0.096 eV can be utilized to produce an efficient polarizing filter for neutrons of energies up to $\sim$ 0.15 eV. A ^{149}Sm polarizing filter is being developed at the Rutherford Laboratory, and neutron tests on a paramagnetic filter material $La_{48}Sm_2Ag_{50}$ are shortly to take place. The nuclear polarization is set up statically using the hyperfine field of the unpaired 4f electrons at the nucleus ($\sim 3 \times 10^2$ Tesla), by cooling the filter to temperatures $\sim$ 0.02 K in the mixing chamber of a dilution refrigerator; a modest magnetic field $\sim$ 0.3 Tesla is applied which ensures complete polarization of the samarium unpaired electrons under the conditions of the experiment. The polarizing efficiency and transmittance of the filter are strongly neutron energy dependent, due to the capture cross-section variation across the resonance, and typical calculated values are $\sim$ 80% for the polarizing efficiency, and 40% for the transmittance of the neutrons of required spin. The energy-variation of these parameters is of little consequence in polarized beam experiments since one is generally interested in the measurement of a flipping ratio, rather than in absolute intensities. This type of filter is easier to construct, less expensive, and simpler to operate than a polarized proton filter, and should be considered for the total scattering polarization analysis instrument, provided that measurements are not required at neutron energies > 0.15 eV.

4.2 TECHNIQUES WITH VERY HIGH ENERGY NEUTRONS

In order to construct the very high energy transfer spectrometer described in Section 3.3.1, energy selection and detection methods which are now available at neutron energies $\sim$ 0.5 eV will require considerable development in order that they can be utilized at energies up to 10 eV.

4.2.1 Selection of Neutrons with 10 eV Incident Energies

A chopper which defines the incident energy of neutrons around $E_o \sim 10$ eV must be constructed of a material which is opaque to neutrons at this energy; this requires the use of boron steel rather than gadolinium. A fast chopper, diameter $\sim$ 0.75 m, and made of aluminium, plastic and steel, with slits defined by a phenolic laminate has been operated over the neutron energy range 1 eV < E < 10 keV at Brookhaven. Extrapolating from the Brookhaven experience, it is probable that a 0.25 m diameter chopper could be built using the conventional Harwell design which can be spun at a frequency $\sim$ 30,000 rpm. This is 10 times the spallation source repetition rate, and for 0.4 mm slit widths, gives a burst width $\sim$ 1 μsec. A straight through rotor of this type only transmits neutrons of energies > 88 eV, therefore a curved slit rotor is needed. In order to achieve 0.8% energy resolution in E_o, we estimate that the (Neutron Speed)/(Tip Speed) ratio required for the curved slit rotor is $\sim$ 100, and this necessitates using very thin slits with small curvature. One method of retaining the material integrity is to have aluminium slits together with heavy metal slats. 0.25 m aluminium has a neutron transmission $\sim$ 10%, and, assuming a slit to slat ratio of 1, the transmission factor for this curved slit chopper is estimated to be only $\sim$ 5%. We emphasise that considerable effect would be required on fast chopper development in order to build a direct geometry instrument suitable for measuring high energy transitions.

4.2.2 Detection of 10 eV Energy Neutrons

In contrast with ionising radiation, neutrons are detected by absorption in a convecter material, which then gives charged particles which are detected by gas ionisation or scintillation. The requirements for good detection are that both the initial capture efficiency of the neutrons and the conversion efficiency to secondary particles must be high. A consideration of neutron capture cross-sections at a neutron energy 10 eV suggests that viable detection systems may be considered using conventional methods with either ^{3}He or ^{10}B as the absorbers.

Two basic types of detector are possible; (a) a gas detector using ^{3}He, and (b) a foil/scintillation detector using ^{10}B. For gas detection systems the

efficiency of conversion to secondary particles is 100%, thus the overall detector efficiency depends only on the neutron capture cross-section, which for ^{3}He at 10 eV is 260 x 10^{-24} cm^2. Estimated values of the detection efficiency for a 10 atm ^{3}He detector as a function of thickness at 10 eV are shown below:

Detector Thickness (cm)	Detector Efficiency (%)
1.5	10
4.0	25
10.0	50
17.0	70

In contrast, foil detection has a much lower collection efficiency of secondary products once the α-range is exceeded, in ^{10}B this is 3.8 x 10^{-4} cm. We have considered a multiple foil detector of 3.8 x 10^{-4} cm thick ^{10}B coils separated by 0.1 cm of scintillator. Using the published cross-section data for ^{10}B (200 x 10^{-24} cm^2 at 10 eV) we have estimated the following efficiencies for the foil detector:

Number of Foils	Total Detector Thickness (cm)	Detector Efficiency (%)
10	1	10
65	7	50
113	12	70

Both the systems considered have comparable efficiencies and thicknesses. However, if high count rates (> 10^{4} n s^{-1}) are expected at the detector, then the lower dead time of the foil detector would give this a distinct advantage over the gas detector.

4.2.3 Simultaneous Energy Selection and Detection at 6 eV

We suggest that a realistic alternative method for measuring very high energy transfers is to use an inverse geometry instrument, in which both the energy analysis and detection are carried out simultaneously using a resonance detector. A possible example is to use ^{238}U which has a sharp (width 0.028 eV) resonance capture peak at a neutron energy 6.67 eV; neutron capture leads to a (n,γ) process and the emitted γ's may be counted using a lithium-drifted germanium

detector. The narrow resonance width allows the instrument to have an energy resolution $\sim$ 0.4%, and the energy transfers could be measured to an accuracy $\sim$ 5 to 10% in $\frac{\Delta\hbar\omega}{\hbar\omega}$. The spectrometer analyses essentially at fixed energy, therefore the detected pulses must be time-sorted so as to extract the inelastic scattering processes. In order to achieve the required energy resolution the incident flight path must again be long $\sim$ 15 m.

SOLID STATE PHYSICS: INSTRUMENTS

Instrument	Moderator	Specification	Field
Total Scattering Polarization Analysis Spectrometer	300K	Q up to 20 Å^{-1} spin analysis of scattered beam	Determination of elastic spin-dependent cross-sections in magnetic and nuclear spin-incoherent systems.
Very High Energy Transfer Spectrometer	300K	$\hbar\omega \sim 1$ eV $\frac{\Delta\hbar\omega}{\hbar\omega} \sim 0.1$ $Q < 4\ \text{Å}^{-1}$	Electronic excitations: Band energies in semi-conductors. Valence fluctuations.
High Energy Transfer Spectrometer	300K	$100 < \hbar\omega < 300$ meV $\Delta\hbar\omega \sim 5$ meV $\Delta Q \sim 0.1\ \text{Å}^{-1}$ low Q bank required	Phonons, magnons, crystal fields, vibrational modes and liquid dynamics.
Moderate Energy Transfer Spectrometer	300/77K	$0 < \hbar\omega < 50$ meV $\frac{\Delta\hbar\omega}{\hbar\omega} \sim 0.02$ $\frac{\Delta Q}{Q} \sim 0.1$	Quasi-elastic scattering from plastic and liquid crystals, intermolecular modes of crystals, magnetic crystal field levels.
Rotating Crystal Spectrometer	300/77K	$0 < \hbar\omega < 50$ meV $\Delta\hbar\omega \sim 0.02$ $\frac{\Delta Q}{Q} \sim 0.1$	Molecular modes, crystal field levels, paramagnets, plastic and liquid crystals.
Inelastic Polarization Analysis Spectrometer	300K	$\hbar\omega \sim 50$ meV $\Delta\hbar\omega \sim 5$ meV $Q \sim 5\ \text{Å}^{-1}$ $\Delta Q \sim 0.1\ \text{Å}^{-1}$ Spin selection of both incident and scattered beam	Separation of spin-flip and non spin-flip scattering.
Constant Q Spectrometer	300/77K	$\hbar\omega < 200$ meV $\frac{\Delta\hbar\omega}{\hbar\omega} \sim 0.05$ $3 < Q < 6\ \text{Å}^{-1}$	Triple axis analogue: scans in energy through $(\underline{Q},\omega)$ space at constant $\underline{Q}$.
Elastic Diffuse Spectrometer	20K	$0.05 < Q < 2\ \text{Å}^{-1}$ Polarized incident beam option	Effects of doping, alloying, heat treating and irradiating condensed systems. Magnetic defects.
Very Low Q Spectrometer	20K	$Q \sim 0.01\ \text{Å}^{-1}$ $\Delta Q \sim 10^{-4}\ \text{Å}^{-1}$	Defects and structural periodicities on the scale ~ 100 Å.

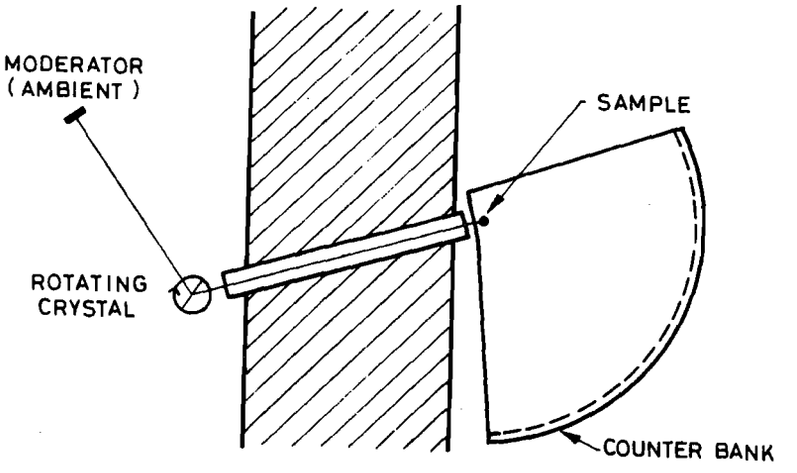

Figure 2.1 Rotating crystal spectrometer

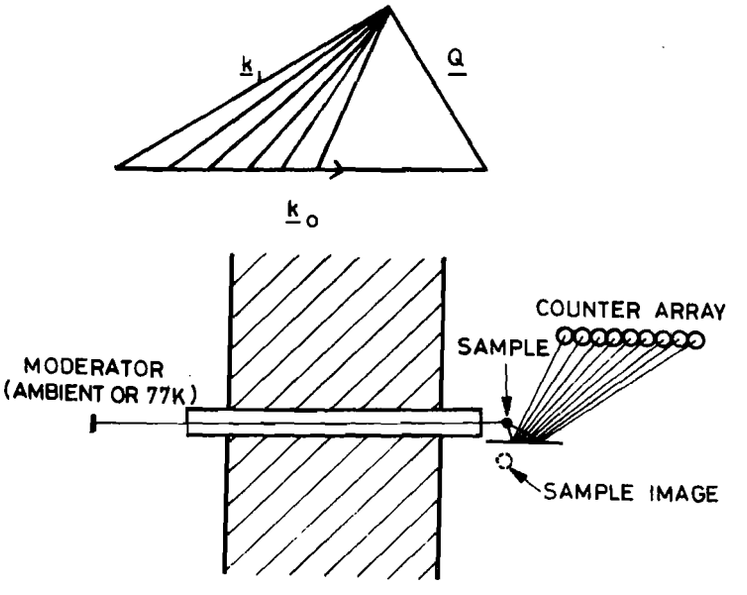

Figure 2.2 The constant Q spectrometer

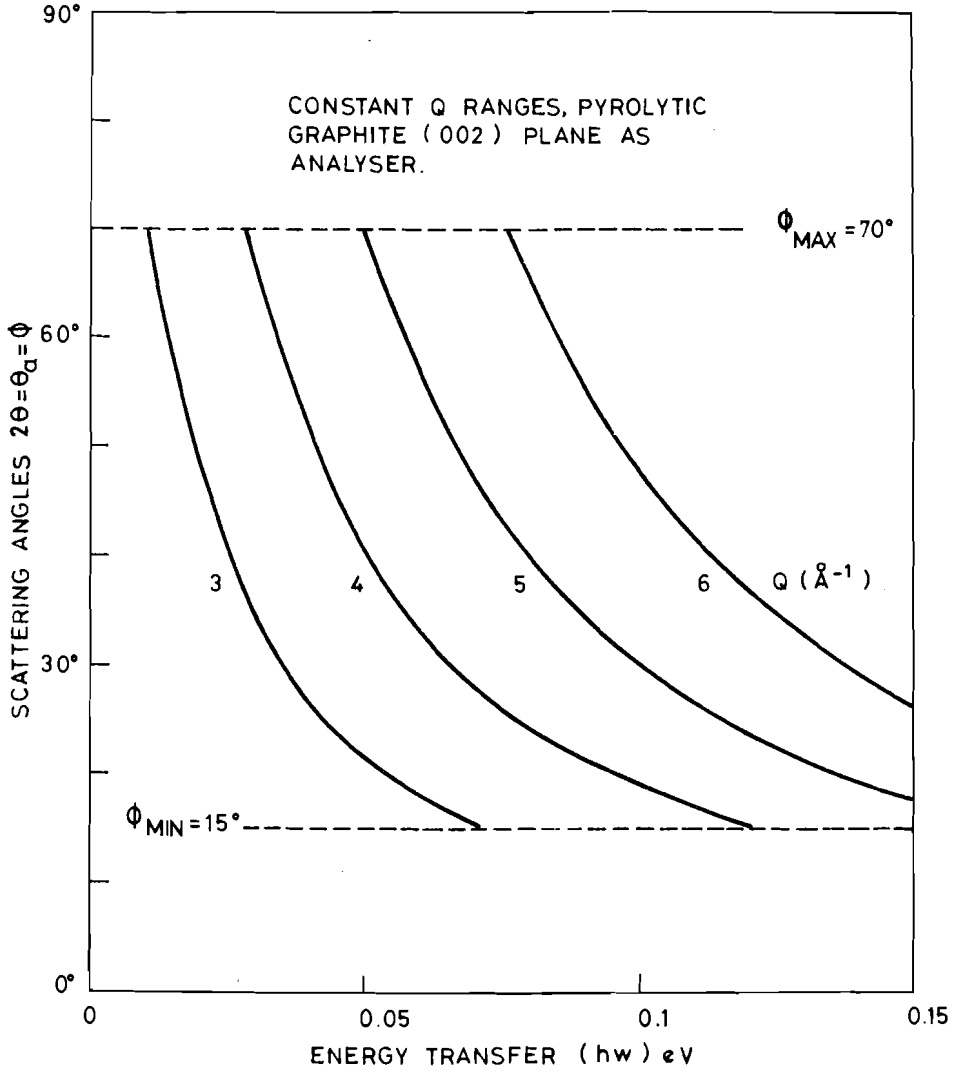

Figure 2.3 Scattering angles as a function of energy transfer for constant Q Spectrometer with pyrolytic graphite (002 plane) as the analyser.

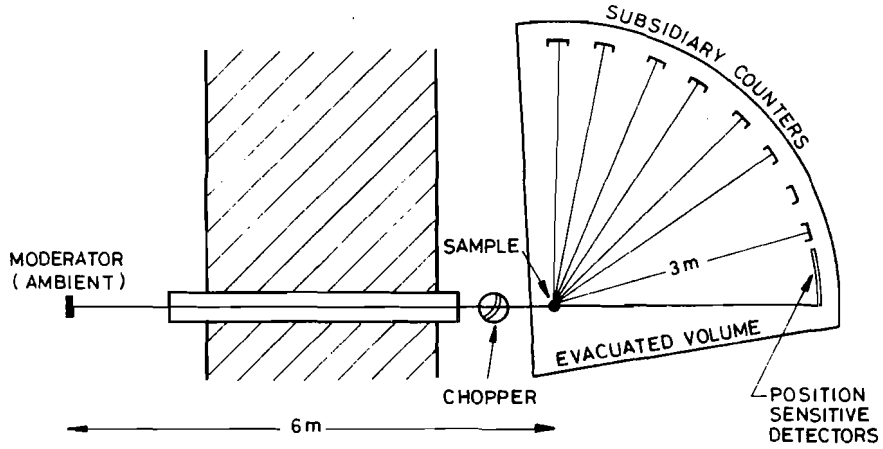

Figure 2.4 High Energy transfer inelastic spectrometer.

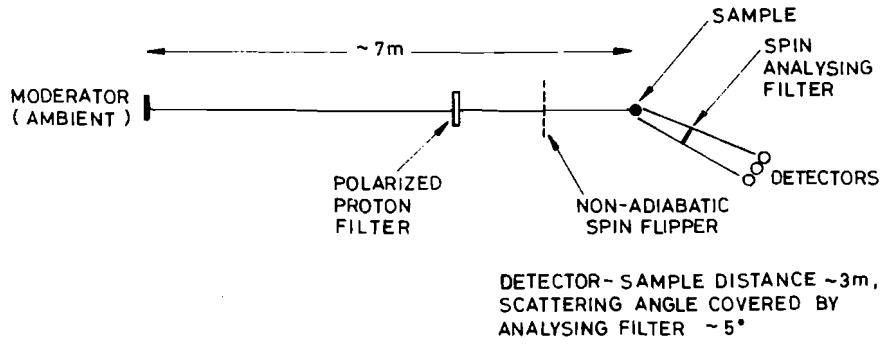

Figure 2.5 Total scattering polarization analysis instrument

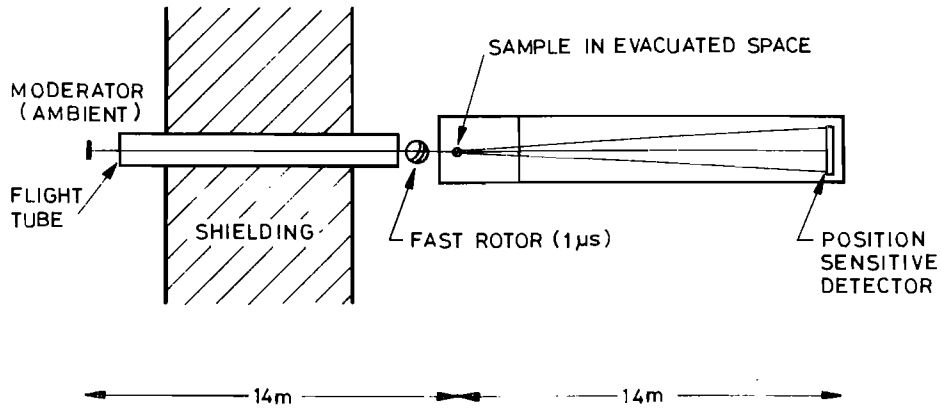

Figure 2.6 Very high energy transfer Spectrometer.

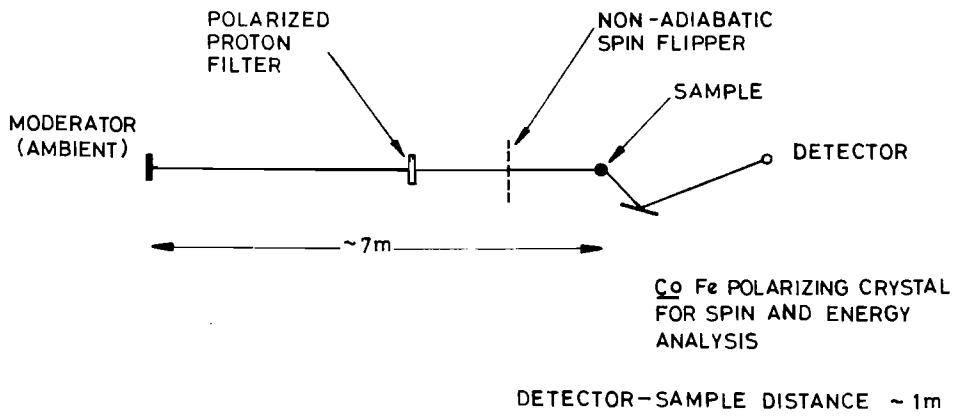

Figure 2.7 Inelastic polarization analysis Spectrometer.

SPALLATION NEUTRON SOURCE SCIENCE PANEL

Working Group B : Fluids and Amorphous Solids

Dr J H Clarke	Physics Department University of Kent
Dr G J Coombs	Physics Department University of Edinburgh
Dr J C Dore	Physics Department University of Kent
Professor J E Enderby (Convener)	Physics Department University of Leicester
Dr M W Johnson	Neutron Beam Research Unit Rutherford Laboratory
Dr B H Meardon (Secretary)	Neutron Beam Research Unit Rutherford Laboratory
Dr G W Neilson	Physics Department University of Leicester
Dr V T Nguyen	Physics Department University of Leicester
Dr B R Orton	Physics Department Brunel University
Dr D I Page	Materials Physics Division AERE Harwell
Professor J G Powles	Physics Department University of Kent
Mr P Schofield	Materials Physics Division AERE Harwell
Dr A C Wright	Physics Department University of Reading

FLUIDS AND AMORPHOUS SOLIDS

TABLE OF CONTENTS

1. THE APPLICATION OF NEUTRON SCATTERING TO GASES, LIQUIDS AND AMORPHOUS SOLIDS

1.1 INTRODUCTION

Over the last ten years, neutron scattering studies of liquids and amorphous materials have had a profound influence on our understanding of these states of matter. In the case of 'simple' liquids, for example, diffraction studies have stimulated advance in the theory of the relationship of the structure factor to the interparticle forces. This has led to procedures for calculation of interparticle potentials, requiring more extensive and more accurate measurements over wide ranges of temperature and pressure. Inelastic scattering, and in particular, quasi-elastic incoherent scattering has given insight into atomic motions in simple liquids revealing that the basic hypotheses on which many theories of transport in liquids were based were wrong.

Current theories of the dynamical structure factor of simple fluids aim to cover the whole range from dilute gas to triple point liquid density. Neutron intensities from present day sources are too low to permit studies on dense gases as detailed as those that have been carried out on liquid argon.

In molecular liquids and glasses, the advantages of a pulsed source have already been demonstrated with the Harwell linac in the determination of molecular bond lengths, through the ability to measure large values of the scattering vector. Higher data collection rates would make possible more extensive studies of the effect on bond length and orientational ordering of the physical state of the systems - in particular the effect of fabrication processes on the structure of glasses.

Neutron molecular spectroscopy again is another area of research - not only in the liquid state - which would benefit from high intensity of neutrons in the appropriate energy range to study the changes in vibration frequency and amplitude induced by changing chemical environment. Such studies have an important role to play in understanding the basic mechanisms of catalysis and corrosion.

In many cases the liquids studied with neutrons have been severely limited to materials with favourable neutron cross-sections for the components. For example, many elements with a high '1/v' cross-section could be studied by using incident neutrons of higher energy where absorption cross-sections are lower. An extension of this is the use of the wide range of wavelength

available from a pulsed source to exploit the variation of scattering lengths with energy. A simple case would be to reduce the effect of absorption in experiments involving He^3 or Cd samples. Furthermore 'anomalous scattering' near resonances can be used to vary scattering amplitudes in structural studies. Test experiments of this type have been carried out on steady state sources but the low flux in the 0.1 to 100 eV range has limited their usefulness. Weakly scattering elements could be studied more effectively with the low background of a pulsed source.

The proposed spallation source will emit pulsed white beams of neutrons and this gives rise to four characteristic features for the study of fluids and amorphous solids. In the following sections these features are discussed in detail. We then show how each of them, either singly or in combinations, allow a wide variety of experiments, necessary for a basic description of disordered systems, to be carried out.

1.2 FEATURES OF THE SPALLATION NEUTRON SOURCE

1.2.1 High Flux

For making comparisons with the present sources it is convenient to divide the energy (E) into three regions.

(a) An epithermal region E > 900 meV, (λ < 0.3 Å)
In this region the SNS will enable measurements to be made which at present are not possible on steady state reactors. Furthermore the gain factor over the present Harwell linac, which at present is the best available high energy source, will be about 15000.

(b) An ambient region 900 meV > E > 20 meV, (0.3 Å < λ < 2 Å)
In this region there is an estimated gain of a few orders of magnitude over current steady state sources.

(c) A long wavelength region E < 20 meV, (λ > 2 Å)
In this region the estimated flux will be comparable to that available at the ILL.

For the studies of fluids and amorphous solids (a) and (b) are the regions of particular interest and it is in these that the greatest gains are to be expected. The higher fluxes can be exploited to enable conventional experiments to be carried out with:

(a) higher statistical accuracy
or
(b) rapid rates of data acquisition
or
(c) small samples

Furthermore the development of entirely new techniques which are at present hampered by inherently low fluxes becomes feasible. For example, the development of useful polarization analysis instruments is at present severely handicapped by the low fluxes available.

1.2.2 Short Wavelengths

Pulsed sources utilising thin moderators have a characteristic undermoderated spectrum, which, in the epithermal region, decays as 1/E. Such a moderator will enable a range of experiments to be performed which is at present inaccessible. The main advantages of this spectrum are summarised as:

(a) At higher energies the absorption of most materials is lower and hence experiments with highly absorbing samples are possible.

(b) To extract structural information from total scattering experiments inelastic scattering corrections have to be made. These corrections are easier to make at higher neutron energies.

(c) The new region opened up by the intense epithermal spectrum enables higher spatial and time resolution to be achieved. Interatomic distances can be measured to better than 0.01 Å and atomic motions measured on a time scale of 10^{-14} secs.

1.2.3 Nature of Source

A pulsed source with a wide energy spectrum offers the following advantages:

(a) A simultaneous measurement can be made of intensities over a wide range of momentum transfer, given by $\hbar Q$ where Q is the scattering vector.

(b) Neutrons are counted between pulses implying low background.

(c) By synchronising the neutron pulse with a sample perturbation (such as magnetic field or pressure) the study of time dependence effects can be developed.

1.2.4 Fixed Scattering Angle

The collection of data over a wide range of momentum transfers at a single angle simplifies the design of furnaces, cryostats, magnets and pressure cells.

1.2.5 Practical Advantages of these Features

These can be summarised conveniently under eight headings and will be referred to frequently in the remainder of the report.

I Data can be obtained with a much higher statistical accuracy, provided, of course, care is taken to keep the background radiation as low as possible.

II Measurements can be made at a higher rate of data collection, for example, a total structure factor for $0 < Q < 100$ Å^{-1} for a multi-component glass could be obtained in ten minutes as opposed to one week as at present.

III The use of much smaller samples than hitherto becomes feasible. This is valuable in the case of expensive materials or for those samples in which isotopes of limited quantity must be used.

IV Experimentation will also be possible on samples which are 'small' in the geometrical sense (eg, surfaces or thin films) or in the chemical sense (eg, dilute solutions where the behaviour of the solute is of particular interest).

V The use of higher energies greater than 1 eV enables studies to be made of highly absorbing samples.

VI Kinematic corrections at high incident energies, particularly for fluid systems, are smaller and better controlled.

VII Wide regions of momentum and energy transfer become accessible to the experimenter. We expect the domain of $(Q,\hbar\omega)$ available to be between $(0.3$ Å^{-1}, 0 eV) and $(100$ Å^{-1}, 0.5 eV).

VIII The use of a fixed scattering angle enables studies of samples to be undertaken under extreme conditions of temperature and pressure which are otherwise difficult or impossible.

2. STRUCTURAL STUDIES

2.1 INTRODUCTION

The study of fluids and amorphous solids by neutron scattering provides information on the structure and dynamics of the materials. These in turn provide information on the interaction of molecules with each other and interactions within the molecule. It is convenient to subdivide the subject into simple fluids, various types of liquids and amorphous solids, although certain problems of interest will span these divisions.

2.2 SIMPLE FLUIDS

The study of pure noble-gas fluids is at present heavily influenced by computer simulation which gives an unambiguous description of kinetics and structures of fluids interacting with realistic and hypothetical pair potentials. There is, however, a lack of very accurate measurements of the structure factor, S(Q), over a wide range of temperature and pressure. Three regions of the p,V,T diagram of particular interest are (a) the dense fluid region, far from the triple point, (b) the liquid region, near to the triple point and (c) the region of the critical point. There will in general be differences between the atomic interactions, derived from S(Q), when these measurements are compared although they may be rather subtle. For such measurements to be of value, structure factor data of better than 1% accuracy are required to give effective pair potentials to a precision of 10%. In addition to calculating pair potentials accurate pressure derivatives of the structure factor will give information related to the triplet distribution function. These measurements can be made with relatively simple pressure cells using the proposed neutron source. Further, this investigation would provide an opportunity to test the various theories of the fluid state. An attempt to investigate the distortion of the structure factor which results from fluid flow, which would have an impact on the theory of transport properties, will also be worthwhile.

As the structure factor for ^{36}Ar at $85^{o}K$ has been determined to an accuracy of 1% (though only to a limited Q_{max}) it could play an important role in testing the accuracy of the proposed instruments associated with the new source. Further, if $S(Q,\omega)$ were obtained for Ar, and integrated over a wide range of ω, the corrections which must be applied to the observed counts can be subject to unprecedented and indeed rigorous scrutiny.

Recent work on the partial structure factors of mixtures of noble gases, in the long wavelength limit, has indicated that the interaction between components departs significantly from ideality. However, very accurate measurements of the partial structure factors at nonzero Q values, using the method of isotopic substitution, are necessary to reveal the expected deviations from ideal mixing. Again, variations of composition, temperature and pressure are required to give complete information about these mixtures and the selection of conditions would be guided by the need to test existing theories.

The broad programme described above exploits the advantages I, III, VI, VII and VIII listed in Section 1.2.5.

2.3 LIQUID METALS AND ALLOYS

The outstanding problem in the physics of liquid metals is to determine the extent to which the distribution of the ions reflects and is influenced by the electron gas. In the simplest case, an effective pair potential, $\phi(r)$, can be thought of as representing the interactions between the ions, appropriately screened by the electron gas. Self-consistent methods which relate $\phi(r)$ to $S(Q)$ require an accurate knowledge of $S(Q)$, particularly in the region for $Q < 2\ \text{Å}^{-1}$, over ranges of temperature and pressure. We therefore wish to exploit the advantages listed as I, VI and VIII in Section 1.2.5. The need to compare x-rays and neutron scattering to a high degree of accuracy has also recently been emphasised. This enables information about electron - ion correlations to be obtained, knowledge of which is basic to our understanding of electronic properties.

Under extreme conditions, liquid metals are known to undergo a metal-insulator transition. A considerable body of knowledge including conductivity, thermopower and density data is now beginning to be assembled. Structural measurements and the related problems of effective ionic pair potentials and electron - ion correlation functions represent a major area where the new source, for similar reasons to those just described, will play a major role.

When one metal is dissolved in another liquid metal, three broad types of behaviour have been observed:

(a) metallic behaviour with a statistical distribution of ions

(b) metallic behaviour with clustering of ions

(c) semi-conducting behaviour implying the existence of ionic or covalent or mixed bonds.

The occurrence of such diverse behaviour is not understood and arises from that area of science common to physicists, metallurgists and chemists. It is therefore proposed to investigate the partial structure factors for a wide range of liquid alloys. Such a programme of research would undoubtedly have a major impact on our understanding of alloy properties generally. The experiments will involve data from isotopically different samples, however, and call for high precision and accuracy. Several alloy systems of interest (eg, Li-Pb, Ag-Te) have substantial absorption. This broad programme utilises features I, III, V and VI, all of which are critical for its success.

It also becomes feasible to consider anomalous scattering close to resonance absorption edges as a method of extracting partial structure factors. Possible isotopes include ^{113}Cd (resonance at 0.68 Å), ^{109}Ag (0.125 Å), ^{115}In (0.237 Å) and ^{133}Cs (0.12 Å). Although this is a relatively new technique, it opens up new and exciting possibilities for liquid alloy work, particularly for systems involving heavy elements and those for which no suitable stable isotopes exist.

A further application of either isotopic substitution or anomalous scattering is in the domain of alloy critical scattering. The occurrence of phase separation in such diverse liquid alloys as Ni-Na and Ga-Bi offers a wide range of possibilities for the study of critical experiments in a variety of metallic systems.

With more highly developed polarization techniques and an intense neutron beam, the nature of magnetism in liquid transition and rare-earth metals - a subject still in its infancy but one which already is beginning to reveal interesting new concepts - will be investigated using the full power of neutron scattering and exploiting particularly advantages I and VII.

2.4 MOLTEN SALTS

The structure of molten salts (ie disordered systems in which there is a strong interaction through Coulomb forces) is a topic of long standing interest. Recently the possible technological applications of superionic conductors such as AgI and of molten salts as battery materials have increased the interest in ionic interactions. Fundamental problems in these types of liquid are:

(a) the short range repulsive part of the ion-ion interaction

(b) the role of polarization

(c) mechanism of ion transport.

A programme to investigate the partial structure factors of molten salts is already under way in the UK and experiments yielding new information have already been carried out on the salts CuCl, NaCl and RbCl. These were chosen because, of all the elements, the isotopes of chlorine show the largest variation in scattering length and hence the effects are easier to measure. If the programme is to be extended to include other elements, and later, tertiary and more complicated systems, the experimental technique will be beyond the capabilities of present day sources and all the advantages listed in Section 1.2.5 can therefore be used to obtain reliable and accurate data.

2.5 AQUEOUS SOLUTIONS

Our knowledge of the structure of aqueous solutions has advanced following a series of experiments using the high flux reactor at Grenoble. These experiments are carried out at fixed concentration on solutions using solute ions of varying isotopic abundance. By first order and second order differencing of data it is possible to determine the ion-solvent and ion-ion arrangement respectively. At present, the investigations are limited to a small number of favourable isotopes where the degree of statistical uncertainty is minimised, eg saturated sodium chloride and nickel chloride solutions.

The new source will increase the statistical accuracy of the data and, for reasons III, V and VI of Section 1.2.5, will enable a study to be undertaken on a wider variety of solutions. A general picture of electrolyte structure will be built up, and tests of the validity of a variety of computer simulated models will be made. Because of the wider range of solute-solvent correlations, it will be possible to assess the degree to which various ions enhance or reduce the bulk water structure, a fundamental problem in electro-chemistry.

With the new source, solutions of higher dilution can be studied. In favourable cases, investigations will be made on the ion-ion correlation to observe where the $c^{1/3}$ behaviour passes over to the $c^{\frac{1}{2}}$ behaviour characteristic of the Debye-Huckel regime. The ion-solvent structure will also be investigated at lower concentrations, corresponding to regions of greater biological significance.

Several interesting structural effects arise under the application of high pressures on electrolyte solutions. It will be possible to complement the indirect structural information obtained from viscosity and conductivity measurements on various salt solutions with those obtained from neutron

scattering, and obtain a more detailed picture of the influence of pressure on the ion-solvent structure. The new source is ideally suited for such studies (VIII of Section 1.2.5).

Polarization analysis techniques can in principle enable new insights to be gained about the spatial distribution of the hydrogen nuclei in water containing systems. As emphasised in Section 1.2.1 such developments are severely limited by the comparatively low level of neutron flux available at present.

Spin analysis techniques using polarized neutrons have shown that coherent and spin-incoherent scattering can be separately determined for deuterium-containing liquids such as heavy water. The increased flux and an improved polarization instrumentation would enable these techniques to be used for hydrogenous materials. This would have immediate importance for the structural study of water as it would enable a third independent measurement to be made, which in principle provides all the required partial structure factors. Furthermore, the methods would lead to the development of facilities for detailed study of the wide range of organic fluids which have previously been neglected in structural studies.

2.6 MOLECULAR FLUIDS

Even the simplest molecular fluids, homonuclear diatomic molecules are, from the point of view of structure, an order of magnitude more complex than the noble-gas fluids discussed in Section 2.2, because of the additional degrees of freedom associated with the relative orientations of the particles.

Neutron structure factor measurements are one means of studying orientational correlations in molecular fluids. It has been possible with the present facilities to determine favourable configurations for pairs of molecules in liquid nitrogen, oxygen and bromine. However, a thorough study of even such simple molecular systems over the thermodynamic phase diagram, combined with an extensive programme of computer simulation would increase our understanding of the liquid state.

For more complex small molecules, studies of the structure of the dense gas phase, not possible with present intensities are desirable: modifications in molecular configuration due to collisions should be detectable and information obtained on the rigidity of the molecules.

At high (liquid) density, studies over a wide Q range are required for a range of temperature and pressure. Intermediate Q is capable of yielding information on the orientational ordering and temperature variation on rotational freedom. Work at high pressure might reveal the existence of different orientational phases (similar to those in liquid crystals). Measurements exploiting the high Q range of the source (up to 100 $\AA^{-1}$) give information on the structure of the molecule and in particular the bond lengths (see Section 2.8).

2.7 QUANTUM FLUIDS

The study of liquid ^{3}He and liquid ^{4}He by neutron scattering shares with other liquids the general advantages to be gained from the use of the new source. However there are specific considerations that apply to quantum liquids.

As far as the static structure factor S(Q) is concerned, ^{4}He may, to a good approximation, be regarded as a dense classical fluid. There is no major change as the temperature is varied through the λ-point. Not unexpectedly, the various more-sophisticated theoretical approaches give reasonable agreement with the experimental results. Thus for a stringent test of theory accurate results are required. The high-Q region, unavailable to x-rays, will become accessible. As these theoretical approaches also give the population of the Bose condensate - a quantity of central importance to the understanding of superfluidity - their critical appraisal is essential.

As a result of the extremely high absorption of ^{3}He there have so far been no measurements of S(Q) with neutrons. The reduction of absorption with increasing incident neutron energy as well as the other advantages of the new source will allow the measurement over an extended range of scattering vector.

The recently discovered superfluid phases of ^{3}He have exhibited a whole new range of behaviour despite the severe technical problems associated with obtaining temperatures in the mK region. Structural studies of ^{3}He - ^{4}He mixtures will allow the nature of the ^{3}He - ^{4}He interaction to be deduced and in turn will help solve the general problem of the interaction potential.

2.8 AMORPHOUS SOLIDS

The structures of amorphous solids are more complicated than those of ionic or molecular liquids so that a greater emphasis is placed on Fourier trans-

formation and the analysis of data in real space. Since the real space resolution obtained in any experiment is inversely proportional to Q_{max} the new source has a decisive advantage over steady state reactors.

Most inorganic glass structures are based on covalently bonded networks ranging from the simple one-dimensional chains found in selenium and many phosphates to the fully three-dimensional silicates. The glasses in common use are multicomponent systems (eg, Na_2O-CaO-SiO_2) and the elements present are not amenable to the technique of isotopic substitution. By far the most effective method of studying the structure of these glasses is by systemmatically varying the composition and we propose a broad programme of structural analysis.

The glass transition region is far from understood and if the time for structural determinations is reduced to the order of a few minutes extremely interesting kinetic studies will be possible. The great advantage of the time of flight technique for kinetic studies is that there is no time lag between measurements at different values of Q. The best glasses for preliminary investigation are those with relatively low glass transition temperatures eg, As_2S_3, BeF_2 or systems based on V_2O_5. High pressure measurements are also of importance particularly on the compacted states of SiO_2 and B_2O_3.

A variety of thin films can be made by vapour deposition (eg, Se, As-S and As-Se) and these have structures which are very dependent on preparation conditions. There is considerable interest in the extent to which the network structure of bulk glasses gives way in thin films to a more molecular character. For example, recent work on As-S indicates that this may have a structure based on a random packing of roughly spherical As_4S_6 molecules. So far the only neutron experiments on thin films have been on As-S and amorphous Ge, the major difficulty being the small amount of sample available. Similar considerations apply to other modes of preparation such as splat cooling and chemical deposition.

There is an increasing interest in the magnetic properties of amorphous solids which can be investigated by means of neutron scattering measurements at low Q. Short range ferromagnetic ordering has been observed in Tb-Fe and antiferromagnetic ordering in vitreous Fe_2O_3 - P_2O_5. In both cases neutron scattering techniques have been used to extract the neutron magnetic correlation function.

For an amorphous solid the equilibrium atomic positions are time independent and it is possible to carry out purely elastic diffraction experiments in order to measure the time averaged space-time correlation function $G(r,\infty)$. These experiments are significant in that they provide an independent check of the dynamic corrections used in total diffraction experiments and can be used to study anharmonicity and to determine the directionally averaged r.m.s. thermal atomic displacements. The advantages of the SNS for elastic diffraction are the same as those for total diffraction with the added benefit that it is possible to employ correlation techniques to increase the scattered intensity.

In summary, then, we see particular advantage in the study of glasses acruing from features II, III, IV, VI and VII in Section 1.2.5.

3. DYNAMICS

3.1 INTRODUCTION

The availability of a high flux of epithermal neutrons will

(a) allow $S(Q,\omega)$ to be established over much of its range with unprecedented accuracy

(b) open up domains of Q-ω space which at present are inaccessible (for example it is not possible with existing facilities to study $S(Q,\omega)$, at $\hbar\omega \sim 150$ meV for $Q < 4.4$ Å^{-1} even though it is known that for the liquid transition metals $S(Q,\omega)$ is, in this region, appreciable).

A general type of investigation which will be applied to a variety of fluids and amorphous systems will be to determine the various frequency moments of $S(Q,\omega)$. The zeroth moment yields $S(Q)$ directly and allows systematic checks to be made on the effectiveness of existing procedures for the dynamical correction as applied to total scattering measurements. The second and fourth moment are of special interest because they represent the only dynamical scattering properties which can be obtained from exact theoretical analysis and they are often simply related to physically understandable properties. For example, the fourth frequency moment is simply related to the mean square force (and thus to the potential) for atomic liquids and to the appropriate generalisation for molecular liquids.

The study of dynamics is not at present as highly developed as that for structural problems and it is therefore appropriate to divide the following

discussion into the broad headings: gases, classical liquids, quantum fluids and amorphous solids.

3.2 GASES

The existence of the SNS will make possible the accurate study of the dynamical structure factor of dense gases of atoms or molecules as a function of density. The features which can be exploited particularly are I, VI and VIII.

The scattering from non-interacting rigid molecules can be calculated exactly. Therefore by studying departures from ideal behaviour as a function of collision rate (by increasing pressure or temperature), it becomes possible to learn about the collision mechanisms themselves. In this way, for instance, it is possible to check whether such models as 'rough spheres' have any validity in representing real gases.

A fundamental problem in the theory of fluids is the treatment of the competition between simple binary collisions, which dominate at low densities, and collective mode-coupling effects which become increasingly important at high densities. These effects most strongly influence the transition region between hydrodynamic and kinetic behaviour. This transition region has been investigated at liquid densities using both neutrons and computer simulation, but the neutron data are at present limited. Light scattering has been used to investigate this transition in the low density region, but it is not useful for denser systems. The intermediate density region has not yet been investigated thoroughly by any technique. It is highly desirable to have good neutron and computer data in this region since we can, as we increase the density, 'turn on' the interesting correlated collision sequences. For this reason, careful and controlled high resolution experiments on a monatomic gas, like ^{36}Ar, should be performed to provide experimental data in a system dilute enough to be described in terms of binary collisions. By extending such measurements to higher densities the onset of higher order collective effects can be monitored. The study described above when applied to simple molecular gases will prove rewarding both for the study of collision processes themselves and their effect on the internal motion of the molecules.

Other low density systems which should be studied are metal vapours and ionised gases. Of particular interest here are the existence and behaviour of dimers and more highly associated groups of atoms or ions in the vapour phase and the most appropriate way to describe the motion of such entities.

3.3 CLASSICAL LIQUIDS

The gains described above by using the SNS in the study of gases are equally applicable to studies of dynamics of liquids. The measurement of the scattering law over a wide range of Q and ω will open up investigations of the dynamics of liquids which are at present poorly understood.

For constant low Q measurements with high energy resolution, the incoherent quasi-elastic peak width shape measurement yields the information on the rotational and translational diffusion. For higher Q the nature of the single particle motion can be investigated. In both cases isotopic variation will allow the investigation of the motion of chemically distinct nuclei in translational and reorientational diffusion processes. In principle one is able to test intermolecular potentials by comparing observed scattering laws with those derived from computer simulations using an assumed potential. The variety of behaviour and interatomic force characteristics described in Sections 2.3 to 2.5 will have parallels in the dynamic behaviour. To this extent we see the study of $S(Q)$ and $S(Q,\omega)$ to be complementary. Furthermore, feature II allows rapid measurements to be undertaken and thereby enables studies to be made of both natural and induced relaxation processes.

Finally, the enhanced flux enables one to consider, for a single element, the separate measurements of $S(Q,\omega)$ and $S_s(Q,\omega)$ (related to the coherent and self motions respectively) by the techniques of polarization and energy analysis. This technique applies in particular to a variety of liquid metals including liquid sodium about which considerable theoretical and experimental knowledge has been built up over the last decade or so.

3.4 QUANTUM LIQUIDS

Existing studies of the collective excitations in superfluid ^{4}He using neutrons, though extensive,have been significantly limited by the nature of present sources.

A much performed experiment has been the attempt to deduce the depletion of the Bose-Einstein condensate from the nature of the scattering in the independent-particle region ie, at large energy transfers. Within the impulse approximation it is expected to observe a sharp peak due to the condensate superimposed on the Doppler broadened distribution. However the experiments so far performed have been at energies insufficiently high for this approximation to be applicable and thus have depended rather heavily in their analysis on theoretical models.

The values obtained for the population of the condensate have been much less than the value of $\sim$ 10% obtained from various theoretical and numerical approaches. Estimates vary, but incident energies of at least in excess of 1 eV are required.

At intermediate scattering vectors a broad distribution is observed at energies above the one-phonon peak. This intensity is usually regarded as being due to multiphonon excitations. It is this distribution that evolves into the independent particle scattering as the scattering vector is increased. It would be of interest to be able to study this distribution with good resolution over a wide range of momentum transfer.

The behaviour of the one-phonon branch at scattering vectors beyond the roton minimum has long been of theoretical interest and recently of experimental interest. After passing through the roton minimum, the energy increases towards a limiting value, twice that at the roton minimum. It has been suggested on theoretical grounds that it should approach this value asymptotically, although recent measurements have obtained peak positions slightly in excess of this value. The problem resides in the fact that the intensity drops rapidly as the scattering vector is increased and the peak has not been observed beyond 3.5 $\AA^{-1}$. The measurement of the peak in this region at improved resolution and statistics and the extension of these measurements beyond this wave vector are highly desirable. The behaviour is dominated by roton-roton interactions and an accurate knowledge of lineshapes would allow a critical test of existing theories.

Although the interaction potential for ^{3}He is similar to that of ^{4}He, its collective excitation spectrum is fundamentally different. Unfortunately the capture cross-section of ^{3}He for thermal neutrons is extremely large and it is only recently that inelastic scattering has been observed and these results are not very extensive. Thus any gain in flux and reduction in the background would be an advantage. An increase in the incident neutron energy would lead to a reduction in the absorption, as the cross-section obeys the '1/v' law at least as high as 11 eV.

On the basis of theory the most prominent feature of the scattering from ^{3}He is the broad distribution of intensity that results from the excitation of particle-hole pairs. This is analogous to the Stoner excitations in itinerant ferromagnets. For large scattering vectors the continum of excitations becomes the independent particle scattering. As for ^{4}He, this region would be accessible with the new source.

3.5 AMORPHOUS SOLIDS

Many glasses sre predominantly coherent scatterers and in order to obtain the density of vibrational states it is necessary to make measurements at high Q where the incoherent approximation is valid. This type of experiment requires a high incident energy coupled with good resolution at low values of $\hbar\omega$.

With the SNS it will be possible to study phonon lifetimes in glasses, which are related to low temperature thermal anomalies. This involves measurements at very low Q, with a high value of incident energy to give an approximately constant Q scan across the low $\hbar\omega$ region. To make such measurements the neutron velocity must be greater than the phonon velocity and typical values for the incident energy should be in the range of 50 - 100 meV with an overall energy resolution of 1 - 2 meV.

4. PROPOSED INSTRUMENTS

We propose the following instruments for the SNS to enable the programme of measurements on fluids and amorphous solids described in the preceding sections to be carried out.

(a) Two Total Scattering Spectrometers

These spectrometers are envisaged as being similar to the present linac TSS. However, for structural studies of fluids and amorphous solids, a minimum momentum-transfer of 0.3 $\mathring{A}^{-1}$, consistent with an incident wavelength of < 1.5 $\mathring{A}$, must be available. If ambient and low temperature moderators are to be constructed, each spectrometer could view a different temperature moderator to take advantage of the different energy distributions available in the polychromatic incident neutron beams. A broad programme of work already exists for such instruments as these, covering most structural work on fluids and amorphous solids.

(b) High-Pressure Spectrometer

The use of a fixed scattering angle to facilitate the construction of high pressure cells for measurements on fluids and both amorphous and crystalline solids, is a big advantage of pulsed sources.

A purpose-built high pressure spectrometer is proposed with a high Q-value resolution ($\frac{\Delta Q}{Q} < 0.01$) to enable accurate subtraction of the

Bragg peaks produced from the windows of the pressure cell. This instrument would be used to study the pressure dependence of the structure and dynamics of many liquids and gases.

(c) Polarization Analysis Spectrometer for Structural Measurements

The availability of more intense polarized neutron beams will be especially useful in structural studies. The determination of spin-incoherent contributions to the observed cross-sections, which contain no structural information, will become possible thereby providing new and useful knowledge about the dynamical corrections. This technique will make a significant contribution to the study of proton and deuteron containing liquids.

A spectrometer is proposed that will use a polarized polychromatic incident neutron beam to study the structure of fluids and amorphous solids by total diffraction. The scattered beam in this spectrometer would be analysed solely for polarization state by a filter. If the instrument were constructed with a sufficiently high Q-value resolution it could also be used for similar experiments on powders.

(d) Polarization and Energy Analysis Spectrometer for Inelastic Measurements

An inelastic polarization analysis spectrometer is also proposed which will enable measurements to be made of $S(Q,\omega)$ and $S_s(Q,\omega)$ for liquids such as sodium and lithium. The instrument will differ from the previous one (c) in that the polarized incident neutron beam would require energy, in addition to polarization analysis. This may be done in several ways; simultaneously as on D5 at ILL using an iron-cobalt or Heusler Alloy crystal analyser, using a conventional crystal analyser and a polarization filter or using a pulsed monochromatic polarized incident beam from a chopper or rotating crystal with a polarization filter and detector.

These experiments are at present not possible on D5 due to the relatively low flux and to the poor energy resolution. Measurements of $S(Q,\omega)$ on liquid sodium would require an energy resolution of $\sim$ 1 meV at $Q \sim 1$ Å^{-1} with a maximum energy transfer of up to 200 meV. On D5 typical energy resolutions vary between 20 and 80 meV depending on the instrument configuration but are usually poor at low Q.

The continued development of polarization analysis techniques such as filters is essential to this work and cannot be overstressed. At present D5 is limited by its low intensity for this type of work and a gain of three orders of magnitude makes many studies an exciting possibility.

(e) An Inelastic High-Energy Transfer Spectrometer with a Maximum Momentum Transfer of up to 30 $\AA^{-1}$

and

(f) A Low Momentum-Transfer Inelastic Spectrometer

The requirements for these spectrometers are at present rather ill-defined. Recent measurements on liquid nickel have been hindered by the inadequate energy transfers available at low Q (eg, $Q < 4\ \AA^{-1}$). Energy transfers of at least 200 meV with good resolution (0.5%) are required to facilitate the determination of the second moment of $S(Q,\omega)$, which at present is hampered by problems of deconvolution and multiple scattering; these problems being caused principally by poor resolution and low beam intensity.

As an upper limit to such instruments studies of liquid helium require energies estimated at > 1 eV to measure the depletion of the Bose-Einstein condensate.

(g) Elastic Diffraction Spectrometer

A spectrometer is proposed using a statistical chopper to provide simultaneously both the total and the inelastic diffraction cross-sections. This information can be used in the study of amorphous solids to provide the purely elastic scattering which, in conjunction with the total scattering, gives information on the anisotropy of the atomic thermal-vibration tensors and also provides additional information on dynamical corrections.

At present this experiment can only be carried out on a triple-axis spectrometer with the attendant problems of limited Q-range and experimental availability which is, of course, linked to the slow way in which such data are collected.

5. SUMMARY AND CONCLUSIONS

It is clear from the foregoing that there is a strong case for the construction of the SNS for wide areas of research in the field of fluids and amorphous materials. The case rests on the possibility of long-term, continuing programmes of investigation of the structure and dynamics of various classes of materials and their relevance to poorly understood properties.

Broadly speaking, the scientific advantages of the proposed source which emerge from the preceding discussions are to permit the study (a) of wider ranges of composition of materials and (b) of materials over a wider range of the thermodynamic phase diagram than is possible with existing sources. Under (a) we have identified, for example; (i) the study of aqueous solutions aimed at understanding the nature of hydration processes and their consequences on the effective interactions of ions in solution; (ii) the study of liquid alloys and the correlation of their structure with electrical and other properties; (iii) the study of multicomponent glasses leading to an understanding of the correlation between structure and physical properties such as strength, durability and hardness; (iv) the structure and dynamics of ^{3}He, ^{4}He and their mixtures as a test of the theoretical understanding of low temperature quantum fluids; (v) the possibility of carrying out kinetic experiments during phase separation and crystallisation processes gives a new dimension to neutron beam studies and the source will provide a new tool for the investigation of such poorly understood phenomena. Under (b) we include: (i) studies of the collision processes in molecular gases, and modifications to bond lengths and inter and intra-molecular configuration as a function of temperature and pressure; (ii) investigations of influences on structure consequences of metal-insulator and other electronic transition, and associations in metal vapours.

Of particular relevance to the study of glasses and molecular fluids is the large range of scattering vectors available from a pulsed source allowing improved precision in the determination of bond lengths and short range atomic correlation.

Although the case for the construction of the source depends crucially on the richness of the scientific programmes for which it may be used - hence the emphasis above on multicomponent and polyatomic systems - its existence will permit the continuation of established areas of research with measurements of greater precision and accuracy. For example, a study of the dynamical structure factor of argon and other rare gases over a wide range of thermo-

dynamic states, including the vicinity of the critical point would provide a stringent test of theories of simple fluids. The existence of observable collective longitudinal excitations in liquid metals and their temperature and density dependence is another important area of research which can be developed in a more effective way with the new source.

FLUIDS AND AMORPHOUS SOLIDS: INSTRUMENTS

Instrument	Moderator	Specification	Field
Total Scattering Spectrometer	300K	$0.3 < Q < 100$ Å^{-1}	Structure factors of fluids and amorphous solids.
High Pressure Spectrometer	300K	$0.3 < Q < 100$ Å^{-1} $\frac{\Delta Q}{Q} \sim 0.01$ Pressures up to 50 kbar	Pressure dependence of structure factors of fluids and amorphous solids. Triplet correlation functions.
Total Scattering Polarization Analysis Spectrometer	300K	Q up to 20 Å^{-1} Spin analysis of scattered beam	Structure factor measurements in presence of spin-incoherent scattering.
Inelastic Polarization Analysis Spectrometer	300K	$0 < \hbar\omega < 200$ meV $\frac{\Delta\hbar\omega}{\hbar\omega} \sim 0.01$ Spin selection of both incident and scattered beam	Separation of the dynamical structure $S(Q,\omega)$ and $S_s(Q,\omega)$.
High Energy Low Momentum Transfer Spectrometer	300K	$0 < \hbar\omega < 200$ meV $\frac{\Delta\hbar\omega}{\hbar\omega} \sim 0.05$ Low Q bank ($Q < 4$ Å^{-1})	Measurements on the dynamical structure factors of liquids, in particular liquid metals.
High Energy High Momentum Transfer Spectrometer	300K	$E_o > 1$ eV $Q_{max} \sim 30$ Å^{-1}	Measurements on the dynamics of the liquids. High Q dependence of $S(Q,\omega)$ for amorphous materials.
Elastic Discrimination Spectrometer	300K	$1 < Q < 25$ Å^{-1} $\frac{\Delta Q}{Q} \sim 0.02$	Simultaneous measurement of elastic and total diffraction patterns to allow separation of elastic and inelastic scattering to study the eccentricity of atomic thermal vibration tensors.
Total Scattering Spectrometer	77/20K	$0.3 < Q < 100$ Å^{-1}	Structure factors of fluids and amorphous solids. High resolution at low Q.

SPALLATION NEUTRON SOURCE SCIENCE PANEL

Working Group C : Structure Determination

Professor G E Bacon	Physics Department University of Sheffield
Dr P H Borcherds	Physics Department University of Birmingham
Dr A K Cheetham	Chemical Crystallography Laboratory University of Oxford
Dr B E F Fender (Convener)	Inorganic Chemistry Laboratory University of Oxford
Dr R H Fenn	Physics Department Portsmouth Polytechnic
Dr J B Forsyth (Secretary)	Neutron Beam Research Unit Rutherford Laboratory
Dr A M Glazer	Cavendish Laboratory University of Cambridge
Dr A J Jacobson	Inorganic Chemistry Laboratory University of Oxford
Dr D W Jones	Chemistry Department University of Bradford
Dr D F R Mildner	Neutron Beam Research Unit Rutherford Laboratory
Dr O S Mills	Chemistry Department University of Manchester
Dr R J Nelmes	Physics Department University of Edinburgh
Dr E Sándor	Physics Department Queen Mary College London
Dr M W Thomas	Materials Physics Division AERE Harwell
Dr P J Webster	Physics Department University of Salford
Dr C Wilkinson	Physics Department Queen Elizabeth College London

STRUCTURE DETERMINATION

TABLE OF CONTENTS

1. STRUCTURAL STUDIES

1.1 INTRODUCTION

Neutron diffraction plays an important role in crystallographic studies because (a) the relatively small range of neutron scattering amplitudes allows the ready detection of light atoms, eg. H, C, N, O in the presence of atoms of high atomic number; (b) the irregular variation of scattering amplitudes often generates significant fluctuations in scattering length between neighbouring atoms in the Periodic Table thus greatly facilitating their identification eg, Mg and Al, O and N, even though the ions be isoelectronic; (c) in many cases absorption is small (compared with x-rays) so that measurements down to liquid helium temperatures or up to 1500°C can be as routine as at room temperature. Experiments at even higher temperatures and at high pressure may also be performed; (d) the magnetic moment of the neutron opens up the whole field of magnetic structure determinations and magnetic moment distributions.

Because of these advantages neutron crystallography has for a number of years formed a major part of the research programmes at medium flux reactors. It also plays a prominent role in the research carried out at high flux sources and at the Institut Laue-Langevin in 1975, 28% of the available instrument time (over 130 experiments) was used for crystal and magnetic structure determination.

Experiments recently reported or currently in progress cover a great variety of compounds. A number are studied for their intrinsic crystallographic interest but most as part of a wider investigation of physical, chemical or biological properties. A few of the topics which have recently benefitted from access to neutron diffraction facilities are:

1.1.1 Phase Transitions

The structures of several important ferroelectric (and piezoelectric) materials are being intensively studied including the KH_2PO_4, $Pb(Zr_{1-x}Ti_x)O_3$ and $Na_xK_{1-x}NbO_3$ systems and the boracites. Often the structural behaviour is complex; in the $Na_xK_{1-x}NbO_3$ system for example there are twenty different phases, half of them being ferroelectric with a high spontaneous polarization - and the crystallographic study is a necessary first step before an examination of the lattice dynamics. In addition, the detailed

structural investigation often gives insight into the chemical factors which influence structure and properties.

A phase transition may be associed with marked changes in electrical conductivity and the structural changes associated with metallic-semiconductor transitions in compounds as diverse as NbO_2 and $CeD_{2.75}$ have recently been investigated. Not infrequently the transition of interest is one which confers enhanced ionic conductivity and the structural properties of a number of superionic conductors have been investigated including αAgI, the β aluminas and high temperature CaF_2. All aspects of the study of phase transitions are likely to remain a focus of interest for a good many years.

1.12 H-Bonded Structures

Most of our accurate information about hydrogen bonded structures has been derived from single crystal neutron diffraction studies. This work continues in studies of hydrates, the clustering of water molecules about H_3O^+, compounds (such as potassium hydrogen bis-phenyl acetate) with very short hydrogen bonds and the exploration of less common hydrogen bond interactions for example with acceptor phenyl rings. Attempts are also being made, combined with x-ray measurements, to elucidate the detailed hydrogen bonding scheme for molecular crystals such as N benzyl-DL-leucyl glycine ethyl ester which can serve as a model for the packing of side chains in globular proteins. More investigations of this kind should prove rewarding.

1.1.3 Molecular Crystals

The relative ease with which accurate neutron diffraction experiments can be carried out at low temperatures, coupled with the rapid development of profile analysis techniques applicable to polycrystalline samples, is stimulating considerable interest in the structure of molecular crystals. Generally there are subtle structural changes with variations in temperature and pressure. The last two or three years have seen substantial investigations on the hydrogen halides, methane, acetylene (and dimethyl diacetylene) and SF_6. We can expect this type of study to extend our understanding of intermolecular forces not only in simple plastic crystals or hydrogen bonded systems but also in the large class of ionic compounds (eg hexafluorides) whose behaviour is intermediate between molecular crystals and simple salts. In selected cases the structural determination will be a necessary prelude to a complete dynamical investigation. The extension to more complex molecular systems, eg organometallic compounds,

pharmacologically important organic molecules and simple polymeric compounds is readily envisaged but it is frequently impossible to obtain crystals of sufficient size (for present fluxes) or sufficient instrumental resolution (also limited by flux) for powder experiments.

1.1.4 Defects and Disordered Solids

The increasing emphasis in recent years on the science of materials has engendered considerable interest in the structure of inorganic solids including ceramics. Many of the important compounds contain light atoms such as oxygen and carbon and frequently the high temperature phases demonstrate broad ranges of non-stoichiometry which contain nominally high concentrations of point defects. Some aspects of the ultra microstructure - short range order and clustering of defects - is revealed by diffuse or small angle neutron scattering and by electron microscopy but the contents of the average unit cell can often only be accurately determined by neutron Braff diffraction. The main leads to our understanding of non-stoichiometry in simple compounds such as fluorite structures (eg $Ca(Y)F_{2+x}$, $Zr(Y)O_{2-x}$) transitions metal oxides and carbides (eg $Fe_{1-x}0$) and perovskites (eg La MnO_{3+x}, $BaFeO_{3-x}$) are derived from such investigations and have stimulated considerable theoretical effect. Even so only a small number of structural types has been studied over limited concentration and temperature ranges. Non-stoichiometric compounds represent one example of very widespread occurrence of order-disorder phenomena in solids. Examples recently studied by neutrons include cation distributions in spinels, layer compounds and crystallographic 'shear' compounds, as well as atom distributions in a number of alloy systems where the atomic scattering factors are unfavourable for x-ray studies.

1.1.5 Intercalation and Surface Solids

A feature of recent crystallographic studies has been the exploration of host-guest structures with host lattices such as the transition metal dichalcogenides and the clays. The molecular orientation of pyridine in $NbS_2(C_5H_5N)_{0.5}$ is one recent determination and the interest result emerges that the pyridine molecules are perpendicular to the sheets with the nitrogen atom (as in NH_3) midway between the sheets. The range of inclusion compounds in this class alone is enormous but we still understand little about the host-guest interaction. In addition, these layer hosts allow the examination of the properties of two dimensional monolayers and could serve as templates for 'tailored' chemical reactions.

As well as the examination of occluded layers, present fluxes just enable - in favourable cases - direct structural investigation of simple gases (eg nitrogen, ammonia, xenon) on high surface area solids (eg graphite). Microcrystalline clusters are observed and in krypton on graphite for instance there is evidence for the existence of two solid phases at coverages between 0.85 and 1.7 with one layer related to the graphite lattice and a compressed phase with Kr-Kr distances close to those in the pure solid. This is a topic which would be considerably extended by the fluxes available from the SNS.

1.1.6 Electron Distributions

In principle it is possible from accurate x-ray and neutron data to derive electron distributions, though in practice the limited Q range, thermal vibrations or the dominance of core electrons restrict the range of compounds which can be studied and diminish the quantitative value of the results. Nevertheless for compounds with elements from the first short period the results obtained are of considerable and growing interest. In one very recent illustration measurements on p-nitro-pyridine N-oxide clearly locate the lone pair electron density in the nitroxo group orthogonal to the bond axis as well as providing information about individual bonds.

1.1.7 Magnetic Studies

The interactions of the magnetic moment of the neutron with the magnetization density resulting from unpaired electrons in solids has led to the determination of hundreds of magnetic structures over the last twenty years. Such investigations will continue to form part of future programmes in magnetic crystallography particularly in connection with novel materials. Much greater emphasis however will be placed in future on the more detailed information which is available by the use of polarised neutrons. In the past complete magnetization density distributions have been restricted to a limited number of relatively simple systems where large crystals were available. Now we can envisage charting the moment distribution for a much wider variety of compounds and reports in the last year include experiments on alloys such as $NdAl_2$, YCo_5, $HoCo_2$, on inorganic salts (eg K_2NaCrF_5, $CrBr_3$ K_2ReCl_6, FeF_2 and $RbCrCl_4$), on UC and the examination of the nitroxide free radical in tanol suberate. In alloys the information obtained can relate the observed macro-

scopic behaviour to atomic properties; thus YCo_5 which exhibits abnormally high magnetic anisotropy it has been shown that this is associated with the extended spin density of Co (in one of the two Co sites) in the basal plane containing Y atoms. For inorganic salts the often marked aspherical moment distribution is related to the extent and nature of the covalent interaction and the measurements, apart from being able to demonstrate effects such as exchange polarization, provide illuminating guidelines for theoretical studies. These moment density maps are much more revealing than the simple determination of atomic moments which have been common hitherto. The evidence from the ILL suggests that with additional polarised beam facilities there would be very little restriction on the type of ligand or on the d and f block elements which could be studied.

Parallel with the greatly extended exploration of unpaired electron distributions there is bound to be a more sophisticated probing of magnetic interactions though a study of magnetic phase diagrams, the influence of pressure and the temperature dependence of correlation lengths in magnetic hains (as in $CsNiF_3$).

2. STRUCTURAL STUDIES USING PULSED SOURCES

2.1 INTRODUCTION

Crystallographic studies are carried out with pulsed sources using white radiation and time-of-flight analysis to replace the monochromated beam at steady state reactors. Direct comparisons with steady state reactors are difficult and frequently misleading because the relative performances in different Q ranges vary. However, it is already clear the the back scattering powder diffractometer on the present linac at Harwell represents significant addition to the UK capability in powder diffraction as carried out on the Harwell reactors. Successful diffraction experiments have been performed on the present Harwell inac, on the electron linac at Tohoku, Japan, and also on the ZING P2 facility on the Argonne proton accelerator. The Working Group is confident that the proposed SNS will enable major advances to be made in structure determination using both single crystal and powdered samples.

2.2 SINGLE CRYSTAL STUDIES

The most efficient method of measuring the integrated intensities of reflections from a single crystal, illuminated by a pulsed beam of white thermal neutrons, is an extension of the classical technique of von Laue. The fixed crystal orientation determines the directions of the diffracted beams from the large number of reflections which occur simultaneously. In turn, the d-spacings of these planes select the wavelength of the diffracted neutrons from the 'white' incident beam. In the classical Laue method orders of the same reflection {nh, nk, nl} are not separated, since they occur at the same scattering angle, but in the time-of-flight method they can be. TOF analysis of the scattered neutrons from a pulsed source enables the orders of any reflection to be separated, since each is produced by neutrons of a different velocity. An extended detector can be used to increase the number of simultaneously observable reflections.

In time-of-flight diffraction the wavelength is determined by measuring the time t for a neutron to cover a distance ℓ

$$\lambda = \frac{h}{mv} = \frac{ht}{m\ell}$$

where m is the neutron mass, v is the neutron velocity and h is Planck's constant. A large number of reflections occurs effectively simultaneously in the TOF stationary single crystal method. The degree to which this property can be exploited to increase the speed of data collection is largely dependent on the detection system. A small area detector receives information from a single direction in reciprocal space, whereas a large area detector is sensitive to a plane or volume in reciprocal space.

The need to have a good resolution for moderately large unit cells suggests than an area position sensitive detector (PSD) will be required for general purpose single crystal diffractometry at the SNS. This principle has already been exploited to a limited extent at the Harwell linac, where a bank of 32 detectors was used in an investigation of the crystal structure of Mn_5Ge_3.

The integrated intensity of a reflection from a given single crystal at the SNS is likely to be comparable to that at the ILL. The TOF technique is normally accompanied by a significant improvement in peak-to-background ratio,

so it is likely that a reduction in specimen crystal size compared to the smallest in use at the ILL can be made. In addition, an increase in the rate of data collection may be achieved with the appropriate detector system and the Laue technique.

2.2.1 Useful Wavelength Ranges for Structural Studies

Below about 1.0 Å the flux of the SNS soon becomes orders of magnitude greater than that of the reactor. This fact, coupled with the much higher data collection rates of the Laue technique, offers the exciting possibility of greatly extending the sin θ/λ limit of neutron single crystal studies. Currently, a value of 0.9 $Å^{-1}$ is seldom exceeded, whereas the corresponding x-ray figure is frequently closer to 1.3 $Å^{-1}$. The improved atomic resolution which could result from extending the lower limit of useable neutron wavelengths to 0.5 Å or beyond is vital to the study of anisotropic and anharmonic thermal vibrations and positional parameter changes at phase transitions. For some current problems, it has been estimated that to distinguish between positional disorder and anharmonic thermal motion, and to determine accurately the anharmonic parameters (higher cumulants) requires a resolution of some 0.1 - 0.2 Å. This resolution can be achieved with wavelengths in the 0.3 - 0.5 Å range and the SNS will allow these measurements to be made for the first time.

At short wavelengths the loss of diffracted intensity, due to the λ^4 dependence of the integrated intensities, places a lower limit to the d-spacings which can be observed. In addition, the demand for data to higher values in sin θ/λ necessitates a corresponding improvement in instrumental resolution at a cost of increased complexity, or a further loss of intensity or both. A lower limit of 0.3 Å is suggested as a compromise; some increase in crystal size might be possible at the shortest wavelengths without introducing an unacceptable degree of extinction.

Studies of materials with large unit cell dimensions are usually limited to much lower values of sin θ/λ. Extinction is not significant so longer wavelengths may be used to improve the instrumental resolution and to increase the scattering.

We may therefore distinguish three principal areas of single crystal investigation which require different ranges of neutron wavelength:

Type of Study	Useful Wavelength Range	Moderator
High resolution structural studies of materials with simple structures having cell dimensions 5 - 10 Å. Extinction usually severe.	0.3 - 0.8 Å	ambient
Normal structural studies. Cell dimensions 10 - 20 Å, extinction moderately important.	0.5 - 1.5 Å	ambient
Complex molecules with large unit cells having dimensions up to 40 Å. Extinction unimportant.	1 - 6 Å	cooled

There is a definite need to be able to carry out accurate studies in the second category much more rapidly than at present. We would aim for a daily rate of some 1000 measurements of integrated intensity with some 2% error.

2.2.2 Detectors for Single Crystal Diffractometry

The provision of an area PSD is much more crucial to the attainment of high data collection rates in TOF diffractometry than it is for the conventional, constant wavelength method. We may assess the relative importance by considering the volume of reciprocal space in which reflections can occur for a beam with say 3% wavelength spread at 1 Å compared to that for the polychromatic method in the wavelength range 0.5 - 1.2 Å.

Constant λ	Constant θ
$\frac{4}{3}\pi\,(0.985^{-3} - 1.015^{-3})$	$\frac{4}{3}\pi\,(0.5^{-3} - 1.2^{-3})$
ie 0.3773 $Å^{-3}$ or 1% of the total	ie 31.086 $Å^{-3}$ or 12% of the total

The volume ratio in this example is about 80 but, in practice, the ratio would increase still further in favour of the polychromatic method. The focussing properties of the monochromator, constant-λ diffractometer and its diffracting

geometry restrict the measurement of good integrated intensities to those reflections which occur to one side of the incident beam and lie in layer lines subtending not more than some 30^{o} to the plane perpendicular to the axis about which the crystal is rotated to achieve integration. In contrast, the detector for the TOF Laue method might conveniently extend over a complete hemisphere, leaving the upper hemisphere free for the specimen support system which might require a cryostat, furnace, pressure cell etc. However, the requirements of the polarized beam technique suggest that an alternative 2π detector, in the form of a band subtending $\pm 30^{o}$ to the horizontal plane containing the specimen, would be suitable for both polarized and unpolarized studies.

The spatial resolution demanded of an area PSD for TOF single crystal diffractometry clearly depends on the unit cell dimensions of the sample to be studied and the atomic resolution ($\sin\theta/\lambda$ limit) to which data are required. Taking 0.5 Å as the lower wavelength limit we find that an angular resolution of 2^{o} (2θ) in the detector is sufficient to resolve reflections from a 20 Å unit cell out to a $\sin\theta/\lambda$ limit of 1.5 $Å^{-1}$. A detector-specimen distance of 0.57 metres would translate this requirement to a 20 mm x 20 mm element and a 2π band detector would require between five and six thousand elements. The same detector would also be suitable for use in polarized neutron diffractometry for the determination of the spatial distribution of magnetisation. It would also provide sufficient resolution for data collection out to 3 $Å^{-1}$ with unit cell dimensions of less than 10 Å, using a lower wavelength limit of 0.3 Å, or out to 0.8 $Å^{-1}$ for dimensions of up to 40 Å.

The time resolution of the diffractometer must be sufficient to resolve reflections which occur on the same radius from the origin in reciprocal space and, hence, occur at the same scattering angle 2θ. For a diffractometer with total length L from moderator to detector, the time-of-flight is given by

$$t = 252.7\ \lambda\ L \quad \mu s \qquad (\lambda \text{ in } Å,\ L \text{ in metres}).$$

In the slowing down region, the pulse width, Δt, is given by

$$\Delta t = 7\ \lambda \quad \mu s \qquad (\lambda \text{ in } Å).$$

The time resolution in the slowing down region is given by

$$\frac{\Delta t}{t} = \frac{7\lambda}{252.7\lambda L} = \frac{1}{36L} \qquad \text{(L in metres)}$$

and is independent of wavelength.

The time separation of adjacent reflections δt is related to their separation in reciprocal space δd^* by

$$\frac{\delta t}{t} = \frac{\delta d^*}{d^*} .$$

The relationship between the width of the peak, Δt, and the peak separation δt is therefore given by

$$\frac{\delta t}{\Delta t} = -36L \frac{\delta d^*}{d^*} .$$

At 135° 2θ for a 20 Å cell edge, 7 metre flight path and at 0.05 Å, $\delta t/\Delta t$ is 3.45 whereas at the same angle at 1.5 Å, $\delta t/\Delta t$ is 10.08. The resolution becomes very high at longer wavelengths and lower diffraction angles. In practice, the resolution is not likely to rise so rapidly since, in the thermal region which follows the slowing down region, the pulse width broadens. The $\delta t/\Delta t$ for an ambient moderator is probably acceptable from the point of view of resolution, but it could be improved by the use of a suitably cooled moderator, though with a loss in intensity.

2.2.3 Extinction Corrections

Extinction corrections remain one of the most serious sources of error in conventional single crystal diffractometry. In the early TOF experiments, only low flux sources were available and data were collected from rather large single crystal specimens over a wide wavelength range, typically 0.5 - 5 Å. All experimenters observed serious extinction effects for strong reflections which happened to be measured at long wavelengths. However, the SNS intensity is sufficiently high to turn what had earlier been a disadvantage into a positive asset. Specimen sizes will be no larger than those for conventional diffractometry at a high flux reactor but data on the wavelength dependence of the observed structure factors will be routinely available. Several orientations of the specimen are required to follow the variation for any particular reflection, but the initial data collection phase should provide sufficient information to isolate those reflections for which further data must be obtained. The method has been successfully used on CuCl single crystals to test recent theories of extinction. It is suggested that an upper wavelength limit of about 1.5 Å should be adopted

for most studies, though this restriction would clearly not apply to the study of weakly scattering substances.

2.3 POLARIZED BEAM STUDIES

2.3.1 Without Polarization Analysis of the Scattered Beam

Traditionally, accurate measurements of magnetisation density distribution have been made on single crystals by a polarized beam technique in which a magnetic field is applied to the specimen in a direction parallel to the incident neutron polarization vector and the scattered beam is measured in the plane perpendicular to this direction (normally the horizontal plane). The ratio of the intensity of a reflection with incident neutron polarization 'up' is measured relative to that with incident polarization 'down'. Useful measurements have also been made with the detector inclined at angles of up to 30^{o} from this plane.

All of the stages involved in this type of experiment can be achieved with a pulsed neutron source. The neutrons can be polarized by an LMN filter with an efficiency of more than 70% over the wavelength range 0.5 to 1.2 Å, and flipped by a Dabbs or Drabkin flipper with an efficiency $\sim$ 99%.

With an extended detector in the form of a band subtending $\pm 30^{o}$ to the horizontal, approximately half of the total area surrounding the specimen can be covered but still allow access for cryostat tails and magnet pole pieces. The gains in the rate of data acquisition are therefore similar to those for single crystal integrated intensities, outlined in Section 2.2. Indeed, with the addition of the LMN filter, the same experimental equipment could be used for integrated intensity and flipping ratio measurements.

The simultaneous determination of both the flipping ratios and the integrated intensities is valuable in studies of weakly magnetic systems, where it has been shown that errors may be introduced if ratios are measured at a single position in the peak of the reflection.

Two other sources of error which have affected the accurate measurement of magnetic structure factors can be overcome by TOF energy analysis of the scattered beam. These are the $\lambda/2$ contamination which accompanies the use of a monochromator, and the preparation of an adequate correction for extinction, which can be serious in the case of mixed magnetic and nuclear reflections.

2.3.2 Polarization Analysis of the Scattered Beam

For the SNS this requires that a second LMN filter be added to the experimental equipment mentioned in Section 2.3.1. Since the dimension of these filters is presently some 60 x 60 mm^2, this limits the area of the detector which can be used to one subtending an angle at the specimen of approximately 5^o. In addition, after scattering from the specimen the neutron polarization must be maintained by a guide field, which also limits the vertical acceptance of the detection system.

The gain in the rate of data acquisition is therefore limited in this case to the simultaneous measurement of reflections lying along a row passing through the origin of reciprocal space. The volume is reciprocal space in which reflections can occur for the wavelength range 0.5 to 1.2 Å is at maximum 0.152 $Å^{-3}$, which is only about 1% of that available to the band detector specified in Section 2.3.1.

2.4 POWDER STUDIES

In the last few years, powder studies have increased greatly, partly because the increased fluxes available have led to the introduction of diffractometers with improved resolution but principally because profile analysis methods enable relatively complicated structures with upwards of 50 structural parameters and unit cell volumes up to 2000 $Å^3$ to be refined. The use of profile analysis techniques is greatly aided by the accurately Gaussian shape of neutron Bragg reflections, but there are some general advantages in studies on polycrystalline samples. The speed of data collection is relatively rapid, and measurements over a range of temperature (and pressure) are more easily performed. The low absorption cross-section of most elements means that large samples can be used without special preparation and preferred orientation (a major bug-bear in x-ray powder studies). The main demand however for powder arises simply because even with high fluxes single crystals of a suitable size are not available. Often, despite the expenditure of very considerable time and effort the crystals produced are too small for a neutron single crystal investigation; in many cases the crystal shatters on undergoing a phase transition which either rules out a study or severely restricts the temperature range over which the compound can be examined. The method of preparation (eg a high pressure solid state reaction) may also preclude the preparation of single crystals.

The proposed new source would supplement existing facilities in a major way but would open up new fields of study because (a) very high resolution at

reasonable counting rates can be readily achieved by the use of the back-scattering mode (b) the rapid simultaneous collection of the whole diffraction pattern can be valuable in following time dependent processes and (c) the sample geometry facilitates measurements under special conditions particularly high pressure studies (d) transient phenomena can be observed by coupling an external influence to the SNS pulse.

2.4.1 Resolution

The time-of-flight method for powders has been intensively studied in the last few years. The Back-Scattering Spectrometer on the present Harwell linac services as a working example for possible SNS diffractometers. A schematic layout of a back-scattering spectrometer is illustrated in Chapter 3 of this Appendix.

The resolution (R) of a TOF diffractometer is given by

$$R = \left(\left(\frac{\delta L}{L} \right)^2 + \left(\frac{\delta T}{T} \right)^2 + \cot^2\theta \ \delta\theta^2 \right)^{\frac{1}{2}} \qquad (1)$$

Where δL is the error in the total path length L and δT is the corresponding uncertainty in total flight time T and $\delta\theta$ is the angular spread of a simple counter in the counter bank.

The intensity (per unit cell) of any reflection I_i is given by

$$I_i = \frac{2 d_i^4 \ j_i \ F_i^2 \ N_s \ \phi}{V_o} \cdot \frac{A \ B \ \sin\theta}{(4\pi)^2 \ L_o^2 \ L_1^2} \qquad (2)$$

where d_i, j_i and F_i are the d spacing, multiplicity, and the structure factor of the i^{th} reflection. V_o is the unit cell volume. N_s is the number of unit cells in the sample, ϕ is the time average flux at the moderator surfaces. L_o and L_1 are the source-sample and sample-detector distances, respectively, and A and B are geometrical factors.

To explore the potential scope of the new source one can envisage two different types of instrument, one designed to achieve the maximum feasible resolution and the second optimising the data collection rate at medium resolution.

2.4.2 A High Intensity, Medium Resolution Diffractometer

For this instrument, the existing Harwell linac diffractometer can be considered as a prototype. In the back scattering mode it has good resolution

$\frac{\Delta d}{d} \sim 3 \times 10^{-3}$. L_o is 12 metres, L_1 is 2.0 metres. With this instrument on the SNS the complete diffraction patterns of simple solids (eg Ni) could be obtained in times less than a minute. Examination of equation (2) shows that substantial decreases in sample size and/or increases in cell volume are possible with total counting times still in the order of about 1 hour.

2.4.3 High Resolution Diffractometry

A major aim of an ultra high resolution diffractometer would be the study of relatively complex crystals with relatively large unit cells. Such crystals, because of the large number of reflections, place a heavy demand on the resolution. Even using profile techniques it is necessary to at least partially resolve the Bragg peak density.

The resolution R_r, to completely resolve one peak between Q and Q + ΔQ can be crudely related to the volume of the unit cell, V_{cell} by

$$R_r = \frac{\Delta Q}{Q} = \frac{2\pi^2}{V_{cell}} \frac{1}{Q^3} . \qquad (3)$$

Ideally one would like to resolve all the Bragg peaks up to some Q_{MAX}. It should be noted that R_r becomes more stringent (smaller) as Q increases. It also turns out that the instrumental resolution becomes better at large θ. Thus the possibility arises of obtaining a fully resolved diffraction pattern using a wavelength band $\lambda_{MAX} - \lambda_{MIN}$ such that low Q Bragg peaks are measured at low θ. Thus if one matches the best instrument resolution with the smallest R_r one gets for R_r = 0.1% the following:

V_{cell} Å^3	Q_{MAX} (resolved) Å^{-1}	λ_{MAX} Å^{-1}	d_{MIN} Å	δT (μs)	
				77K	300K
80	6.3	2	1	25	43
1000	2.7	4.6	2.3	70	

For the larger unit cell the resolution limit is reached for quite low Q but in a practical case full resolution of the peak is unnecessary so that useful information is obtained at considerably higher Q.

In order to specify the instrument requirements one must consider the terms of equation (1) in some detail. The contribution from the pulse width, δT,

will dominate at large θ values. For 2 Å neutrons and a 77K moderator a flight path of 100 m will be required for 0.1% resolution.

If one neglects vertical divergence and guide tube effects the other terms in equation (1) can be shown to be

$$\cot\theta\ \delta\theta = \frac{\cot\theta}{2}\left[\left(\frac{\delta X_o}{L_o}\right)^2 + \left(\frac{\delta X_o}{L_1}\right)^2 + (\delta X_s)^2\cos^2\theta\left(\frac{1}{L_o}+\frac{1}{L_1}\right)^2 + (\delta Y_s)^2\sin^2\theta\left(\frac{1}{L_o}-\frac{1}{L_1}\right)^2\right]^{\frac{1}{2}} \quad (4)$$

$$\text{and } L = \left[(\delta Y_o)^2 + (\delta Y_1)^2 + 4\sin^2\theta\,(\delta X_s)^2\right]^{\frac{1}{2}} \quad (5)$$

with $\delta X_s \parallel \underline{Q}$ and $\delta Y_s \perp \underline{Q}$. At low θ the uncertainty in the angular contribution becomes important.

Assuming the above equations and that a chopper removes neutrons with a wavelength > 2 Å, then with detectors 3 metres from the sample and only 0.5 cm across and with a flight path of 100 m, resolutions between 10^{-3} and about 3×10^{-4} can be achieved over a useful Q range provided a cold moderator is used. The largest d spacing observed in the back scattering counters ($\theta > 82^\circ$) would be 1 Å but with counter banks at $2\theta = 15^\circ$ this would be increased to 8 Å. Collimation before the counters would give a resolution of 3×10^{-2}. By selecting only one pulse in two, the maximum d spacings could be increased to 2.8 Å and 16 Å respectively. At the normal repetition rate intensities would be up to 100 - 200 times smaller than for the high intensity instrument (with similar sample volumes) but counting times would generally still fall in the range from half an hour to two or three days assuming the back-scattering counting is maximised.

2.4.4. Applications of High Resolution Powder Diffractometry

The high resolution diffractometer would very considerably extend the power of powder methods in structure determination. Not only is a resolution 2 - 3 times better than conventional diffractometers achieve, but the resolution is only slowly dependent on $\sin\theta/\lambda$. With such an instrument the refinement of structures with at least 100 structural parameters should be feasible, over a very wide range of experimental conditions. In these cases, even with the high resolution, profile analysis techniques would be employed.

There are further applications however which do not involve profile analysis. They include the observation of phase transitions involving small changes of symmetry and, with the highest resolutions under consideration, d-splittings of about 1 in 2000 could be detected. At these very high resolutions it would also be possible to examine, in the vicinity of the Bragg peak, the critical scattering associated with a phase transition or the diffuse scattering associated with point defects in the sample. A high resolution instrument could also be used for the accurate determination of the lattice parameter(s) of a small amount of precipitated phase occluded in the bulk material. Particle line broadening effects can also be followed at this resolution.

For a number of these experiments the separation of elastic and inelastic effects is desirable and the possibility of using a statistical chopper for this purpose should be explored in detail.

2.5 NEW EXPERIMENTS IN DIFFRACTION

This section of the report deals with the novel applications of a high intensity, pulsed neutron source. These new possibilities arise primarily for three reasons. First, the white nature of the beam enables diffraction experiments to be carried out using time-of-flight techniques. Under these conditions the whole of the diffraction pattern is obtained at the same time and only a narrow aperture is necessary for the incident and scattered beam. This facilitates the study of samples in special environments, where the path of the beam may otherwise be obstructed. Of particular interest in this respect are measurements under very high pressures and temperatures. Second, the very high intensity of the beam adds a further dimension to the study of time-dependent processes, for example reaction mechanisms and transient phenomena. In addition the high flux of the spallation source allows the use of small samples and hence opens up the neutron technique to many materials previously only suitable for study by x-ray and electron diffraction. The third factor is the pulsed nature of the beam. This affords an exciting opportunity to examine relaxation processes in the solid state by synchronising some external perturbation with the pulse frequency of the beam.

2.5.1 Studies in Special Environments

There is currently a strong interest in structural studies of materials in a controlled environment, for example, under high pressure, temperature, electric field, etc. Though measurements in electric fields can be carried out using diffractometry on conventional neutron sources, with the high intensity of the

spallation source small samples can be used and hence considerably smaller and more manageable applied voltages are needed. For example, with a typical ferroelectric crystal the coercive field may be around 10 $kVcm^{-1}$ or possibly more; with a weaker neutron source, large crystals obviously require large voltages. In the case of powder specimens, the problem is even more severe. It might also be possible to extend the range of applied magnetic fields in neutron experiments by a factor of up to 5 over those currently available on steady state sources (100 kG). This could be achieved by pulsing the field synchronously with the neutron beam, thus reducing the average heat load in the magnets.

The use of TOF methods solves many of the problems of sample accessibility. The incident and scattered beams pass through two small apertures (or even the same aperture), thus imposing minimal restrictions on the bulk of the surrounding apparatus. Moreover, in the case of single crystal studies, the sample can remain stationary in contrast with conventional methods, a feature which makes the application of special environments relatively simple.

In principle, the advantages described above are also offered by x-radiation from a synchrotron source. However, the high degree of collimation of this radiation enhances preferred orientation effects so that powder specimens require some rotation. Moreover, the solid state detectors used in energy dispersive analysis of the synchrotron radiation have very poor resolution compared with the neutron TOF methods. A further problem is that accessibility is more difficult using x-rays because of the greater absorption effects.

The provision of continuous windows clearly restricts the high pressure limit of a cell. Windows with limited aperture, of the type envisaged for a TOF instrument, can sustain higher pressures. Cells of this type have been described by several groups of workers including one which has been utilized up to 73 kbars in the temperature range between $-50^{o}C$ and $600^{o}C$. Cells suitable for x-ray work which are capable of hydrostatic pressures in excess of 100 kbars have also been reported, and with suitable modification could be used for neutron work. Particularly in the case of powders, it is necessary to use small samples if the effects of line broadening due to pressure gradients are to be minimised.

The main areas of crystallography in which high pressure studies have been carried out are the fields of structural and magnetic phase transitions.

These include studies on the systems KNO_3, thallium metal, ice, NH_4Cl, chromium metal, Au_2Mn and NiS. Most of these studies were performed outside the UK. A facility operating up to 100 kbars on a back scattering TOF diffractometer on the SNS would add an important new dimension to the structural facilities available in the UK. In addition to studies on phase transitions at critical points (eg $BaTiO_3$), it would open up the way for structural measurements on a wide range of geophysical problems. A further area of interest would be the investigation of new phases which exist only under high pressure conditions.

Neutron diffraction studies on samples held at temperatures up to 1600°C can in principle be carried out using a tantalum vacuum furnace on a conventional powder or single crystal diffractometer. For very high temperatures (up to 3000°C) it is necessary to use an induction furnace, in which access to the sample is restricted by the structure of the susceptor, so the TOF method is again more attractive. The range of applications here is obviously restricted to materials which are stable at very high temperatures. These include metal carbides and oxides and a wide range of alloys and minerals.

2.5.2 Relaxation Studies

The pulsed nature of the proposed source allows relaxation phenomena on the millisecond time scale to be studied. Here we consider the applications of some periodic perturbations which are correlated with the frequency of the beam pulse. Modulation techniques then allow diffraction profiles to be obtained over the interval within the cycle of perturbation. Typical perturbations that may be applied are: elastic and magnetic fields, stress (shock waves), thermal fluctuations and light stimulation.

As mentioned above the high intensity of the source allows one to use the small samples and consequently small applied voltages. Since electric fields can be switched very rapidly (less than one microsecond) very fast relaxation processes can be studied. There are many ways in which electric field studies could be carried out. The application of a small periodic field to a piezo-electric crystal (or ceramic) or to a liquid crystal would cause structural changes which could be conveniently investigated. A large periodic field (around 10 $kVcm^{-1}$ or more) applied to ferroelectrics will cause the dipoles to switch direction. With modulation methods it is possible to determine the precise mechanism by which the dipoles switch. Indeed, experiments of this type have already been achieved on $NaNO_2$ using an electron linac source.

Another interesting experiment would be to oscillate the field across a phase boundary between an antiferroelectric, say, and a ferroelectric phase. Such phase boundaries are known to occur in, for example, $NaNbO_3$ and $PbZrO_3$.

Similar ideas apply to the use of magnetic fields, although one should bear in mind the difficulties of switching large magnetic fields rapidly. For this reason, magnetic relaxation effects may be limited to those occurring over 1 or 2 seconds. On the other hand, small but rapid oscillation of the field about some mean value is possible and would open up studies of metamagnetic phase transitions in compounds such as $FeCl_2$.

These techniques can be applied both to single crystals and to powders, and it would be desirable to combine them with temperature variation.

An intriguing although speculative possibility is to carry out experiments on muscle specimens during the cycle of contraction stimulated by an electric field. This has been done in part using x-rays but not as yet with neutrons. The main limitation is that the muscle dies after only 1,000 contractions and therefore a high intensity beam is vital. Very low Q scattering techniques would be required to examine the large lattice spacings inherent in muscles. The hope would be to obtain information about the mechanism of contraction at the molecular level. Moreover, since muscle is a hydrogen-containing material, interesting inelastic scattering effects could also be studied with neutrons.

If an instantaneous stress or shock wave is applied periodically to a crystal, structural studies can be performed as described earlier. This would be of use not only in solids but also in liquids and gases. A typical example would be afforded by the application of a rapid stress to a piezoelectric material, eg $BaTiO_3$, quartz. It is even feasible to examine the structural changes as the shock wave travels through a long crystal.

In studies of relaxation processes at thermally-induced phase changes the temperature could be oscillated across the phase transition in order to follow the progress of the structure through the transition. In the case of first order transitions, important insight would be gained into thermal hysterisis and coexistence effects. This could be combined with rapid neutron topography and particle-size analysis. Ideal second order phase transitions are instantaneous and the structural parameters may be changing rapidly just below the transition. By modulating the temperature in the vicinity of the transition with a periodicity which is some multiple of the pulse frequency, the structural changes close to the transition could be monitored.

The combination of the pulsed neutron source with a pulsed laser excitation permits a much higher light intensity than is attainable with a continuous source. This could facilitate the study of excited states using neutrons and there is clearly the possibility of examining structural changes due to electronic excitations and thermal effects due to vibrational excitations. Some very interesting inelastic scattering experiments could also be envisaged.

2.5.3 Time-Dependent Processes

In this section we consider rapid but precise data collection of time-dependent systems. For this type of experiment two criteria must be met:

(a) high incident flux

(b) white radiation profile so that the whole diffraction pattern can be collected simultaneously. (In conventional diffractometry, the counter must scan across the diffraction pattern during which time the pattern may be changing).

An extrapolation of the performance already obtained on the ZING prototype, at the Argonne National Laboratory, suggests that, with the proposed facility, it will be possible to obtain reasonable diffraction patterns of normal polycrystalline materials in a few seconds. Time scales of this order have already been achieved with x-rays using a synchrotron source and it is clearly desirable to have a complementary facility with neutrons.

Diffraction patterns taken at short time intervals will allow the progress of solid state reactions and decompositions to be followed. This would give structural information relating to the mechanisms of the reactions and could be complemented by information from neutron topography and line-profile analysis (for particle size). The progress of a reaction between ammonia and TaS_2 has been followed by neutron diffraction studies at the ILL. The increased flux of the proposed source would increase the scope of such studies by at least one order of magnitude. An important additional application would be to the structures of unstable materials with short lifetimes.

2.5.4 Anomalous Dispersion

By collecting data with the crystal in several orientations, each structure factor can be obtained at a number of different wavelengths. When the crystal contains strongly absorbing nuclei and anomalous dispersion effects are present,

it is possible to solve the phase problem using data collected in this manner. This experiment could be done on a conventional reactor, but with the proposed source the high rate of data collection increases the precision with which the weak anomalous scattering effects can be measured. Furthermore, with monochromatic radiation it is necessary to collect data sets separately at different wavelengths, a very time-consuming process. With the proposed source this technique could become part of the routine process of any single-crystal structure determination.

STRUCTURE DETERMINATION: INSTRUMENTS

Instrument	Moderator	Specification	Field
Single Crystal Diffractometer	300K	$0.3 < \lambda < 1.5$ Å $\quad \frac{\Delta Q}{Q} \sim 0.03$ Polarized incident beam option	Single crystal structure determination. Magnetization density distributions. Structural investigations as a function of temperature, pressure, etc..
High Intensity Medium Resolution Powder Diffractometer	300K	$Q > 2.5$ Å^{-1} ($\phi = 170^{\circ}$) $\frac{\Delta Q}{Q} \sim 3\ 10^{-3}$ $Q > 0.6$ Å^{-1} ($\phi = 30^{\circ}$) 12 m incident flight path	Structural determination using powder samples. Kinetic processes, eg diffusion of gases into solids.
Single Crystal Diffractometer	77K	$1 < \lambda < 6$ Å $\quad \frac{\Delta Q}{Q} \sim 0.03$	Structure determination of crystals with large unit cell dimensions.
High Resolution Powder Diffractometer	77K	$Q > 6$ Å^{-1} ($\phi = 170^{\circ}$) $Q > 0.8$ Å^{-1} ($\phi = 15^{\circ}$) $\frac{\Delta Q}{Q} = 0.001$ 100 m incident flight path	Resolution of closely spaced peaks in powder diffraction profile.

In addition, a Laue facility has been requested.

SPALLATION NEUTRON SOURCE SCIENCE PANEL

Working Group D : Molecular and Biological Sciences

Dr M R Anderson	Physical Chemistry Laboratory University of Oxford
Dr J P Baldwin	Biophysics Laboratory Portsmouth Polytechnic
Dr C J Carlile	Neutron Beam Research Unit Rutherford Laboratory
Dr P G Hall	Chemistry Department University of Exeter
Dr J S Higgins	Department of Chemical Engineering and Chemical Technology Imperial College London
Professor A J Leadbetter (Convener)	Chemistry Department University of Exeter
Dr G S Pawley	Physics Department University of Edinburgh
Professor Sir John Randall	Department of Zoology University of Edinburgh
Dr D K Ross	Physics Department University of Birmingham
Dr G C Stirling	Neutron Beam Research Unit Rutherford Laboratory
Dr A D Taylor (Secretary)	Neutron Beam Research Unit Rutherford Laboratory
Dr R K Thomas	Physical Chemistry Laboratory University of Oxford
Professor J J Turner	Chemistry Department University of Newcastle
Professor T C Waddington	Chemistry Department University of Durham
Dr C J Wright	Materials Physics Division AERE Harwell
Dr D L Worcester	Materials Physics Division AERE Harwell

TABLE OF CONTENTS

4. MAGNETIC SCATTERING AND POLARIZATION ANALYSIS

4.1 MAGNETIC ELASTIC SCATTERING

4.1.1 Surface Magnetism

4.1.2 Covalency

4.1.3 Defects

4.2 MAGNETIC INELASTIC SCATTERING

4.3 POLARIZATION ANALYSIS

5. SMALL ANGLE (LOW Q) SCATTERING

5.1 INTRODUCTION

5.2 SMALL ANGLE SCATTERING ON THE SNS

6. POLYMERS

6.1 INTRODUCTION

6.2 SMALL ANGLE NEUTRON SCATTERING (SANS)

6.3 QUASI-ELASTIC SCATTERING

6.4 INELASTIC SCATTERING

6.5 WIDER ANGLE NEUTRON SCATTERING

7. BIOLOGY

7.1 INTRODUCTION

7.2 SMALL ANGLE NEUTRON SCATTERING FROM MACROMOLECULAR PARTICLES IN SOLUTION

7.3 SMALL ANGLE STUDIES OF BRAGG DIFFRACTION IN SEMI-CRYSTALLINE BIOLOGICAL SPECIMENS

7.4 STUDIES OF SINGLE CRYSTALS OF MACROMOLECULES

7.5 NEUTRON QUASI-ELASTIC AND INELASTIC SCATTERING

7.6 NEUTRON POWDER DIFFRACTOMETRY

7.7 KINETIC EXPERIMENTS USING THE PULSED NATURE OF THE NEW SOURCE

8. IN-BEAM NMR, AND POSSIBLE NQR STUDIES

8.1 NMR

8.2 NQR

1. INTRODUCTION

1.1 NEUTRON SCATTERING IN THE MOLECULAR AND BIOLOGICAL SCIENCES

The areas of research considered by this group encompass chemical physics, chemistry and molecular biology. In all of these areas neutron scattering techniques have made a major impact in the last few years, particularly since the advent of the facilities at ILL, Grenoble.

Structural studies at $Q > 1$ $\mathring{A}^{-1}$ are in the main discussed elsewhere but we shall refer briefly in this report to structural work of surface chemical or biological interest. The other techniques of major interest are

- Quasi-elastic scattering
- Inelastic scattering
- Small angle scattering
- Non scattering techniques such as in-beam NMR and NQR

High resolution quasi-elastic scattering experiments have led to major advances in the understanding, for example, of liquid and plastic crystalline phases, the behaviour of hydrogen in metals and long range conformational motions of polymer chains. Many studies have been made of vibrational modes inactive in or inaccessible to conventional spectroscopy such as the torsional modes of molecular groups or ligands, and H bonding modes. Very recently observations have been made of tunnelling splittings in the librational ground state of a number of molecules at low temperatures. Neutron scattering investigations of structure, vibrations and diffusional motions of adsorbed or intercalated species on a variety of substrates hold promise of major contributions to surface chemistry but available fluxes have so far limited experiments to systems of relatively large surface area. Most of the above experiments utilise the high and incoherent scattering cross-section of the proton and here deuterium substitution often provides a very powerful diagnostic tool. For coherent scatterers the measurement of phonon dispersion curves provides a unique means of investigating intermolecular forces, but a major difficulty is often the preparation of sufficiently large single crystal specimens. In small angle scattering studies of polymeric and biological structures the use of the scattering contrast provided by H/D substitution has led to quite unique results and growth in

this area has been particularly rapid in the last two or three years. The use of non-scattering techniques such as in-beam NMR is in its infancy but even at ILL is restricted by inadequate fluxes.

1.2 THE SPALLATION NEUTRON SOURCE

Comparison of the SNS parameters with those of the present Harwell linac shows immediately that in the epithermal energy region the effective flux will be very much greater than that from the best reactors. Hence for inelastic scattering experiments at high energy transfer the performance of a spectrometer on the SNS must be overwhelmingly superior to that on a reactor. At the outset, it was not immediately obvious over what energy range this is true nor what relative performance is to be expected at lower energy transfers. Furthermore the feasibility of high resolution and quasi-elastic scattering experiments in the Q-range of interest, and of small angle scattering experiments, was completely unknown. Effort has therefore been devoted to considering the neutron fluxes available from cold moderators on the SNS and to the performance of possible instruments compared with those currently in use.

The conclusion reached is that experiments of all the above types can be performed on the SNS with efficiencies which, with a few exceptions, are at least as good and often orders of magntiude better than those of current instruments. Higher count rates can be utilised to do experiments more quickly, more accurately or on smaller samples than is currently possible and should, moreover, allow the development of new techniques such as in-beam NMR and useful polarization analysis. Furthermore, the special features of the SNS permit the extension of current techniques to regions of energy transfer and resolution (and hence of space and time in molecular motions) which are not now accessible, and the pulsed nature of the source should help in reducing backgrounds and in making measurements to low scattering angles.

The above points will be developed and amplified below but it must first be emphasised that in the whole area of the molecular and biological sciences the instrument time currently available on the best quality spectrometers is quite inadequate. This results in experiments which require 2 or 3 weeks of beam time being extended over perhaps 2 years, so that it os often possible to examine only model systems; experiments requiring long counting

times or detailed studies as a function of temperature and composition are generally not feasible. Thus the availability of further instruments only comparable in performance to those at ILL would make a major scientific impact. When the performance is orders of magnitude better, and when new types of experiment are also possible, the case becomes overwhelmingly strong.

2. QUASI-ELASTIC SCATTERING

2.1 INTRODUCTION

Quasi-elastic neutron scattering experiments study motions of a diffusive (non-periodic) nature in condensed phases and these motions may be translational or rotational in character. Most cases investigated so far have been concerned with incoherent scattering from protons and hence the determination of self correlation functions. It is expected that with the advent of the SNS there will be a considerable increase in work on other nuclei and an increased study of coherent scattering and hence of collective aspects of the diffusional motions.

A great impetus was given to this area when the new generation of high resolution instruments at ILL became available, in particular the multi-chopper instrument IN5 and the back scattering spectrometer IN10. High resolution is needed to observe slow dynamical processes which give instrinsically narrow lines and also to determine the quasi-elastic line shape which contains detailed information about geometric and temporal aspects of the diffusional motions. This high resolution has been achieved in the above instruments by two different methods. The first involves the use of long wavelength neutrons (since $\Delta E/E$ is approximately constant) which severely restricts the available range of momentum transfer $\hbar Q$ ($Q_{max} = 4\pi/\lambda$). Experiments to higher Q value ($Q > 5$ $\AA^{-1}$) would often be desirable in order to probe the diffusional motions more finely in space and time. The second technique utilises the very high energy definition obtained by back scattering from a crystal monochromator and analyser, coupled with an energy modulation achieved by Doppler or crystal expansion methods. The restriction in this case is the extremely limited energy scan which may be achieved.

2.2 QUASI-ELASTIC SCATTERING ON THE SNS

The above limitations may be overcome using the SNS. Three types of instrument are proposed to carry out the quasi-elastic scattering programme. These are

I A White Beam Back Scattering Spectrometer

II A Time-of-Flight, Multi Angle Reflecting Crystal (MARX) Spectrometer

III A Long Wavelength Chopper Spectrometer

The source is assumed to be a methane moderator at 20K or 77K as appropriate.

The basic principle of Spectrometer I is that of the back scattering spectrometer (IN10) except that the incident energy variation is achieved by allowing a broad band of wavelengths $\Delta\lambda$, selected from the pulse by a helical velocity selector, to separate in energy by drifting to the sample along a guide tube of length L. Neutrons whose energy is changed by interaction with the sample to exactly the analyser energy are detected after back scattering from a large d-spacing crystal analyser. The use of neutron guide tubes allows long flight paths, thus giving adequate time resolution without a dramatic loss in intensity. The performance of this spectrometer is compared with those at ILL (IN10 and the proposed IN13) in Table I, assuming the use of identical analyser systems.

TABLE I

COMPARISON OF WHITE BEAM BACKSCATTERING SPECTROMETER WITH ILL INSTRUMENTS

	Intensity at sample ($n\ cm^{-2}\ s^{-1}$)	Rate of Data Acquisition (Intensity/ Unit Energy Channel)	$\Delta\hbar\omega$ (μeV)	$\hbar\omega$ Range (μeV)
IN10	$1\ 10^4$	1	1	20
IN13 (proposed)	$\sim 10^5$	1	5	200
SNS (L=25m)	$8\ 10^6$	8	15	2000
SNS (L=75m)	$2\ 10^6$	6	5	600
SNS (L=100m)	$1\ 10^6$	5	2	400

The most important gain is the achievement of a large energy window covering the entire quasi-elastic region, overcoming IN10's major drawback without significant loss of resolution. It is to be noted that, although for the spectrometer of Table I the intensity per unit energy channel is not greatly improved over present instruments, the mosaic of the secondary spectrometer may in fact be greatly relaxed for the shorter flight paths, matching it to the time resolution. The overall resolution would not be significantly degraded, but a greatly increased count rate would be obtained.

The time-of-flight MARX Spectrometer is a white beam instrument which uses all the neutrons from the source. The incident energy is determined by time-of-flight and the scattered energy by detection position. This is a very versatile instrument in which the resolution and range of Q and $\hbar\omega$ investigated may be varied within wide limits. Thus, for example, it is possible to make quasi-elastic measurements at $Q \sim 6$ Å^{-1} with an energy resolution of 200 μeV, corresponding to $\Delta E/E \sim 1\%$. This overcomes the other major disadvantage of current instruments mentioned above. At longer wavelengths, comparable resolution to that of IN5 may be readily achieved, and with higher effective count rates. This instrument is particularly suitable for use with oriented samples.

Spectrometer III is a single chopper instrument with time-of-flight analysis and a large counter bank. The low repetition rate of the SNS avoids the frame overlap problem encountered on IN5 without recourse to a multichopper design. A comparison with IN5 is given in Table II which shows that the pulsed instrument provides a gain in intensity at comparable resolution for all wavelengths. The advantage of this instrument is its high data collection rate.

The instruments outlined above would provide a uniquely powerful set for high resolution quasi-elastic scattering measurements over a wide Q-range and with resolution and energy window adjustable to suit the particular application.

TABLE II

COMPARISON OF LONG WAVELENGTH CHOPPER SPECTROMETER WITH IN5

	Intensity at sample ($n\ cm^{-2}\ s^{-1}$)		$\Delta\hbar\omega$ (μeV)	λ (Å)
SNS	2.5	10^5	140	6
IN5	6.0	10^4	125	6
SNS	1.2	10^5	78	8
IN5	2.5	10^4	50	8
SNS	4.7	10^4	40	10
SNS*	1.2	10^4	30	10
IN5	0.9	10^4	27	10

*Reduced Burst Time on Chopper

2.3 THE SCIENTIFIC PROGRAMME

2.3.1 Molecular Rotations in Crystals

The object of this type of measurement is to elucidate the details of the rotational motions of groups within molecules, and of the molecules themselves, and hence to investigate the angular parts of intra- or intermolecular potentials. Thus there is need for resolution good enough to separate elastic and quasi-elastic components of the scattering and a Q range large enough to distinguish between different models for the motion, which will often require $Q > 2\ Å^{-1}$. Furthermore, the most useful measurements will be on single crystals which may well be small. Finally, in characterising the behaviour of a material as a function of temperature, and particularly in different phases, the rotational correlation times must be expected to vary over a wide range so that instruments of variable resolution and energy scan, and high data collection rates, will have great advantages. All of these requirements can be met by the spectrometers proposed above.

2.3.2 Liquid Crystals and Intercalated Systems

The essential requirements for these systems are similar. Often two

components of the molecular motions are of interest, namely those perpendicular and parallel to the sample planes and there may be translational diffusion which in the case of intercalates must be separated from the elastic scattering of the host. These systems may have complicated peak profiles extending over a wide energy range and in this respect the wide energy window backscattering spectrometer would be of enormous benefit. The study of collective molecular motions in such systems has hardly begun and is hampered by low inelastic structure factors and small sample sizes resulting from the requirement for fully deuterated samples. The proposed SNS spectrometers, and particularly Spectrometer II, should go a considerable way towards overcoming these difficulties.

2.3.3 Surface Chemistry

The study of surfaces is one in which the high counting rates and low background of the SNS will open up exciting areas for study. The problem in all surface work is in detecting the scattering from the surface species in the presence of that from substrate plus general background. Increase of flux allows the ratio of surface to substrate counts to drop proportionally to (flux increase)$^{\frac{1}{2}}$ for a given experimental accuracy, but for small amounts of surface species it is clearly important to minimise substrate and background scattering. In favourable cases, such as the measurement of incoherent quasi-elastic scattering from a hydrogenous species adsorbed on a good quality coherently scattering crystal, the SNS should make it possible to study monolayers on single crystal surfaces with substrate areas of less than 1 m^2 (how much less will depend on the level of the parasitic background). This could lead the way to major advances in the study of catalysis (see also § 3, 'Inelastic Scattering').

The SNS should make it possible to study many other interesting systems such as multiple water layers on silver iodide crystals, not easily available as high surface area samples, which are of great interest in relation to heterogeneous nucleation of water vapour in the atmosphere. It should also be possible to extend investigations into other areas where the ratio of signal to unwanted background scattering is currently too small, such as concentrated colloids and non-hydrogeneous adsorbed species.

2.3.4 Hydrogen in Metals

The particular interest in measurements of quasi-elastic neutron scattering due to hydrogen diffusing in metals is to extend the measurements to values beyond the first reciprocal lattice point in the defect lattice and measurements would also be made, where possible, using single crystals. The proposed MARX spectrometer would be ideal for these requirements.

High intensity and low background are also important, because systems of technological interest are mainly concerned with very low hydrogen concentrations. Here one would like to be able to measure the effect of various metallurgical treatments such as the introduction of defects, dislocations and impurity atoms or clusters on the diffusion coefficient of the hydrogen. It is also of interest to extend measurements to studies of correlation effects in diffusion and this would involve coherent quasi-elastic scattering using deuterium. This type of investigation would probably require spin analysis to separate the coherent and incoherent parts of the deuterium cross-section, which in view of the equally necessary resolution and intensity is unlikely to be feasible on existing sources.

A further interest here is in the extension of measurements to low temperatures where very high resolution would be required. Such measurements are important from the point of view of correlation effects and comparison with NMR. They are also useful because they increase the ratio of residence time to Debye frequency, which improves the separation between quasi-elastic and inelastic events. Measurements have already been made of the diffusion of Ag in superionic AgI and such measurements could be extended to other nuclei with cross-sections small relative to that of the proton. The study of carbon in metals or alkali ions in glasses might be a future objective.

2.3.5 Very Low Energy-Transfer Inelastic Scattering

Many systems can be expected to show sharp excitations at very low energy (eg tunnelling states) and the availability of a very high resolution spectrometer with a wide energy window will make possible the study of a much greater variety of systems.

3. INELASTIC SCATTERING

3.1 INTRODUCTION

Inelastic neutron scattering experiments are of two basic types, coherent and incoherent. In chemistry the latter is principally proton scattering and is essentially molecular spectroscopy of vibrations involving proton motions. Its development has been hampered by low fluxes resulting in rates of data collection which are very slow in comparison with infra-red spectroscopy and also in the necessary use of rather poor resolution spectrometers. Another limitation has been on the upper limit of energy transfer (generally < 250 meV) because of the poor flux of high energy neutrons. Coherent scattering studies of phonons have been most limited by the availability of suitable single crystals. This is also to some extent a question of flux since a higher flux will permit the use of smaller crystals.

3.2 INELASTIC SCATTERING ON THE SNS

The important features of the SNS for inelastic scattering are the epithermal flux and the pulsed nature of the source. This means that measurements will be possible at energy transfers not accessible with reactors and must be made by time-of-flight methods to utilise fully the advantages of the source; they will generally involve neutron energy loss. In considering how these measurements might be made and what count rates are achievable two broad regions may be distinguished.

3.2.1 The region $\hbar\omega$ < 600 meV

Measurements in this region may conveniently be made using a single-chopper time-of-flight technique and the energy range includes all the fundamental vibration frequencies. The flight path and chopper speed are variables in determining resolution and energy range and it seems likely that two instruments would be needed, optimised to higher and lower energy transfers within this region, with the quasi-elastic instruments also serving as inelastic spectrometers for the region $\hbar\omega$ < 20 meV. An exciting possibility here is the use of the backscattering instrument as an ultra-high resolution inelastic spectrometer, as the spectrometer window may be moved to higher energies relative to the detector energy by adjusting the velocity of the helical

slot rotor. This also has the effect of widening the energy window and changing the resolution. For example, energy transfers between 2 and 20 meV with resolutions of 26 to 150 μeV and good count rates could be observed in a single experiment. This performance far exceeds anything currently possible.

Table III compares the performance of an inelastic chopper spectrometer with that of IN4, the nearest equivalent instrument at ILL. The flux at the sample is shown for various incident energies and for resolutions chosen to be comparable with those of IN4; for the same secondary spectrometer this gives a true comparison of data collection rate.

TABLE III

INELASTIC SCATTERING: COMPARISON OF CHOPPER SPECTROMETER ON SNS WITH IN4

Incident Energy (meV)	IN4		SNS		
	Intensity ($n\ cm^{-2}\ s^{-1}$)	Resolution (meV)	Intensity ($n\ cm^{-2}\ s^{-1}$)	Resolution (meV)	
12	$3\ 10^4$	0.84	$2\ 10^5$	0.62	†
12			$9\ 10^5$	0.52	*
80	$5\ 10^3$	4.0	$5\ 10^5$	3.7	†
200	-	-	$1\ 10^5$	6.7	†

* 77K Moderator

† 300K Moderator

At low incident energies the flux gain at the sample on the SNS is one order of magnitude but this increases rapidly to 10^2 at 80 meV and is immeasurably greater at E_o > 200 meV, still with a high absolute flux. Even higher data collection rates could be achieved by relaxing the Q resolution in some way as with a beryllium filter spectrometer, and we envisage the possibility of such an instrument for use as a routine service spectrometer.

When measuring inelastic spectra it is in general very important to keep Q as small as possible. This is because of diffusional and recoil broadening in liquids

and gases and recoil broadening in solids at high enough Q, together with the increasing importance of multiphonon contributions with increasing Q and form factor effects in magnetic scattering. Low Q scattering is achieved by measuring with small scattering angles and it is envisaged that a low angle counter bank ($< 5^{o}$) would be included on the inelastic spectrometers. The SNS is particularly suited to low angle scattering measurements because the pulsed operation minimises background counts near the straight through beam.

For coherent scattering measurements where constant-Q operation is important, a time-of-flight MARX spectrometer may be used. This is similar to the one considered for quasi-elastic scattering but requires finer incident beam collimation.

3.2.2 The region $\hbar\omega > 600$ meV

This energy range will be quite new for neutron scattering experiments and will involve measurement of vibrational harmonics and more particularly electronic transitions. It in unlikely that a chopper technique will be used because of the fast chopper speeds required but a promising possibility is the use of resonant absorbers like ^{238}U ($E_r \sim 6$ eV) to determine scattered energies, with time-of-flight being used to determine incident energies.

3.3 INCOHERENT SCATTERING

The great increase in effective flux possible with the SNS can be used to

- improve the statistical accuracy
- reduce the time taken for an experiment
- improve the resolution
- examine small or dilute samples

Some of the consequences of this, together with the higher energy transfers available, are examined briefly below.

3.3.1 Rapid Experiments

Measurements with the PLUTO Beryllium Filter Spectrometer or the IN4 spectrometer at ILL currently require several hours. A factor of 10^2 or more in

flux thus implies a run time of seconds or minutes, which opens up a whole new range of possible applications, for example, in repeated scanning for kinetic experiments where the ease of data collection should then be comparable with current infra-red techniques.

3.2.2 Kinetic Experiments

Related to this type of kinetic work, but capable of examining kinetic phenomena which are very much faster, is the technique of applying an external perturbing force to a specimen in phase with the neutron pulses. By this technique it should be possible to observe phenomena such as relaxation processes, and indeed the Japanese have recently reported the direct observation of polarization reversal in a ferroelectric by this method. It has been suggested that the method could be used to observe dynamic instabilities in nematic liquid crystals, and more speculatively in biophysical applications such as muscle contraction. The lower limit of accessible relaxation times is determined by the pulse width and so is $\sim$ 100 μs.

3.3.3 High Resolution Experiments

In principle, for fixed statistical accuracy, the energy resolution may be improved proportionately to the flux increase if the Q resolution is completely relaxed. If the Q resolution is also improved then this gain will be reduced, but in practice a ten-fold improvement in $\Delta\hbar\omega$ should be possible on virtually any instrument. Improvement in energy resolution is of enormous importance since at the moment the low resolution of inelastic neutron scattering spectrometers compared to optical techniques limits severely the complexity of the compounds that can be examined because of the problem of overlapping peaks. The necessity for high resolution is enhanced because of the need to obtain data at low Q which implies relatively high incident energies as well as low scattering angles. The SNS is thus specially suitable for these high resolution inelastic experiments and the possibility of a very high resolution inelastic spectrometer has already been mentioned.

Very high resolution inelastic spectroscopy is potentially very useful in the measurement of diffusive type motions from an analysis of the inelastic band shape. Thus in quasi-elastic scattering from chemical systems there may be contributions from more than one species but if one of these has a suitable vibrational transition it would be possible to study its diffusion from the

vibrational band shape, and hence separate the contributions to the quasi-elastic peak. A trivial example is the tetramethyl-ammonium ion in aqueous solution. This type of analysis to follow rotational diffusion is commonly used in infra-red and Raman spectroscopy. It would require high resolution ($\sim$ 300 eV) in conjunction with low Q techniques. The proposed very high resolution inelastic spectrometer would be most appropriate for such measurements.

3.3.4 Small Samples and Dilute Systems

The high effective flux should make possible experiments with the same accuracy on samples which are up to a thousand times poorer scatterers than can currently be examined. As indicated above in §2.3.3 the exact gain factor will depend on the details of the system under study but this possibility has very considerable importance in the following areas:

- inelastic scattering from biological membranes and lipid bilayers.
- inelastic scattering from chemisorbed monolayers. At present, experiments are only possible from chemisorbed monolayers on polycrystalline materials with surface areas of tens of $m^2\ g^{-1}$ but it now becomes possible to contemplate scattering experiments from stacks of thin oriented single crystals of total area $< 1\ m^2$. The situation is particularly favourable for inelastic scattering of hydrogenous species on tightly bonded, highly perfect, single crystals with coherently scattering nuclei, where most of the scattering is in the Bragg reflections.
- inelastic scattering from matrix isolated systems:

  (a) Unstable species isolated at low temperatures in host gas matrices, currently studied almost exclusively by infra-red techniques (b) Species isolated at low concentrations in alkali halide matrices. These include molecular ions, such as NH_4^+, and H^- (c) Hydrogen in metals at low concentrations. As well as taking the already faily well-studied systems, such as hydrogen in palladium, to much lower concentrations than is possible at the moment there is considerable technological interest in the study of hydrogen in steels. Here the concentrations which markedly affect the properties are too low to be studied by neutron scattering at the moment.

3.3.5 High Energy Transfer Vibrational Spectroscopy

The most important application here is the study of hydrogen stretching frequencies which are largely inaccessible on current instruments. Some particular areas are as follows:

- The study of the vibrations of hydrogen chemisorbed on a surface since for many metals the M-H stretching vibration may lie above 200 meV. Also it is desirable to examine the region of 500-600 meV to see if any molecular hydrogen is present on the surface, identifiable by the H-H stretching vibration.
- The study of the hydrogen stretching frequency in hydrogen-bonded systems where detailed measurements of the intensity of inelastic neutron scattering will provide a good deal of information about the potential well in which the hydrogen is moving.
- The study of metal-hydrogen stretching vibrations in transition metal hydride compounds. In some cases it has proved virtually impossible to identify the stretching frequency in these compounds by conventional optical techniques.
- At higher energies the measurements of the relative intensities of overtone modes derived from hydrogen stretching frequencies should enable a much more precise definition of the potential energy curve experimentally in X-H bonds. The study of overtone modes of hydrogen in transition metal lattices is also of considerable importance.

3.3.6 Electronic Transitions

Apart from vibrational transitions the availability of a good flux of epithermal neutrons up to 5 eV suggests that a range of direct observations of electronic transitions should become possible. Observations of this type have been confined to the examination of crystal field transitions in lanthanide compounds, since the separation between levels tends to be small. This has proved particularly useful in optically opaque materials.

Measurements so far have not been made for normal 'd' block (transition metal) systems because the separation between the levels has been too great. However, the transitions are broad and most fall conveniently below 5 eV in the range 1 to 3.5 eV. It should be of particular value to use neutrons to observe such transitions in optically opaque materials.

3.4 COHERENT SCATTERING

Studies of phonons in single crystals should give the most definitive results on intermolecular forces. Such studies require neutrons in the 1 Å range, and a pulsed source does not yield the same advantage as a triple axis spectrometer using monochromatic neutrons from a reactor which will, in general, be preferable for such work. An exception, however, lies in the use of a time-of-flight constant Q MARX spectrometer in a 'phonon search' mode. This is especially important for the molecular sciences where investigations of complex molecular crystals and polymers may necessarily be undertaken without prior calculation of expected dispersion surfaces and inelastic structure factors. The biggest problem in this area is in the growth of suitable single crystals rather than getting the neutrons but the availability of fluxes $\sim 10^3$ times greater will permit the use of much smaller crystals and this in itself will constitute a major advance.

Studies of the dispersion of internal modes would use the advantage of the spallation source as more energetic neutrons are required. However, we are sceptical of the future of such studies, in view of calculations of what to expect for the modes in naphthalene and hexamethylene-tetramine which show not very much variation. Any variation that exists must be measured accurately to be of any help with understanding the intermolecular forces. Certainly there are experiments which must be done, but it will not be until we have results from the new Harwell linac that we will be able to assess these experiments.

4. MAGNETIC SCATTERING AND POLARIZATION ANALYSIS

4.1 MAGNETIC ELASTIC SCATTERING

Areas of elastic magnetic scattering which can be envisaged as of future and continued interest are studies of surface magnetism, covalency and defects.

4.1.1 Surface Magnetism

This has been little investigated experimentally but it could well be of great significance in the study of catalysis. Questions about the magnetic properties of small particles, concerning their magnetic diameters in contrast to their nuclear diameters, and the influence on these of the

adsorption of gas at the particle's surface could all be answered with the diffuse scattering of polarized beams. It is known from bulk susceptibility measurements that there is a one to one relationship between the number of protons adsorbed at the surface of nickel particles and the number of free (unpaired) electrons lost by the particle. It would be very important to determine from where in the particle these electrons were lost.

4.1.2 Covalency

This is studied by measuring the unpaired electron spin density with neutron scattering, but only a few inorganic complexes (eg K_2NaCrF_6) have so far been investigated. In principle more complex ligands may well be easier to investigate with neutron scattering than with resonance techniques, and the extension of measurements to H_2O and NH_3 ligands would be interesting.

4.1.3 Defects

The small angle scattering of polarized beams from magnetic defects is of interest in systems where nuclear polarization can be obtained. Apart from the well known lanthanum magnesium nitrate dihydrate (LMN) in which the protons can be polarized using the solid effect, protons can also be polarized in the vicinity of free radicals in radiation damaged materials such as polyethylene. Answers can be obtained to questions such as the size of the polarized domains, whether or not these domains cluster, and how fast they increase in size after initiation. To be able to investigate free radical clustering in radiation-damaged materials would be of great interest. To be able to follow the proton polarization propagation in LMN over the period of days in which a single crystal slowly becomes completely polarized at $T < 0.6K$ could yield valuable information on the uncertain mechanism of this process.

4.2 MAGNETIC INELASTIC SCATTERING

Theoretical studies are presently in progress to investigate the neutron cross-sections of 'forbidden' electronic excitations (eg singlet to triplet) in molecular solids. Initial order of magnitude calculations suggest that they will be observable with the flux intensity available from the proposed source, although very small angles of scatter will be needed to avoid the form factor decay at the large values of momentum transfer associated with $1 \rightarrow 4$ eV energy transfers.

Further progress in this area may allow the determination of the dispersion of collective electronic excitations and the investigation of exciton-phonon interactions; a detailed discussion is given by the Solid State Physics Working Group.

4.3 POLARIZATION ANALYSIS

The major chemical application of polarization analysis will be in the separation of coherent from spin-incoherent scattering. (In spin-incoherent systems, the spin non-flip cross-section is the coherent cross-section plus one-third of the spin-incoherent cross-section whereas spin flip scattering is given by the remaining two-thirds of the incoherent cross-section.)

Applications of the study of coherent scattering from materials with normally large incoherent cross-sections include the measurements of scattering from oriented natural materials which are very difficult to deuterate completely, and from biological materials in *in vivo* conditions, ie in light water.

The elastic and quasi-elastic coherent scattering from polymer chains could lead to interesting information about velocity correlation lengths and the influence of entanglements upon polymer dynamics.

The reverse application, that of removing unwanted coherent scattering would be invaluable in the measurement of elastic incoherent structure factors. At present experiments are limited to those ranges of momentum transfer, often small, where coherent scattering is absent. Research areas which have been especially hindered in this manner are those where interest lies in the dynamics of adsorbed gases, such as CH_4 on graphite or C_2H_4 on zeolites, or in the dynamics of ions in ionic conducturs such as silver iodide.

Applications can also be envisaged to the general areas of dilute systems where, for example, a low concentration of a spin-incoherent material is immersed in a coherently scattering matrix, and to materials maintained in extreme environments. In this latter case the containment materials could be constructed of coherently scattering nuclei if the sample of interest was an incoherent scatterer.

5. SMALL ANGLE (LOW Q) SCATTERING

5.1 INTRODUCTION

A large number of experiments has been performed using small angle scattering of long wavelength neutrons to study the structure of biological and physical materials, especially for structures in the range 10-100 Å. These will be considered in more detail in §6 and §7 but they are broadly of two types:

(a) structural studies of materials with very long periodicities, eg some polymer work, which requires measurements at $Q < 0.005$ Å^{-1}

(b) experiments to measure conformation over shorter distances, eg biological and other polymer work, defect clusters in crystals etc, requiring $Q > 0.005$ Å^{-1} and poorer absolute resolution. The first type is less frequent and it turns out that these very low Q experiments will still best be done on a high flux continuous source using very long flight paths to give low scattering angles, such as with D11A at ILL. On the other hand there is a very large and, to a considerable extent, unsatisfied demand for the second type of experiment with Q up to about 1 Å^{-1}, beyond which other instruments take over.

5.2 SMALL ANGLE SCATTERING ON THE SNS

The basic requirement is for an instrument to cover the range $0.005 < Q < 1$ Å^{-1} with a resolution of 5-10%. This needs long wavelength neutrons $4 < \lambda < 12$ Å and small scattering angles $10^{-3} < \phi < 10^{-1}$ rad, and is equivalent to D11A at ILL with the detector at 10 m from the sample.

The conventional method on a reactor defines an incident wavelength spread $\Delta\lambda$ about λ using a helical slot velocity selector and a 2-dimensional position-sensitive detector to determine the intensity as a function of scattering angle. The required angular resolution is achieved by adjusting the lengths of primary and secondary flight paths, and the wavelength spread is often the dominant contribution to the resolution. For an instrument on a pulsed source the intensity is determined as a function of Q using a white incident beam with time-of-flight techniques and a fixed low angle detector. Measurements at the lowest Q thus employ the longest wavelengths, and the Q range is limited by frame overlap with the next pulse. This limits the use

of long flight paths, unless $\Delta\lambda$ or the pulse repetition rate are reduced, so that the overall resolution is determined by the angular resolution since adequate time resolution is given for even the slowest neutrons by use of only modest path lengths ($\sim$ 10 m). It is this which prevents experiments at very low Q values from being competitive with instruments on a high flux reactor.

An outline design for a spectrometer has been considered in which the sample views a cold moderator (methane at 20K) at a distance of 10 m with the detector situated at 2.5 m from the sample, and consisting of an annular ring of inner radius 15 cm and outer radius 30 cm, comprising 0.5 x 0.5 cm^2 elements. This will give count rates comparable to those on D11A at ILL, with a resolution $\Delta Q/Q \sim 10\%$, for $Q > 0.06$ $\AA^{-1}$, and by extending the inner radius to 10 cm measurements can be performed to $Q = 0.04$ $\AA^{-1}$ with 15% resolution. For lower Q values to be reached with reasonable resolution longer flight paths and/or smaller detector elements are required. The former may be achieved by using only one half or less of the pulses and the latter appear to be quite feasible using solid state detectors. A further possibility which stems from the pulsed nature of the beam is the separation of elastic and inelastic scattering. This is feasible if a wavelength spread of less than 20% is used and could be useful in many cases in separating temperature diffuse from structural scattering.

6. POLYMERS

6.1 INTRODUCTION

The application of neutron scattering techniques to polymerised systems has involved the study of rubbers, glasses, partially crystalline materials and polymer solutions. Apart from the intrinsic interest in relationships between chemical structure and physical property for materials composed of long chain molecules there are very important technological applications.

Neutron scattering has made a unique contribution to the understanding of the structural conformations of polymer molecules and to their molecular dynamics. This is due to the particular wavelength - energy characteristics of neutron beams, and also to the enormous difference in scattering cross-section of hydrogen and deuterium combined with the fact that these isotopes can be substituted for each other with little effect on the general physical

properties of the materials. The phenomena of principle interest are;

- Small angle coherent elastic scattering
- Coherent and incoherent quasi-elastic scattering
- Coherent and incoherent inelastic scattering

In each section paragraph (a) outlines the current situation and paragraph (b) deals with the impact of the new source.

6.2 SMALL ANGLE NEUTRON SCATTERING (SANS)

(a) Most of the work in this field has been carried out using D11A at ILL. The work has extended our knowledge of polymer chain conformation to polymers in bulk. Light scattering and small angle x-ray scattering techniques, which hitherto provided all available information, are only applicable to polymer solutions. Neutron scattering results have in the past three years raised Flory's hypotheses on chain conformations in rubbers and glasses (the basis of all theories of amorphous polymers) to the status of fact. Equally important information on the effects of bulk deformations and also of crystallisation on chain conformations is now beginning to emerge.

(b) The enormous backlog of experiments and pressure on time available at ILL (taking D17 into account also) means that a SANS instrument even of only comparable efficiency would be important especially in extending the polymer work to technological problems which will demand more time than do science problems. However, with count rates improved by an order of magnitude, entirely new experiments on the time dependence of chain conformations (relaxation phenomena) will be possible. This would enable the asymmetry of scattering to be measured as a function of time in a sample undergoing bulk relaxation on a technological time scale. Thus a whole new area of polymer science and technology could be opened up.

6.3 QUASI-ELASTIC SCATTERING

(a) Some of the conformational reorientational motions of polymer chains associated with the onset of main chain motion which occurs at the glass-rubber transition, or occuring in polymers in solution, have been investigated by quasi-elastic scattering. In solution, for example, the results

support the Zimm model (with hydrodynamic interactions) rather than the Rouse model. The range of interest is $0.01 < Q < 1.0$ Å^{-1} and $\Delta\hbar\omega \sim 1$ μeV.

(b) Extension of this work is seriously hindered by pressure of time on ILL instruments and this entirely prevents extension to technological problems which demand periods of time longer than are allocated at ILL. The quasi-elastic instruments discussed in §2 will be invaluable in extending the work on rubbers and gels which, in the current situation, are restricted to model systems only.

6.4 INELASTIC SCATTERING

(a) In amorphous systems inelastic neutron scattering has been used mainly to study side-group motions. Measurements on crystalline polymers have involved powders, stretch oriented specimens and in two or three instances specimens approximating to single crystals having macroscopic dimensions. Phonon frequencies have been measured and using perdeuterated samples dispersion curves have been determined. Generally, cold neutron time-of-flight instruments have been used together with triple axis spectrometers for the single crystal work.

(b) In the single crystal work advance is limited by single crystal growth technology rather than by neutron fluxes, but the much greater effective fluxes available with the SNS would make possible the use of significantly smaller crystals. The new source could provide additional capacity for the remaining inelastic work with the possibility of much improved resolution being especially valuable. The pulsed nature of the source would make possible the study of rotational isomerism in relaxing systems, which is important because the rotational isomeric model of the polymer chain is the one which underpins all accepted models concerning the influence of chemical structure.

6.5 WIDER ANGLE NEUTRON SCATTERING

The determination of radial distribution functions in the high Q region will give information on local molecular packing in both crystalline and amorphous states. Despite the work done on D11A this is a subject of current controversy. Even more important might be kinetic studies made in this range using a pulsed source while the sample is subjected to relatively low frequency mechanical deformation. The very high epithermal flux should make such kinetic experiments easily possible.

7. BIOLOGY

7.1 INTRODUCTION

Broadly, the experiments of interest can be classified as follows:

- Studies of single crystals of macromolecules (eg proteins such as myoglobin, lysozyme etc. and nucleotides). Here the wavelength range is 1 to 2 Å.
- Studies of semi-crystalline macromolecules where Bragg diffraction peaks are observed even though there is inherent disorder (eg fibre diffraction from proteins and DNA, diffraction from collagen, muscle and membranes). Typically 4 to 12 Å neutrons would be involved with these experiments and small angle scattering equipment (eg D11A or D17 at ILL) used.
- Neutron quasi-elastic and inelastic scattering studies of the dynamical properties of biological molecules and macromolecular structure.
- Small-angle scattering studies of separated macromolecules in solution (λ = 4 to 12 Å).
- Kinetic experiments using the pulsed nature of the source (λ = 1 to 12 Å say).

7.2 SMALL ANGLE NEUTRON SCATTERING FROM BIOLOGICAL PARTICLES IN SOLUTION

These experiments enable the determination of the spherically averaged Patterson function of the macromolecules in contrast against scattering from the solvent. In the absence of crystals of the macromolecules this information is vital to the determination of the low resolution structure and the technique requires that the solvent scattering-length density (usually water) is changed by choosing different D_2O/H_2O mixtures for the solvent and by choosing different small molecule concentrations. Because of the coherent elastic scattering-length-density difference between D_2O and H_2O a variety of contrast conditions are achieved and one can obtain 'fundamental scattering functions' which are related to:

- the outer profile of the particle
- the internal structure
- a 'cross' term of the inner and outer structures
- the distribution of D/H sites within the particle

Measurements at low Q, in the so-called Guinier region, yield information on the spherically symmetrical component of the scattering-length-density distribution within the macromolecules, but there is interest developing in higher Q, measurements, say $Q > .1$ Å^{-1}, where the deviations from spherical symmetry can be determined and where the details of the internal structure of the particles can be seen. These higher angle measurements where structural detail is revealed need careful discrimination of the scattered intensities against a background of incoherently scattered neutrons. Here a high flux of neutrons will be most useful. A minimum of seven separate experiments if necessary to determine the 'scatter functions' and ideally regression analysis involving some 16 to 20 spectra would be needed. Again the higher effective flux will cut down measurement times.

Deuteration of the macromolecules at non labile sites permits the determination of the position of the deuterated sites within the structure. One technique, the so-called triangulation method involves accurate measurements of differences of scattered intensity as a function of Q for two solutions. The first solution is a mixture of ribosome subunits with both proteins deuterated and both proteins protonated. The second solution is a mixture of ribosome subunits containing the first protein protonated and the second protonated. An interference function in the measured difference of intensities as a function of Q gives information about the distance between the scattering-length centres of the proteins and a distribution of length between extreme surfaces of the two proteins. By obtaining information on a large number of proteins in the ribosome subunits the positions of the proteins are obtainable by triangulation and it should be possible to determine the shape of the proteins. This technique will be applied to many other macromolecular assemblies (eg chromatin subunits, eukaryotic ribosomes etc) and it requires accurate determination of small intensity differences between two samples which are alternately switched in and out of the neutron beam. Clearly high statistics for the scattered neutrons are necessary, particularly since the conditions of the measurements are such that the molecules are nearly 'contrast matched' by the solvent. The ribosome experiments

will take several years to complete so that the increase in flux will add considerably to the speed at which these very time-consuming experiments can be done.

In studying dispersions of biological membranes and membrane components in solution the neutron scattered intensity falls off more rapidly than for globular particles in solution. In this case again therefore, a higher neutron flux will be a big advantage.

7.3 SMALL ANGLE STUDIES OF BRAGG DIFFRACTION IN SEMI-CRYSTALLINE BIOLOGICAL SPECIMENS

Neutron studies of small-angle Bragg peaks in specimens such as muscle, collagen, biological membranes etc. are revealing much information on the intact systems and on changes on activating a given system. For example, differences between contracted and relaxed muscle, and between retinal membranes in the dark and activated by light, may be studied.

Changes of the D_2O/H_2O ratios in the Ringer solutions give information on how the various parts of a structure contribute to the Fourier harmonic corresponding to the amplitude of a given Bragg peak. Many of these specimens are quite highly oriented and therefore information is available at particular Q values. Clearly information would be lost on spherically averaging the neutron data from an area detector (in an attempt to improve statistics) so that better count rates are a great help in studying the details of a particular Bragg peak.

7.4 STUDIES OF SINGLE CRYSTALS OF MACROMOLECULES

Studies of crystals of biological macromolecules using neutrons are in progress both at the ILL and at Brookhaven. The advantage of using neutrons may be listed as follows:

- The form factor for neutrons does not fall off with angle, so inherently the neutron technique is capable of higher resolution than x-rays.
- The coherent-elastic neutron scattering lengths for H and D are large and vastly different and, as with the small

angle scattering studies, this enables the location of D/H sites. The positions in the structure of hydrogen atoms, deuterium atoms and bound water molecules can therefore be studied.

Single crystal studies of small biological molecules have already provided valuable information about hydrogen bonding and the detailed structures of the macromolecular building blocks of amino acids and nucleotides. If it were possible (by virtue of a very high flux of neutrons of $\sim$ 1.5 Å wavelength) to carry out a complete structure determination in a few days, one could look in fine detail at D/H exchange at highly localised sites in the structure. Work at high pressures with cooled samples will reduce the thermal motion in the crystals and enable the full potential of the high resolution capabilities of neutrons to be obtained. These experiments will clearly gain from the high flux of neutrons at 1.5 Å wavelength which would be available from the SNS. The disadvantage of these experiments is that the measurements are not carried out *in vivo*, but there is the potential for a wealth of information of biological importance.

7.5 NEUTRON QUASI-ELASTIC AND INELASTIC SCATTERING

In biological studies this work has investigated the normal modes of vibration and force constants of poly-α-amino acids. At present the studies have concentrated on polyglycine (the simplest amino acid). More complex systems are now beginning to be investigated. These neutron studies supplement infra-red and Raman studies because they are most sensitive to displacements of hydrogen atoms in vibrational modes and are not restricted by optical selection rules. In this area the possibility of performing an energy analysis in conjunction with small angle scattering is very attractice.

7.6 NEUTRON POWDER DIFFRACTOMETRY

This work has not yet been extensively applied to studies of biological molecules. This may be in part because the numbers of scattering-lengths in the unit cells of even small biological molecules are too large for productive study by powder diffractometry. With the development of increasingly high resolution powder diffractometers, however, such experiments have become more feasible. The further advances offered by the SNS are therefore very attractive.

7.7 KINETIC EXPERIMENTS USING THE PULSED NATURE OF THE NEW SOURCE

There is quite a lot of interest in the dynamical aspects of biological processes, eg the kinetics of enzyme action, the rates for H/D exchanges within a structure, changes of structure with electrical signals, magnetic fields, exposure to light, temperature, pressure etc..

In principle the kinetics of many of the above processes could be studied with high resolution using the scattering from each neutron pulse to follow the process but in practice the statistics available from a single neutron pulse may not be good enough. For example the experiments using the stop-flow apparatus on D11A at Grenoble to study the dynamics of H/D exchange would benefit considerably from an increase in the mean flux, but information from single pulses would not be sufficient.

However, there are processes which can be repeated in phase with the proposed neutron pulses (for example, activation and relaxation of muscle, light activation of retinal membranes) and one could envisage rapid sample changes to study processes which could not be continuously recycled. Since these processes are phased in with the neutron pulses, good statistics could be built up for processes occurring at some particular small time delay after the activation process.

8. IN-BEAM NMR, AND POSSIBLY NQR STUDIES

8.1 NMR

Experiments with an in-beam NMR apparatus with two main modifications:

(a) in-beam production of the observed polarized probe nuclei during the measurement
(b) polarization and signal detection via the non isotropic nuclear β-radiation

are already being carried out at the ILL using a thermal guide with a polarized beam of $5\ 10^{7}$ neutrons $cm^{-2}\ s^{-1}$ and a polarization ratio of 80%.

The nucleides that have been examined are ^{8}Li, ^{12}B, ^{20}F, ^{28}Al, ^{38}Cl, ^{66}Cu, ^{108}Ag, ^{110}Ag, ^{116}In and the total number of usable nucleides is of the order

of 25, though extension to γ emitters may increase this number. The observed quantity is the polarization of the probe nucleus detected via the β decay asymmetries.

$$A = \frac{\beta_N - \beta_S}{\beta_N + \beta_S}$$

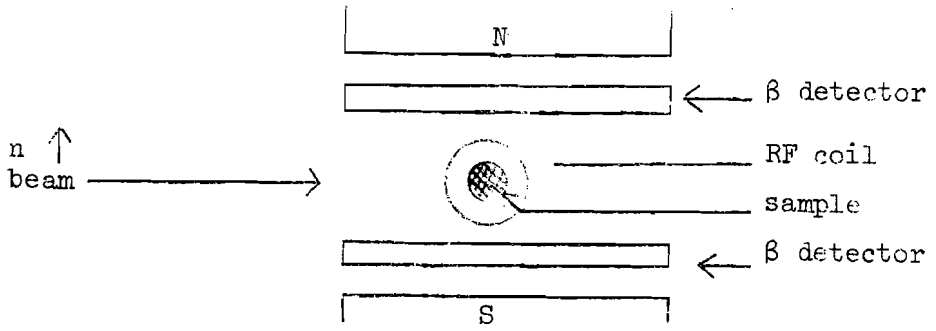

One can either detect stationary asymmetries $A(t) = A_o\ (1 + t_\beta/T_1)$,

where T_1 is the spin-lattice relaxation time and,

t_β is the β decay lifetime

as functions of the applied RF field or, using a chopped neutron beam, detect transients $A(t) = A_o\ e^{-t/T_1}$.

The sensitivity of the method is in principle high and extremely isolated probe nuclei are examined. So there is no problem with homopolar broadening and it is possible to use techniques already developed in classical NMR, for example the production and detection of very narrow ^{20}F NMR lines in solids by decoupling of ^{19}F spins due to strong irradiation at the ^{19}F frequency. Quadrupolar splitting can in favourable circumstances be obtained from rotating polycrystalline samples.

The problem with the method at the moment is that, since one is looking at a small difference between two large quantities, β_S and β_N, the counting times for good statistical accuracy tend to be long and this is particularly true of the examination of a quadrupolar split spectrum. It has been

estimated that for experiments on bifluorides at ILL times of the order of a month may be required. By using a pulsed NMR system and synchronising the application of the RF pulses with the bursts from the SNS significant improvements should be possible.

So far most of the experiments using this technique have been in the field of solid state physics but there are potentially interesting applications in chemistry, particularly if quadrupolar splittings are observable.

8.2 NQR

An attractive possibility which has not been exploited is an in-beam NQR experiment. The experimental arrangement would require four β detector units (N, S, E and W) rather than two and N and S would be connected together, as would E and W, so that the asymmetry A would now be

$$A = \frac{\beta_N+\beta_S - (\beta_E+\beta_W)}{\Sigma\beta}$$

and the sample could either by a single crystal or polycrystalline. In the latter case A would be zero in the absence of a resonant RF field, other things being equal, but a resonant RF field would perturb the nuclear magnetic dipolar orientation in those atoms where the principal electric field gradient was perpendicular to the coil and thus produce a change in A from zero.

The advantage of this technique is that one could look at nuclei whose stable isotopes are non-quadrupolar and where therefore it is difficult or impossible to obtain information about the electric field gradient at the nucleus. A prime example of this is fluorine, where ^{19}F has a spin of $\frac{1}{2}$ and no quadrupole moment but ^{20}F is quadrupolar.

MOLECULAR AND BIOLOGICAL SCIENCES: INSTRUMENTS

Instrument	Moderator	Specification	Field
Very High Energy Transfer Spectrometer	300K	$\hbar\omega \sim 1$ eV $\frac{\Delta\hbar\omega}{\hbar\omega} \sim 0.1$ $Q < 4$ Å^{-1}	Crystal field levels in opticall opaque transition metal compounds. Electronic excitations.
High Energy Transfer Chopper Spectrometer	300K	$100 < \hbar\omega < 600$ meV $\Delta\hbar\omega \sim 5$ meV low Q bank required	Vibrational spectroscopy, in particular the study of hydrogen modes on surfaces, in H-bonded systems and in metal hydride complexes.
Moderate Energy Transfer Chopper Spectrometer	300K	$10 < \hbar\omega < 100$ meV $\frac{\Delta\hbar\omega}{\hbar\omega} \sim 0.02$ low Q bank required	Conventional inelastic spectroscopy. Very low angle bank required for observing inelastic modes in liquids on the energy gain side - the 'small Q method'.
Inelastic Polarization Analysis Spectrometer	300K	$0 < \hbar\omega < 100$ meV $\frac{\Delta\hbar\omega}{\hbar\omega} \sim 0.1$ Spin selection of both incident and scattered beams	Separation of coherent and spin-incoherent contributions to scattering. Magnetic studies.
Constant Q Spectrometer	300K	$10 < \hbar\omega < 100$ meV $\frac{\Delta\hbar\omega}{\hbar\omega} \sim 0.05$ $1 < Q < 6$ Å^{-1}	Energy scans through (Q,ω) space at constant value of Q. Coherent excitations in molecular crystals and polymers.
High Count Rate Spectrometer	300K	$0 < \hbar\omega < 200$ meV $\frac{\Delta\hbar\omega}{\hbar\omega} \sim 0.1$ ΔQ relaxed	High data collection rate inelastic spectrometer (cf IR and Raman machines).
Time-of-flight MARX Spectrometer	77K	$0 < \hbar\omega < 50$ meV $\frac{\Delta\hbar\omega}{\hbar\omega} \sim 0.02$ $\frac{\Delta Q}{Q} \sim 0.1$	Conventional inelastic scattering. Quasi-elastic scattering at good resolution and high Q, diffusive modes of plastic and liquid crystals, hydrogen in metals, etc..
Long Wavelength Chopper Spectrometer	20K	$4 < \lambda < 10$ Å $\Delta\hbar\omega/E$ comparable to that of IN5	High resolution quasi-elastic studies. Low energy inelastic modes (< 20 meV) observable in neutron energy gain.
Very Low Q Spectrometer	20K	$0.005 < Q < 1$ Å^{-1} $\frac{\Delta Q}{Q} \sim 0.1$ $4 < \lambda < 12$ Å	'Small Angle Neutron Scattering': studies of polymers and biological systems.
White Beam Backscattering Spectrometer (L = 25 m)	20K	$\Delta\lambda = 3$ Å Quasi-elastic mode: $\Delta\hbar\omega \sim 15$ μeV $-1000 < \hbar\omega < 1000$ μeV Inelastic modes: scan up to 100 meV with $\frac{\Delta\hbar\omega}{\hbar\omega} < 8\ 10^{-3}$	Slow diffusive processes. Tunnelling transitions. Inelastic band shapes.
White Beam Backscattering Spectrometer (L = 100 m)	20K	$\Delta\lambda \sim 1$ Å $-200 < \hbar\omega < 200$ μeV $\Delta\hbar\omega \sim 2$ μeV	Very slow diffusive processes.

CHAPTER 3 INSTRUMENTATION

PULSED SOURCE INSTRUMENTS

3.1 Instruments suitable for condensed matter research using pulsed neutron sources may be broadly categorised thus:

(a) diffractometers, which use techniques identical to time-of-flight diffractometry on a continuous source. This method is rarely employed at reactors in comparison to the usual constant wavelength technique, whereas it is ideally suited to a pulsed source since no instrumentation is required in the incident beam and all incident neutrons are used. The efficiency of the instrument may be further increased by detecting over a large solid angle.

(b) direct geometry inelastic spectrometers, for which the incident energy is selected by some monochromatizing system (eg a single chopper) and the final energy is analysed by time-of-flight (similar to a double chopper instrument on a reactor). The lengths of the primary and secondary flight paths are usually similar. Only a small fraction of the primary neutrons is selected so that the efficiency of direct geometry spectrometers can only be increased significantly by the use of more detectors.

(c) inverted geometry inelastic spectrometers, for which the final energy is selected by some analysing system and the initial energy deduced by

time-of-flight. The instrumental resolution is dependent on the length of the incident flight path, whereas the analysing system may be placed close to the sample. As in time-of-flight diffractometry all the neutrons incident on the sample are used, and the efficiency of inverted geometry spectrometers may be further increased by using more than one analysing arm.

Twenty-six pulsed source instruments have been identified, based on the reports of the Working Groups and from other deliberations. A brief description of each is given below and table 3.1 provides an outline summary of their important characteristics.

TABLE 3.1

PULSED SOURCE INSTRUMENTS

	Instrument	Moderator	Specification	Field
1.	Single Crystal Diffractometer	300K	$0.3 < \lambda < 1.5$ Å $\frac{\Delta Q}{Q} \sim 0.03$ Polarized incident beam option	Single crystal structure determination. Magnetization density distributions. Structural investigations as a function of temperature, pressure, etc.
2.	High Intensity Medium Resolution Powder Diffractometer	300K	$Q > 2.5$ Å^{-1} ($\phi = 170^{\circ}$) $\frac{\Delta Q}{Q} \sim 3\ 10^{-3}$ $Q > 0.6$ Å^{-1} ($\phi = 30^{\circ}$) 12 m incident flight path	Structural determination using powder samples. Kinetic processes, eg diffusion of gases into solids.
3.	Total Scattering Spectrometer	300K	$0.3 < Q < 100$ Å^{-1}	Structure factors of fluids and amorphous solids.
4.	High Pressure Spectrometer	300K	$0.3 < Q < 100$ Å^{-1} $\frac{\Delta Q}{Q} \sim 0.01$ Pressures up to 50 kbar	Pressure dependence of structure factors of fluids and amorphous solids. Triplet correlation functions.
5.	Total Scattering Polarization Analysis Spectrometer	300K	Q up to 20 Å^{-1} Spin analysis of scattered beam	Determination of elastic spin-dependent cross-sections. Structure factor measurements in presence of spin-incoherent scattering.
6.	Elastic Distrimination Spectrometer	300K	$1 < Q < 25$ Å^{-1} $\frac{\Delta Q}{Q} \sim 0.02$	Simultaneous measurement of elastic and total diffraction patterns to allow separation of elastic and inelastic scattering to study the eccentricity of atomic thermal vibration tensors.
7.	Very High Energy Transfer Spectrometer	300K	$\hbar\omega \sim 1$ eV $\frac{\Delta\hbar\omega}{\hbar\omega} \sim 0.1$ $Q \sim 4$ Å^{-1}	Electronic excitations: Band energies in semiconductors. Valence fluctuations. Crystal field levels in optically opaque transition metal compounds.
8.	High Energy, High Momentum Transfer Spectrometer	300K	$Q_{max} \sim 30$ Å^{-1} ($\phi = 150^{\circ}$)	Measurements on the dynamics of the helium liquids. High Q dependence of $S(Q,\omega)$ for amorphous materials.
9.	High Energy Transfer Chopper Spectrometer	300K	$100 < \hbar\omega < 600$ meV $\Delta\hbar\omega \sim 5$ meV $\Delta Q \sim 0.1$ Å^{-1} low Q bank	Vibrational spectroscopy, in particular the study of hydrogen modes on surfaces, in H-bonded systems and in metal hydride complexes. Phonons, magnons, crystal fields, vibrational modes and liquid dynamics.
10.	Crystal Analyser Spectrometer	300K	$50 < \hbar\omega < 300$ meV $\Delta\hbar\omega \sim 5$ meV $\Delta Q \sim 0.1$ Å^{-1}	Vibrational spectroscopy. Phonon, magnon and crystal field studies.
11.	High Count Rate Spectrometer	300K	$0 < \hbar\omega < 200$ meV $\frac{\Delta\hbar\omega}{\hbar\omega} \sim 0.1$ ΔQ relaxed	High data collection rate inelastic spectrometer (cf IR and Raman machines).

Continued

	Instrument	Moderator	Specification	Field
12.	Inelastic Polarization Analysis Spectrometer	300K	$0 < \hbar\omega < 200$ meV $\frac{\Delta\hbar\omega}{\hbar\omega} \sim 0.01$ Spin selection of both incident and scattered beams	Spin dynamics. Separation of magnon and phonon scattering. Measurements of the dynamical structure factors $S(\underline{Q},\omega)$ and $S_s(\underline{Q},\omega)$ for spin-incoherent scatterers.
13.	Moderate Energy Transfer Chopper Spectrometer	300/77K	$\hbar\omega < 100$ mcV $\frac{\Delta\hbar\omega}{\hbar\omega} \sim 0.02$ low Q bank required $\Delta Q \sim 0.1$ Å^{-1}	Measurements on the dynamical structure factors of liquids. Conventional inelastic spectroscopy. Very low angle bank required for observing inelastic modes in liquids on the energy gain side - the 'small Q method'. Phonon, magnon and crystal field studies.
14.	Rotating Crystal Spectrometer	300/77K	$0 < \hbar\omega < 50$ meV $\Delta\hbar\omega \sim 5$ meV $\Delta Q/Q \sim 0.1$	Conventional inelastic spectroscopy. Molecular modes, crystal field levels, paramagnets, plastic and liquid crystals.
15.	Constant Q Spectrometer	300/77K	$10 < \hbar\omega < 200$ meV $\frac{\Delta\hbar\omega}{\hbar\omega} \sim 0.05$ $3 < Q < 6$ Å^{-1}	Triple axis analogue: scans in energy through $(\underline{Q},\omega)$ space at constant $\underline{Q}$. Coherent excitations.
16.	Cross-Section Spectrometer	300K	$0.025 < E_o < 1$ eV $\frac{\Delta E_o}{E_o}$ 0.01	Total cross-section measurements.
17.	Single Crystal Diffractometer	77K	$1 < \lambda < 6$ Å $\frac{\Delta Q}{Q} \sim 0.03$	Structure determination of crystals with large unit cell dimensions.
18.	High Resolution Powder Diffractometer	77K	$Q > 6$ Å^{-1} ($\phi = 170^o$) $Q > 0.8$ Å^{-1} ($\phi = 15^o$) $\frac{\Delta Q}{Q} = 0.001$ 100 m incident flight path	Resolution of closely spaced peaks in powder diffraction profile.
19.	Time-of-Flight MARX Spectrometer	77K	$0 < \hbar\omega < 50$ meV $\frac{\Delta\hbar\omega}{\hbar\omega} \sim 0.02$ $\frac{\Delta Q}{Q} \sim 0.1$	Conventional inelastic scattering. Quasi-elastic scattering at good resolution at high Q, diffusive modes of plastic and liquid crystals, hydrogen in metals, etc. Intermolecular modes of crystals, magnetic crystal field levels.
20.	Total Scattering Spectrometer	77/20K	$0.3 < Q < 100$ Å^{-1}	Structure factor of fluids and amorphous solids. High resolution at low Q.
21.	Elastic Diffuse Spectrometer	20K	$0.05 < Q < 2$ Å^{-1} Polarized incident beam option	Effects of doping, alloying, heat treating and irradiating condensed systems. Magnetic defects.
22.	Very Low Q Spectrometer (SANS)	20K	$0.005 < Q < 1$ Å^{-1} $\frac{\Delta Q}{Q} \sim 0.1$ $4 < \lambda < 12$ Å	'Small Angle Neutron Scattering': studies of polymers and biological systems. Defects and structural periodicities on the scale ~ 100 Å.

Continued

	Instrument	Moderator	Specification	Field
23.	Very Low Q Inelastic Spectrometer	20K	$0.01 < Q < 1\ \text{Å}^{-1}$ $\frac{\Delta Q}{Q} \sim 0.1$	Separation of elastic and inelastic scattering at very low Q.
24.	Long Wavelength Chopper Spectrometer	20K	$4 < \lambda < 10$ Å $\Delta\hbar\omega/E$ comparable to that of IN5	High resolution quasi-elastic studies. Low energy inelastic modes (< 20 meV) observable in neutron energy gain.
25.	White Beam Backscattering Spectrometer (L = 25 m)	20K	$\Delta\lambda$ = 3 Å Quasi-elastic mode: $\Delta\hbar\omega \sim 15$ μeV $-1000 < \hbar\omega < 1000$ μeV Inelastic modes: scan up to 100 meV with $\frac{\Delta\hbar\omega}{\hbar\omega} < 8\ 10^{-3}$	Very high resolution quasi-elastic studies. Slow diffusive processes. Tunnelling transitions Inelastic band shapes.
26.	White Beam Backscattering Spectrometer (L = 100 m)	20K	$\Delta\lambda \sim 1$ Å $-200 < \hbar\omega < 200$ μeV $\Delta\hbar\omega \sim 2$ μeV	Very slow diffusive processes.

1. SHORT WAVELENGTH SINGLE CRYSTAL DIFFRACTOMETER

$0.3 < \lambda < 1.5$ Å

$\frac{\Delta Q}{Q} \sim 0.03$

Serious extinction effects occur for strong reflections in single crystals which are measured at long wavelengths on neutron diffractometers. Short wavelength neutrons available on a pulsed source enable high resolution diffraction studies of the structure of single crystals with cell dimensions of the order of 5-10 Å, for which extinction is usually severe. The instrument will both improve the quality and extend the range in Q of the data available from the hot source diffractometer at Grenoble. In addition, structural studies may also be performed on crystals with larger cell dimensions of 10-20 Å for which extinction is generally less acute. The short wavelengths will improve the atomic resolution for the study of anisotropic and anharmonic thermal vibrations, and for studying phase transitions.

A large area detector is required to measure with reasonable resolution reflections in a large range of Q for moderately large unit cells. The single crystal diffractometer on the Harwell linac used a bank of 32 detectors, though here is envisaged a large 2π detector with thousands of elements of size 2 cm at a distance of ∿ 0.5 m from the sample. Specimen sizes are typically 10 mm^3 for which reasonable resolution is available when a 10 cm ambient temperature moderator is viewed at a distance of 6.5 m. However this primary flight path must be increased somewhat for the inclusion of a polarized filter and a spin flipper, so that polarized neutron diffractometry may be performed for the structural determination of magnetic materials. Provision can also be made for the inclusion of a cryostat, furnace and pressure cell.

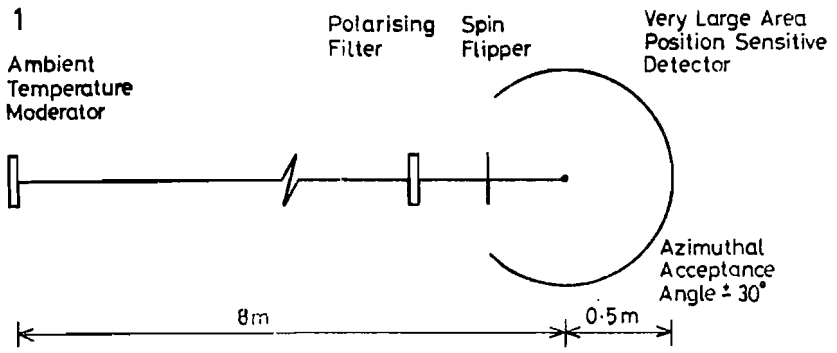

2. HIGH INTENSITY POWDER DIFFRACTOMETER

$Q > 2.5$ Å^{-1} ($\phi = 170^\circ$) $\frac{\Delta Q}{Q} \sim 0.003$

$Q > 0.6$ Å^{-1} ($\phi = 30^\circ$)

High intensities at short wavelengths available on pulsed sources may be used for the diffraction of powdered crystalline samples with high resolution by backscattering. Developments in the technique of profile analysis can be used in the analysis of time-of-flight powder diffraction to examine complicated structures with large unit cells. This method has been tested successfully on an instrument on the Harwell linac.

The primary flight path from the ambient temperature moderator is 12 m, with the scattered flight path of 2 m. Detectors are placed on the Debye-Scherrer cones with an extended counter bank along the focussing curve for the back-scattering angle of $\phi = 170^\circ$, and with a smaller area detector solid angle at $\phi = 30^\circ$. The counters are contained in an evacuated box with the sample environment which may have up to 5 positions on the sample changer. The sample size is of the order of 5 cm, and may be incorporated with a furance, cryostat or pressure cell. Frame overlap will occur at wavelengths of ∿ 5 Å, so that it would be useful to exclude longer wavelengths

by a simple chopper which may be placed first outside the biological shield, since filters tend to cut off at too high energies.

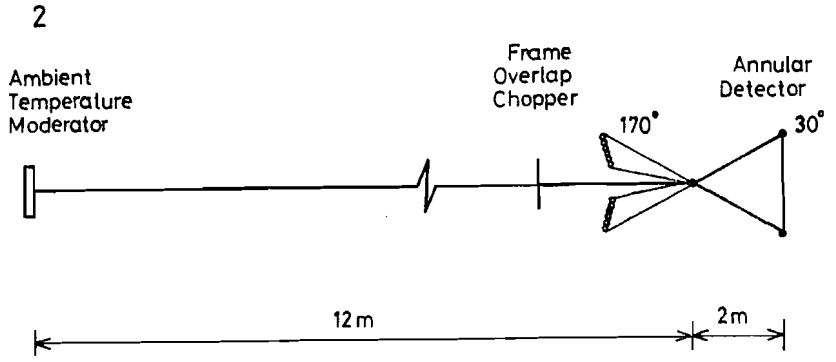

3. TOTAL SCATTERING SPECTROMETER

$\lambda > 0.12$ Å

$0.3 < Q < 100$ Å^{-1}

$0.6 > \frac{\Delta Q}{Q} > 0.015$

An active programme has continued for many years on the Harwell total scattering spectrometer for the measurement of structure factors of fluids and amorphous materials. Time-of-flight diffraction has the ability to extend the range in Q available on a diffraction instrument on a conventional reactor source on account of the abundance of short wavelength neutrons. Fluid and amorphous material structure factor measurements do not require a high degree of resolution and hence high intensities can be obtained by relaxing resolution particularly for the detectors at high scattering angles. Consequently the use of an extended time-focussed detector in a backward geometry allows the time-of-flight diffraction instrument even on a modest pulsed source, to gain in intensity down to low values in Q over a conventional instrument on a reactor hot source.

The instrument is constructed with a 7.5 m incident flight path and has 6 counter banks at angles of 150°, 90°, 58°, 20° and 10°. Each counter is at a scattered flight path of 0.5 m and is designed with curved slits of appropriate curvature to follow the Debye-Scherrer cones. The sample is placed in the polychromatic beam of

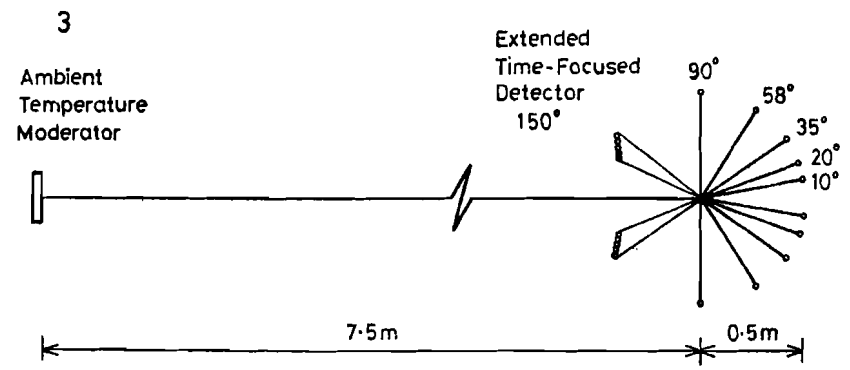

neutrons, and sample sizes of up to 5 x 5 cm^2 may be adapated by varying slits in the primary beam. The sample region is sufficiently large to accommodate a cryostat, furnace or pressure cell. A 6 position sample changer is available to allow simultaneous acquisition of data for the sample, empty can, vanadium reference and background. Monitor counters before and after the sample allow estimates of the absorption.

4. HIGH PRESSURE SPECTROMETER $2 > \lambda > 0.2$ Å

$0.3 < Q < 30$ $Å^{-1}$ $\frac{\Delta Q}{Q} \sim 0.01$

This instrument is essentially a total scattering spectrometer with high Q resolution and scattering angles restricted to $\phi < 10^o$ and $\phi > 170^o$. The use of a fixed scattering angle to facilitate the construction of high pressure cells for measurements on fluids and both amorphous and crystalline solids is a big advantage of pulsed sources. A purpose built nigh pressure spectrometer would have a high Q resolution to enable accurate subtraction of the Bragg peaks produced by the windows of the pressure cell. The windows would be limited to an entrance window with a field of view of 10^o and an exit (transmission) window also of 10^o view (these windows would also act for both the main beam and scattered beams).

The high resolution demands a moderator-sample distance of 12 m, with a maximum sample size of 1 cm viewing the full 10 cm ambient temperature moderator. Adequate resolution is given for the backward scattering angle if the sample-detector is 2 m, and the counter bank has high count rates for $Q > 6$ $Å^{-1}$ if detectors are placed in a time-focussed geometry throughout the entire Debye-Scherrer cone. The two detector angles allow an overlap in Q and between them cover the full Q range required. The forward detector is most important since it measures in the region of the first diffraction peak, and its small size (and hence small count rate) for adequate resolution determines the measurement time. It consists of a ring detector of thickness 0.5 cm to cover the entire Debye-Scherrer cone at an angle of 8^o and at a distance of 4 m from the sample.

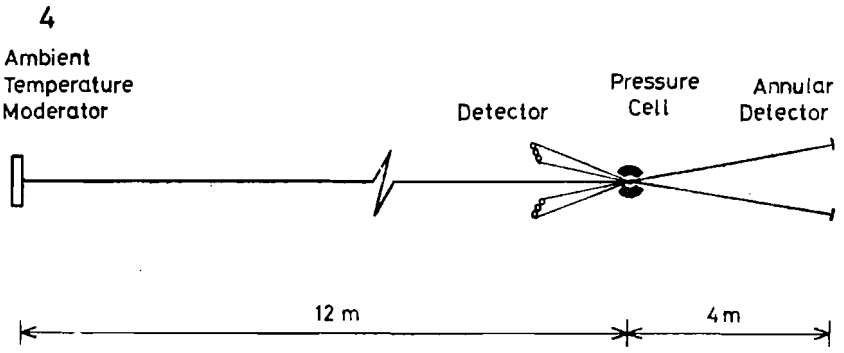

5. TOTAL SCATTERING POLARIZATION ANALYSIS SPECTROMETER Q up to 20 $Å^{-1}$

Polarization analysis on this modification of a total scattering spectrometer will allow measurements of elastic spin-dependent cross-sections when inelastic scattering may be ignored, eliminated, or evaluated separately. Q values of up to ~ 20 $Å^{-1}$ will be attainable.

A polarized proton white beam polarizing filter is required for the incident beam, as well as a non-adiabatic spin flipper which can operate over a large neutron energy range. The spin analysing filter would contain

polarized ^{149}Sm nuclei for scattered neutron energies $E_1 < 0.15$ eV, but for spin analysing at all neutron energies a second polarized proton filter is required.

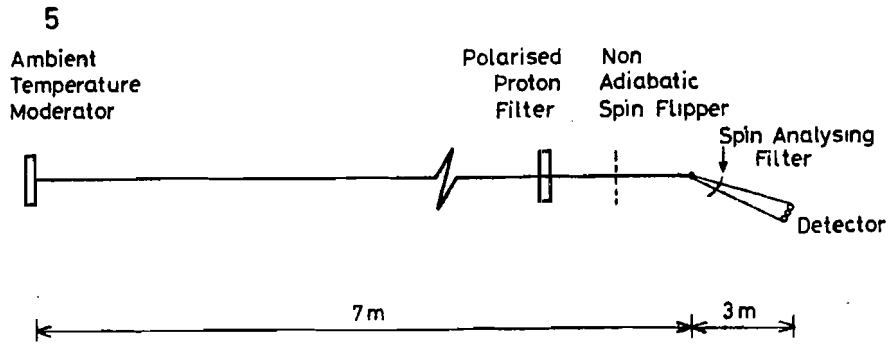

6. ELASTIC DISCRIMINATION SPECTROMETER

$1 < Q < 25\ \text{Å}^{-1}\ \ \frac{\Delta Q}{Q} \sim 0.02$

The use of a correction chopper on a pulsed source allows the separation of elastic and inelastic scattered neutrons in diffraction experiments, and permits the simultaneous measurement of both the elastic and the total diffraction patterns of amorphous materials. This information can be used to study the eccentricity of the atomic thermal-vibration tensors, and also provides data for the dynamical corrections to total scattering experiments. At present elastic diffraction can only be carried out on a triple-axis spectrometer which has both a restricted Q-range and a limited experimental availability.

The sample is located in a primary polychromatic beam and neutrons of all energies are measured by the detectors. The correlation chopper is run asynchronously with the pulsed source and data analysis is dependent on both time-of-flight referred to the pulsed source and simultaneous correlation referred to the chopper. The best resolution is obtained for equal primary and secondary flight paths, and both are taken as 8 m, so that the full size (10 x 10 cm^2) of the ambient temperature moderator is viewed. The sample may have dimensions of a few cm and is located immediately behind the chopper for the best resolution. This limits the scattering angle to 90°,

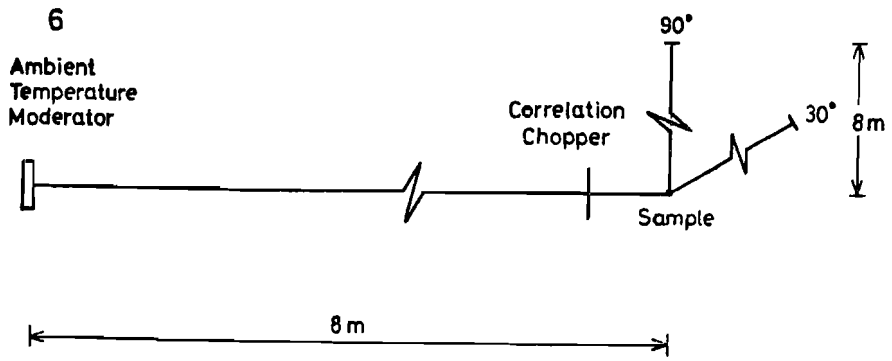

which corresponds to Q_{max} of ~ 25 Å^{-1}, sufficiently high for many materials. Secondary flight paths are placed at scattering angles of 30^{o} and 90^{o} and large area detectors are required. The method has been tested at the Munich reactor using a periodic rotor for a chopped beam, though this method of separation of elastic and inelastic scattering is most suited for a pulsed neutron source.

7. VERY HIGH ENERGY TRANSFER SPECTROMETER

$\hbar\omega \sim 1$ eV $\quad \Delta\hbar\omega/\hbar\omega \sim 0.1$

$Q \sim 4$ Å^{-1} $\quad \Delta Q/Q \sim 0.1$

A spectrometer to measure energy difference $\hbar\omega$ of ~ 1 eV as are found in transitions between electron bands in semi-conductors requires incident neutron energies of ~ 10 eV. A specification of 10% energy transfer resolution with a wavevector change $Q \sim 4$ Å^{-1} demands a small ($\sim 2^{o}$) scattering angle and an incident energy resolution $\Delta E_o/E_o$ of about 0.7%. A fast chopper with this resolution will require considerable development and will have only a small transmission.

A resonance detector may be used as an inverse geometry spectrometer, in which the energy selection and neutron detection are performed simultaneously. ^{238}U has a very sharp and well separated resonance absorption at an energy of 6.67 eV with a total width of 0.028 eV, allowing an energy resolution of 0.4%. The gammas emitted after the neutron capture are detected in coincidence by sodium iodide crystals or liquid scintillators. To prevent large background, the U^{238} can be surrounded by a thin layer of $^{10}B_4C$. The incident energy is measured by time-of-flight and the narrow resonance width allows the energy transfer to be measured to about 5-10%. Such a resonance absorption detector is being tested at Oak Ridge. Matching the contributions to the energy resolution gives a primary flight path length of the order of 14 m. The secondary flight path should be as short as possible, about 2 m, consistent with the angular definition and shielding. In order to minimise the spread of the Q resolution of the spectrometer, the ^{238}U slab will be placed at an angle to the scattered flight path. Focussing will also require the sample and the ambient temperature moderator to be placed at an angle to the primary flight path.

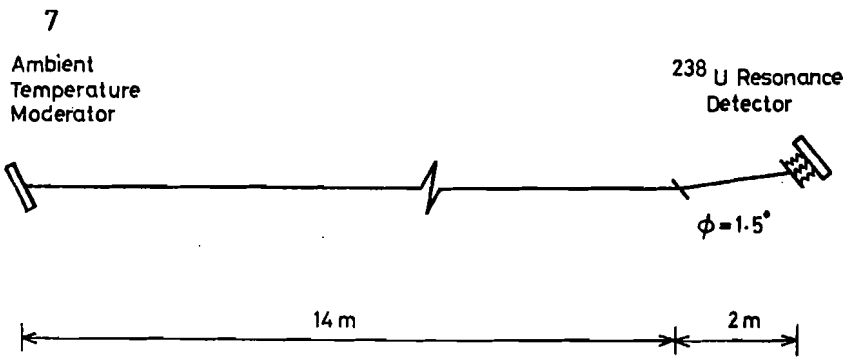

8/9. HIGH ENERGY TRANSFER, HIGH/LOW MOMENTUM TRANSFER SPECTROMETER

$100 < \hbar\omega < 600$ meV $\quad \frac{\Delta\hbar\omega}{\hbar\omega} \approx 0.05$

$Q < 4\ \text{Å}^{-1} \quad \Delta Q \sim 0.1\ \text{Å}^{-1}$

$Q_{max} \sim 30\ \text{Å}^{-1}$

An inelastic rotor spectrometer is required to perform energy scans simultaneously over a large Q range. The epithermal intensity available on the SNS will allow the useful range of neutron inelastic spectroscopy to be extended beyond that possible on the Harwell linac (IRS) or the hot source at ILL. To achieve the required specification on a direct geometry machine would place very stringent demands on a chopper system ($\sim$ 2 μs burst time required). Direct geometry, nowever, has considerable advantages, particularly for liquids work (simultaneous data collection at a set of ϕ values). It may, therefore, be worthwhile putting effort into a chopper development programme. With a feasible chopper ($\sim$ 7 μs) this spectrometer will out perform IN1 at ILL.

A low Q bank (possibly in the form of a PSD) would be a useful feature for the study of inelastic excitations. A backward angle, high Q, bank is required for studies of quantum fluids.

An inverted geometry crystal analyser spectrometer will compete with this spectrometer if spectra at only a few values of Q are required.

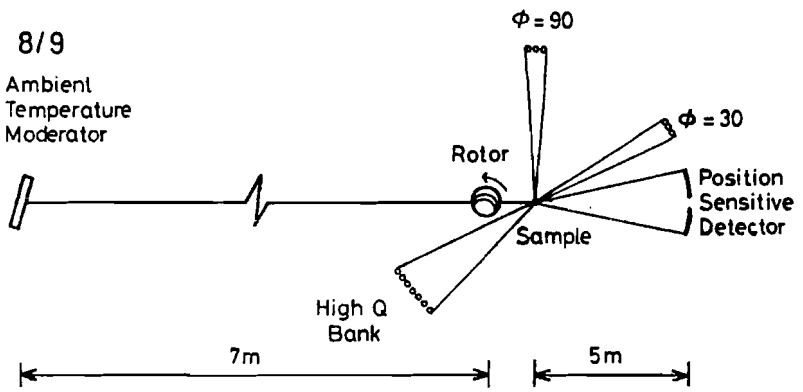

10. CRYSTAL ANALYSER SPECTROMETER

$50 < \hbar\omega < 300$ meV $\quad \hbar\omega \sim 5$ meV

$\Delta Q \sim 0.1\ \text{Å}^{-1}$

This instrument is required to make measurements at lower energy transfers than those measured on the inelastic rotor spectrometer, though measurements of $S(Q,\omega)$ can also be made in the energy transfer range up to 500 meV at medium Q values. It can be used for the study of diffusional broadening effects in liquids and amorphous materials, of liquid and paramagnetic scattering law distributions, of phonon and magnon dispersion curves in single crystals, and of molecular excitations of incoherent scattering samples. Up scattering of cold neutrons is limited to energies below 80 meV by the Boltzmann factor. Down scattering using a beryllium filter detector can be extended to study energy transfers up to 400 meV, but these high Q measurements allow multi-phonon effects, which are proportional to Q^4, to obscure the observation of high energy excitations. Measurements at low Q to minimise these effects requires large incident energies, and small scattering angles.

The inelastic rotor spectrometer performs down scattering measurements from a fixed high energy E_o to a range of final energies, whereas the crystal analyser spectrometer has a final energy fixed by the crystal, and the whole of the inelastic scattering distribution may be analysed by time-of-flight. The incident flight path L_o is 7 m, and analyser is held at a distance 1.5 m from the sample at a scattering angle of 10^o. A series of detectors are set at a further 1.5 m from the analyser, and the sample, analyser and detectors are placed in a focussed condition to minimise the resolution broadening. The analyser crystal and its particular reflection should be chosen such that the final energy analysed is of the order of the energy transfer. Second order contamination may be eliminated by the use of filters. Such an instrument has been successfully tested at Argonne, in which a beryllium filter was placed between the curved graphite analyser and the helium-3 detector.

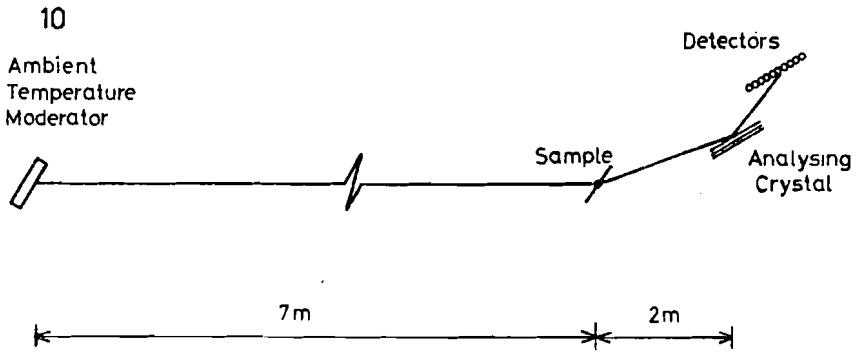

II. HIGH COUNT RATE SPECTROMETER

$0 < \hbar\omega < 200$ meV $\quad \frac{\Delta\hbar\omega}{\hbar\omega} \sim 0.1$

ΔQ relaxed

In the spectroscopic study of undispersed modes (eg the internal vibrations of molecules) the data acquisition rate may be improved by relaxing the Q definition of the instrument. Thus, for example, a scan of the region 25 meV $< \hbar\omega <$ 125 meV may currently be made on the Pluto Beryllium Filter with adequate statistics in less than half a day. A decrease in counting time of two orders of magnitude would bring inelastic neutron scattering into the regime of infrared and Raman studies. Run times of a few minutes would make possible the investigation of systems as a function of temperature and composition, and would allow kinetic studies to be performed. Such an instrument, run on a service basis, would be valuable as a "fingerprint" tool, and would permit technological exploitation of the technique.

Such a spectrometer may be realised on the SNS in a variety of ways:

(a) by summing the signal over a large angular range on a chopper spectrometer (instruments 9, 13 and 24).

(b) by a Filter (Be) or Filter-difference (Be-BeO; Be-Fe).

(c) in an inverted geometry mode, by using a curved crystal analyser.

(d) by using a band-pass mirror system.

As with steady state sources, method (b) has the disadvantage of having $Q \sim k_o$.

11b

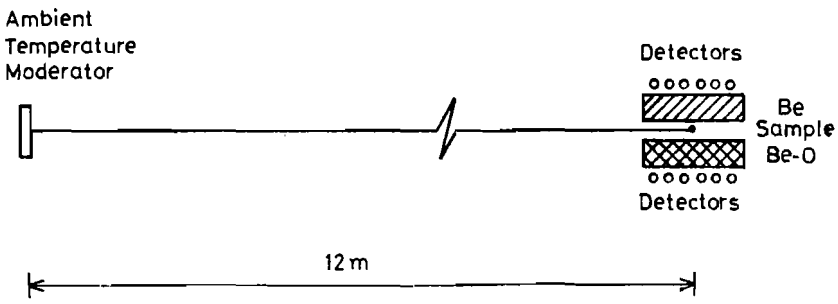

11c

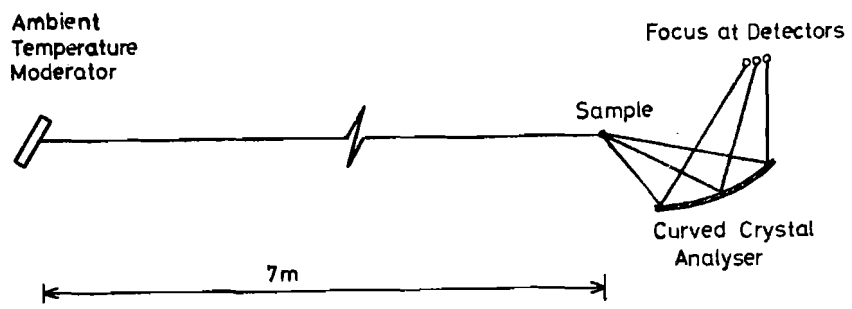

12. INELASTIC POLARIZATION ANALYSIS SPECTROMETER

$0 < \hbar\omega < 200$ meV

$\frac{\Delta\hbar\omega}{\hbar\omega} \sim 0.01$

$Q < 5$ Å^{-1} $\quad \Delta Q \sim 0.1$ Å^{-1}

Polarization analysis of the incident and scattered beam on an inelastic spectrometer permits the determination of the spin-flip and non spin-flip cross-sections. Interest in these cross-sections extends beyond the field of simple magnetic scattering because of the following relationship:

$$\sigma_{\text{spin-flip}} = \frac{2}{3}\sigma_{\text{inc}}$$

$$\sigma_{\text{non spin-flip}} = \frac{1}{3}\sigma_{\text{inc}} + \sigma_{\text{coh}}$$

Their determination thus allows the separation of the coherent and spin-incoherent contributions to the scattering, and hence the determination of the dynamical structure factors, $S(\underline{Q},\omega)$ and $S_s(\underline{Q},\omega)$. For reasons of intensity, such experiments are at the limit of present facilities.

On the SNS, one possible design for such a spectrometer would be an inverted geometry machine, final state spin and energy analysis being performed by a Co:Fe polarizing crystal. The incident beam may be defined by a primary spectrometer similar to that described for Instrument 5 above.

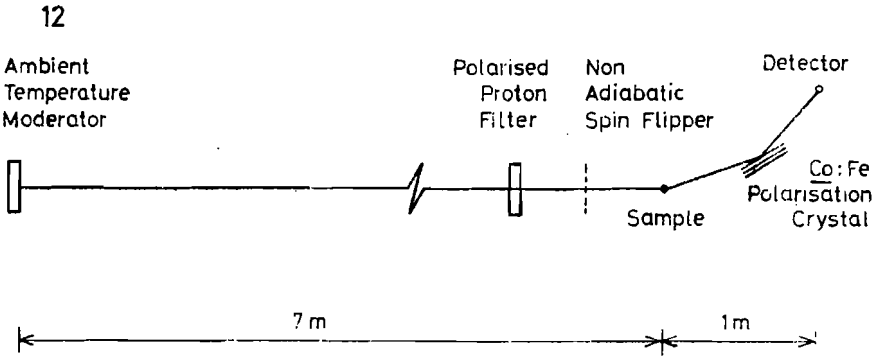

13. MODERATE ENERGY TRANSFER SPECTROMETER

$\hbar\omega < 100$ meV $\quad \frac{\Delta\hbar\omega}{\hbar\omega} \sim 0.02$

$50 < E_o < 150$ meV

The energy range covered by this spectrometer is that classically associated with inelastic neutron scattering on medium or high flux reactors. The diverse programme of research which already exists for such a machine would greatly benefit from two orders of magnitude increase in flux. Such an increase would also permit the development of inelastic kinetic experiments.

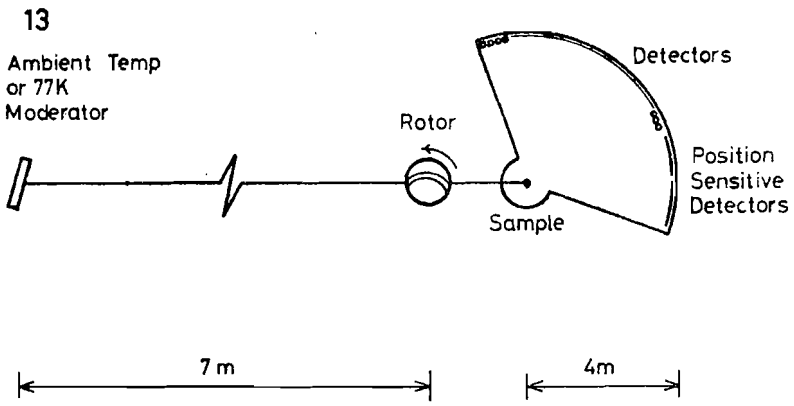

A single chopper spectrometer with a 4 m radius time-of-flight detector bank would meet the above requirements. The demand on the chopper of a burst time in the range 10-50 μsec is realisable. The large detector bank allows a set spectra to be accumulated simultaneously. By using a very low angle counter bank and a high incident energy, a relatively small value of Q may be associated with energy transfers ∿ 25 meV. (This is in sharp contrast to the locus associated with a conventional cold neutron spectrometer.) This 'small Q' method allows

inelastic features to be observed which would normally be washed out by recoil/diffusive effects. It is to be noted, however, that since inelastic cross-sections vary as Q^2, the increased flux of the SNS will be essential for such experiments performed at small scattering angles for which only a small solid angle is available.

14. ROTATING CRYSTAL SPECTROMETER

$0 < \hbar\omega < 50$ meV
$\Delta\hbar\omega \sim 5$ meV
$\Delta Q/Q \sim 0.1$

Low energy transfer measurements at relatively relaxed Q resolution may be made using a rotating crystal spectrometer. Such an instrument has already been tested on the Toronto electron linac. The rotating crystal suppresses reflections from undesired lattice planes since reflections of order higher than the first are eliminated by time-of-flight. The monochromatic beam is diffracted from the main beam so that the instrument allows measurements to be made with relatively low background. In addition the rotating crystal gives high energy resolution to the measurements.

It is best for the rotating crystal to be located within a few metres of the moderator with a 4 m flight path from the crystal to the sample and a similar flight path from the sample to the detector. The detectors should be enclosed with an evacuated chamber and be placed in an arc which extends from a small scattering angle to over 90°.

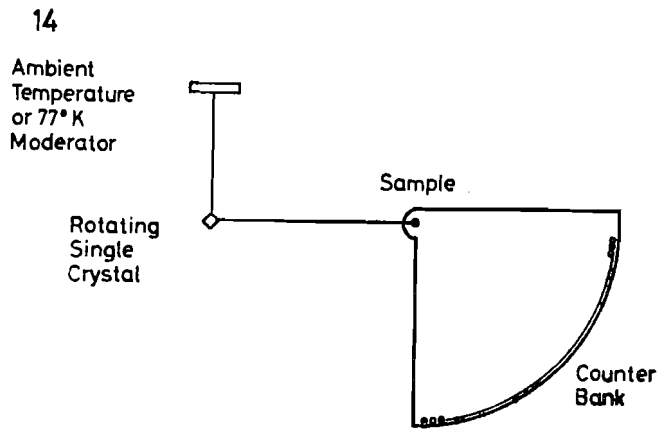

15. CONSTANT Q SPECTROMETER

$10 < \hbar\omega < 200$ meV $\quad \frac{\Delta\hbar\omega}{\hbar\omega} \sim 0.05$
$3 < Q < 6$ Å^{-1}

Many experiments on excitations in single crystals require data only along high symmetry directions. Unless the excitation spectrum is already known, only the constant Q type of scan can ensure that the observed excitation lies at the required high symmetry position. This is the reason for the high demand for reactor triple-axis spectrometers.

On a pulsed source, it is natural to use time-of-flight analysis at some stage of the scattering process. If a constant Q scan is employed, then the momentum and energy transfer both vary non-linearly across the spectrum. By using an extended analysing crystal and a position sensitive detector, however, a constant Q scan may be achieved.

The constant Q spectrometer is a special configuration of the Time-of-Flight MARX Spectrometer (Instrument 19). Both the analyser crystal planes and the PSD are parallel to the incident beam; the initial wavevector is

determined by time-of-flight and the final state wavevector by positon on the PSD. The constant Q scan is obtained by picking the appropriate time-of-flight channel at each position on the PSD. A prototype of this spectrometer is being tested on the present Harwell linac.

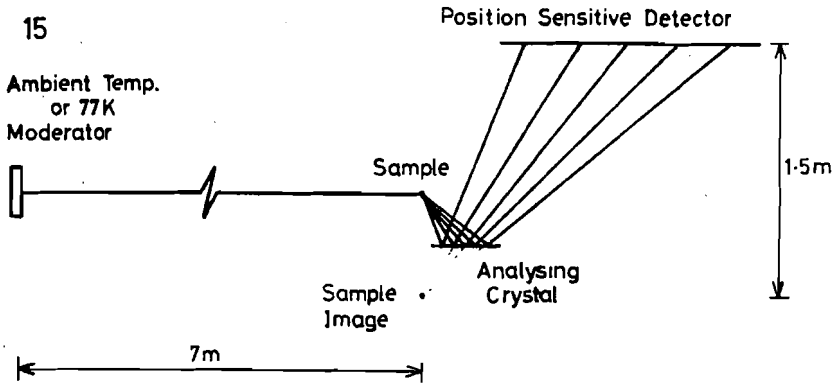

16. CROSS SECTION SPECTROMETER $0.025 < E < 10$ eV $\frac{\Delta E}{E} = 0.01$

All neutron scattering experiments sustain attenuation and multiple scattering to varying extents, though often they may either be ignored or accounted for. In some cases an extra transmission experiment must be performed. Structural measurements of, for example, liquids and amorphous materials, performed by time-of-flight diffraction require the knowledge of the total cross section for the specimen over the range of incident wavelengths used in the experiment. This is obviously best performed by a transmission experiment using the same incident flux as that on the main experiment rather than on a reactor whose spectrum has relatively few neutrons at the higher energy range. A facility for this measurement has existed on the Harwell linac. In addition the spectrometer can also be used for nuclear data work, for example, the study of low energy resonance parameters and as a test-bed facility.

The sample is placed at a distance of 6 m from the ambient temperature moderator, with a helium-3 or BF_3 detector placed a further 6 m beyond the sample position. Collimation is provided by variable shutters in the

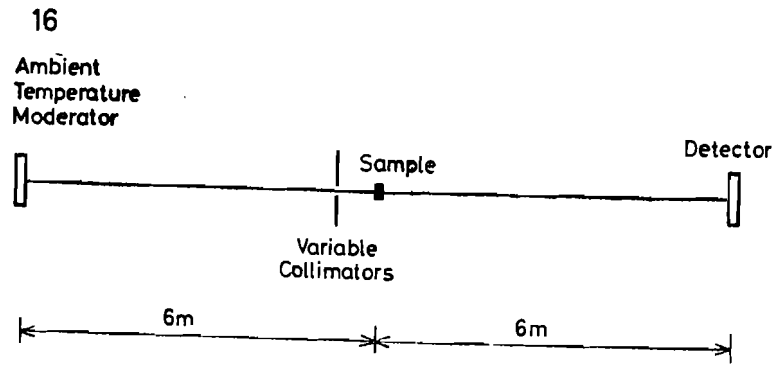

primary path length. Wavelength selection is provided by time-of-flight. A total flight path of 12 m can allow a time resolution of the order of 0.003, which will provide better energy resolution that is required. It is possible for this instrument to be incorporated with, for example, a total scattering spectrometer.

17. LONG WAVELENGTH SINGLE CRYSTAL DIFFRACTOMETER

$1 < \lambda < 6$ Å

$\frac{\Delta Q}{Q} \sim 0.03$

Complex molecules having large unit cells with dimensions as great as 40 Å may be studied with neutrons of wavelength $1 < \lambda < 6$ Å. The problem of extinction is usually unimportant so that the longer wavelengths may be used to increase the instrumental resolution. The advantage of a pulse source can be realised by the use of a large area position sensitive detector to enable high count rates with good resolution. However a position sensitive detector does not allow any focussing technique for the instrument, so that the elements should be small. It appears that a detector with the same angular resolution (2°) for its elements as that proposed for the short wavelength instrument will be appropriate, though some restricting to lower scattering angles may be acceptible.

The total flight path is of the order of 8 m with a distance of 7.5 m between the 10 cm low temperature moderator and the small ($\sim$ 3 mm) sample position. The detector may be placed over half the scattering sphere at a distance of 0.5 m from the sample, to allow the possibility of temperature or pressure changes to the sample environment.

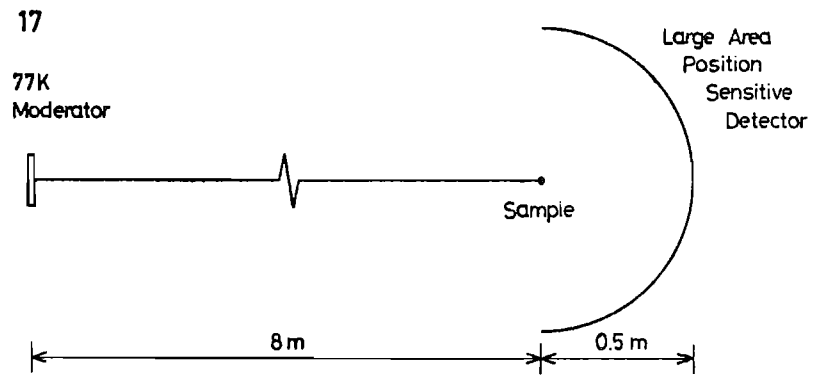

18. HIGH RESOLUTION POWDER DIFFRACTOMETER

$Q > 6$ Å^{-1} $\theta = 170^{\circ}$

$Q > 0.8$ Å^{-1} $\theta = 15^{\circ}$

$\frac{\Delta Q}{Q} \sim 0.001$

High resolution time-of-flight powder diffraction has been demonstrated at Garching using a long primary flight path and a backward angle of scattering with the detectors placed at the focussing angle. This technique is most suited to a pulsed source, and is necessary for the study of complex crystals with relatively large unit cells with a large number of reflections requiring high resolution. This is given by very long flight paths which can produce both good angular collimation and adequate time resolution.

The use of a cold moderator extends the slowing down region of the neutron spectrum to wavelengths beyond 2 Å, so that the instrumental time resolution may be minimised. The primary flight path may be contained within a neutron guide tube, and a length of the 100 m is required for a resolution of 0.1% for the back scattering angle. However, this long flight path will cause frame overlap for a source of repetition rate of 53 Hz. Consequently a simple disc chopper defined by cadmium is required to be placed immediately beyond the biological shield, so that

1 pulse in 3 may be available. Another similar chopper could be employed further down stream as a neutron tail cutter so that a narrower spread in wavelengths can be used. Detectors are placed at a distance 3 m from the sample both in the back scattering direction ($\theta = 170^{\circ}$), and in a forward direction ($\theta = 15^{\circ}$), where the angular contribution to the resolution becomes more significant. This ultra high resolution diffractometer considerably extends the powder method in structure determination, and can benefit by a reduction in the repetition rate of the spallation source.

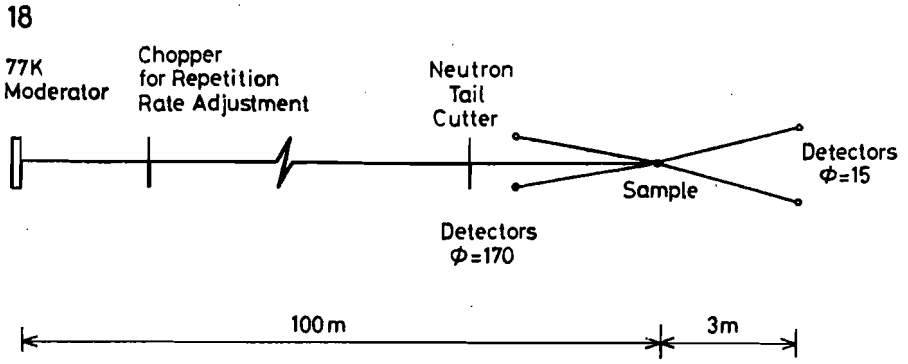

19. TIME-OF-FLIGHT MARX SPECTROMETER

$0 < \hbar\omega < 50$ meV

$\frac{\Delta\hbar\omega}{\hbar\omega} \sim 0.02 \quad \frac{\Delta Q}{Q} \sim 0.1$

The restriction generally imposed by the demand for high resolution in quasi-elastic scattering studies is that the spectrometers have to operate at long wavelengths. This results in a limitation of the Q range available. ($Q_{max} = 4\pi/\lambda$). By operating at shorter wavelengths, the Time-of-Flight MARX overcomes this problem, allowing, for example, the diffusion of hydrogen in metals to be followed up to the zone boundary.

The Time-of-Flight MARX Spectrometer is a white beam instrument which uses all the neutrons from the source. The incident energy is determined by the time-of-flight and the scattered energy by detection position. This is a very versatile instrument in which the resolution and the range of Q and $\hbar\omega$ investigated may be varied within

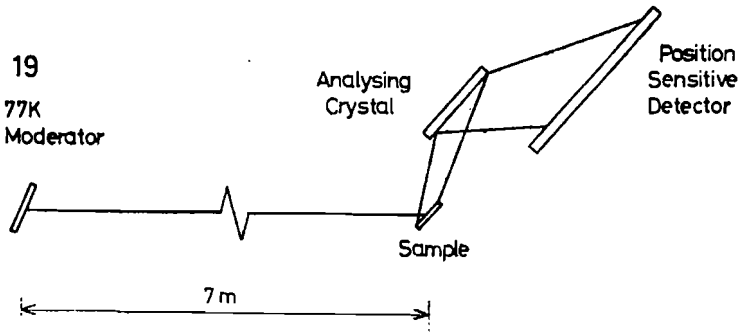

wide limits. Thus, for example, it is possible to make quasi-elastic measurements at $Q \sim 6$ Å^{-1} with an energy resolution of 200 μeV, corresponding to $\Delta E/E \sim 1\%$. At longer wavelengths, comparable resolution to that of IN5 may be readily achieved, and with higher effective count rates. This instrument is particularly suitable for use with oriented samples, where only particular $\underline{Q}$ scans are of real value.

20. TOTAL SCATTERING SPECTROMETER

$\lambda > 0.1$ Å $\quad 0.3 < Q < 100$ Å^{-1}

Structure factor measurements of liquids and amorphous materials require modest resolution data for Q values greater than some value (about $Q \sim 0.5$ Å^{-1}) below the first diffraction peak. Since even at $Q \sim 0.3$ Å^{-1}, the spallation source total scattering spectrometer gives much higher intensities than the hot source diffractometer D4 at Grenoble, it should be expected that the bulk of this type of work would transfer to the pulsed source. Consequently a second total scattering spectrometer is required on the cold moderator with similar parameters to instrument 3.

An advantage of the time-of-flight diffractometer over a conventional reactor instrument is that the instrumental integration path in (Q,ω) space more closely follows a constant Q cut. As a result the static approximation distortions which depend on the ratio of the secondary to the primary flight paths may be minimised. Corrections for these distortions are made easier when the incident flux spectrum index is constant over a large wavelength range; that is, when the slowing down spectrum is extended to lower energies. A cold moderator extends the epithermal region from 0.5 Å to 3 Å for a 20 K moderator, and though there is a reduction in the intensity in the Maxwellian region corresponding to the ambient temperature moderator, this is offset by an improvement in the quality of the data in this region. In addition provision can also be made for variable secondary flight paths as has been made on the Harwell linac instrument to investigate further the details of the dependence of these static approximation distortions.

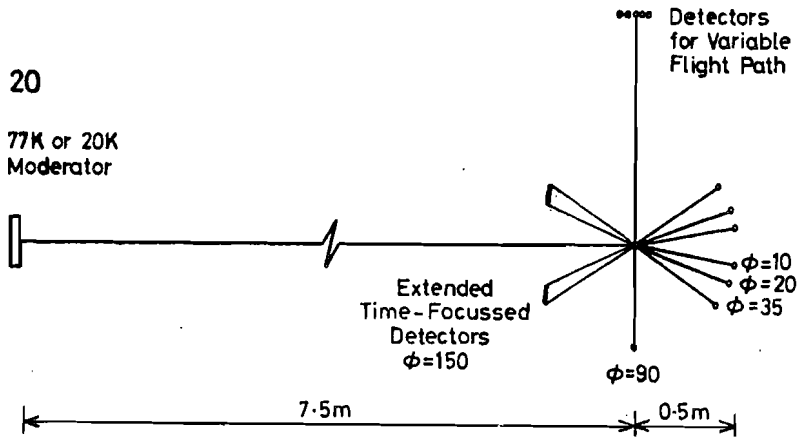

21. ELASTIC DIFFUSE SCATTERING SPECTROMETER

The design of this instrument has to fulfil both high and low resolution requirements for both total and purely elastic scattering measurements. To operate in the total scattering mode, generally with samples at low temperatures, no energy analysis of the scattered beam is needed. However, to discriminate against inelastic scattering, for example with high temperature samples, analysis of the scattered beam is required. This could most simply be performed with an analyser crystal at low scattering angle as shown below. To convert to the total scattering mode the analysers could be removed and the detectors moved to view the sample directly.

The total sample detector distance would need to be greater than 3 m to prevent frame overlap between 2 Å and 10 Å neutrons. This would then enable an overall range of momentum transfer of 0.04 Å < Q < 6 $Å^{-1}$.

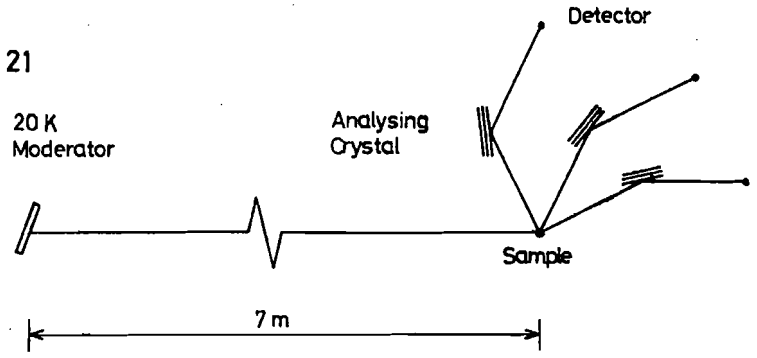

22. VERY LOW Q SPECTROMETER $0.005 < Q < 1\ Å^{-1}$ $\frac{\Delta Q}{Q} \sim 0.05 - 0.1$

The small angle ($10^{-3} < \phi < 10^{-1}$ rad) scattering of long wavelength ($4 < \lambda < 12$ Å) neutrons is required for experiments investigating the structure of biological and physical specimens over the spatial range 10-100 Å. Measurements are to be performed in the wavevector transfer range $0.005 < Q < 1\ Å^{-1}$ with reasonable resolution (5-10%), equivalent to experiment at the 10 m position on the small angle neutron camera at Grenoble. A small angle scattering instrument has been built at the pulsed reactor at Dubna, and a prototype instrument for $Q > 0.1\ Å^{-1}$ is planned on the electron linac at Harwell.

The spectrometer has an incident flight path of 10 m with the 0.5 x 0.5 cm^2 sample viewing a 5 x 5 cm^2 cold moderator at 20K. A total flight path of 12.5 m determines a maximum wavelength of 6 Å and a minimum scattering angle of 0.005 rad allows measurements for $Q > 0.005\ Å^{-1}$. A large area position sensitive detector with a spatial resolution determined by elements of area 0.5 x 0.5 cm^2 is placed at a distance 2.5 m from the sample. A two dimensional multi-detector similar to that at Grenoble placed at this distance can give count rates an order of magnitude greater than that presently available for specimens scattering within this Q range. Each element

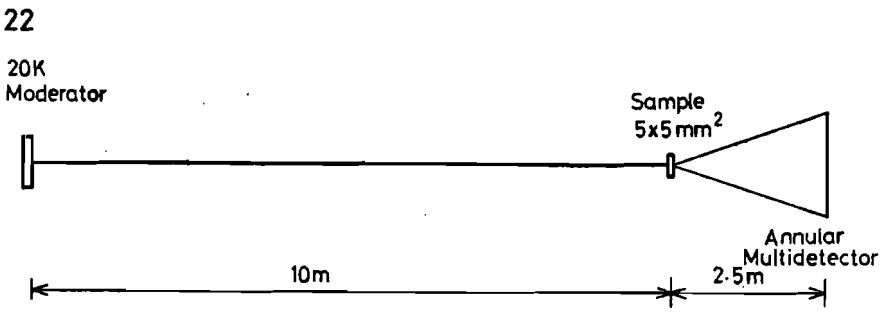

scans a different range of Q with a different resolution depending on its distance from the spectrometer axis, and a series of annular rings with differing thicknesses can allow measurements with similar resolutions over the entire Q range. The ring detector also allows $S(\underline{Q})$ to be measured with the same resolution for a given ring of elements, with values with the same $|\underline{Q}|$ measured at the same time-of-flight.

23. VERY LOW Q INELASTIC SPECTROMETER

$0.01 < Q < 1\ \text{Å}^{-1}$

$\frac{\Delta Q}{Q} \sim 0.1$

An advantage of a pulsed neutron beam is the possibility of separation of elastic and inelastic scattering events, provided that the incident wavelength spread of the beam is limited to less than 20 Å. Usually little gain can be expected from the use of guide tubes for diffraction on account of frame overlap, unless some coarse form of wavelength selection is performed, and at low Q the time-of-flight mode is preferable. However, a velocity selector in conjunction with a curved guide tube can act as a filter of long wavelength neutrons, and this inelastic mode of operation is a technique which cannot be used on a conventional low Q spectrometer. The ability to discriminate between elastic and inelastic scattering can be useful for the study of the structure of molten alloys and the distribution of precipitates in metallurgical specimens at high temperatures.

The instrumentation of this spectrometer would be similar to that of the neutron small angle camera at Grenoble, though since the instrument is in an inelastic mode the count rate would be greatly inferior. A helical slot velocity selector close to the 20K cold moderator provides the necessary wavelength selection. The angular divergence of the incident beam required for a given sample detector distance could be achieved by using various collimators grouped in pairs at right angles to each other to obtain the required point geometry. These are placed in an accessible position outside the biological shield through which runs the curved guide tube to reduce the fast neutron flux and to maintain maximum flux at the input of the collimation system. Primary and secondary flight paths are evacuated, and the sample position requires the provision of a furnace. A two dimensional position sensitive detector is necessary since many samples exhibit anisotropic scattering around the incident beam direction. A multi detector with 128 x 128 0.5 x 0.5 cm elements which could be set at distances between 1 and 10 metres from the sample would provide a Q range of $0.03/\lambda$ to $3.0/\lambda\ \text{Å}^{-1}$ for an incident wavelength λ. The scattering in an experiment could be sorted into about a dozen channels, one of which could be for the total inelastic scattering, the rest to separate the different incident wavelengths.

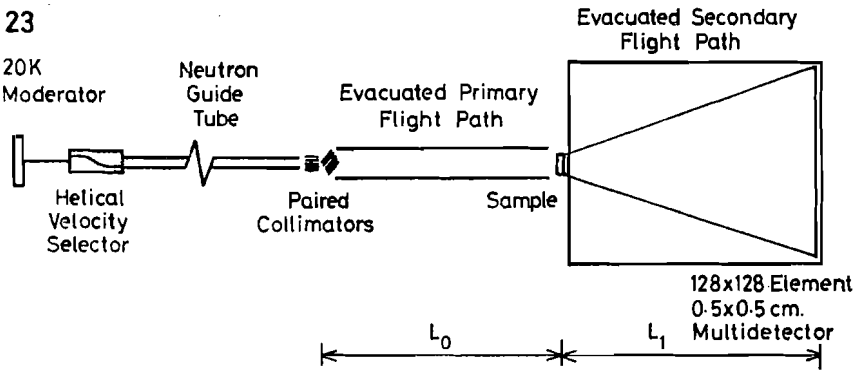

24. LONG WAVELENGTH CHOPPER SPECTROMETER

$4 < \lambda < 10$ Å

$0 < \hbar\omega < 20$ meV $\quad \frac{\Delta E}{E} \sim 0.05$

The long wavelength high resolution time-of-flight spectrometer IN5 at ILL is heavily oversubscribed in its use for the studies of the diffusive motions of molecules. A 'replica' of such an instrument (with slightly improved performance) may be built on a pulsed source.

A monochromatic beam of neutrons may conveniently be produced on a pulsed source by utilising the phase relationship between the production pulse and a single chopper. As on the conventional machine the final state energy is determined by time-of-flight over a path length $\sim$ 4 m to a large counter bank array. There should be no technical problem in matching the burst time of the chopper to that of the neutron pulse (25λ μs). This spectrometer may also be used to study the near inelastic region ($\hbar\omega < 20$ meV) in a neutron energy gain mode.

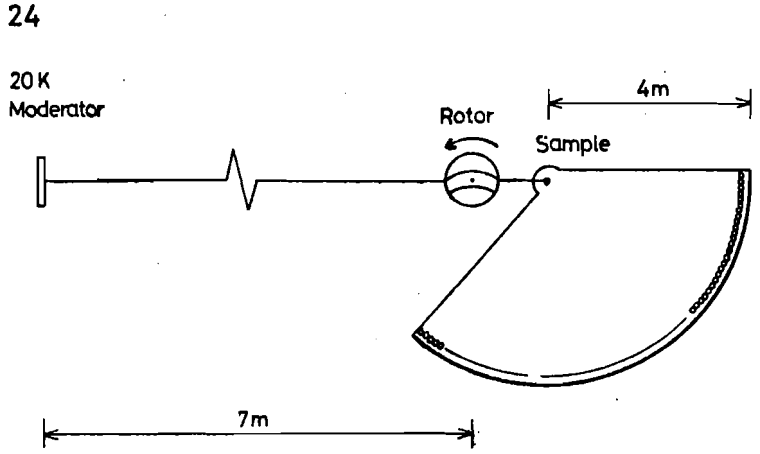

25/26. WHITE BEAM BACKSCATTERING SPECTROMETER

$L = 25$ m, $\Delta\lambda = 3$ Å

$-1000 < \hbar\omega < 1000$ μeV $\Delta\hbar\omega \sim 15$ μeV

$L = 100$ m, $\Delta\lambda = 1$ Å

$-200 < \hbar\omega < 200$ μeV $\quad \Delta\hbar\omega \sim 2$ μeV

These pulsed source spectrometers utilise the high energy definition achieved in direct backscatter from a crystal analyser to determine the final state energy, E_1. A broad band in λ, selected by a helical velocity selector is incident on to the sample. Only neutrons whose energy is changed to E_1 by interaction with the sample are detected. E_0, the incident energy may be determined by the neutron's time of arrival. The use of neutron guide tubes allows adequate time resolution to be achieved without a dramatic loss in intensity.

Two spectrometers are envisaged:

(i) Instrument 25 with a flight path of 25 m, giving an overall quasi-elastic resolution of $\sim$ 15 μeV and an energy window of 2000 μeV

(ii) Instrument 26 with a flight path of 100 m

Both machines have secondary spectrometers identical to IN10.

It is to be noted that the rate of data acquisition (Intensity/unit energy channel) has not significantly improved over IN10. In practice, however, for the L = 25 case, the mosaic of the secondary spectrometer would be greatly relaxed, matching it to the time resolution. The overall resolution would not be significantly degraded, but a greatly increased count rate would be obtained.

By offsetting the $\Delta\lambda$ band from around λ_1, truly inelastic features may be observed, still with very high energy definition. The 'window' of $\hbar\omega$ space available in neutron energy loss as a function of $\bar{\lambda}$ (wavelength acceptance band defined as $\bar{\lambda} \pm \frac{\Delta\lambda}{2}$) is plotted in figure 3.2 for a given Spectrometer configuration (L = 25 m, $\Delta\lambda = 3\ \text{Å} \rightarrow \frac{\Delta E}{E} < 8\ 10^{-3}$). Figure 3.1 explicitly defines the window and resolution available for a set of $\bar{\lambda}$.

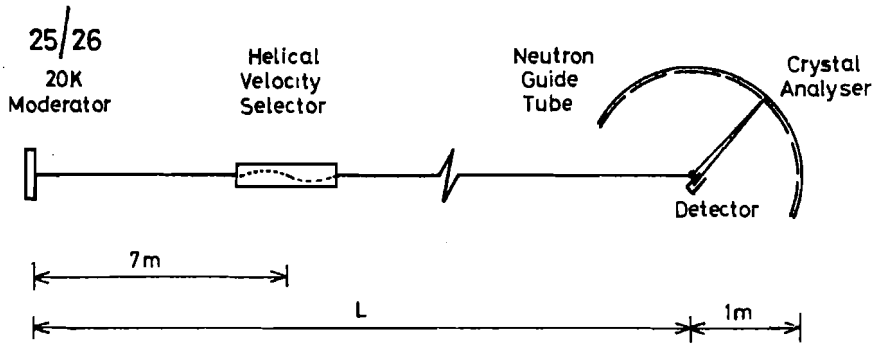

3.2 The preceding section provides a comprehensive list of pulsed source instruments from which one can select a balanced set to carry out the science identified by the Working Groups as likely to benefit from the SNS. In table 3.2 a basic group of fourteen instruments has been specified which would cover most of the range of this scientific programme within the limitations imposed by cost and by the number of beams that may be accommodated around one spallation target at the stated high flux. This may be achieved in a number of ways:

(a) It is possible for instruments to be built which have more than one operating configuration, similar to D5 at ILL. For example, the basic design of instruments 5 and 12 (of table 3.1) are similar. Instrument 4 may be incorporated with instrument 2, etc. In the melding of these instruments, however, it may be necessary to sacrifice some of the features in the performance of the proposed spectrometer.

(b) In some instances two instruments which have flight paths differing greatly may be incorporated on to the same beam hole. For example, instruments which require only long wavelength neutrons from a cold moderator can be placed on the same beam hole by the use of guide tubes, though this may introduce problems of frame overlap in the case of diffraction and inverse geometry instruments.

(c) It is seen that different areas of science may be performed on the same spectrometer, though this will necessarily cut down the available beam time of each proposed instrument. For example, the high Q and low Q banks on a chopper spectrometer will simultaneously satisfy the requirements of instruments 8 and 9.

The performance of some instruments may be improved by viewing the moderator at an angle other than the normal to the moderator surface. Suitable positioning of the various instruments will therefore allow the most efficient use of the available beam tubes.

3.3 In the long term, consideration may be given to increasing the number of instruments, either by addition of different types of spectrometer, or by duplicating those in heavy demand. It is convenient to place 6 or 7 beam tubes within a half-angle of 30^{o} to the normal of the moderator surface, and

the reference design allows for two such moderators, each viewed from a single side to maximise the reflector efficacy. To accommodate extra beam tubes it would be necessary to expose further moderator faces. This could be accomplished either by four moderators surrounding the spallation target, or by allowing both faces of each moderator to be open to neutron beam holes. In either case, not only are there physically a very large number of instruments in the experimental hall surrounding the source on both sides of the proton beam line, but also the moderator requirements necessitate the removal of a large part of the reflector around the moderators. This results in reduced beam intensities from those quoted earlier which would be a disappointing use of such a powerful new neutron source. An alternative solution is to have two target stations each with two moderators, that is, four moderators in all, two at ambient temperature, one at liquid nitrogen temperature, and the fourth at liquid hydrogen temperature. If each target is fed from the proton accelerator in turn, then the repetition frequency is halved, so that the time-averaged neutron flux available to each instrument is reduced only by a factor two. This is less important for the instruments which predominantly require neutrons of short wavelength since this is the region where pulsed sources score most heavily over reactor sources. At the longer wavelengths, some instruments could benefit by a reduction in the repetition rate, since the greater spread in wavelengths available without frame overlap can increase the performance of these spectrometers.

3.4 The precise determination of the instruments to be built and their priority will be determined after an up-to-date reassessment of the scientific programme and in the light of experience gained on the new Harwell linac. During the planning stage instruments of advanced conception to match novel applications are likely to emerge.

TABLE 3.2

INSTRUMENTS FOR THE SNS : AMBIENT TEMPERATURE MODERATOR

Instrument	Specification	Field
I. Single Crystal Diffractometer	$0.3 < \lambda < 1.5$ Å $\frac{\Delta Q}{Q} \sim 0.03$ Polarized incident beam option	Single crystal structure determination. Magnetisation density distributions. Structural investigations as a function of temperature, pressure, etc..
II. (a) High Intensity, Medium Resolution Powder Diffractometer	$Q > 2.5$ Å^{-1} ($\phi = 170^{\circ}$) $\frac{\Delta Q}{Q} \sim 3\ 10^{-3}$ $Q > 0.6$ Å^{-1} ($\phi = 30^{\circ}$)	Structural determination using powder samples. Kinetic processes, eg diffusion of gases into solids.
(b) High Pressure Spectrometer	$0.3 < Q < 100$ Å^{-1} Pressures up to 50 kbar	Pressure dependence of structure factors of fluids and amorphous solids. Triplet correlation functions.
III.(a) Elastic Discrimination Spectrometer	$1 < Q < 25$ Å^{-1} $\frac{\Delta Q}{Q} \sim 0.02$	Simultaneous measurement of elastic and total diffraction patterns to allow separation of elastic and inelastic scattering to study the eccentricity of atomic thermal vibration tensors. Structure factors of fluids and amorphous solids.
(b) Total Scattering Spectrometer	$0.3 < Q < 100$ Å^{-1}	
IV. Very High Energy Transfer Spectrometer	$\hbar\omega \sim 1$ eV $\frac{\Delta\hbar\omega}{\hbar\omega} \sim 0.1$ $Q < 4$ Å^{-1}	Electronic excitations: Band energies in semiconductors. Valence fluctuations. Crystal field levels in optically opaque transition metal compounds.
V. (a) High Energy Transfer Chopper Spectrometer	$100 < \hbar\omega < 600$ meV $\Delta\hbar\omega \sim 5$ meV $\Delta Q \sim 0.1$ Å^{-1} low Q bank	Vibrational spectroscopy, in particular the study of hydrogen modes on surfaces, in H-bonded systems and in metal hydride complexes. Phonons, magnons, crystal fields, vibrational modes and liquid dynamics.
(b) High Energy, High Momentum Transfer Spectrometer	$Q_{max} \sim 30$ Å^{-1} ($\phi = 150^{\circ}$)	Measurements on the dynamics of the helium liquids. High Q dependence of $S(Q,\omega)$ for amorphous materials.
VI. (a) Total Scattering Polarization Analysis Spectrometer	Q up to 20 Å^{-1}, with spin analysis of scattered beam	Determination of elastic spin-dependent cross-sections. Structure factor measurements in presence of spin-incoherent scattering.
(b) Inelastic Polarization Analysis Spectrometer	$0 < \hbar\omega < 200$ meV $\frac{\Delta\hbar\omega}{\hbar\omega} \sim 0.01$ Spin selection of both incident and scattered beams	Spin dynamics. Separation of magnon and phonon scattering. Measurements of the dynamical structure factors $S(\underline{Q},\omega)$ and $S_s(\underline{Q},\omega)$ for spin-incoherent scatterers.
VII. Moderate Energy Transfer Chopper Spectrometer	$\hbar\omega < 100$ meV $\frac{\Delta\hbar\omega}{\hbar\omega} \sim 0.02$ low Q bank required $\Delta Q \sim 0.1$ Å^{-1}	Measurements on the dynamical structure factors of liquids. Conventional inelastic spectroscopy. Very low angle bank required for observing inelastic modes in liquids on the energy gain side - the 'small Q method'. Phonon, magnon and crystal field studies.

Continued

INSTRUMENTS FOR THE SNS : COLD MODERATOR

Instrument	Specification	Field
VIII. High Resolution Powder Diffractometer	$Q > 6\ \text{Å}^{-1}$ ($\phi = 170^\circ$) $Q > 0.8\ \text{Å}^{-1}$ ($\phi = 15^\circ$) $\frac{\Delta Q}{Q} = 0.001$	Resolution of closely spaced peaks in powder diffraction profiles of complex crystals with large unit cells.
IX. (a) Very Low Q Spectrometer (SANS)	$0.005 < Q < 1\ \text{Å}^{-1}$ $\frac{\Delta Q}{Q} \sim 0.1$ $4 < \lambda < 12$ Å	'Small Angle Neutron Scattering': studies of polymers and biological systems. Defects and structural periodicities on the scale ~ 100 Å.
(b) Elastic Diffuse Spectrometer	Polarised incident beam option	Effects of doping, alloying, heat treating and irradiating condensed systems. Magnetic defects.
X. Total Scattering Spectrometer	$0.3 < Q < 100\ \text{Å}^{-1}$	Structure factors of fluids and amorphous solids. High resolution at low Q.
XI. Constant Q Spectrometer	$10 < \hbar\omega < 200$ meV $\frac{\Delta\hbar\omega}{\hbar\omega} \sim 0.05$ $3 < Q < 6\ \text{Å}^{-1}$	Triple axis analogue: scans in energy through (Q,ω) space at constant Q. Coherent excitations.
XII. Time-of-flight MARX Spectrometer	$0 < \hbar\omega < 50$ meV $\frac{\Delta\hbar\omega}{\hbar\omega} \sim 0.02$ $\frac{\Delta Q}{Q} \sim 0.1$	Conventional inelastic scattering. Quasi-elastic scattering at good resolution and high Q, diffusive modes of plastic and liquid crystals, hydrogen in metals, etc.. Intermolecular modes of crystals, magnetic crystal field levels.
XIII. Long Wavelength Chopper Spectrometer	$4 < \lambda < 10$ Å $\Delta\hbar\omega/E$ comparable to that of IN5	High resolution quasi-elastic studies. Low energy inelastic modes (< 20 meV) observable in neutron energy gain.
XIV. White Beam Backscattering Spectrometer (L = 25 m)	$\Delta\lambda = 3$ Å Quasi-elastic mode: $\Delta\hbar\omega \sim 15$ μeV $-1000 < \hbar\omega < 1000$ μeV Inelastic mode: scan up to 100 meV with $\frac{\Delta\hbar\omega}{E} < 8\ 10^{-3}$	Very high resolution quasi-elastic studies. Slow diffusive processes. Tunnelling transitions. Inelastic band shapes.

with the energy uncertainty of the analyzer crystal, $\sim$ 0.7 μeV.

The magnitude of the wavelength spread $\Delta\lambda$ is limited for a given flight path of L metres by the frame overlap condition, viz:

$$\frac{10^6}{f} = (\lambda_{max} - \lambda_{min})\ 252.7L = \Delta\lambda\ 252.7L$$

For a repetition rate f of 53 Hz and a flight path of 25 m we have a wavelength spread $\Delta\lambda \sim 3$ Å. The resultant energy scan is illustrated in figure 3.1. High resolution may be obtained by going to much longer flight paths at the expense of reducing the energy window allowed before frame overlap occurs. The intensity of neutrons at the sample may be calculated from

$$I(E)\Delta E = \frac{10^{13}\ F(E)\ \Delta E_W}{L^2}\ \eta_{GT}$$

where L is 7m, the distance of the helical velocity selector from the source

η_{GT} is the efficiency of the neutron guide, $\sim$ 0.5

F(E) is an intensity factor at an energy E eV defined in Chapter 1

ΔE_W is the energy window corresponding to the wavelength spread $\Delta\lambda$ defined by the helical velocity selector.

For $\Delta\lambda$ centred on 6.5 Å we have

$$I(E)\Delta E = \frac{10^{13} \times 390 \times 1.99\ 10^{-3}}{49\ 10^4}$$

$$= 8\ 10^6\ cm^{-2}\ s^{-1}$$

3.10 The performance of this spectrometer is compared with those at ILL (IN10 and IN13) in Table 3.3, assuming the use of identical analyzer systems. A significant gain over the steady state source is achieved by the utilization of both the pulsed characteristics and the white beam nature of the SNS spectrum. The large energy window covers the entire quasi-elastic region, which is a major shortcoming of IN10, without serious loss in resolution.

3.11 It is to be noted that the rate of data acquisition (Intensity/unit energy channel) has not been improved significantly over that of IN10. In practice

TABLE 3.3

COMPARISON OF WHITE BEAM BACKSCATTERING SPECTROMETER WITH ILL INSTRUMENTS

	Intensity at sample (n cm^{-2} s^{-1})	Rate of Data Acquisition (Intensity/ Unit Energy Channel)	$\Delta\hbar\omega$ (μeV)	$\hbar\omega$ Range (μeV)
IN10	$1\ 10^4$	1	1	20
IN13 (proposed)	$\sim 10^5$	1	5	200
SNS (L=25m)	$8\ 10^6$	8	15	2000
SNS (L=75m)	$2\ 10^6$	6	5	600
SNS (L=100m)	$1\ 10^6$	5	2	400

for the L = 25 case, however, the mosaic of the secondary spectrometer would be greatly relaxed, matching it with the time resolution. While the overall resolution would not be degraded substantially, a greatly increased count rate would be obtained.

Long Wavelength, High Resolution Quasi-Elastic Studies

3.12 For the long wavelength chopper spectrometer, the pulsed source analogue of IN5, a monochromatic beam of neutrons is defined by the phase relationship between the pulsed source and a single chopper. The secondary spectrometer is taken to be identical with that of IN5, so that the intensity at the sample may be taken as the figure for comparison.

3.13 The burst width of neutrons in the thermal region produced by the 20K moderator is given in figure 1.3 and may be approximated by $\Delta t = 25\lambda$ μs Å^{-1} in the wavelength range $4 < \lambda < 8$ Å. The contribution to the time uncertainty at the detectors from the pulse width at 6 Å is $\Delta t_p = 25\lambda = 150$ μs. The relationship between the time taken for a neutron of wavelength λ and energy E to travel a distance L is given by

$$t = 252.7L\ \lambda \text{ μs m}^{-1} \text{ Å}^{-1}, \text{ so that}$$

$$dt = 252.7L\ d\lambda = 1.56\ \lambda^3\ L\ dE \qquad \text{μs Å}^{-3}\ \text{m}^{-1}\ \text{meV}^{-1}$$

This equation will be used to calculate the overall energy resolution of the spectrometer.

3.14 At a distance L metres from the moderator, a chopper whose open time is matched to this pulse width will accept neutrons in the energy interval ΔE. The above relationship between the time and energy uncertainty gives an energy spread ΔE of 64 μeV, assuming a 7 m primary flight path between the moderator and the chopper. If this spread in energy is passed by the chopper, the time uncertainty at the detector a distance of 4 m from the sample is given by $\Delta t_c = 84$ μs.

Uncertainties in path length (~ 0.045 m) due to finite sample and detector size contribute a further time uncertainty at the detectors $\Delta t_L = 68$ μs.

The overall time uncertainty Δt_T is then $\Delta t_T = (\Delta t_p^2 + \Delta t_c^2 + \Delta t_L^2)^{\frac{1}{2}} = 186$ μs. which corresponds to a resolution of 140 μeV.

The neutron intensity at the sample is given by

$$I(E)\Delta E = \frac{10^{13}\, F(E)\, \Delta E\, \eta_c}{L^2}$$

where L is the distance from the moderator to the rotor, 7m

η_c is the chopper transmission factor, 0.5

F(E) is the intensity factor at an energy E eV

which for a 20K moderator is 392 for a wavelength of 6 Å and ΔE is the transmitted energy interval, 64 μeV. This equation gives a flux of 2.5 10^5 neutrons $cm^{-2}\ s^{-1}$ at the sample.

3.15 The disadvantage of the undermoderated nature of the neutron spectrum from a pulsed source for long wavelength work is compensated by the low repetition rate of the SNS which avoids the need of a further chopper to overcome frame overlap problems. A comparison of the two spectrometers is given in Table 3.4. The pulsed instrument provides a gain in intensity and comparable resolution at all wavelengths. The resolution may be improved at the expense of intensity, by reducing the burst time of the chopper below that required to match the moderator burst. Indeed the SNS resolution can be improved to 30 μeV at 10 Å with an intensity which is still competitive with IN5.

Intermediate and High Energy Transfer Studies

3.16 A similar comparison has been made between IN4 and a pulsed source analogue.. Again, the secondary spectrometers are assumed to be identical. In the pulsed case, the primary spectrometer consists of a single chopper, at a distance of 7 m from the source, with burst widths which vary between 7 s at 200 meV to 50 s at 12 meV. Table 3.5 shows the distinct advantage of the SNS in both intensity and resolution, even for an incident energy of 12 meV, the optimum operating condition for IN4. All quoted resolutions refer to the elastically scattered peak, and since the spectrometers operate in a neutron energy loss mode, this figure will improve as the energy trans fer becomes greater, corresponding to slower final state neutrons.

TABLE 3.4

COMPARISON OF IN5 WITH THE DOUBLE CHOPPER ANALOGUE

	INTENSITY AT SAMPLE ($n\ cm^{-2}\ s^{-1}$)	ΔE(μeV)	λ(Å)
SNS	$2.5\ 10^5$	140	6
IN5	$6.0\ 10^4$	125	6
SNS	$1.2\ 10^5$	78	8
IN5	$2.5\ 10^4$	50	8
SNS	$4.7\ 10^4$	40	10
SNS*	$1.2\ 10^4$	30	10
IN5	$0.9\ 10^4$	27	10

* Reduced Burst Time on Chopper

TABLE 3.5

INELASTIC SCATTERING: COMPARISON OF IN4 WITH SNS

	IN4		SNS	
Incident Energy (meV)	Intensity at Sample ($n\ cm^{-2}\ s^{-1}$)	Resolution (meV)	Intensity at Sample ($n\ cm^{-2}\ s^{-1}$)	Resolution (meV)
12	$3\ 10^4$	0.84	$2\ 10^5$	0.62 †
-	-	-	$9\ 10^5$	0.52 *
80	$5\ 10^3$	-	$5\ 10^5$	2.7 †
200	-	-	$1\ 10^5$	6.7 †

* 77K Moderator

† 300K Moderator

3.17 Figure 3.3 shows the cuts in (Q,ω) space available for small angles of scattering for an inelastic rotor spectrometer, and the interdependence of the incident energy, the energy transfer and the momentum transfer. Measurements of peaks corresponding to high energy transfers ($\hbar\omega > 100$ meV) at low momentum transfers ($Q < 4$ Å^{-1}) may be achieved by such a spectrometer by using neutrons of high incident energies ($E_o > 200$ meV) and detector banks at low scattering angles ($\phi < 15^o$). This spectrometer will allow high energy transfers in molecular and magnetic systems to be observed at lower values of Q than can be obtained on conventional instrumentation available on steady state reactors.

High Energy Inelastic Scattering Studies at Well Defined Wavevector

3.18 While it is relatively straightforward to compare the performance of reactor based time-of-flight instruments with similar instruments on the SNS, there remains the very important class of continuous source instruments using monochromatic neutron beams diffracted from a crystal, which cannot be translated in any straightforward way onto a pulsed neutron source. These include the two most important and widespread instruments used in neutron scattering - the single crystal elastic diffractometer and the triple axis crystal spectrometer. For these instruments a comparison can be made if the time-of-flight scan from the pulsed source is used simply to pick out neutrons of a desired incident wavevector $\underline{k}_o$ with corresponding spread $\Delta\underline{k}_o$. We assume that all other incident neutron wavevectors will be discarded from the time-of-flight scan in just the same way that the crystal monochromator discards all incident wavevectors except that satisfying the Bragg condition. We show that in the short wavelength range, energies above 200 meV, the SNS can exceed the ILL hot source in performance even for this type of experiment.

3.19 The comparison of continuous and pulsed source instruments is illustrated in figure 3.4. The single crystal elastic diffractometer of figure 3.4a and the triple axis crystal spectrometer of figure 3.4b both use crystal monochromators to select from the reactor white beam a band of incident wavevectors centred on $\underline{k}_o$ and of width $\Delta\underline{k}_o$. Both quantities are represented as vectors since the direction of $\underline{k}_o$ within the axis of the single crystal sample must be defined, and the spread must be defined not only along k_o as $\Delta k_o^{//}$, but also in

the horizontal and vertical planes, Δk_o^{α} and Δk_o^{β}. Figures 3.4c and 3.4d show the corresponding pulsed source instruments. In this case the required incident wavevector k_o is separated in time-of-flight from the other wavevectors present in the incident pulsed white beam. It is a restriction on this comparison that the time-spread of scattered neutron flight times be no larger than those on the incident neutrons. This will be true in the examples shown in figure 3.4, but is not true in, for example, a beryllium filter spectrometer where there are large spreads in the scattered neutron flight times. In the pulsed source method we collect a time-of-flight spectrum which includes a wide range of incident wavevectors k_o and select from these a time range corresponding to the desired wavevector range $\Delta k_o^{//}$ in the incident beam. The width of the included time gates thus plays a role similar to the mosaic spread and horizontal collimations α_o and α_1 in a crystal monochromator case, with the difference that the optimum compromise between intensity and resolution can to some extent be chosen after the experiment.

3.20 The separate points on a diffractometer scan or a triple axis scan at constant Q or E must then be sequentially measured. For each point on the scan the crystal angle, the included time range, and possibly the analyzer angle must be changed. (We ignore in this discussion the so-called Constant Q Spectrometer which allows a constant Q scan to be derived from one set of time-of-flight scans recorded on a position sensitive MARX analyzer).

3.21 The continuous curve in figure 3.5 shows incident beam intensities on the IN1 beam hole on the hot source at the ILL reactor at Grenoble, measured by a calibrated fission chamber. The intensity values were normalized by the ratio of the fission cross-sections for the energy diffracted by the crystal and for 25 meV, the energy at which the fission chamber had a known sensitivity. This curve agrees well with other similar calculations but is a factor of 2 lower than some gold foil measurements. The curves make no correction for the presence of higher order peaks, but are corrected for non-Bragg reflected neutrons. Below the flux curve is shown the corresponding parallel fractional resolution $\Delta k_o^{//}/k_o$. This is calculated from the expression $\Delta k_o^{//}/k_o = \cot\phi\Delta\phi$ where the scattering angle ϕ is calculated for copper (331) planes. The spread $\Delta\phi$ is given by $\sqrt{(\alpha_o^2 + \alpha_1^2)}/2$, where $\alpha_o = 30'$ is the before-monochromator horizontal angular spread, and $\alpha_1 = 30'$ is the

after-monochromator spread with the $\frac{1}{2}^{o}$ collimator in place. Thus $\Delta\phi \sim 0.0062$ radians. The horizontal and vertical spreads $\Delta k_o^{\alpha}/k_o$ and $\Delta k_o^{\beta}/k_o$ are essentially constant at 0.009 and 0.01 respectively..

3.22 The fractional resolutions shown in figure 3.5 are generally poor compared with those possible on the proposed spallation source. Even at the shortest practicable incident flight path of about 6 m, $\Delta k_o^{\parallel}/k_o$ is equal to about $\frac{1}{2}^{o}$, and is independent of neutron energy. The neutron flux at the sample position at this distance is

$$I(E) = 2.8\ 10^{7}/E \text{ neutrons } eV^{-1}\ cm^{-2}\ s^{-1}$$

The flux accepted within the wavevector range $\Delta k_o^{\parallel}$ about k_o is therefore given by

$$I(k_o)\ \Delta k_o^{\parallel} = 5.6\ 10^{7}\ \Delta k_o^{\parallel}/k_o \text{ neutrons } cm^{-2}\ s^{-1}$$

The dashed curve in figure 3.5 shows the flux calculated in this way for the same resolution characteristics as those given for the IN1 case. The other components of Δk_o are determined by the moderator dimensions ($\sim$ 100 mm) compared to the incident flight path, and in this case are slightly larger at $\Delta k_o^{\alpha} \simeq \Delta k_o^{\beta} \simeq 0.016$.

3.23 Thus over this whole epithermal energy range (E_o = 0.2-0.4 eV) the proposed spallation source outshines the Grenoble hot source hole even for studies using a well defined incident wavevector. The energy resolution is in general better, though the transverse resolution $\Delta k_o^{\perp}/k_o$ is slightly worse because of the large incident solid angle. Focussing properties involving the systematic change of neutron energy across the beam are of course different, but this may allow the new source a more complimentary role, especially for the focussing of steep dispersion curves.

Structural Measurements on Fluids and Amorphous Solids

3.24 A comparison is made between a proposed instrument on the SNS, the Total Scattering Spectrometer (TSS), and the present best available reactor-based instrument for measuring the structural parameters of non-crystalline

materials namely D4 on the hot source at Grenoble. Structure factors are measured as a function of momentum transfer $|\underline{Q}|$ where $|Q| = 4\pi/\lambda \sin \phi/2$ and ϕ is the scattering angle. For the continuous source instrument data are collected as a function of $|\underline{Q}|$ by stepping a single detector around in ϕ for a fixed incident wavelength, which for D4 may be either 0.35 Å, 0.5 Å or 0.7 Å. In the case of the pulsed source instrument data are collected at a few fixed scattering angles as a function of wavelength, or time-of-flight, with the complete Q-range being measured simultaneously.

3.25 The parameters used for the D4 instrument are those taken from the 1974 ILL handbook. The TSS used for the comparison is the Mark I Total Scattering Spectrometer at the Harwell linac with the addition of a single low angle detector at 4°. This detector is taken to have the same solid angle as the D4 detector and furthermore the energy resolution is adjusted to give the same $|\underline{Q}|$ resolution as D4 at 0.3 $Å^{-1}$ momentum transfer. The resolution of the data from the linac instrument is better than that of the best available on D4, with the energy resolution being 2% for the highest angle detectors. Table 3.6 shows the various parameters for the two instruments.

3.26 The factor to be used as a figure of comparison of the SNS instrument to D4 is the time taken to complete a given Q scan. The intensity at the detector is proportional to the neturon flux I at the sample and the detector solid angle Ω. The time required to complete a given scan in Q on the D4 instrument is $Nn/I_{D4}(\lambda)\ \Omega_{D4}$, where N is the number of counts required at each data point and n is the number of data points. The TSS, however, measures all the data simultaneously and the time required for such a Q scan is $N/I_{TSS}(Q)\ \Omega_{TSS}$. The flux in this case is dependent on the incident wavelength, so that the count rate at a given detector position varies with the measured momentum transfer. The figure of comparison is defined as:-

$$\frac{\text{time for Q scan on D4}}{\text{time for Q scan on TSS}} = \frac{nI_{TSS}(Q)\ \Omega_{TSS}}{I_{D4}(\lambda)\ \Omega_{D4}}$$

TABLE 3.6

PARAMETER	VALUE FOR THE TSS	VALUE FOR D4	UNITS
Incident Wavelength	Limited to 0.12 - 1.5	(i) (ii) (iii) 0.35, 0.5, 0.7	Å
Incident Energy	Limited to 5.6 - 0.036	0.68, 0.3, 0.17	eV
Angular Ranges (2θ)	Fixed detectors at a) 4 b) 15 c) 28 d) 60 e) 150	2 to 140	degrees
$\lvert\underline{Q}\rvert$ Range	a) 0.3 - 3.6 c) 2.0 - 25 e) 8 - 101	i) 0.6 - 34 ii) 0.4 - 24 iii) 0.3 - 17	$Å^{-1}$ " "
Moderator-Sample Distance	7	-	m
Sample-Detector Distance	0.4	1.4	m
Beam Size	5 x 2	5 x 2	cm x cm
Detector Solid Angle	a) 5.1×10^{-4} c) 0.015 e) 0.28	5.1×10^{-4}	ster " "
Divergence of incident beam horizontal	0.16	0.33	degrees
vertical	0.41	0.83	"
Divergence of scattered beam horizontal for 1 cm sample	minimum (a) 0.58 maximum (e) 12.9	0.58	degrees "
Flux at sample	For $\Delta\lambda/\lambda = 0.02$ flux at 0.7 Å is $2\ 10^6$	i) 1.3×10^6 ii) 10^7 iii) 2×10^7	n cm^{-2} s^{-1}
Moderator temperature	ambient	ILL hot source	
Moderator thickness	5	-	cm

3.27 The comparison is shown on figure 3.6 for each of three wavelengths available on D4 (0.35 Å, 0.5 Å and 0.7 Å) and for each of three scattering angles on the TSS (4^{o}, 28^{o} and 150^{o}). These figures were computed assuming steps of 0.3^{o} in scattering angle for the fixed wavelength instruments, so that 460 steps are required to scan the available range of Q. The intensity values of the TSS have been computed assuming a total flight path of 7 m. The 4^{o} scattering angle data on the TSS appear better than the 28^{o} data on account of better matching of the energy resolution to that of D4. The range in Q covered by the TSS is from 0.3 $Å^{-1}$ to 100 $Å^{-1}$ and is measured simultaneously, whereas the range of D4 extends only to 35 $Å^{-1}$. The SNS spectrum determines the shape of the figure of comparison as a function of Q. The figures of comparison range from 300 at medium Q values to greater than 10^{5} at high Q values. Furthermore the range from 35 $Å^{-1}$ to 100 $Å^{-1}$ is totally inaccessible on conventional reactor-based instruments.

Very Low Q Spectrometer

3.28 Experiments to study the structure of physical and biological materials in the range of 10 - 100 Å require the measurements of neutrons in the momentum transfer range $0.005 < Q < 1$ $Å^{-1}$ with the availability of good (5 - 10%) resolution. This means the diffraction of neutrons with long wavelengths ($4 < \lambda < 12$ Å) through small scattering angles ($10^{-3} < \phi < 10^{-1}$ rrad).

3.29 The conventional method on a continuous reactor source is to define an incident wavelength λ with a wavelength spread $\Delta\lambda$ using a helical slot velocity selector, and to measure the intensity of radiation scattered from the sample as a function of scattering angle for small values of ϕ using a multi-dimensional detector. The angular resolution $\Delta\phi/\phi$ is improved by increasing the lengths of the primary and secondary flight paths, though in some experiments its contribution to the overall Q resolution may be small compared to that from the wavelength resolution.

3.30 On the pulsed source instrument, a small angle of scatter is defined by one detector subtending a small solid angle at the specimen, and the intensity of scattered radiation is measured as a function of wavelength using time-of-flight techniques. Measurements at the lowest Q are performed by the longest wavelengths at the longest times-of-flight, and are limited by frame overlap from the next burst.

The wavelength resolution which is inversely proportional to the length of the spectrometer gives a small contribution to the overall Q resolution. Indeed adequate time resolution is given for the slowest neutrons with modest path lengths (10 m). The dominant factor in the overall resolution of the spectrometer is the angular resolution which necessitates long flight paths. Unlike the conventional method, however, the angular resolution cannot be improved simply by increasing the lengths of the flight paths, since for a given repetition rate the maximum wavelength before frame overlap is inversely proportional to the length of the spectrometer. Since very long flight paths cannot be used without frame overlap for diffraction measurements, guide tubes are not only unnecessary but actually impair the resolution. Consequently tight collimation is necessary to achieve adequate resolution; indeed the ideal would be two-dimensional Sollers along the flight paths.

3.31 The proposed spectrometer has an incident flight path of 10 m with the 0.5 x 0.5 cm^2 sample viewing 5 x 5 cm^2 of the moderator at 20K. A position sensitive detector with spatial resolution determined by elements of area 0.5 x 0.5 cm^2 is placed at a distance 2.5 m from the sample. Typical biological samples are fractions of millilitres in volume, with usual dimensions about 0.5 x 0.5 cm^2. Consequently the major contribution to the angular resolution will be that from the moderator area viewed by the sample. Since both the intensity and the angular resolution depend on the same factor (moderator area/(primary path length)^2), there is little to be gained by extending the primary flight path beyond that necessary for adequate time resolution.

3.32 The total flight path of 12.5 m allows a maximum wavelength of 6 Å and the minimum scattering angle of 0.005 rad allows measurements for $Q > 0.005$ $Å^{-1}$. Each element scans a range of Q with different resolutions, with the minimum Q increasing and the resolution improving as the distance of the element from the spectrometer axis is increased. Consequently measurements may be made with a resolution of less than 10% for the range $Q > 0.06$ $Å^{-1}$, with poorer resolution for lower values of Q. A decrease in the frequency of the pulsed source would be useful since it allows a corresponding increase in the flight path lengths which may be used to extend the lower limit of the Q-range measurable by the detector and to improve the angular resolution measured at any given value of Q.

3.33 Many low Q experiments are performed on samples whose scattering function is dependent only on the magnitude of Q, so that azimuthal symmetry may be included in the design of the spectrometer. An annular position sensitive

detector facilitates the analysis of the data since the resolution of each element in the ring is the same. Consequently for azimuthally symmetric scattering, the elements may be summed directly. On the other hand, an increasing number of experiments is being performed on samples exhibiting anisotropic scattering around the incident beam direction. The use of a ring detector allows values of $S(\underline{Q})$ to be measured with the same angular resolution for a given detector, and values with the same $|\underline{Q}|$ to be measured with the same time-of-flight. The complete range of Q may be measured by using only a few annular detectors; their angular resolution may be matched by making the outer rings thicker than the inner ring. For example, a ring of radius 15 cm and thickness 0.5 cm enables measurements for $Q > 0.06$ Å with 10% resolution; a ring of radius 20 cm can measure in the range $Q > 0.08$ Å and may have a thickness of 1.8 cm for 10% resolution.

3.34 A comparison of conventional and pulsed source low Q spectrometers requires the determination of the total count rate at the detector for a given sample. The total count rate for the pulsed method is determined by the integral of the incident wavelength spectrum with the differential cross-section of the sample, provided that the low Q measurement is performed in the Maxwellian part of the spectrum. The comparison is easily made when the incident spectrum and the differential cross-section may be expressed analytically. The Maxwellian spectrum is given by

$$I(\lambda,\underline{\Omega}) \sim 2I_o \frac{\lambda_T^4}{\lambda^5} e^{-(\lambda_T/\lambda)^2}$$

and the differential cross-section in the small Q region for a sample having a Guinier radius R_G is given by

$$\frac{d\sigma}{d\Omega} \sim C\, e^{-R_G^2 Q^2/3} = C\, e^{-(2\pi R_G \phi/\lambda)^2/3} = C\, e^{-\alpha^2/\lambda^2} .$$

The total number of neutrons at the detector per second is given by

$$\int_{\lambda_{min}}^{\lambda_{max}} d\lambda \; 2I_o \frac{\lambda_T^4}{\lambda^5} e^{-(\lambda_T/\lambda)^2} \frac{A}{L_1^2} Nt\, C\, e^{-\alpha^2/\lambda^2} \Delta\Omega_2$$

where N is the atomic density of the sample of thickness t and area A. $\Delta\Omega_2$ is the solid angle of the detector subtended at the sample, and L_1 is the

primary flight path. Provided that $\alpha \sim \lambda_T$, most of the measurement will be performed in the thermal region of the spectrum and the minimum and maximum wavelengths may be taken as zero and infinity respectively. Integrating over the thermal region of the spectrum only

$$\int_o^\infty 2\, d\lambda \; \frac{\lambda_T^4}{\lambda^5} \; \exp\{-\frac{\alpha^2 + \lambda_T^2}{\lambda^2}\} \; = \; \frac{\lambda_T^4}{(\alpha^2 + \lambda_T^2)^2} \; ,$$

and the total number of neutrons at the detector per second is given by

$$I_o \frac{\lambda_T^4}{(\alpha^2 + \lambda_T^2)^2} \; \frac{A}{L_1^2} \; Nt\, C\, \Delta\Omega_2 .$$

3.35 Assume that the equivalent measurement is performed on a conventional low Q diffractometer using a unique wavelength λ^* and a multidimensional detector. If $I(\lambda^*)$ is the neutron intensity at the sample, then the total number of neutrons at the detector per second is given by

$$\int_{\phi_{min}}^{\phi_{max}} I(\lambda^*)\, A\, Nt\, C\, e^{-\beta^2\phi^2} \; 2\pi\phi d\phi$$

where $\Delta\Omega_2 = 2\pi\phi d\phi$ is the solid angle of an annular detector element at a small scattering angle ϕ with an angular spread $\Delta\phi$, and ϕ_{min} and ϕ_{max} are the angular limits of the detector. β is given by the form of the cross-section

$$\frac{d\sigma}{d\Omega} \; = C\, e^{-(2\pi R_G \phi/\lambda)^2/3} \; = C\, e^{-\beta^2\phi^2} \; ,$$

so that $\alpha^2/\lambda^{*2} = \beta^2\phi^{*2}$

where ϕ^* is the angle of the detector of the low Q diffractometer on the pulsed source. Integrating over the scattering angle ϕ, and assuming that $\phi_{min} \sim 0$ and that the maximum angle ϕ_{max} contained by the multidimensional detector is sufficiently large to accept all the low Q scattering, then

$$\int_{\phi_{min}}^{\phi_{max}} e^{-\beta^2\phi^2} \; \phi d\phi \sim \int_o^\infty e^{-\beta^2\phi^2} \; \phi d\phi \; = \frac{1}{2\beta^2} \; .$$

Thus the total number of neutrons at the detector per second is given by

$$I(\lambda^*)\ A\ Nt\ C\ \frac{2\pi}{2\beta^2}\ .$$

3.36 The ratio of the number of neutrons at the detector of the low Q diffractometer on the pulsed source to that on the reactor is given by

$$\frac{N_{PS}}{N_{CS}} = \frac{I_o}{I(\lambda^*)} \frac{\lambda_T^4}{(\alpha^2 + \lambda_T^2)^2} \frac{\beta^2 \Delta\Omega_2}{\pi L_1^2}\ .$$

Take a sample with a Guinier radius R_G of 35 Å so that significant small angle scattering occurs for $Q < 2\pi/R_G \sim 0.2$ Å^{-1}. For a wavelength λ^* of 4 Å on a conventional instrument, $\beta^2 \sim 1000$ rad^{-2}. For the 2-metre position on D11A, $Q_{max} \sim 0.25$ Å^{-1}, so that most of the low Q scattering is recorded by the detector, and the above approximation is valid. Additionally take $I(\lambda^*)$ as $3\ 10^7$ neutrons cm^{-2} s^{-1} at 4 Å with an 8% wavelength resolution. The pulsed source instrument has a primary flight path L_1 = 10 m. An annular detector of width 0.5 cm at a mean radius of 15 cm gives a solid angle subtended by the detector at the sample of $\Delta\Omega_2 \sim 7.5\ 10^{-4}$ ster. The scattering angle ϕ of 0.06 rad gives $\alpha^2 \sim 58$ Å^2. The flux at the maximum of the spectrum (4.25 Å) for a 20K moderator is $I_o = 2\ 10^{13}$ neutrons ster^{-1} Å^{-1} s^{-1}. For this moderator λ_T = 6.7 Å and

$$\frac{\lambda_T^4}{(\alpha^2 + \lambda_T^2)^2} \sim 0.2.$$

3.37 With this particular experiment the time averaged count rate for the pulsed source instrument is thus 0.03 of the total count rate of the two-dimensional multidetector at the 2 m position on the D11A instrument with an incident wavelength of 4 Å ($\Delta\lambda/\lambda \sim 8\%$). However, an array of annular detectors may be used on the pulsed source low Q spectrometer, so that overlapping regions of Q space may be measured with different resolutions. For example, a two-dimensional array of detectors with inner and outer radii of 15 and 30 cms, and with elements 0.5 cm thick, can be used to give count rates comparable to those on D11A, and with a resolution of 10% for $Q > 0.06$ Å^{-1}. In addition, by reducing the inner radius, measurements may be performed at lower values of Q, though with poorer resolution. For example, with an inner radius of 10 cm, measurements can be carried out at $Q = 0.04$ Å^{-1} with 15% resolution.

3.38 It is possible to perform low Q measurements on the SNS in the range $Q > 0.005$ Å^{-1}. In the pulsed mode, adequate time resolution is obtained, and

very long flight paths with guide tubes are unnecessary. The dominant contribution is the angular resolution at the sample from the moderator. A two-dimensional detector with a spatial resolution of 0.5 x 0.5 cm^2 is most useful. Since the resolution of the instrument described here is sufficiently good, many experiments would require a comparison with the D11A instrument at flight paths longer than 2 m, and with longer wavelengths. Consequently an array of ring detectors may allow certain measurements to be made with count rates which can be up to an order of magnitude greater than those available on the small angle neutron camera.

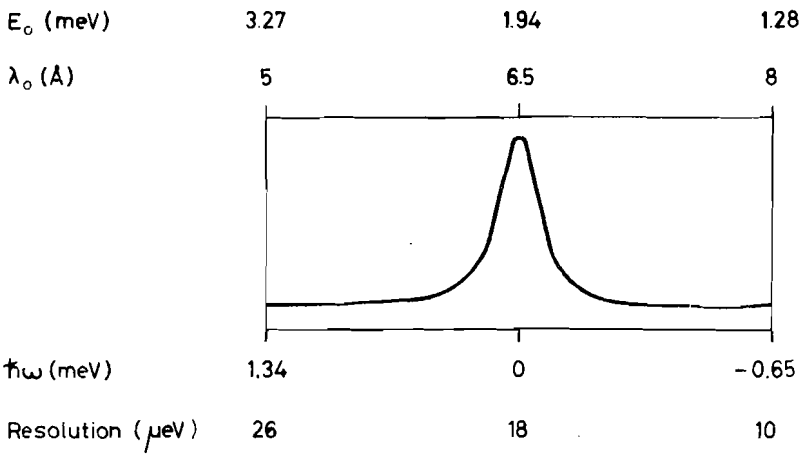

FIGURE 3·1 The quasi-elastic scan obtained on the White Beam Backscattering Spectrometer at 25 m.

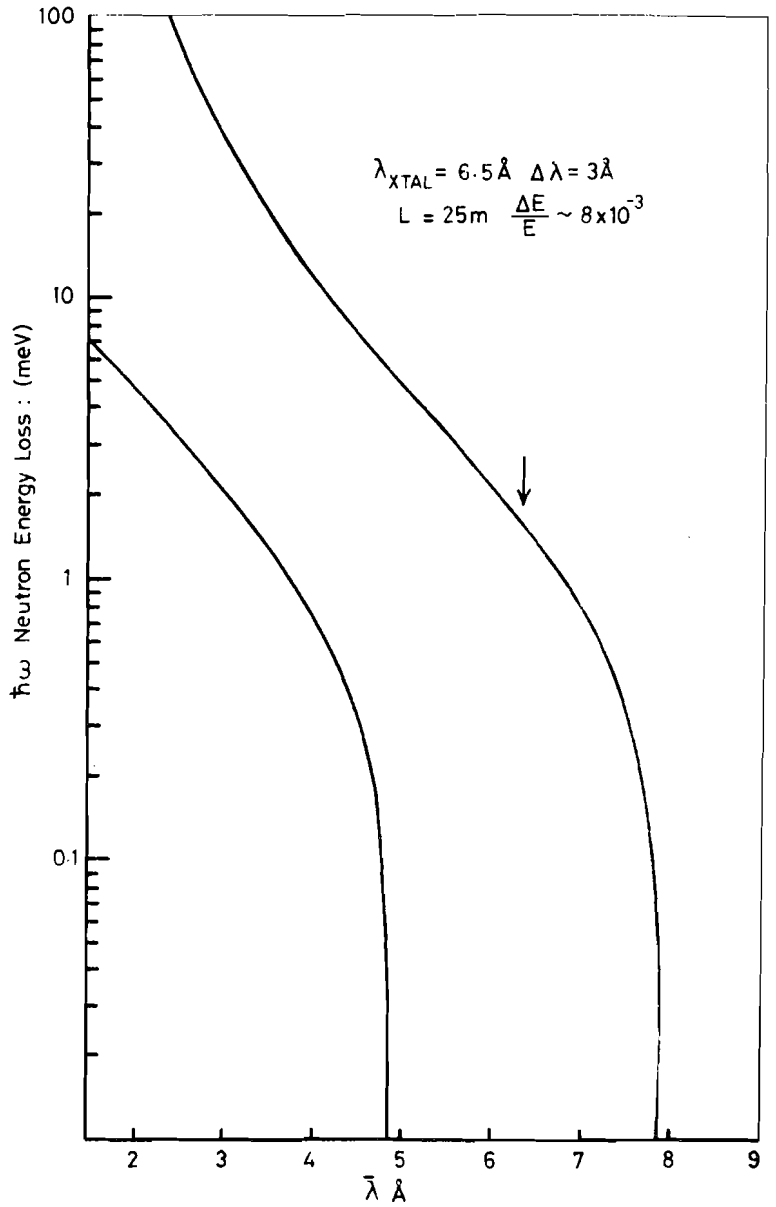

FIGURE 3·2 The 'window' of $\hbar\omega$ space available in neutron energy loss as a function of $\bar{\lambda}$, the mean value of the wavelength band accepted. The scan illustrated in Figure 3·1 corresponds to the arrowed position.

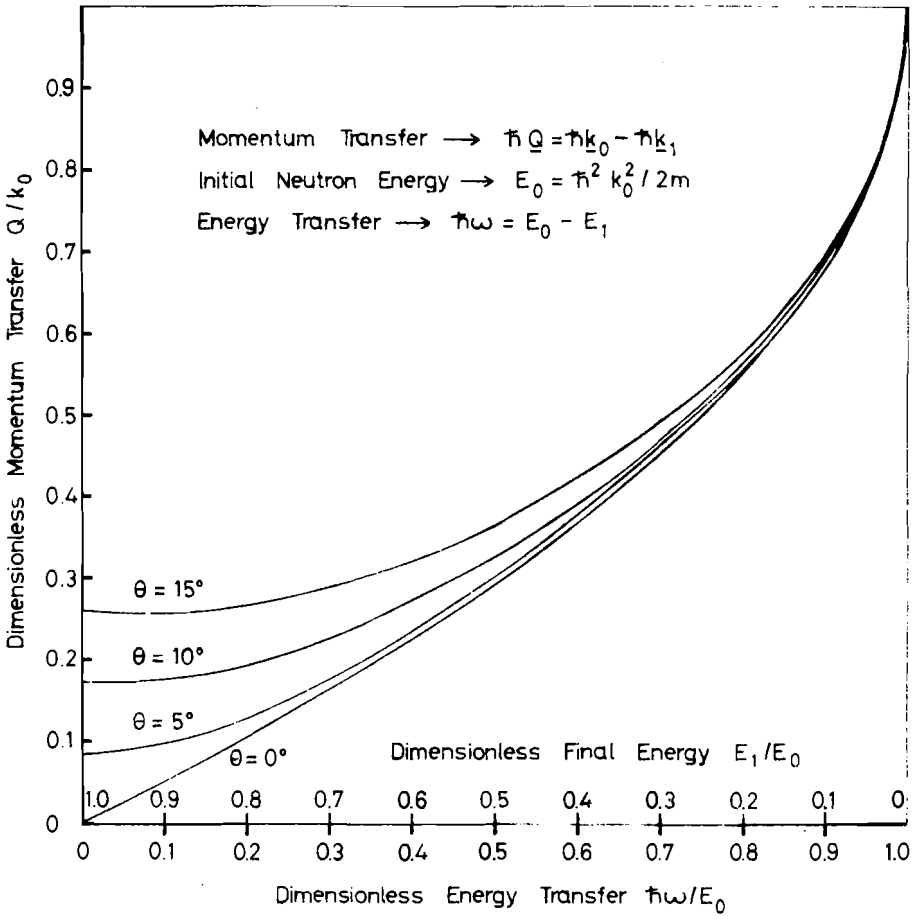

FIGURE 3·3 The constant ϕ loci in (Q, ω) space expressed in terms of the dimensionless variables $\hbar\omega/E_0$ and Q/k_0

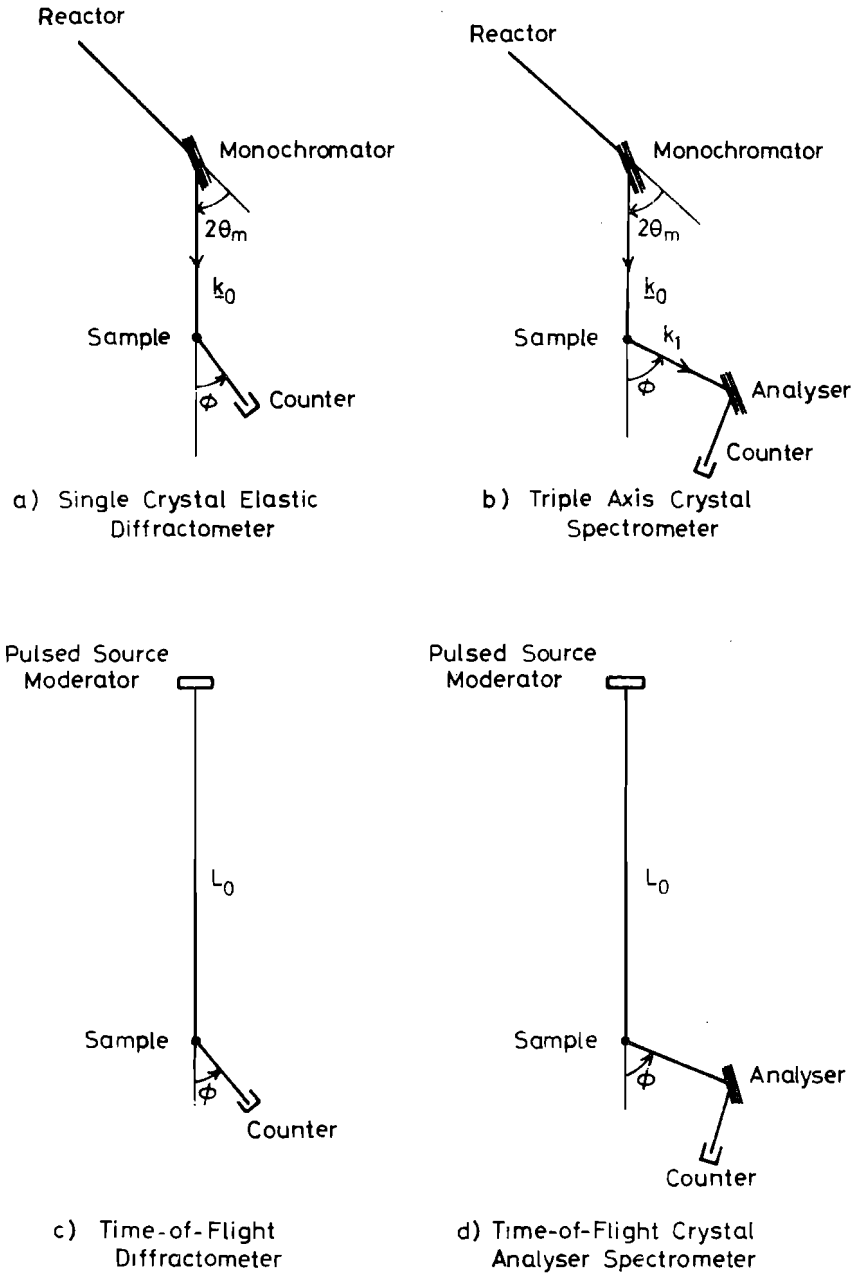

FIGURE 3.4 Pulsed source and reactor analogues of elastic and inelastic instruments.

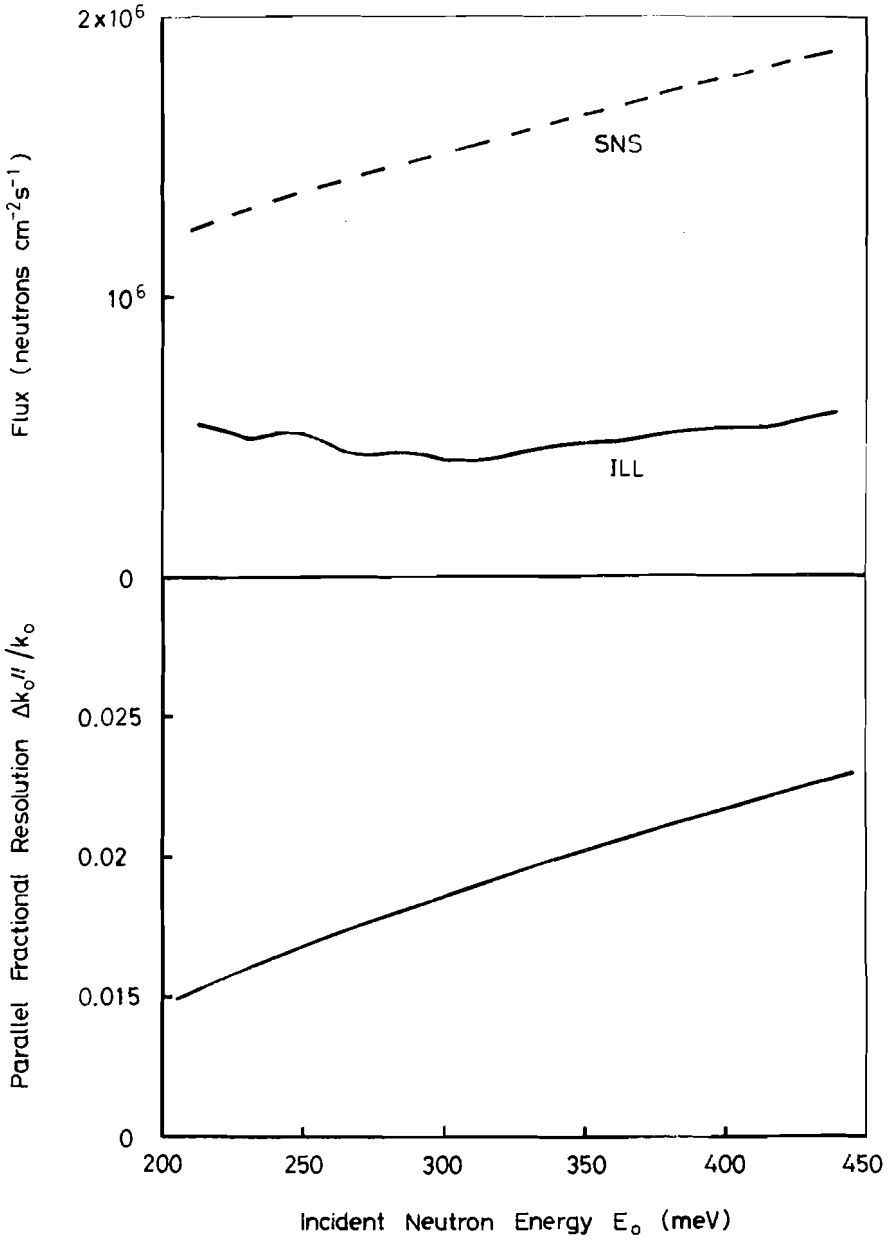

Figure 3.5 A comparison of the triple-axis spectrometer IN1 on the ILL hot source and a crystal analyser spectrometer on the SNS under the same resolution conditions.

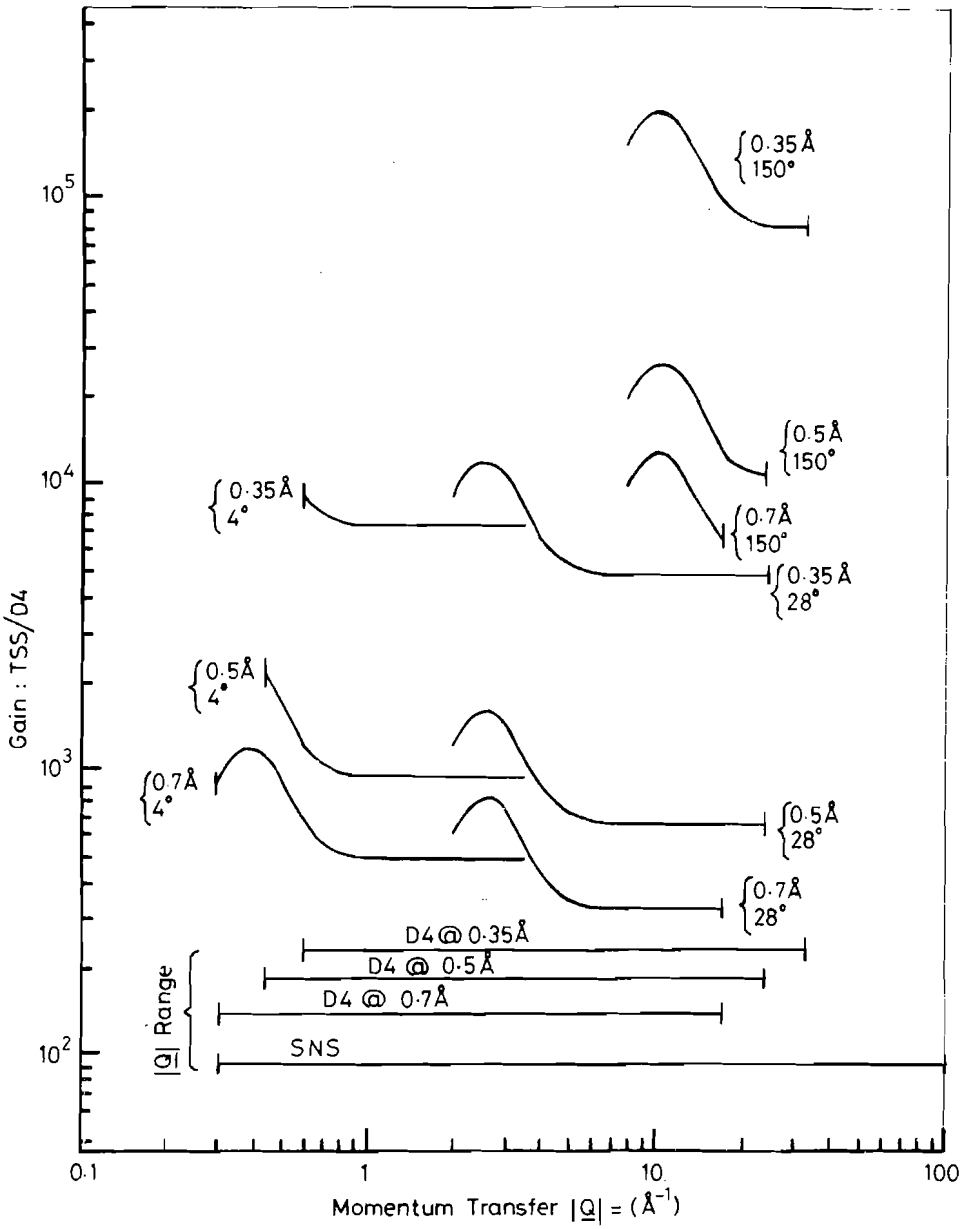

FIGURE 3.6 The gain of a Total Scattering Spectrometer on the SNS over D4 at ILL for a wide range of conditions.

CHAPTER 4. OTHER (NON THERMAL NEUTRON) USES

In this chapter are collated various suggestions which have been made for possible use of the proposed facility additional to its major application in condensed matter research by thermal neutron scattering. The material has been compiled by

Dr C J Batty	SRC Rutherford Laboratory
Dr J D Davies	University of Birmingham
Dr K Green	SRC Rutherford Laboratory
Professor E W J Mitchell	University of Reading
Dr D H Reading	SRC Rutherford Laboratory
Dr G C Stirling	SRC Rutherford Laboratory

CHAPTER 4 OTHER (NON THERMAL NEUTRON) USES

INTRODUCTION

4.1 The interaction of the 800 MeV proton beam in the heavy metal target gives rise to fragmentation of the target nuclei and to the evaporation of neutrons whose use, after moderation, forms the basis of the proposed SNS. However as well as these evaporation neutrons, intense beams of higher energy neutrons, π and μ mesons, neutrinos and other particles are produced. In this chapter we consider possible uses for such particles outside the field of neutron scattering in condensed matter research. These other uses cover a wide range of disciplines, both pure and applied.

4.2 The fact that the accelerator will be a world class machine and could provide first class multi-disciplinary facilities using elementary particles is shown in the following table, where comparisons are made with the energies, intensities and duty cycles of the major 'pion factories' of the world.

Facility	Country	Proton Energy MeV	Planned Maximum Beam Intensity μA	Duty Cycle
LAMPF	USA	600-800	1000 (100 achieved)	6×10^{-2}
TRIUMF	CANADA	180-520	200 (100 achieved)	1.0
SIN	SWITZERLAND	590	100	1.0
SNS	UK	800	200	1×10^{-5}

4.3 It can be seen from the table that the proposed facility has a proton intensity superior to any in the world, save perhaps that of LAMPF if its final design intensity is reached. The duty cycle of 10^{-5} is however several orders of magnitude lower than the other machines. This feature can be exploited in situations where the precise timing information of the pulsed source is used, as for example in neutron or muon time-of-flight work, or in situations where the dominant background is uniform in time, as for example in neutrino interactions where the cosmic ray background is important. However for many applications the capabilities of the machine could be considerably enhanced if provision were made for increasing the duty cycle closer to 100%. A possible means for doing this to part of the main beam, by extraction and stretching the basic 0.2 μs pulse in a storage ring, is discussed later. This method for increasing the duty cycle has two particularly attractive features - it does not in any way affect the design of the basic proton synchrotron, and it would allow the stretched beams to be used simultaneously with the pulsed beam to the SNS neutron target.

4.4 An 800 MeV proton beam entering a heavy metal target will interact to produce intense fluxes of pions as well as large numbers of neutrons and protons over a broad energy spectrum. The pions can then decay

$\pi^o \rightarrow 2\gamma$ with a half-life $\sim 10^{-16}$s

$\pi^+ \rightarrow \mu^+ \nu_\mu$ or $\pi^- \rightarrow \mu^- \bar{\nu}_\mu$ with a half-life $\sim 2.6 \times 10^{-8}$s

and the muons from the charged pions then decay

$\mu^+ \rightarrow e^+ \nu_e \bar{\nu}_\mu$ or $\mu^- \rightarrow e^- \bar{\nu}_e \nu_\mu$ with a half-life $\sim 2.2 \times 10^{-6}$s.

4.5 The source intensity of these particles to be expected from 10^{15} protons per second interacting in a target is $\sim 2 \times 10^{14}$ pions per second, which if allowed to decay lead to similar numbers of muons, electrons and neutrinos. This source could be used to provide practically realisable beams from a thin target:

$\sim 2 \times 10^9$ π^+/s
$\sim 2 \times 10^8$ π^-/s } in the energy range 100-600 MeV

$\sim 2 \times 10^7$ stopping pions/s

$\sim 1 \times 10^7$ stopping muons/s

and from a thick target:

$\sim 4 \times 10^{16}$ spallation neutrons at source
$\sim 8 \times 10^{6}$ neutrons cm^{-2} s^{-1} at 800 MeV
$\sim 4 \times 10^{9}$ stopping π/s at 100 MeV/c
$\sim 2 \times 10^{14}$ neutrinos $(\nu_\mu)/cm^2$ at 30 MeV/c at source
$\sim 2 \times 10^{14}$ neutrinos $(\nu_e \bar{\nu}_\mu)/cm^2$ in the range 0-53 MeV/c at source
$\sim 4 \times 10^{7}$ stopping μ^+/s at 30 MeV/c

4.6 The relative fluxes and energies of neutrinos from the different laboratories of the world are shown in the accompanying figure; the energy region of 0-53 MeV very nicely fills in the gap between the reactor neutrinos ($\bar{\nu}_e$ only) and those from the high energy accelerators (ν_μ $\bar{\nu}_\mu$ primarily). This facility could provide all types of neutrinos, though from a massive target ν_μ (30 MeV), ν_e, $\bar{\nu}_\mu$ (0-53 MeV) will dominate over the anti-neutrinos $\bar{\nu}_\mu$, $\bar{\nu}_e$, ν_μ by a factor of 10^3. This factor could be brought nearer to unity in a system if the π^- were allowed to escape from the target and decay in flight.

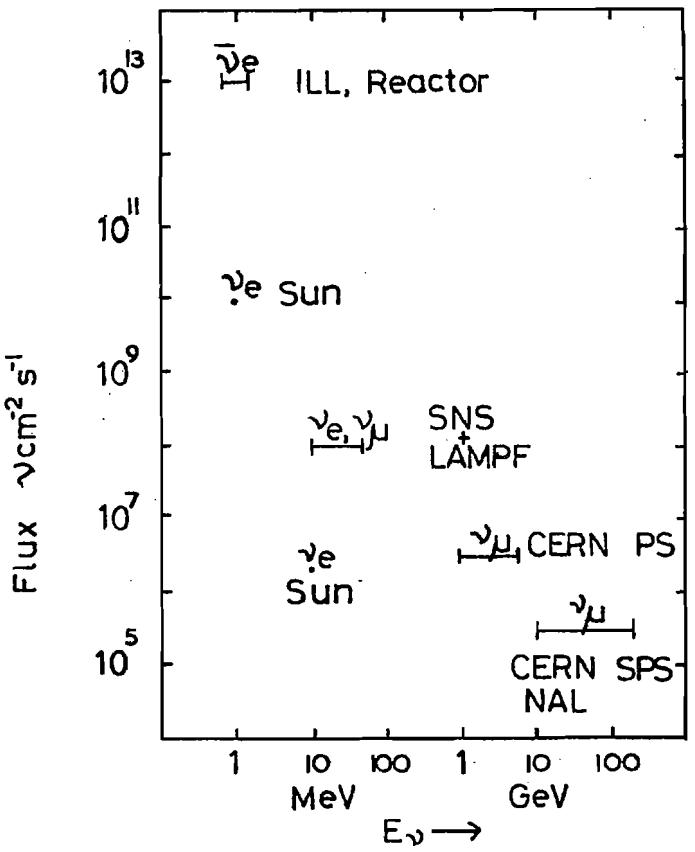

Intensities and Energies of Neutrinos from Various Sources

4.7 The production of ultra cold neutrons (UCN) at the SNS may also be considered. The UCN facility at present being installed at the ILL reactor in Grenoble is sited on a beam tube in the reactor thermal flux of 10^{15} n cm^{-2} s^{-1} and is expected to yield a UCN flux of $\sim 5 \times 10^{4}$ n s^{-1}. The equivalent time-averaged thermal flux to be expected from the SNS is 2×10^{13} n cm^{-2} s^{-1} so that the equivalent UCN flux would be around two orders of magnitude less than that available at ILL. However there may be means whereby the pulsed beam conditions of the SNS could be exploited.

4.8 The pulsed nature of the particle beams can be exploited in specific cases where it is not required to count particles individually in the incident beam, but where this feature is required it is necessary to spread out the spill time of the beam. The simplest way to lengthen the spill time of the protons from the rapid cycling synchrotron and the one which minimises interference with the basic operation of the machine for the spallation neutron facility, is to extract part of the main beam and temporarily put it in a separate storage ring. An outline design study has shown that a ring using standard Nimrod beam line magnets could be accommodated in the existing experimental Hall 1 of the Nimrod complex, with adequate space for external beam lines and equipment. 10-15% of each 0.2 μs pulse from the 800 MeV proton beam would be transferred to the ring, then slowly spilled during the 20 ms before the arrival of the next pulse. In this way a nearly uniform proton current could be generated ($\sim$ 20 μA) for subsequent use in the generation of secondary beams. This 'stretcher' ring could be operated simultaneously with the main spallation neutron facility which would suffer only 10% loss in beam intensity.

APPLICATIONS

Muon Spin Rotation

4.9 Muons are created in the decay of pions, and can be collected into beams which are nearly 100% polarized. When slowed down in a sample the muon spin precesses about the local magnetic field at a frequency determined by this field and the muon magnetic moment, until such time as it decays $\mu^{+} \rightarrow e^{+} + \nu_{e} + \bar{\nu}_{\mu}$. The positron ($e^{+}$) is preferentially emitted along the muon spin direction, and a positron detector in the plane of precession reflects the

mean muon lifetime (2.2 μs) together with the Larmor precession frequency arising from the local magnetic interaction. The uses to which this so-called muon spin rotation technique (μSR by analogy with NMR, ESR) can be put are many and varied, and include the study of internal fields in magnetic materials, diffusion processes, critical phenomena and fluctuations in the region of magnetic phase transitions, relaxation times down to 10^{-8}s, and investigations into impurity centres in semiconductors and insulators. In the process of slowing down the positive muon forms muonium (μ^+e^-); negative muons form μ^- atoms (see below). Muonium is an analogue of the H atom with virtually identical properties, except that the mass of muonium is only about 1/9 that of H. Consequently the chemical reactions of muonium provide a unique context in which to examine dynamic isotope effects in chemical kinetics, in particular quantum mechanical tunnelling; the μSR technique has been used for studying chemical reactions in both the liquid and gaseous phase.

4.10 Muon beams from the SNS will be capable of feeding research of this kind, possibly with a 30 MeV/c μ^+ beam from the neutron target station. This beam will be fully polarized and pulsed with the characteristics of the main machine. The intensity of beam muons will preclude individual particle counting so that the precision with which the precessional frequency can be observed will be limited by the 0.2 μs pulse length. Of more general use would be the provision of muons from the stretcher/storage ring, in which case the muons in the beams, both positive and negative,could be individually counted.

Chemical Effects with π and μ Mesic Atoms

4.11 As indicated above when π^- and μ^- mesons traverse sufficiently thick material they will interact, slow down and stop in a time (10^{-10} s) which is considerably less than their lifetime. Being negatively charged they will be attracted by the coulomb field of the nucleus and captured into orbits about the nucleus. These 'exotic-atoms' will then de-excite by the emission of x-rays, the meson coming closer to the nucleus at each transition until it is finally captured by the nucleus and is 'lost'.

4.12 The orbits of the meson about the nucleus are described by angular momentum (ℓ) and principal (n) quantum numbers. The energy of the emitted x-rays depends almost entirely on the charge of the nucleus and the principal quantum numbers of the atomic states involved. However the probability of nuclear capture depends on the ℓ-value, and for π-mesons will be complete for all angular moments below a certain critical value.

4.13 Measurement of the energy of the x-rays clearly allows the nuclear charge to be determined and it is possible with μ-mesons to distinguish between isotopes of the same element even at high Z. It is also known that the capture of the meson into the initial high n states is considerably affected by the atomic or molecular electron cloud and hence by chemical and solid state effects. This probably arises through different populations of the ℓ-states for a given n-value. It is these two features which are of particular interest in considering the use of exotic atoms for chemical analysis and for studies in atomic physics, chemistry and solid state physics.

4.14 As an example, muons have been used at LAMPF to study the elemental composition of tissue. The x-ray spectra from several types of tissue were used to determine the amounts of carbon, nitrogen and oxygen present. These determinations agreed with the results of more conventional chemical analysis and showed that muonic x-rays offer a non-destructive technique for determining the amounts of the more abundant elements present in selected regions of the body. Other work has looked at the use of muonic x-rays to analyse active fissionable material and again promising results have been obtained. Whilst in many cases neutron activation or x-ray fluorescence techniques will be more convenient it seems that in certain specialised cases, exotic atom analysis could have significant advantages.

4.15 It has been known for some time now that the chemical form of a substance can affect the relative intensities of exotic atom x-rays for a particular element. More recent work has shown that absolute intensities are also affected and these variations have been correlated in a very direct way with the variation with Z of the electron density in the outer part of the target atoms. Extensive programs of work using muon beams are now in progress at several laboratories to study these effects further. Additional experiments using pions would be useful since the nuclear capture from low ℓ-states would give information on the ℓ-distribution for different n-values.

4.16 It is now clear that mesic x-ray spectra carry a lot of information about the structure of the outer electronic shells. However improved and systematic experiments, of the types in progress, and detailed comparisons with realistic theoretical models will be necessary before exotic atoms can become a serious and reliable tool for studies of atomic and molecular structures. The SNS fitted with a proton storage ring would be well suited to studies of this type.

Stored Neutrons

4.17 There is considerable interest in research with ultra cold neutrons at a number of reactor centres. The potentially most powerful facility is now under construction at the ILL and experiments to measure the neutron lifetime and to search for a neutron electric dipole moment are now being prepared. Results from these experiments are of fundamental significance for elementary particle theory. Ultra cold neutrons are likely to be used to study the surface properties of materials. Where experiments can be designed to exploit the high pulse intensity of the SNS it may be possible to augment these applications.

Neutrino Physics

4.18 The neutrino, an apparently massless, chargeless, spin $\frac{1}{2}$ particle is an enigma. It was first postulated as the carrier of the missing energy in nuclear β-decay and has subsequently been observed to interact with other particules at a level consistent with just the weak interaction process. It appears to exist in at least two forms, one associated with electrons and the other in association with muons.

4.19 Neutrinos will in general excape from the target station yielding fluxes of $\sim 10^{8}\ \nu\ cm^{-2}\ s^{-1}$. The known cross-sections for neutral current processes for example (a form of the weak interaction only discovered in 1975) are extremely low and of the order $10^{-45}\ E_{\nu}$ (MeV) cm^{2} where E_{ν} is the neutrino energy, and the more usual charge current interactions will exist with similar cross-sections. The process of charged muon production ($\nu_{\mu} + n \rightarrow \mu^{-} + p$, $\bar{\nu}_{\mu} + p \rightarrow \mu^{+} + n$) can only occur above a neutrino threshold energy of 111 MeV. As the neutrinos from the SNS target come essentially from π's and μ's at rest they have energies less than 53 MeV and hence in the case of the muon neutrinos are unable to initiate charge current interactions. These neutrinos therefore form a unique source of particules whose only interaction is through the weak neutral current. In particular the line source of ν_{μ} at 30 MeV allows the possibility of detailed investigation of this interaction by observations of excitations to specific nuclear energy levels of known quantum numbers.

4.20 In addition to studies of the form of the weak neutral current the neutrinos can be used to investigate the purely leptonic weak charged current interaction; the form of the lepton conservation laws, whether multiplicative

or additive; the muon conservation law; coherent nuclear scattering and anomalous neutrino effects in general as, for example, in neutrino oscillations which might exist if their masses are not exactly zero.

4.21 All of these experiments are intrinsically very difficult with, for example, cross-sections at the level of 10^{-41} cm^2 for neutral current excitations implying event rates of around 0.05 events/day/kgm of detecting material. This is a low, but not impossible, detection rate and one whose signal to background is considerably enhanced by the short pulses of the SNS. Any machine generated delayed background or cosmic ray background is suppressed by 10^{-5}, the duty cycle of the machine.

Nuclear Physics

4.22 Beams of neutrons, protons, pions and muons at a level of 10^7 to 10^8 per second will provide opportunities for wide ranging studies in nuclear properties, nuclear interactions and elementary particle interactions through both strong and weak interactions. In general the pulsed nature of the machine with its low duty cycle of 10^{-5} is a hindrance for most of these studies and considerable benefit would be obtained by the provision of a storage ring to stretch out the beam to a 100% duty cycle. One exception to this might be in the provision of a low energy muon beam (30 MeV/c) from the neutron production target where the muons coming from pion decay at rest in the surface of the target are very nearly 100% polarized. This intense burst of muons could be used after the prompt burst of background has subsided and, in cases where observation of the beam muon was not necessary, experiments on rare decays and interactions would be possible, the known polarization of the incident muon being an additional useful factor for correlation experiments. Other possible uses for the pulsed beam would be in those cases where time-of-flight information could be exploited and, in particular, total cross-sections of low energy neutrons in the energy range 10 keV to 10 MeV are of importance with reference to astrophysical problems and measurements of (n,γ) reactions for nuclear structure studies. Neutrons with times-of-flight of 75 ns m^{-1} at 10 MeV should be readily available from the SNS.

4.23 Experiments that will be possible, given the storage ring, will include medium energy (100-700 MeV) interactions of pions and nucleons with nuclei and nucleons. These experiments with both polarized and unpolarized targets will probe the nature of the strong interactions to higher precision than presently known and also probe the content of the nucleus. The single pion contribution

clearly dominates the nuclear force at large distances and is responsible for the bulk of the total cross-section; higher energies and intensities will enable this force to be investigated at shorter and shorter distances. The contribution of resonance effects within a nucleus are also of importance and can be probed in this way. Although much of this work will be undertaken by the existing pion factories, the energy region above 500 MeV, the maximum of the TRIUMF machine, will be largely unexplored. The provision of large volume spectrometers like the Rutherford Multiparticle Spectrometer will also considerably aid these studies. Stopping pion and muon beams will be an essential feature of these new facilities. Capture of these particles into well defined atomic states will yield characteristic x-ray spectra and with finally nuclear capture taking place information will be obtained on weak interaction coupling constants and parameters as well as more general information on nuclear structure. Intense beams of pions and muons will also enable investigations on rare decay modes of these particles as well as more detailed information on the normal decays. Conservation laws and symmetry principles will be able to be tested to a greater precision than heretofore.

Biomedical Applications

4.24 The basic principles in the use of pions for biomedical purposes and, in particular, for the treatment of tumors were pioneered in this country. Negative pions offer advantages over the usual γ-ray treatment because being heavy charged particles they can penetrate deeply to a target volume and deposit much of their kinetic energy in a stopping region. They are absorbed there, causing further local ionization to be deposited by fragments of atomic nuclei shattered by the liberation of the pion rest mass. The result is a variation of dose with depth such that an initial flat region, 'the plateau', is folled by a high dose region, 'the peak', which would be located in the region of the tumor. Beyond the peak the dose falls rapidly to a low value. The biological damage is further enhanced at the peak because the fragment nuclei are densely ionizing and more efficient than fast particles. Further, the absence of oxygen, as occurs in tumors with a poor blood supply, produces less radio-resistance to the fragments than to γ-rays, so that pions are expected to be particularly effective in the treatment of large deep seated tumors.

4.25 Experiments to study these effects are being carried out at several laboratories around the world including the Rutherford Laboratory. Beam lines are being commissioned which are designed as radiotherapy units, and some

'human biology' exposures have been made on volunteer patients. For studies on biological systems where duty cycle is no problem but the highest intensities are required, a pion beam derived from the main SNS proton beam would give does in the region of 10 to 100 rad/min over a litre volume and would enable a great variety of work to be carried out. However, for more detailed dosimetry studies where the individual particles have to be counted a beam derived from the storage stretcher ring would be ideal.

4.26 Protons of, say, 200 MeV are simpler to use and more abundant than pions and are also claimed to have advantages over γ-rays because of more precise localisation of the radiation dose within the tumor volume. They are used for radiotherapy in several centres particularly for the precision demanding irradiation of pituitary gland tumors. Similarly neutrons as produced from 70 MeV protons (eg, parasitically using the injector) are used for radiotherapy as effects are even less dependent on the presence of oxygen than with pions although the neutron dose is localised no better than γ-rays.

Isotope Production

4.27 The interactions of 800 MeV protons in a target (A,Z) generates products (A', Z') through reactions of the type

$$(A, A)\ (p, xp\ yn)\ (A', Z')$$

where x and y can be large numbers greater than 10 and lead to neutron deficient spallation products. The higher the incident energy the larger x and y can be so that an 800 MeV machine has advantages over the lower energy machines already in use such as the Harwell Variable Energy Cyclotron. Reactors are also a source of isotopes but in this case they are generally neutron ricy. The neutron deficient isotopes provide new elements with suitable products and short life-time. Further, by positron emission, which on annihilation produces two back to back γ-rays, tomographic information may be obtained without the need of a collimator.

4.28 The use of isotopes is now widespread throughout industry, research and the commercial world covering such diverse topics as x-ray fluorescence, Mössbauer effect, ionization effects, neutron activation and measurement and tracing methods. An isotope production facility at the 800 MeV SNS would almost certainly find commercial outlets.

Radiation Damage Studies

4.29 Fast neutrons can make eleastic collisisions with nuclei which lead to atoms recoiling with high energies ($\sim 10^5$ eV) through crystals. At these energies the primary knock-on atoms are not only displaced from their lattices positions but, in slowing down, undergo atom-atom collisions which produce many more displacements. A primary knock-on may produce 10^2-10^3 further displacements, affecting the physical properties of the material. The subject of radiation damage is one of both scientific interest - the details of how the defects are created, their stability and how they affect the physical properties - and technological interest - since passive materials (electronic materials) are seriously modified in radiation environments. Neutron irradiations are an important part of this subject and although extensive studies have been made using reactors the subject is still not fully understood. The question arises as to whether a neutron irradiation cell on the SNS would make a useful contribution to the field. Such contributions might come from:

(a) the damaging flux
(b) 'cleaner' spectrum
(c) the pulsed nature

We discuss each in turn.

(a) Flux

SNS will give a time averaged (fast) neutron production rate of 4×10^{16} n s^{-1} in pulses about 0.2 μs at 53 Hz. This gives in certain positions close to the target fluxes $\sim 10^{14}$ fast n cm^{-2} s^{-1}. This is a useful flux but comparable figures can be obtained in some MTRs (Materials Testing Reactors), always provided that they are not closed down. There is, therefore, no gain in total fast neutron flux so that the SNS is not going to contribute on this ground, better than existing high power MTRs, to the solution of problems relating to high accumulated fast neutron dose.

(b) Cleaner spectrum

The neutron spectrum is expected to be not unlike a fission spectrum, except the SNS will give a high energy tail extending to several hundred MeV. The important difference is, however, that there should be considerably less γ-ray production. In low temperature irradiation experiments (say 1-10K) γ-heating in the cryostat is a considerable problem requiring large refrigeration power.

Such low temperature experiments are critically important in understanding radiation damage and there seems to be no doubt that they would be at the SNS than in a reactor of comparable flux. There would be cases also in which the damage so produced may be studied at slow neutron beam scattering instruments at the SNS.

(c) The pulsed nature of the source

The intensity in a pulse in a favourable flux position could be $\sim 5 \times 10^{17}$ n cm^{-2} s^{-1}. This has two consequences of potential interest. It allows damage to be accumulated corresponding to a very high flux while a lower rate could be achieved by using a different position. Thus some information about the flux dependence of damage production could be obtained. The other possibility which makes use of the pulsed nature of the source is to use a very sensitive property (minority carrier recombination in semiconductors; quenching of luminescence) to study the response of the crystal to a short, high intensity damaging flux. During one pulse in a favourable position one could expect a damage dose of $\sim 2.5 \times 10^{11}$ n cm^{-2}. The effects of one pulse should be observable and a number of interesting experiments could be carried out. The method would not be generally available because the dose per pulse will not be sufficient for most properties in most materials. However, in a few special cases it could be of considerable interest.

4.30 We cannot see that the SNS would have a generally useful role in radiation damage studies. However, in a few special instances the characteristics of SNS have some potential advantages over reactors of equivalent average flux. It would be sensible to arrange permanent structures near the target area in such a way that the incorporation of a radiation cell, without prejudicing the moderated beams, could be achieved from time to time if irradiation topics such as those discussed became of clear scientific or technological importance

SUMMARY

4.31 The uses for a high intensity rapid cycling 800 MeV proton synchrotron are in principle many and varied, as indicated in the preceding pages. The primary use if of course the generation of spallation neutrons for thermal and epithermal neutron scattering in condensed matter research, but provisions for other uses could possibly be made so as to create a broadly based multi-disciplinary facility. These additional uses could cover the full spectrum of interests, from

the pure research of elementary particle and nuclear physics, to the application of these tools and techniques in condensed matter research using beams of pions and muons, to the commercial and immediately useful fields of isotope production and medical physics.

PROPOSAL FOR A SPALLATION NEUTRON FACILITY

Appendix II - PROJECT DESCRIPTION

C O N T E N T S

ACKNOWLEDGEMENT

This document is based on work by the following Rutherford Laboratory staff:

F Atchison
R Bendall
J R J Bennett
C J Carlile
A Carne
R J Elsey
J B Forsyth
R G Fowler
P Goodyer
D A Gray
M Greenwood
M R Harold
J A Hirst
L C W Hobbis
J T Hyman
J Lidbury
B G Loach
B H Meardon
D F R Mildner
J D Milne
A R Mortimer
M O'Connell
D R Perry
C W Planner
G H Rees
J Rimen
R Sidlow
A Slater
W A Smith
G C Stirling
A D Taylor
B C W Ward
N D West
A Wheldon
W G Williams
R Wimblett

CHAPTER 1: 800 MeV SYNCHROTRON

1.1 INTRODUCTION

An outline description of the proposed facility is given in the main proposal document. A rapid-cycling synchrotron is used to provide an intense pulsed beam of 800 MeV protons at a well-shielded external target station. The source is estimated to provide 4 x 10^{16} spallation and fission neutrons per second in a uranium (^{238}U) target. The neutrons are brought to thermal and epithermal energies in 2 moderator assemblies which are adjacent to the target. Special openings are made in the target shield wall to provide for 14 external neutron beam lines.

A design and costing for the proposed 800 MeV proton synchrotron was issued as a Rutherford Laboratory report[1] in December 1975. Since that time, a more detailed evaluation of the synchrotron has been undertaken together with an initial study of the neutron spallation target station and a survey of the attendant radiation problems expected at the site. Further aspects of the source design are given in a series of internal RL notes[2,3,4,5].

A schematic lay-out of the facility is shown in Fig 1.1, and a more detailed diagram of the synchrotron components in Fig 1.2. No new buildings are required as full use is made of the services and buildings that form the Nimrod complex. Use is also to be made of the existing 70 MeV proton linac injector and of the magnet power supply system from the NINA accelerator. The scale of the project is indicated by reference to Photographs 1.1, 1.2 and 1.3 which show, respectively, the Nimrod Magnet Hall, Experimental Hall 3 and the 70 MeV injector during their construction phases.

The synchrotron is designed to provide 2.5 x 10^{13} protons per pulse, at a kinetic energy of 800 MeV, with a pulse duration of approximately 200 ns and a pulse repetition frequency of nominally 53 Hz. This is the resonant frequency of the present NINA magnet power supply. It is probable that the new synchrotron will operate at a slightly lower repetition frequency, with the system phase-locked to the frequency of the mains supply.

Emphasis is given in this Appendix to the solution of those features of the project which are considered to be the more difficult: the prevention of radiation damage to machine components, the problems associated with induced radioactivity,

the control of the high intensity beam in the synchrotron and aspects of the synchrotron vacuum chamber design.

To provide the large circulating beam current in the synchrotron, charge exchange injection of negative hydrogen ions is used. The existing proton ion source for the 70 MeV injector will thus be replaced by an H^- source. Some other modifications to the injector are also required for rapid-cycling operation and these are discussed in Section 1.8.

The single bunch of 800 MeV protons in the synchrotron will be extracted as a 200 ns pulse and transported to the target station in Experimental Hall 3 using Nimrod beam line elements within a well shielded enclosure. Experimental Hall 1 will be reserved initially for testing of machine components. Future possibilities for the Hall are a second neutron target station or the installation of a small stretcher storage ring to contain 10% of the main proton beam in a long duty cycle mode. Such a beam is of interest for a wide range of non-neutron applications, and an outline design for a possible stretcher ring has been given in an internal RL note[2]. If it is decided to allow for either of these possibilities, then a different orientation of the synchrotron from that shown in Fig 1.1 will be adopted, together with a more complex beam line from the synchrotron to the target station in Hall 3.

Existing Nimrod services, such as water cooling, air conditioning and electrical distribution, are more than adequate for the proposed source and can be used with little modification. Also, most of the shielding for the target station is available on site. Steel shield thicknesses of 4-5 m are required plus additional layers of concrete and special linings for the beam openings.

It is planned to locate the main control room in the building that presently houses the Nimrod 15 MeV linac. Control of the 70 MeV injector, 800 MeV synchrotron and the target station will be undertaken by a central computer system together with separate computers for the individual sub-systems. The use of a sophisticated control system is considered an important feature for the successful operation of the high intensity source and for the display of adequate data to ensure high standards of radiation protection.

1.2 SYNCHROTRON DESIGN AND PARAMETERS

The 800 MeV synchrotron is designed to fit into the Nimrod Magnet Hall and to be compatible with a modified NINA magnet power supply. Components of the synchrotron are arranged in 5 superperiods as shown in Fig 1.2, and the details of a superperiod are given in Fig 1.3. Each superperiod has 1 long straight section, 3 quadrupole doublets, 2 dipoles, 1 octupole and 1 skew quadrupole, plus a trim quadrupole next to each main quadrupole. Of the 5 long straights, 1 is for injection, 1 for extraction, 2 for RF cavities and 1 is free for diagnostics and developments. A list of synchrotron parameters is given in Table 1.1, and a noticeable feature is the relative values of bending radius and mean radius (ratio 0.27).

A 'missing-magnet', separated function design is chosen for the magnet lattice for the following reasons:

a. It provides long straight sections, which are needed for extraction, without recourse to the use of special matched insertions.

b. It readily allows fast extraction in the vertical plane, which is the favoured plane for extraction, as described in Section 1.9.

c. It provides straight section lengths sufficient to simplify the design of the RF system.

d. It leads to a lattice with a high value of the transition energy, well above the operating energy of the synchrotron.

There are two reasons for introducing trim quadrupoles into the lattice:

a. To allow the betatron Q-values to be varied independently of the main magnet resonant power supply, by the separate powering of small, associated, correction units.

b. To enable the main F and main D quadrupoles, which have a common design, to operate with equal current levels and field gradients in the chosen Q range around $Q_h = 4.2$ and $Q_v = 3.9$.

The first feature is important for Q correction during injection and acceleration, with the specific requirement of continuous correction during the injection interval. The second feature leads to a completely symmetrical mode of operation for the modified NINA magnet power supply. The choke unit of the NINA system is designed to feed 10 identical magnet sectors. Such sectors are formed by a series

arrangement of 1 dipole magnet, 1 quadrupole doublet and 1 other F or D quadrupole. Each superperiod conveniently subdivides to provide 2 sectors.

The superperiod resonance lines in the vicinity of the operating point are shown on the tune diagram, Fig 1.4. The operating point (4.2, 3.9) is better placed with respect to the superperiod resonances than alternative operating points (3.7,3.9),(4.2,3.3) and (4.2,4.3). In particular, the third order resonance lines $3Q_h = 10$, $2Q_v + Q_h = 10$ and $2Q_v - Q_h = 5$ are far removed, as is the coupling resonance $Q_v - Q_h = 0$ and all the fourth order resonances except $4Q_v = 15$. This last resonance is discussed in Section 1.3.

The nominal betatron tunes of $Q_h = 4.2$ and $Q_v = 3.9$ are obtained by normalised quadrupole field gradients of 0.805 m^{-2} in the main quadrupoles and 0.02 m^{-2} in the trim quadrupoles, when all the trim units are radially defocusing. These values assume trim quadrupole lengths of 0.3 m, main quadrupole lengths of 0.6 m, a spacing between the main quadrupoles of 0.5 m and other lengths in the superperiod as in Fig 1.3.

Fig 1.3 also gives the lattice functions in a superperiod for the nominal Q-values. The effect of the 'missing-magnet' is indicated by the ripple in the peak values of the horizontal β-function and of the dispersion function, α_p. It may be seen that the largest maxima of β_h and α_p do not occur at the same machine azimuth. There is no corresponding ripple in the peaks of the vertical β-function because the 36^o dipoles are constructed as sector magnets, with consequently no effect on the vertical focusing.

As a consequence of the shape of the dispersion function, the transition energy of the lattice is high, with $\gamma_t = 6.39$. The minimum value of α_p, approximately 0.2 m, which occurs in one of the 2.9 m straight sections of each superperiod, is advantageous for the location of octupole and skew quadrupole correction magnets. There will be an octupole in each superperiod at the point marked O in Fig 1.3, and an adjacent skew quadrupole in either all or just two of the superperiods. A minor disadvantage of the lattice is the large maximum value of α_p, 5.7 m, which occurs in the F quadrupoles at the upstream ends of the five, 7.99 m, long straight sections. Beam scrapers will be positioned near these locations to intercept the beam lost at trapping, when the momentum spread is increasing rapidly as indicated in Fig 1.5.

During the magnet cycle the field in the main dipole magnets varies sinusoidally between 0.176 T and 0.697 T. The dipoles are located near positions of minimum β_v so as to reduce their vertical aperture requirements. This feature is also an advantage for vertical fast extraction as it enables the fast kicker and extraction septum magnet to be located near positions of maximum β_v and minimum β_h. There are 3 lattice 'cells' in each superperiod, and the phase shift of the vertical betatron motion per cell is approximately $\pi/2$. Vertical rather than horizontal extraction is preferred because the beam emittance, which is large, is smaller in the vertical than the horizontal plane, with $E_v/E_h = 0.56$.

The quadrupole vertical apertures and the extraction system elements are designed to allow extraction at 800 MeV of a beam which has an increase of 2 in its momentum-normalised transverse emittances at peak energy. This safety factor is introduced because of the large transverse and longitudinal space charge forces at the design intensity.

There are no sextupole magnets in the synchrotron because it is best, from the standpoint of transverse instabilities, to operate with the natural values of the chromaticities (see Section 1.3). Within the range $\Delta p/p = \pm 6 \times 10^{-3}$, the chromaticities are almost constant, with $\Delta Q_v = -.027$, $\Delta Q_h = -.029$ for $\Delta p/p = 6 \times 10^{-3}$ and $\Delta Q_v = .028$, $\Delta Q_h = .03$ for $\Delta p/p = -6 \times 10^{-3}$. The absence of sextupoles leads to the requirement for continuous Q correction during the injection interval, when the instantaneous orbit moves from the inside edge to the centre of the aperture. The equivalent momentum error at the start of injection is $\Delta\tilde{p}/p = -18 \times 10^{-3}$ and injection continues until $\Delta\tilde{p}/p = 0$. The trim quadrupoles must be programmed in this interval to keep the Q-values constant. A stability requirement of ± 1% is set for the injection process, and this may be related to an equivalent tolerance for the regulation of the minimum value of the guide field in the synchrotron of ± 2 parts in 10^4.

A special RF shield is installed within each dipole magnet as described in Section 1.7 and the necessity for the shield is discussed in Section 1.3. Care will also be taken in the design of all components within the vacuum chamber so as to limit the electromagnetic coupling impedances between the beam and its environment.

To minimise beam loss in the synchrotron, and the resulting build up of radioactivity, there will be accurate RF beam control and closed orbit correction. Beam phase detectors, current monitors, envelope detectors and position

indicators will all be installed. Envelope detectors will be at orbit positions of both low and high dispersion to obtain estimates of the beam momentum spread during the cycle. Such information is important for optimising RF acceleration. For the closed orbit correction system there will be a position detector adjacent to each of the main quadrupoles.

TABLE 1.1: SYNCHROTRON PARAMETERS

Proton Design Intensity	2.5×10^{13} ppp
Maximum Proton Kinetic Energy	800 MeV
Injection Energy	70 MeV
Nominal Repetition Frequency	53 Hz
Injection Scheme	H^- charge exchange
Mean Radius of Synchrotron	26.0 m
Bending Radius of Dipoles	7.0028 m
Number of Superperiods	5
Length of Superperiod	3 x 10.89085 m
Number of Dipoles	10
Number of Main and Trim Quadrupoles	30 (each)
Number of Octupoles	5
Number of Skew Quadrupoles	2 or 5
Length of Dipole	4.4 m
Length of Main Quadrupole	0.6 m
Length of Trim/Skew Quadrupole	0.3 m
Dipole Field at 800 MeV	0.69700 T
Dipole Field at 70 MeV	0.17582 T
Tolerance on Minimum Dipole Field	± 2 parts in 10^4
Approximate Horizontal Betatron Tune, Q_h	4.2
Approximate Vertical Betatron Tune, Q_v	3.9 (or 3.4)
Horizontal Beam Emittance at 70 MeV (Area$\div\pi$)	950×10^{-6} rad m
Vertical Beam Emittance at 70 MeV (Area$\div\pi$)	535×10^{-6} rad m
Linac Beam Emittance (Area$\div\pi$)	60×10^{-6} rad m
Duration of Injection Interval	472 μs
Number of RF Cavities	4
Number of Acceleration Gaps/Cavity	3
Number of Vertical Fast Extraction Systems	1
Maximum β_v in Dipoles	7.24 m
Maximum β_v in Lattice	15.44 m
Maximum β_h in Dipoles	14.73 m
Maximum β_h in Lattice	18.77 m
Maximum α_p in Lattice	5.725 m
Gamma Transition γ_t	6.39

1.3 INTENSITY LIMITATIONS

The transverse space charge limit of the synchrotron is set by the design values of the injection energy, the magnet repetition frequency, the transverse acceptances, the momentum spread of the injected beam and the amplitude of the RF fields during the initial period of acceleration. The maximum bunching factors, $\bar{B}$, and hence the maximum limits, are obtained when the amplitude of the accelerating field is adjusted so as to just contain the longitudinal phase space area of the trapped beam.

A momentum spread of $\pm 1.2 \times 10^{-3}$ is assumed for the injected beam, and a longitudinal phase space area after trapping of 0.6 eV.s. The optimum voltage amplitude of the accelerating field is given in Fig 1.5, together with the resulting momentum spread and bunching factor. The peak momentum spread is approximately $\pm 5.4 \times 10^{-3}$. The estimates for the RF voltage include the effect, at peak intensity, of the longitudinal space charge forces within the bunch for a perfectly conducting chamber wall, but there is no allowance for inductive wall effects. Use of a larger RF voltage than that indicated will increase the momentum spread and decrease the bunching factor.

Maximum transverse space charge forces occur after approximately 1.25 ms of acceleration. The value of $\bar{B}$ is then 0.245 for uniform transverse beam density distributions. A space charge tune shift, $\Delta Q_v = 0.25$, is reached with the chosen transverse machine acceptances for a beam of 2.7×10^{13} protons.

It is possible to obtain an improved bunching factor by the use of RF acceleration systems where the basic system of harmonic number 1 is complemented by a second system operating on harmonic number 2, but the proposal and costing do not include this feature. One long straight section is free, however, for such a scheme.

The direction in which the operating point moves under the detuning effect of the transverse space charge forces is indicated by the dashed line in Fig 1.4. If the transverse beam density distributions are not uniform there will be increased space charge forces for a given intensity. Non-linear octupole components of the forces introduce a variation of the betatron tunes as a function of oscillation amplitude and also may excite fourth order resonances of the betatron motion. The space charge detuning moves the operating point away from the fourth-order coupling resonance $2Q_v - 2Q_h = 0$ but towards the resonance $4Q_v = 15$.

Preliminary studies indicate that partial compensation is possible for the transverse space charge forces that drive the $4Q_v = 15$ resonance, when the forces arise from a beam with a parabolic particle distribution. This is achieved by the use of the 5 octupole magnets in the lattice, all with equal strength and sign. A given value of octupole strength is adequate to cancel the relevant space charge excitation at the instant of maximum injected beam, but subsequently, as the beam is trapped and particles execute synchrotron oscillations, individual particles may repeatedly cross the resonance line and only partial compensation is achieved.

Transverse Instabilities

The octupole magnets not only provide partial compensation for the space charge excitation of the $4Q_v = 15$ resonance but also introduce an additional Q-spread in the beam to help combat transverse instabilities. The resulting stabilisation is commonly referred to as Landau damping.

The natural chromaticity of the lattice, $\xi = (\Delta Q/Q) \div (\Delta p/p)$, is approximately equal to - 1.2. This is the correct sign of the chromaticity to avoid the dipole mode of the bunched-beam transverse instability for an accelerator in which the proton energy lies below the transition energy of the lattice.

Theory for bunched-beam transverse instabilities has been given by Sacherer[7]. For acceleration from 70 MeV to 800 MeV, the protons have $\gamma << \gamma_t$ (gamma transition) so that the difference in phase, ψ, of the coherent betatron motion between the head and tail of the accelerated bunch is large:

$$\psi = wQ\xi\tau/(\gamma_t^{-2} - \gamma^{-2})$$

where w is the particle revolution frequency and
τ is the time duration of the bunch.

With the numerator and denominator in this expression both negative, ψ is positive, increasing from the value of + 17.5 radians at 70 MeV to + 27.5 radians at 800 MeV. Such values of ψ ensure that not only the m = 0 (dipole mode) of the bunched beam transverse instability is stable, but also that the m = 1 (quadrupole mode), m = 2 (sextupole mode) and m = 3 modes are stable[7].

Instability thresholds and growth rates are a function of the transverse electromagnetic coupling impedance between the beam and its environment. If the synchrotron operates with its natural values of chromaticity, only the higher order modes of the bunched-beam transverse instability should occur and these modes have reduced growth rates compared to that of a coasting unbunched beam. Thus the most stringent requirements, on the allowable transverse coupling impedances, arise not during acceleration but during the injection interval before the beam has become bunched.

The definition of the transverse coupling impedance, $Z_\perp$, is given together with a stability criterion for an unbunched circulating beam:

$$Z_\perp = j \int_0^{2\pi R} \frac{(E + v_\wedge B).ds}{\beta I \Delta}$$

$$|Z_\perp| < 2\pi E_o \gamma Q \mid \tilde{\Delta Q} \mid / Ne^2 c$$

$$\tilde{\Delta Q} = \tilde{\Delta Q}\,(\text{octupole}) + \frac{\Delta p}{p} \left[(n-Q)\,(\gamma^{-2} - \gamma_t^{-2}) - \xi Q \right]$$

where R is the mean radius of the synchrotron
s is measured along the beam orbit
v is the beam velocity (= βc)
I is the beam current
Δ is the coherent transverse beam displacement
B,E are the transverse magnetic and electric fields respectively at the position of the beam, due to the beam interaction with the surrounding environment
$E_o\gamma$ is the proton energy
N is the number of protons (assumed 4×10^{13} at injection)
e is the proton charge
c is the velocity of light
n is the number of wavelengths of the coherent motion in one circumference
$\tilde{\Delta Q}$ is the full Q-spread at the half maximum point of the beam distribution, and
$\Delta p/p$ is the full momentum spread at the half-width of the distribution.

At 70 MeV injection, if $\Delta\hat{Q}$ (octupole) = 0.01, $\frac{\Delta p}{p} = 1.2 \times 10^{-3}$ and $\xi = -1.2$:

$$\left| \frac{Z_\perp}{n} \right| < 12.5 \text{ k}\Omega/\text{m} \qquad \text{for n large}$$

$$\left| Z_\perp \right| < 200 \text{ k}\Omega/\text{m} \qquad \text{for } n = 4,\ Q_v = 3.9$$

Thus, to ensure the stability of the unbunched beam at modes of high n value, all resonant structures coupled to the beam must be adequately damped, with values of $|Z_\perp/n| < 12.5$ kΩ/m. The stability limit is also quoted for the low mode number n = 4. This is because the transverse coupling impedance will be a maximum at this mode for a resistive wall type of coupling impedance and for the chosen vertical Q-value of $Q_v = 3.9$.

For a resistive vacuum chamber wall, the transverse coupling impedance is related to a longitudinal coupling impedance, Z_{11}, by:

$$Z_\perp = 2c\ Z_{11}/b^2(n-Q)w$$

where b is the inner radius of the vacuum chamber wall (assumed .09m), $(n-Q)w$ is the angular frequency of the coherent mode defined by n, and $(4-Q_v)\ w/2\pi = 67.2$ kHz.

There would be no difficulty in meeting the stability criterion of $|Z_\perp| < 200$ kΩ/m at 67.2 kHz if the synchrotron had a conventional metallic vacuum chamber of wall thickness greater than the skin depth at this frequency. Estimates for such a stainless steel chamber give Z_{11} (67.2 kHz) $\sim$ 0.2 Ω or $Z_\perp$ (67.2 kHz) $\sim$ 36 kΩ/m.

However, because of the rapid-cycling nature of the synchrotron, it is not feasible to install such a solid metallic chamber within the main dipole magnets. Excessive eddy current heating and sextupole error fields would result. It is therefore planned to install an RF shield between the beam and the magnet laminations. Such a shield is described in section 1.7, and model measurements will be made to establish that the shields meet the stability requirement. Estimates indicate that Z_{11} would be very large if there were no shields present and if the magnet laminations were allowed to form the boundary of the machine aperture. The resistive component of Z_{11} (67.2 kHz) is estimated

TABLE 1.2: RF SYSTEM PARAMETERS

RF Harmonic Number	1
RF Frequency Range	0.6719 to 1.5448 MHz
Number of RF Cavities	4
Number of Acceleration Gaps/Cavity	3
Capacitive Load/Cavity	45,000 pF
Peak RF Voltage Amplitude/Turn	133 kV
Peak RF Power (4 stations)	910 kW
Peak Beam Loading Power	612 kW
Total number of Ferrite Toroids	640
Number of Bias Turns on Ferrite Resonators	2
Peak Bias Current	5000 A
Ferrite Specification:	
Ferrite Type	Ni - Zn
Outside Diameter of Toroid	500 ± 0.2 mm
Inside Diameter of Toroid	300 ± 0.2 mm
Thickness of Toroid	25 ± 0.1 mm
Concentricity of Cylindrical Surfaces	Within 0.2 mm
Parallelism of Plane Surfaces	Within 0.1 mm
Initial Incremental Permeability (μ)	250-450
Lower Limit of μ under DC Magnetisation	5
DC Magnetisation for $\mu = 5$	$\leq$ 10,000 A-t
Dielectric Constant	$<$ 25
Dielectric Loss Tangent at 1 MHz	$\leq$ 0.002
μQf Factor at 220 Gauss Peak RF Flux	$\geq 8\ 10^9$

1.5 MAGNET SYSTEM

The magnet parameters are given in Table 1.3. Magnet apertures are made as large as possible within the restriction that 800 MeV is not beyond the capability of the proposed power supply. The magnetic cycle (0.176 T to 0.697 T in the dipoles) is such that remanent and saturation effects are small. The magnet cores will be made from 0.5 mm thick laminations of high permeability steel, these being glued together and mounted on base plates. Excitation coils will be wound with stranded conductor, and indirectly cooled by means of tubes embedded in the insulation. The insulation itself will be glass cloth impregnated with radiation resistant epoxy resin.

Dipoles

Each of the 10 dipoles is 4.4 m long. The large sagitta of 0.34 m means that the magnets will have to be curved, being made from short, parallel-sided blocks with the inter-block wedges filled with part laminations. The good field region (where $\Delta B/B \lesssim 0.1\%$) is made up in the following way:

	Horizontal (mm)	Vertical (mm)
Betatron motion	241	126
Dispersion	19	0
Closed orbit distortion	10	10
RF shield	0	4
Totals	270	140

Shims will be used to keep the pole width, and hence the inductance, as small as possible. The end blocks will have flared apertures to prevent excessive eddy-current heating of the laminations. A cross-section of the dipole is shown in Fig 1.7(a).

Quadrupoles

The 15 F- and 15 D- quadrupoles are identical in all respects save that of polarity. Since they are powered in series with the dipoles, the integrated field gradients must match as closely as possible those required by the lattice design. This results in the minimum demands to be made upon the correction quadrupoles.

The good field region, in which $\Delta K/K$ is less than 0.8%, is 312 mm horizontally by 200 mm vertically. After allowing for extraction and the RF shield, the inscribed radius of the quadrupoles is set at 123.8 mm. In order to minimise the inductance, an asymmetric design has been chosen, illustrated in Fig 1.7(b).

Correction Elements

Small trim quadrupoles will be adjacent to each of the 30 main quadrupoles. They allow the Q-values to be varied by approximately ± 0.3, and will be designed to be compatible with the power supplies developed for the NINA trim quadrupoles. Because their length (0.3 m) is comparable with the beam dimensions, the pole profiles will be modified to take account of end effects.

Symmetrically placed round the machine (in the 2.9 m straight sections) will be 5 octupoles. These are 0.25 m long, and have a constant third derivative field of 40 T m^{-3}, sufficient for the purpose of Landau damping. In the same straight sections up to 5 skew quadrupoles will be introduced to eliminate any coupling effects due to the $Q_h + Q_v = 8$ resonance. These will be identical to the trim quadrupoles mentioned above. Means for correcting closed orbit errors, important for reducing beam loss and for extraction, will also be provided.

General

Even though beam loss will be kept to the minimum, the components of the machine will be subject to considerable radiation fields. Insulators, and particularly the magnet coils, will be very vulnerable to damage from this source. The greatest care will therefore be taken in the choice of materials and in manufacturing technique. If a magnet should fail, it will be quickly removed and replaced with a spare. In the cost estimate there is provision for 2 spare dipoles and 4 spare quadrupoles plus additional spare coils.

TABLE 1.3: MAGNET PARAMETERS

General		
	DC current	682 A
	Peak AC current	407 A
	RMS current	740 A
	Current density	2.0 A mm^{-2}
Dipoles		
	Number of turns	72
	Gap height	0.14 m
	Peak field	0.697 T
	Resistance	0.039 Ω
	Inductance	0.09 H
	I^2R loss	21.4 kW
	Hysteresis loss	10.0 kW
	Core weight	15.5 tonnes
	Core dimensions	1.02 x 0.65 x 4.4 m^3
Quadrupoles		
	Number of turns/pole	22
	Inscribed radius	0.1238 m
	Peak field gradient	3.93 T m^{-1}
	Resistance	0.012 Ω
	Inductance	0.0144 H
	I^2R loss	6.5 kW
	Hysteresis loss	1.3 kW
	Core weight	2.1 tonnes
	Core dimensions	0.974 x 0.864 x 0.6 m^3

1.6 MAGNET POWER SUPPLIES

Resonant Magnet Network

The synchrotron magnets will be sinusoidally excited at a nominal frequency of 53 Hz in a distributed resonant circuit. DC bias will be added to the AC waveform in order to obtain the field conditions necessary for injection, giving a time variation of magnet current of the form:

$$I_M = I_{DC} - I_{AC} \cos wt$$

where w = accelerator angular repetition frequency.

The use of a biased waveform rather than pure AC excitation has the well recognised advantages of an increased sinusoidal duty cycle, reduced dB/dt at injection, lower AC circuit losses and reduced RF accelerating voltages.

The resonant circuit, which is based upon that of the NINA accelerator, is shown in Fig 1.8 and consists of a series arrangement of magnet groups, each connected to the next via one winding of a central energy storage choke. In parallel with each choke winding is a capacitor bank designed to resonate the whole network at the chosen machine frequency. One winding of the choke is split for circuit earthing and to provide a connection point for the DC bias power supply.

Auxiliary windings on the energy storage choke allow the injection of energy to make up AC losses. The total input power to the system at 50 Hz is estimated at 1300 kW which is comfortably within the ratings of existing site supplies.

Magnet parameters have been selected to allow the main components of the existing NINA resonant power supply[8] to be adapted to drive the new synchrotron. This, taken together with the proposed extensive re-use of site power distribution equipment and services, will result in a considerable saving in power supply costs. A resonant configuration matching the NINA power supply requirements will be achieved by grouping the 40 SNS magnets into 10 sectors, each having 3 quadrupoles and 1 dipole. Typical ratings are given in Table 1.4. With this grouping, and the simple series connection of magnets illustrated, the distribution of magnet types within the group potential gradient alternates from sector to sector. This leads to variations in

capacitive earth leakage effects. The connection sequence ultimately chosen will therefore aim to equalise, as far as is possible, the operating voltage conditions for magnets of a given type. Steps will also be taken to compensate for the stray capacitances associated with connecting cables and the major network components.

The NINA synchrotron is at present powered in a self-resonant mode at 53 Hz. Although it would be possible for the SNS to run at this frequency, it is believed that line frequency operation at a nominal 50 Hz could offer considerable advantages in both RF power supply costs and in the reduction of accelerator/line beat frequency effects. The possibility of adapting the NINA power supply to allow line locked operation, while retaining the free running option for diagnostic purposes, is currently under investigation.

Programmable Trim Supplies

For the precise control of machine Q-values necessary throughout the injection and acceleration cycle, a system of 30 programmable quadrupoles will be provided. The computer controlled power supplies required to drive these magnets will be based upon the PQ power supplies designed at Daresbury Laboratory by J B Lyall[9]. A typical magnet/power supply layout is given in Fig 1.8, the number of magnets per power supply being determined by drive waveform requirements and magnet constants.

Power supply output waveforms will be calculated by computer from a knowledge of machine and magnet parameters. Each waveform will be stored as 500 ordinates in a microprocessor/DAC system capable of reproducing the waveform as an analogue reference at accelerator frequency. The power supplies will then amplify this low level reference signal to a maximum of 300V for application to the trim magnets. Circuit control will be achieved by comparison of the voltage developed by auxiliary windings on the trim magnets with the incoming reference signals.

Each power supply will contain an energy storage inductor from which energy will be transferred, during the acceleration period, to capacitors and thence to the trim magnet. The transfer is controlled by transistor switching banks. During the remainder of the cycle, most of this energy can be returned to the inductor by a similar process, thus limiting input energy requirements to the make up of system losses.

TABLE 1.5: VACUUM SYSTEM PARAMETERS

Pressure	$< 5 \times 10^{-7}$ Torr
High Vacuum Pumps	
12" Oil Diffusion Pumps:-	
Number	32
Nominal Speed (air)	4000 $\ell\ s^{-1}$
Nominal Speed with liquid nitrogen trap and baffle.	800 $\ell\ s^{-1}$
12" Liquid Nitrogen Traps	
Number	32
Nominal Speed (water vapour)	7000 $\ell\ s^{-1}$
Roughing and Backing Pumps	
Combination Roots and rotary mechanical pumps:	
Number	3
Nominal Speed (air)	500 $\ell\ s^{-1}$

1.8 INJECTION SYSTEM

The full accelerated beam intensity of 2.5×10^{13} protons per pulse corresponds to a circulating current of 2.69 A at the injection energy of 70 MeV. To accumulate such a large current, H^- stripping injection is proposed. This method of charge exchange at injection by the use of a stripping foil, or a gas jet, removes the acceptance limitation of normal multi-turn injection and the accumulated beam is limited only by space charge and instability effects in the magnet ring. Charge exchange injection has been successfully demonstrated at INP (Novosibirsk) and at ANL.

Nimrod 70 MeV Injector

The new Nimrod 70 MeV injector linac, recently commissioned as a proton accelerator, will be modified to provide a 20 mA H^- beam in approximately 470 μs pulses at 53 Hz. (The linac has already accelerated twice this intensity as proton beam current). The modifications required are:

a. Installation of an H^- ion source able to deliver up to 40 mA.
b. A polarity change for the voltage of the pre-injector.
c. Uprating the RF modulators from the present 1.0 Hz operation to 53 Hz.
d. Uprating the cooling plant for the linac tanks.
e. Installation of new drift tubes in Tank 1 with DC powered quadrupoles.
f. Additional shielding.

The H^- ion source will be of the hollow discharge duoplasmatron type, incorporating caesium to enhance the negative ion yield, and similar to that under investigation at BNL. All other major components remain unchanged, including the beam transfer line between the linac and the entrance to the Nimrod Magnet Hall.

70 MeV Beam Transport Line

The beam transport line from Magnet Hall entrance to the injection point in the lattice is shown schematically in Fig 1.9. All the components exist at the Rutherford Laboratory. The beam from the linac is 0.685 m above the median plane of the machine and is brought to the correct height by 2 vertical bending magnets (Nimrod Type III magnets[23]) spaced 5 m apart. Horizontal bends of $+ 22^{\circ}$ and $- 25^{\circ}$ at 5 and 15.5 m from the Magnet Hall entrance direct the beam into a septum magnet which steers it into the machine. Eight quadrupoles are used to give a beam of the correct transverse dimensions at the location of the stripping foil, where dispersion effects are required to be minimal.

Injection into the Synchrotron

The ideal location of the H^- stripper is one which:

a. provides as uniform a filling of the transverse phase space as possible;
b. maximises the duration of the injection interval.

The input H^- beam emittance (area $\div \pi$) is assumed to be the same as the linac proton emittance, 60×10^{-6} rad m, and is much smaller than either transverse acceptance of the synchrotron. In the vertical plane the input beam is appropriately mismatched so that successive turns fill up the acceptance area. As the circulating current increases, so do the transverse space charge forces. These are larger in the vertical plane than in the horizontal, but will be enhanced in both if there is not uniform filling in each plane.

The ring magnetic field varies sinusoidally with time (period 18.87 ms). Injection is from the inside of the ring as the guide field decreases from a given value to its minimum, 0.17582 T, after which RF trapping and acceleration begin. The instant at which injection may start is set by the input beam characteristics, the horizontal acceptance of the machine, the values of the lattice functions and the stripping foil location. The acceptance limitation for protons is set after acceleration has started. The incoming H^- beam has an equivalent negative momentum error which reduces to zero by the end of injection. Studies indicate a maximum time interval for injection of 470 μs, with an initial equivalent momentum error $\Delta\tilde{p}/p = -18 \times 10^{-3}$.

The stripping foil is situated between the quadrupole doublets of a long straight section. The centre of the incoming H^- beam is aligned to strike the foil in the direction of a specific off-momentum particle's closed orbit, whose $\Delta p/p$ value equals the value of $\Delta\tilde{p}/p$ at the start of injection. The relative merits of 2 alternative injection schemes are currently being assessed. In the first scheme 3 steering magnets (marked as CO in the injected beam line schematic, Fig 1.9) are used to create a suitable horizontal closed orbit bump, and the centre unit of the 3 provides the required separation between the incoming H^- beam and the proton beam circulating in the ring. In the second scheme, there is no orbit bump and injection is ahead of the upstream doublet of the straight to give the necessary separation. Both schemes employ an injection septum magnet. An example of a horizontal phase plane plot for the beam at a stripper azimuth is given in Fig 1.9(a).

During the injection interval, use will be made of the lattice trim quadrupoles to give constant values of the horizontal and vertical Q-values. As injection commences with $\Delta\tilde{p}/p = -18 \times 10^{-3}$, there is need for the corrections to prevent associated Q-shifts of approximately + 0.09.

Stripping Mechanism

The stripping mechanism will be a foil mounted from the edge of a circular disk rotating at the machine repetition frequency. The disk is driven by a synchronous motor so that the foil is seen by the incoming beam for a precise interval of time.

The stripping material must have a low atomic number to reduce the effects of multiple scattering. It must be self-supporting when held on just one side, it must not melt or decompose from heating due to energy loss during the traversals of the beam and its tensile strength must last for a reasonable time, of the order of 8 hours. Calculations show that 262 $\mu g.cm^{-2}$ of carbon are sufficient to strip 99% of the H^- ions to protons, and the carbon will be used in the form of polyparaxylene foils. Radiative cooling is sufficient to limit the temperature to well below the melting point. Loss of material by evaporation and nuclear interaction is roughly 3% per 24 hours.

Also under consideration is the use of a stationary foil system, in which case the circulating beam is removed from the foil region by reducing the closed orbit bump to zero in a short time interval after H^- injection has ceased.

1.9 EXTRACTION SYSTEM AND EXTRACTED BEAM LINE

The Extraction System

The 'missing magnet' lattice allows the possibility of extraction in a single long straight. At full energy the vertical and horizontal emittances (area $\div \pi$) are $E_v = 270 \times 10^{-6}$ and $E_h = 475 \times 10^{-6}$ rad m (ie $E_v/E_h \sim 0.56$). This, and inspection of the lattice dynamic functions at possible kicker and septum locations (see Fig 1.3) suggest that:

a. Vertical extraction is used.

b. A full aperture fast kicker and large aperture septum magnet(s) are required.

The extraction system consists of a single fast kicker magnet 1.4 m long, with centre located 1.3 m from the neighbouring machine dipole, and 2 septum magnets centred 2.2 m upstream of the trim quadrupole T_1 at the end of the extraction region. The phase difference of the vertical betatron motion between the kicker magnet and the centre line of the septum magnets is $\pi/2$. Beyond the septum magnets the beam is transported over the machine and then brought down to standard height (1.905 m) prior to transport to Experimental Hall 3 and the target station. Fig 1.10 shows a schematic of the extraction system, also of the vertical beam position. The parameters of the components of the extraction system are given in Table 1.6.

Since the synchrotron is rapid-cycling, critical components of the extraction system (particularly the thyratron switches) must operate well within their maximum ratings to ensure adequate lifetime.

Fast Kicker Magnet

At 800 MeV full energy the circulation time is 650 ns. The bunch length is expected to be 90^o, but an allowance for 120^o is made, hence the required kicker rise time is 432 ns. The kicker magnet must produce a deflection of 14.2 mrad to lift the beam 114 mm into the septum magnet and this is obtained by a field of 4.95×10^{-2} T over an actual length of 1.4 m. The magnet aperture is determined only by the beam size at injection and no allowance for sagitta is required since the beam dimensions reduce by a factor roughly $\sqrt{2}$ at full energy: hence the gap width is 160 mm and height 175 mm. The kicker magnet itself will be of the ferrite-loaded, delay line type, mounted in a vacuum chamber 1.8 m long. The magnet is split vertically into two halves or 'modules', each module being excited

through a single turn winding. Each module is split into sections, of number determined by the rise time and characteristic impedance. With the rise time set at 430 ns a 14-section module has a characteristic impedance conveniently equal to 10 Ω. The major advantage of this type of kicker magnet is that each module is driven through a single thyratron switch. The switches are electrically separate and possible magnetic coupling has been found to be very small. The excitation current is half that of an equivalent full aperture magnet, but the inductance is doubled. The V-A rating per module is well within the specification of known thyratron switch tubes, so a good lifetime performance can be expected. The main disadvantage is the complexity of a sectionalised magnet requiring many high voltage feed-through capacitors. However, an alternative lumped element magnet, which retains the required pulse characteristics, is possible and will be investigated.

Septum Magnet

The septum magnet must deflect the beam through an angle large enough to clear the machine components immediately downstream, the actual angle depending on the components in the extracted beam line. It is proposed to use an existing Nimrod Type II dipole as the vertical bending magnet located over the machine main dipole, as can be seen in Fig 1.10, and this requires a deflection angle of 12.9° (total angle 13.73° to the plane of the machine). The septum magnet must have a field of 0.63 T over an effective length of 1.75 m. The aperture to contain the 800 MeV beam is w = 110 mm, h = 115 mm. The required performance is best obtained by using a combination of a short thin septum magnet (thickness t = 10 mm, N = 12 turns) and a thick septum magnet. The lengths of the two magnets, and t and N for the second, are determined by the need to keep the thick septum clear of the circulating beam and the need to minimise the total power consumption. The lengths of the two magnets are respectively 0.65 m and 1.1 m, and in the second magnet t = 30 mm, N = 36. Both magnets will use standard (nominal 10 mm square) water-cooled conductor and total power consumption is expected to be 202 kW. The specifications for the two septum magnets S_1 and S_2 are given in Table 1.6.

Extracted Beam Line

After extraction the beam is transported over the main ring and is then bent vertically into the standard horizontal plane for Nimrod components of 1.905 m height above floor level. A 3° horizontal bend at the entrance to Tunnel 8 (see Fig 1.1) gives the beam its final direction towards the target in Experimental Hall 3. Inside Tunnel 8 the beam is matched into a periodic FODO structure, and close to the target, the beam is again matched to yield the required spot size.

Apart from two Daresbury large aperture quadrupoles used near the target, all the magnets and quadrupoles, and their power supplies, already exist at the Rutherford Laboratory.

Fig 1.10 shows schematically the extracted beam line components close to the main ring. A Type II dipole is located 1.9 m above the plane of the main ring and bends the beam vertically through - 25^{o}; a Type I dipole bends the beam through 11.27^{o} into the horizontal direction. On either side of the Type II dipole is a pair of Type III quadrupoles to confine the beam within the aperture of a standard (197 mm diameter) beam pipe. The horizontal bend required to direct the beam into Tunnel 8 to Hall 3 is provided by a Type I or Type IV dipole. Some simplification of this system may be possible by using Type X dipoles in place of the vertical bending magnets. Following the horizontal bend into Tunnel 8, four quadrupoles, equally spaced with 3 m drift lengths, match the beam into the FODO structure of the beam line in Hall 3.

The matched periodic FODO structure uses equally spaced quadrupoles, with drift length 3.6 m. The unit FODO cell occupies 8.64 m and provides a phase advance of 72^{o} in both horizontal and vertical planes. There are 6 such cells in the complete beam line. The beam envelope size is ± 92 mm horizontally, ± 34 mm vertically at the centre of an F quadrupole, and respectively ± 48 mm, ± 65 mm in the centre of a D element.

The required spot size at the target is 70 mm (h) by 50 mm (v). The shielding immediately before the target is 4-5 m thick and must be free of beam transport elements. To meet these constraints there is a 16 m long matching section at the end of the FODO structure, requiring the use of 2 large aperture quadrupoles. The Daresbury Type 35 quadrupoles would be adequate for this purpose. Fig 1.11 shows schematically the extracted beam line in Experimental Hall 3, with the last of the 6 FODO unit cells and the matching system to the target spot size. Also shown are the horizontal and vertical beam profiles.

TABLE 1.6: EXTRACTION SYSTEM PARAMETER LIST (800 MeV)

KICKER MAGNET

Angular Deflection	$\Delta\Theta$	14.2	mrad
Magnetic Field	B	4.951×10^{-2}	T
Length	ℓ	1.4	m
Gap Height	h	175	mm
Gap Width	w	160	mm
Sagitta	s	0	
Rise Time	τ	0.43	μs
Number of Modules (of gap $\frac{1}{2}$h)		2	
Length per Module		1.4	m
Number of Sections	n	14	
Characteristic Impedance	Z_o	10	Ω
Excitation Current (single turn/module)	I	3.45×10^{3}	A
Charging Voltage	(2V)	68.9	kV
Pulse Duration		0.65	μs
Mean Dissipation per Module Load Resistor		4.1	kW

SEPTUM MAGNETS

		S_1	S_2	
Deflection Angle	Θ	4.803	8.128	deg
Magnetic Field	B	0.6295	0.6295	T
Length	$L_{1,2}$	0.65	1.1	m
Bending Radius	ρ	7.7535	7.7535	m
Gap Height	h	115	115	mm
Gap Width	w	110	110	mm
Septum Thickness	t	10	30	mm
Number of Turns	N	12	36	
Current	I	4.801×10^{3}	1.600×10^{3}	A
Current Density		72.0	24.0	A mm^{-2}
Inductance	L	1.125×10^{-4}	17.136×10^{-4}	H
Voltage (DC)	V	28.30	47.71	V
Dissipation	P	135.9	66.8	kW

1.10 CONTROL SYSTEM

The computer control system for the SNS has several roles to play, namely: the control of major sub-systems, both for stand-alone operation and as part of the complete system; the integration of the sub-systems into a coherent whole and the provision of a sophisticated operator interface. A schematic layout of the system is shown in Fig 1.12. Separate computers will be used for each of the sub-systems shown, while a larger central computer will be responsible for the system integration, maintenance of the central library, console service duties and any large computations required. The central computer will be assisted, in its operator interface work, by a comprehensive graphics system. Apart from peripherals, specific to the computers, the SNS equipment will be interfaced through CAMAC. The computer data-link system will use serial transmission at about 20 kBaud and have CAMAC terminal modules.

The software system will be based on the use of a control language interpreter, a technique pioneered at Rutherford Laboratory and used successfully at the CERN SPS. All application level programs will be written in a high level control language. Hardware control subroutines and time-critical routines will be written in assembler code. The whole system will have true distributed processing capabilities.

Because the synchrotron will be rapid-cycling, it will be necessary to restrict fast closed-loop controls (ie where time constants less than the machine cycle time of approx. 20 ms are involved) to individual computers. Much of the control therefore will be of the "set point" or "supervisory" type. All equipment will have normal hardwired interlocks which are monitored by the computer system.

Since the control system for the 70 MeV injector was conceived with computer involvement in mind and it already uses CAMAC, comparatively little modification will be required for the SNS. The scope of the existing system will be extended to include vacuum monitoring, additional beam line diagnostics and interfacing of the beam line and injection controls.

Normal control facilities for the four RF stations will be provided through a single computer, which will also handle the correction magnet supplies. A particularly attractive feature of this arrangement is that most of the time-dependent (or rather B-dependent) control facilities can be brought together. To alleviate the I/O load on this computer, extensive use will be made of micro-computer function generators for the programmed correction magnet power supplies.

Although they are numerous and widely distributed around the machine, the control requirements of the vacuum system are fairly simple. Similarly widespread are the monitoring requirements for general alarms, water and other services. While special electronics involving sample and hold circuits, analogue and digital processing will be used for the beam monitoring systems, the control/monitoring requirements will not be dissimilar to those of the vacuum and alarm systems. It is convenient therefore to handle all three of these subsystems together in one computer, with a serial CAMAC system providing the required long distance data path.

Separate computer(s) will be used for the highly important job of controlling and monitoring the target station(s) and beam line(s). The required rapid acquisition of target data will be the responsibility of "mini data loggers" controlled by micro computers.

In addition to the graphics hardware, previously mentioned, the operator consoles will employ special devices such as computer controlled knobs, tracker balls and touch screens. Much information will be presented to the machine operators through TV displays and the system will include the use of colour. Signal display will be on conventional oscilloscopes with signals routed via a distributed switching matrix.

Because of its very nature, the controls for the main ring resonant power supply are few. The present proposal is based on the use of the existing NINA power supply which has an acceptable manual control system. This will be used with little modification other than the addition of status monitoring by the central control computer.

For a number of reasons, including the re-use of existing equipment, greater back-up safety etc, the radiation monitoring and access control system will be separate from the computers but will supply information to the rest of the control system for display and logging purposes. Both the main power supply controls and radiation access equipment will be housed in racks in the main control room, to be built in the present Nimrod 15 MeV Injector building. This is at the centre of gravity of the new accelerator and target station, giving minimum lengths of control cables and freeing the existing, over-large Nimrod control room for other use.

CHAPTER 2: TARGET STATION

2.1 INTRODUCTION

The complete SNS target assembly consists of the target, the moderators and the shielding. These components are clearly interrelated and must be considered concurrently in the overall design. Some aspects, however, are still in the early stages of analysis, so the discussion of the moderator arrangements is given separately in Chapter 4. The target has been chosen bearing in mind as far as possible the requirements of the other components, but some of the performance parameters should be regarded as preliminary until the detailed studies are complete.

The proposed target material is depleted Uranium 238. This material has been chosen since it gives a neutron yield twice that of non-fissile heavy metals. In the context of neutron facilities this factor of 2 represents a significant advantage. The technical problems associated with spent targets, containing active fission products, are within existing active handling experience. All handling and disposal will be within the appropriate codes of practice.

2.2 TARGET MATERIAL, NEUTRON YIELD AND HEAT DEPOSITION

Of the possible target materials it is proposed to use Uranium 238. The gross yield of neutrons from uranium is roughly double that of a normal heavy target metal, for example lead or tungsten, the increased production being due both to fissions that occur in the interactions with primary protons and cascade nucleons, and to fast fission by the evaporation neutrons. The use of uranium, however, brings several technological problems which are discussed in the following paragraphs. The heat of production per neutron is roughly twice that in heavy metals, so heat removal is more difficult. Uranium is chemically active, especially at elevated temperatures, so cladding must be provided which has high corrosion resistance to the coolant. Also uranium suffers from radiation damage effects which manifest themselves in several ways and which set the limit to the target lifetime. Nevertheless, the increased neutron yield makes it worthwhile obtaining solutions to these problems, many of which are available from reactor technology. Other materials will continue to be studied and indeed a 'back-up' target based on a non-fissile heavy metal, eg tungsten, will be designed.

Estimates of yield of neutrons from ^{238}U with incident 800 MeV protons vary between 35 n/p[10] and about 26 n/p[11,12] for thick targets, whilst measurements on thick targets[13] have given 32 n/p. For the proposed target the following values are used as a basis for the design:

800 MeV protons: Yield 30 n/p Heat of Production 55 MeV/n

For an incident proton beam of intensity 3×10^{13} ppp, 53 pps there will be:

Gross Yield 4.8×10^{16} n/s Mean Target Heating 420.3 kW

The yield assumes a higher input proton intensity than given elsewhere in this proposal, to anticipate future improvements in the synchrotron performance and/or to give a safety margin. The target power includes heating from the beam and from exothermic reactions (eg fast fission in the uranium).

The target will be about 300 mm long and will be divided into clad plates separated by cooling channels. The overall length corresponds to 1 range-length of 800 MeV protons in ^{238}U; the effect on the gross yield due to the cladding and cooling channels will be small, but the source length is increased. The distribution of neutrons and heat deposition may be obtained from the experimental data[11] and the range-energy relations in ^{238}U. The results can be

seen in Figs 2.1 (a) and 2.1 (b). The peaks in both curves are expected to occur about 30 mm (ie $\sim$ 1 beam radius) into the target, having values of 2.6 n p^{-1} cm^{-1} and energy deposit 150 MeV p^{-1} cm^{-1} for incident 800 MeV protons. Beyond the peaks the curves decrease as exp $(-x/\lambda)$ where $\lambda \sim 12.3$ cm corresponds to the nucleon mean free path in ^{238}U over the energy range 800-250 MeV. At the ends of the target there is fall-off because of the loss of neutrons through the ends. Computed data[12] indicates that some 90% of the neutrons are produced within the beam diameter and that the most probable energy of the escaping neutrons is not 2-3 MeV as would be expected from an evaporation/fission spectrum, but about 0.2 MeV due to degradation by neutron inelastic and multiple production processes.

2.3 TARGET COOLING

Because of the poor thermal properties of uranium, the target must be segmented to remove the total 420 kW dissipation and it will consist of a number of plates cooled by parallel flow through narrow cooling channels. Fig 2.2 shows a possible geometry of the target. The thickness and number of plates depend on:

a. The type of coolant used.
b. The maximum acceptable temperature in the uranium; and
c. The temperature distribution within a plate.

For this target, with its modest total power and heat flux, cooling by nucleate boiling of water is proposed, which is technically simpler and less costly than liquid metal cooling. Cladding of the uranium is necessary and Zircaloy-2 (thickness 0.25 mm) will be used, which bonds well, has low neutron absorption cross-section and high corrosion resistance to water. For reasons to be discussed in Section 2.4, the maximum temperature in the uranium is limited to 600°C, but the minimum (at the interface between the uranium and the Zircaloy-2 cladding) depends on the axial position of the plate in the target and varies between about 300°C and 220°C.

Fig 2.3 shows the maximum uranium thickness in the plates against axial position in the target for an input proton beam of spot size 50 mm (v) by 70 mm (h) after transport from the synchrotron. The proton beam is assumed to have a parabolic intensity distribution, ie where the peak intensity is 1.5 times greater than the equivalent uniformly charged beam. Other data are given in the Figure and Table 2.1: in particular, the thermodynamic values have been taken from known data[14] on nucleate boiling as readily achievable in a practical system. The maximum steady state heat flux is not more than 80% of 'burn-out' flux at which film boiling could occur. The cooling channels have been chosen to be 2 mm wide to guard against boiling proximity effects and to minimize problems of plate buckling and radiation swelling. Each channel will be fed and monitored individually to ensure its integrity. However some simplification of this arrangement and cost saving can be obtained by grouping the plates into 3 or 4 batches of constant thickness; also by batching the cooling feeds.

The pulse behaviour of the plates has also been analysed. The plate temperatures remain close to the steady state values, varying by less than ± 10° during the 0.2 μs energy input pulse. The heat flux is a maximum immediately after the pulse, due to heat release from close to the surface of the Zircaloy-2 cladding. Apart from a small peak after about 4 ms, the heat flux is roughly constant due to the poor thermal diffusivity of both uranium and Zircaloy-2.

2.4 RADIATION EFFECTS ON THE TARGET

The maximum temperature of the uranium is set at 600°C, being below the α-β phase transition temperature of 660°C at which large thermal cycling growth can occur. The minimum temperature should ideally be well above 300°C. Below this temperature, uranium in the α-phase experiences under neutron bombardment large radiation growth. There is rapid elongation of the crystal in a preferred direction, but no volume change. Elongation growth factors, G, of several hundred are possible. This problem can be alleviated by 'normalising' the uranium, ie by heating above 800°C (into the γ-phase) and rapidly quenching to produce a polycrystalline material, giving G less than unity. Thermal cycling growth can also occur in the α-phase, but because of the relatively small temperature changes during the pulse, this is not expected to be serious. In addition to these non-volume growth effects, irradiation swelling can also occur due to several causes, with an accompanying true volume change:

a. Solid fission product swelling, producing a volume increase of 0.2% per 0.1% burn-up of fissionable atoms (since there are two atoms from each fissioned ^{238}U atom). This volume increase is independent of temperature and is inexorable; it forms a lower limit to the volume change expected.

b. Cavitation swelling is the formation of voids due in part to mechanical straining during an irradiation of a polycrystal. This is the most serious form of swelling, the maximum rate occurring at about 425°C. Cavitation swelling can be reduced by an order of magnitude to a 2% maximum per 0.1% burn-up by 'adjusting' the ^{238}U, ie alloying with carbon, aluminium and iron (total about 3000 ppm).

c. Stress-free bubble swelling, due to the formation of bubbles of the inert gases xenon and krypton which constitute 10-15% of the fission product atoms. This effect increases with temperature, but in the present range has an average value 0.35% per 0.1% burn-up.

The sum of the above effects leads to a 7.5% volume change for 0.6% burn-up of fissionable atoms. These figures allow an estimate of the target lifetime to be made. An uncorrected cooling gap closure of 0.5 mm corresponds to a volume change of about 9%, ie little more than 0.6% burn-up (the dominant cavitation swelling is non-linear beyond 0.5% burn-up). With an input beam of 2.5×10^{13} ppp and assuming a multiplicity of neutron production of 2, then at the axial peak 1.7×10^{15} nuclei/s are destroyed. This leads to a minimum target lifetime of

about 8 weeks, which may be extended by a factor 2 by:

a. optimising the swelling resistance by selection of the 'adjusted' uranium;

b. bowing the plates; and

c. controlling the gross movement of the target.

Thus the target is expected to have a useful lifetime, but must be considered expendable.

example, replacing the parallel flow cooling channels by a single baffled reversible flow system requires a pressure drop 12 times greater than the simple hydrostatic pressure. Further, the risk of neutronic coupling (cross-talk) between moderators is increased, with consequent degradation of the pulse characteristics from the moderators, especially at epithermal energies. Thus, at this stage, a horizontal target is preferred on cost and technical grounds.

TABLE 2.1: STEADY STATE THERMODYNAMIC PARAMETERS FOR TARGET

Proton Intensity for Target Design		1.59×10^{15}	pps
Beam Size at Target	vertical	50	mm
	horizontal	70	mm
Total Heat Deposit in Target		4.203×10^{5}	W
Range of 800 MeV Protons	^{238}U	253.3	mm
	Zr	577	mm
	H_2O	0.235	m
Thermal Conductivity	k_u	0.34	$W\ cm^{-1}\ {}^{o}C^{-1}$
	k_z	0.119	$W\ cm^{-1}\ {}^{o}C^{-1}$
Thickness of Zr-2 Cladding	t_z	0.25	mm
Width of Water Channel	t	2	mm
Target Plate Cross-Section (Nominal)		80 x 80	mm x mm
Maximum (centre line) Uranium Temperature	T_u	600	^{o}C
Water Saturation Temperature	T_{sat}	131	^{o}C
Hydrostatic Pressure	P	40	psia
Maximum Heat Flux in Target	q	644.5	$W\ cm^{-2}$
Water Flow in Channel		12.127	$m\ s^{-1}$
Water Bulk Temperature		48	^{o}C
Sub-Cooled Water Temperature Difference	ΔT_{sub}	83	^{o}C
Corresponding Burn-out Flux	$q_{b.o.}$	800	$W\ cm^{-2}$
Gross Water Flow		33.35	$\ell\ s^{-1}$
Gross Temperature Difference	ΔT_{bulk}	3	^{o}C

CHAPTER 3: SHIELDING, RADIOACTIVITY AND RADIATION DAMAGE

3.1 INTRODUCTION

The recommendations of the International Commission on Radiological Protection (ICRP) provide the primary standards for protection against ionising radiations. These form the basis of national codes of practice and legislation which must be observed in the design and operation of the SNS. Consultations will be held with the Health and Safety Executive and the Radiochemical Inspectorate on all aspects of the facility relevant to radiation protection. No particularly difficult problems not already met in other reactors have been identified.

Target Cooling

Direct activation of pure water will produce the spallation products of oxygen, of which only tritium (12 years) and ^{7}Be (53 days) will be significant after a few hours decay. Estimates give yields of the order of 0.1 curie of tritium and 1 curie of ^{7}Be per day. The target design will minimise activity due to corrosion of other active material and from the activation of impurities.

Ideally, the primary coolant would be in a closed, sealed circuit. However, the radiolysis of water will lead to the evolution of hydrogen (contaminated with tritium), a build-up of corrosive peroxides and a consequent loss in volume (possibly 1 litre per day). Provision will therefore be made for gas venting, make-up and bleed-off points, all suitably protected against the spread of contamination. For the early detection of abnormal radioactivity, use will be made either of a sophisticated gamma spectrometry system, or, if it proves adequate, a simple NaI detector with a low energy cut-off.

Environmental Radioactivity

a. Air

The radiation exposure from the air surrounding the synchrotron will be much smaller than that from the solid objects exposed to the same radiation field. Despite this fact, a delay will be introduced for the short-lived elements in the air to decay, before the air will be discharged to the external atmosphere and personnel are allowed to enter the accelerator areas. Filtration is not necessary except in the target enclosure, for which special provision will be made.

b. Ground Water

This problem was studied for a chalk site (not Chilton) during the 300 GeV SPS design study[19]. Activity in the ground water near the accelerator arises either directly by the spallation of oxygen or by leaching out from irradiated solid material. It was concluded that tritium would be the most significant activity, especially after a long time, but also that the contamination level would always lie well within acceptable limits. The SNS is not expected to produce higher levels than would have occurred with the SPS.

Control of Induced Activity

A beam loss monitor system around the synchrotron ring and the external beam line will provide relevant information for machine operators to assess synchrotron performance and make estimates of induced activity levels. This system will be

based on a suitably designed ionisation chamber. It must operate without saturation at high dose rates and be resistant to radiation damage.

REFERENCES

1. J R J Bennett et al: 'A High Intensity, 53 Hz, 800 MeV Proton Synchrotron'. RL Report, RL-75-189 (Dec 75).

2. G H Rees: 'Possible Use of Beam Line Magnets to Build a Stretcher Ring for a 10% Long Duty-Cycle Proton Beam from the SNS'. RL Int. Note SNS/MC/6 (June 76).

3. G H Rees, A Carne & D R Perry: 'Progress Reports on Synchrotron, Shielding and Target Station', RL Int. Note SNS/MC/3 (May 76).

4. G H Rees: 'Synchrotron Lattice with Trim Quadrupoles', RL Int. Note SNS/MC/4 (June 76).

5. A Carne: 'Extraction from the 800 MeV, 53 Hz Synchrotron'. RL Int. Note SNS/MC/5 (July 76).

6. F J Sacherer: 'A Longitudinal Stability Criterion for Bunched Beams'. Proc. 1973 Particle Accel. Conf., IEEE Trans. Nucl. Sc. NS-20, No.3, 825 (1973).

7. F J Sacherer: 'Transverse Bunched Beam Instabilities - Theory'. Proc. 9th Int. Conf. on High Energy Particle Accel., SLAC (1974) p.347.

8. J A Fox: 'Resonant Magnet Network and Power Supply for the 4 GeV Electron Synchrotron NINA'. Proc. IEE, Vol.112 (1965).

9. N Marks, J B Lyall, M W Poole: 'NINA Programmed Quadrupoles'. Proc. 1975 Particle Accel. Conf., IEEE Trans. Nucl. Sc. NS-22, No.3, 1586 (1975).

10. J M Carpenter, Ed: 'Draft Proposal for an Intense Pulsed Neutron Source'. ANL, Oct. 75.

11. J S Fraser, G A Bartholomew and P R Tunnicliffe (Eds). AECL-2600, July 1966.

12. R R Fullwood et al: 'Neutron Production by Medium Energy Protons on Heavy Metal Targets'. LA-4789 (LASL) 1972.

13. J S Fraser et al. Phys in Canada, 21 (2), 17 (1965).

14. W R Gambill: 'Design Curves for Burn-Out Heat Flux in Forced Convection Subcooled Light Water Systems'. ORNL-TM-2421, 1968.

15. W A Coleman & T W Armstrong: 'The Nucleon-Meson Transport Code NMTC'. ORNL 4606, Oct 1970.

16. H W Patterson & R H Thomas. Accelerator Health Physics. Academic Press, New York & London (1973).

17. P J Gollon. Fermilab Report TM-609 (1975).

18. M Barbier: Induced Radioactivity. North-Holland, Amsterdam & London (1969).

19. G B Stapleton & R H Thomas. Health Physics 23, 689 (1972)

20. J F Kircher & R E Bowman (Eds): Effect of Radiation in Materials and Components. Reinhold, New York (1964).

21. M H Van de Voorde. CERN Report 70-5 (1970).

22. H Kumpfert (DESY). Private communication.

23. Nimrod Magnet Types specified in 'Nimrod Beam Line Equipment Data Handbook'. Rutherford Laboratory 1968.

PHOTOGRAPH 1.1 NIMROD HALL

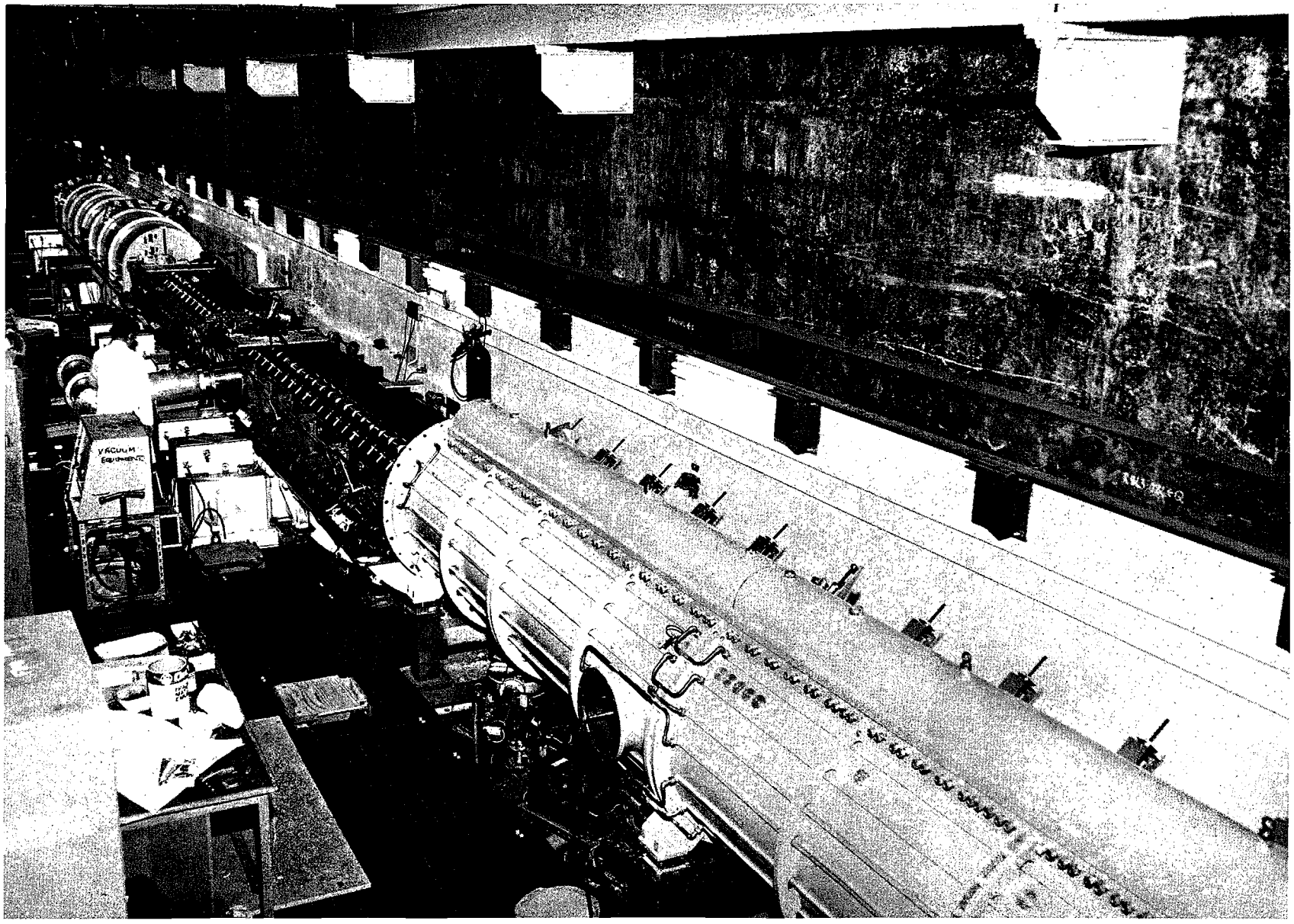

PHOTOGRAPH 1.3 70 MeV PROTON LINAC (DURING CONSTRUCTION)

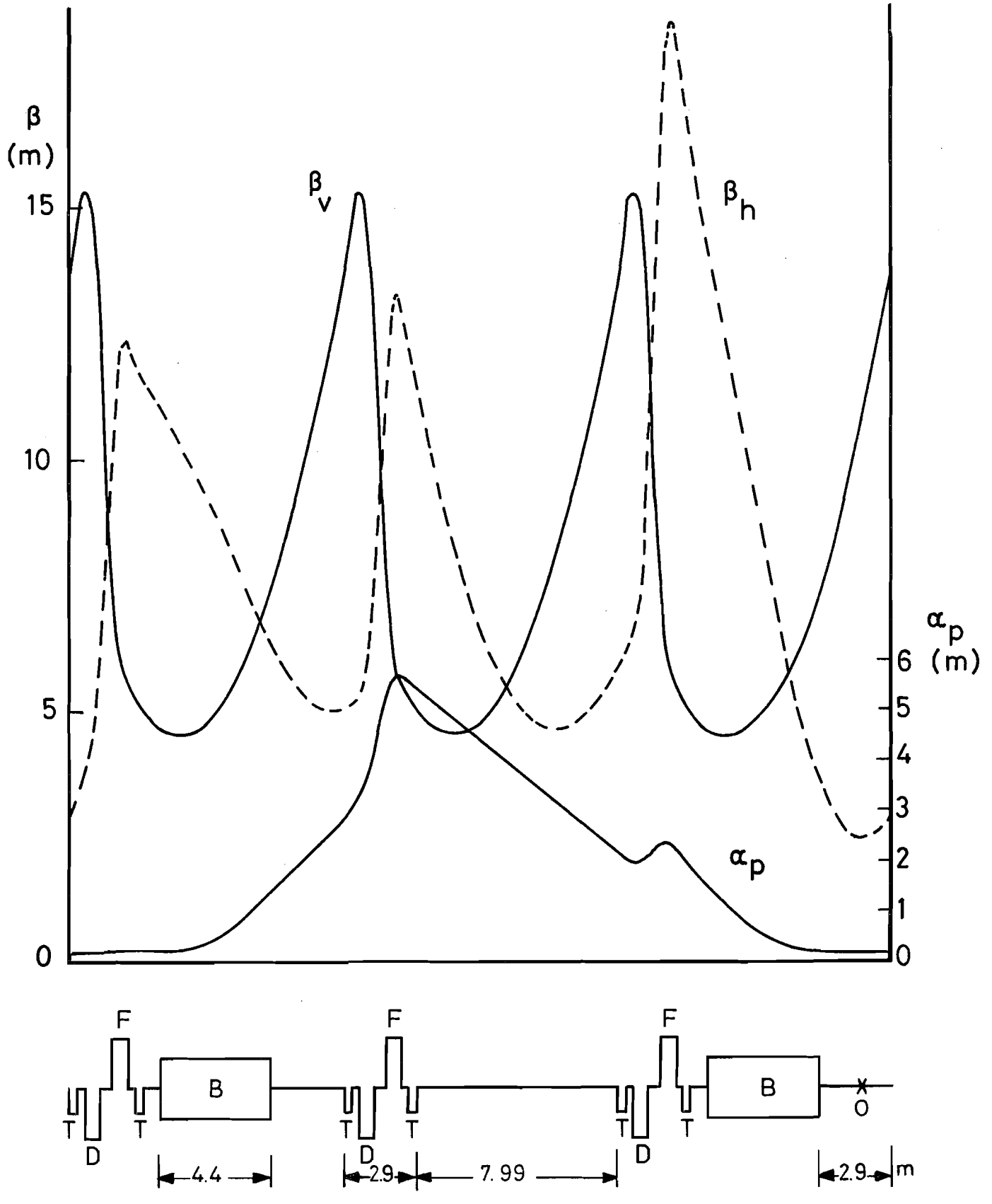

FIG. 1.3 LATTICE FUNCTIONS

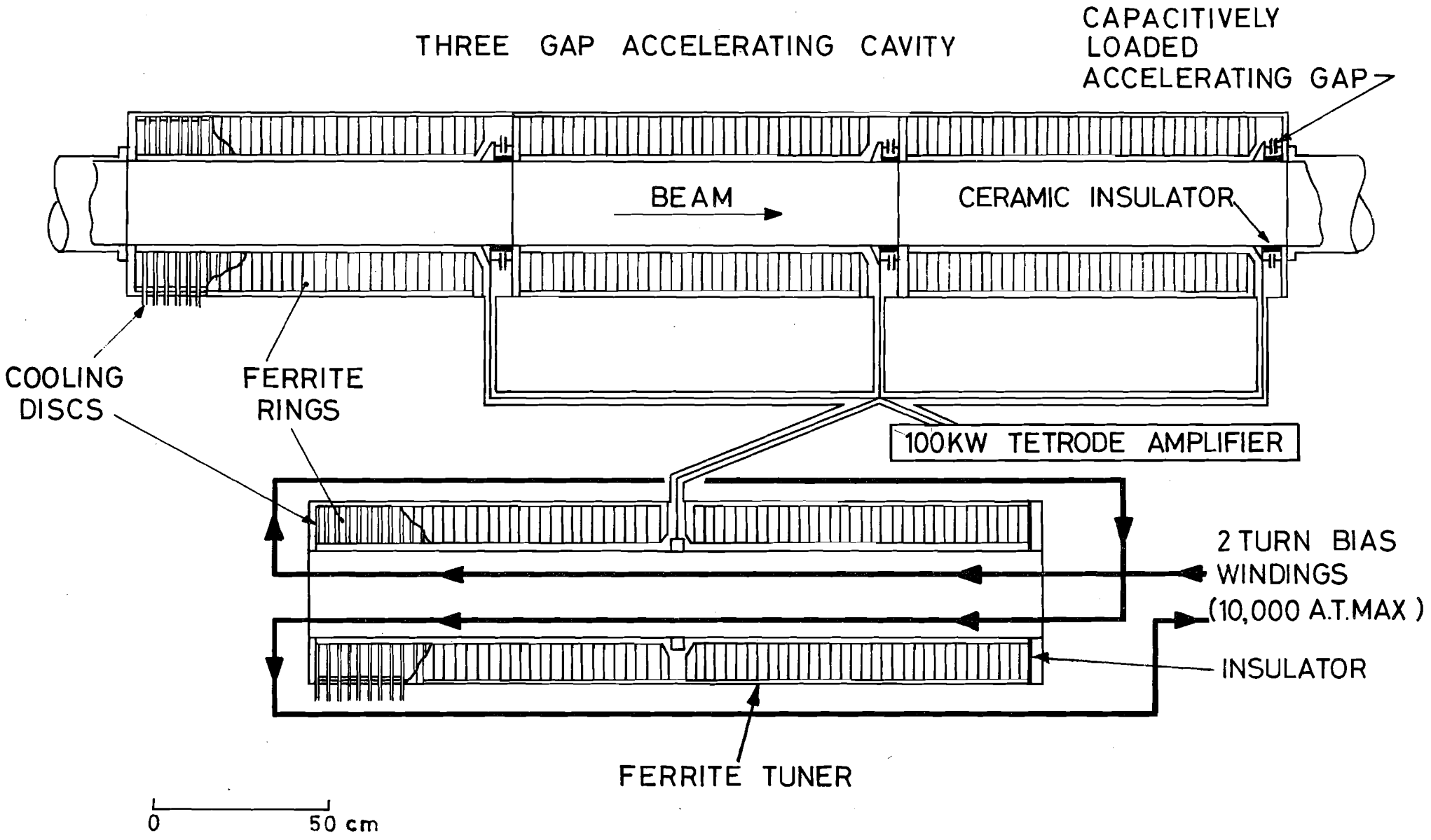

FIG.1.6 SCHEMATIC DIAGRAM OF R F CAVITY

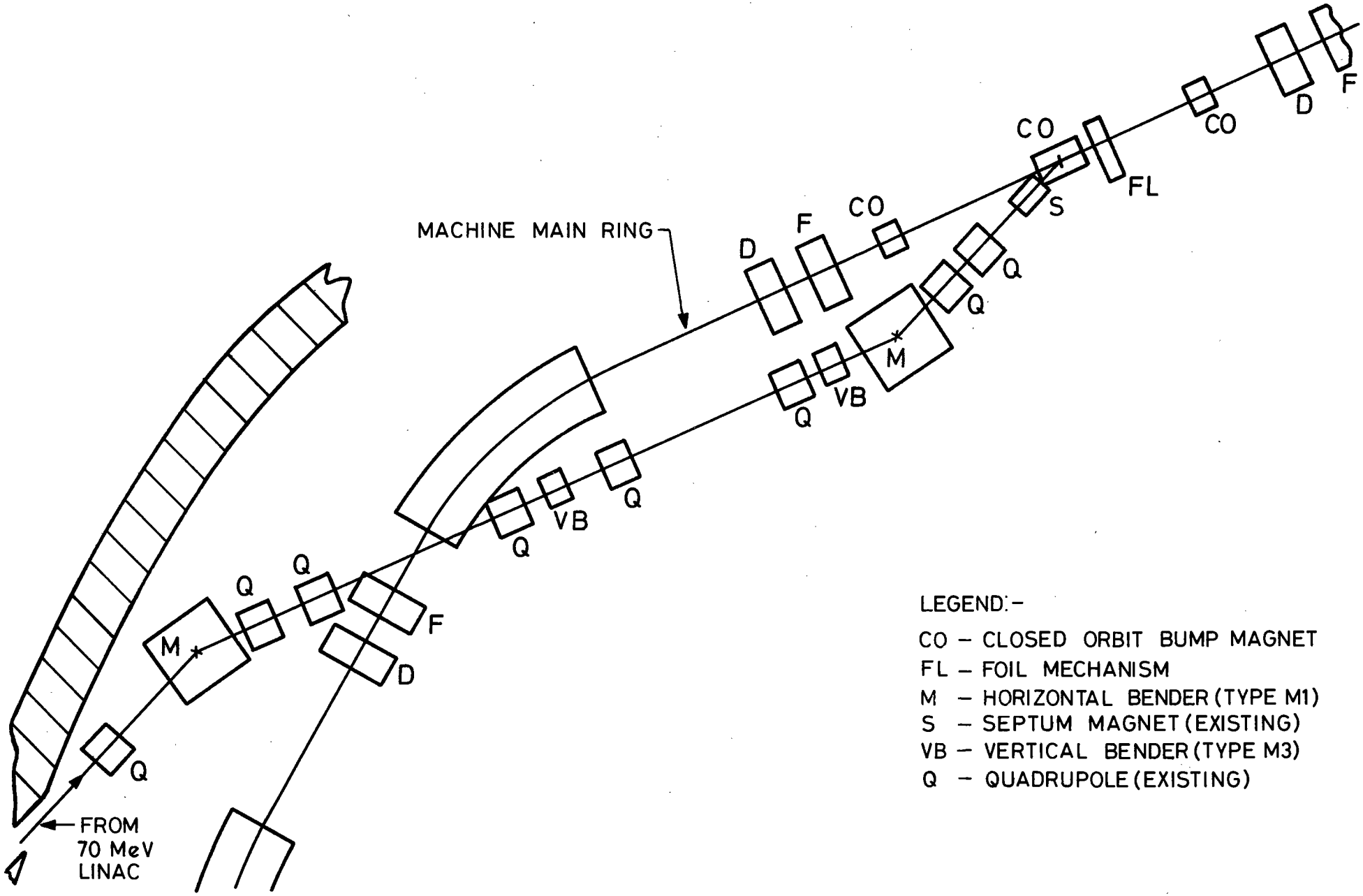

FIG.1.9 SCHEMATIC LAYOUT OF INJECTION BEAM LINE

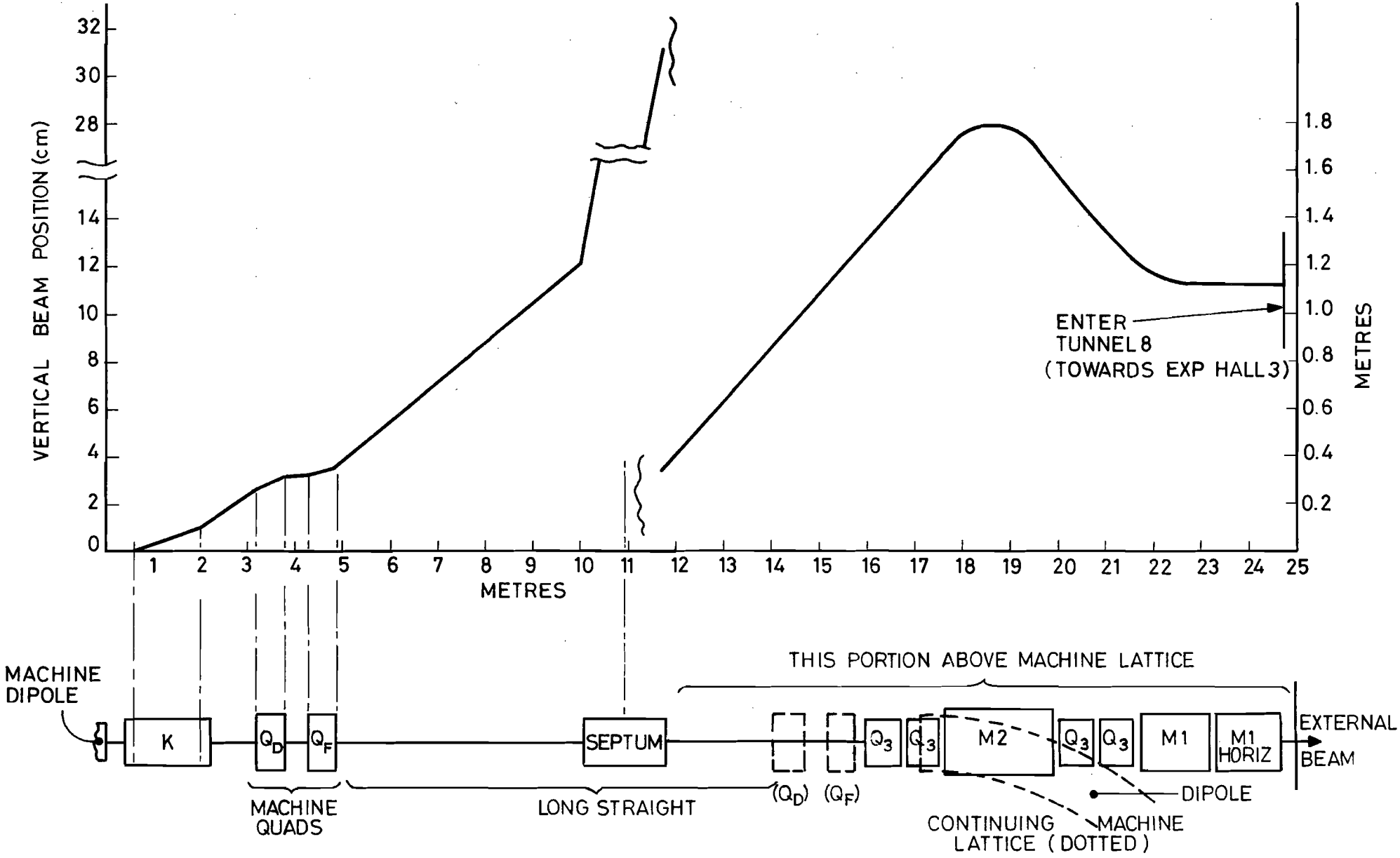

FIG. 1.10 VERTICAL BEAM POSITION AND SCHEMATIC PLAN OF EXTRACTION SYSTEM

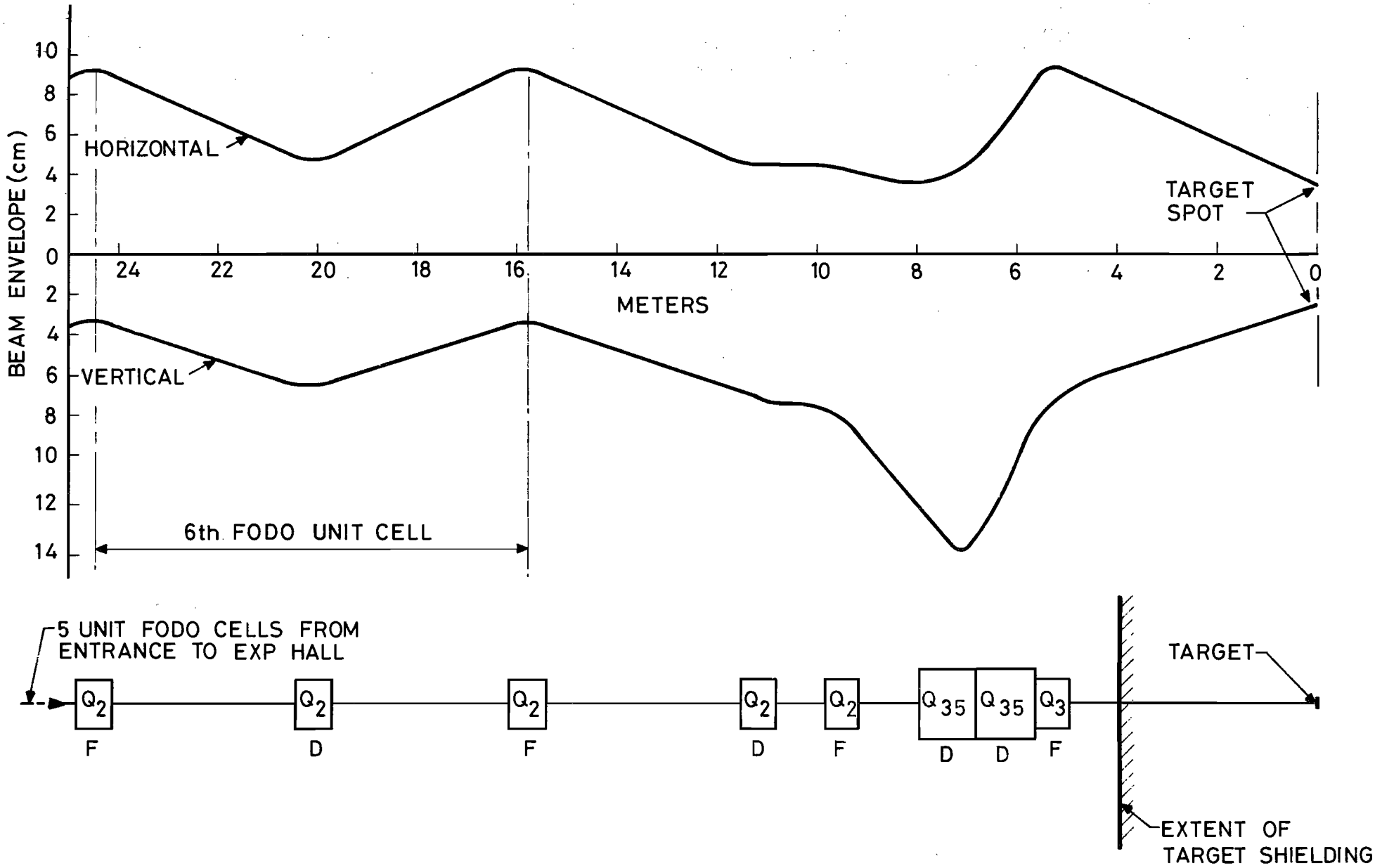

FIG. 1.11 EXTERNAL PROTON BEAM LAYOUT, WITH HORIZONTAL AND VERTICAL BEAM ENVELOPE

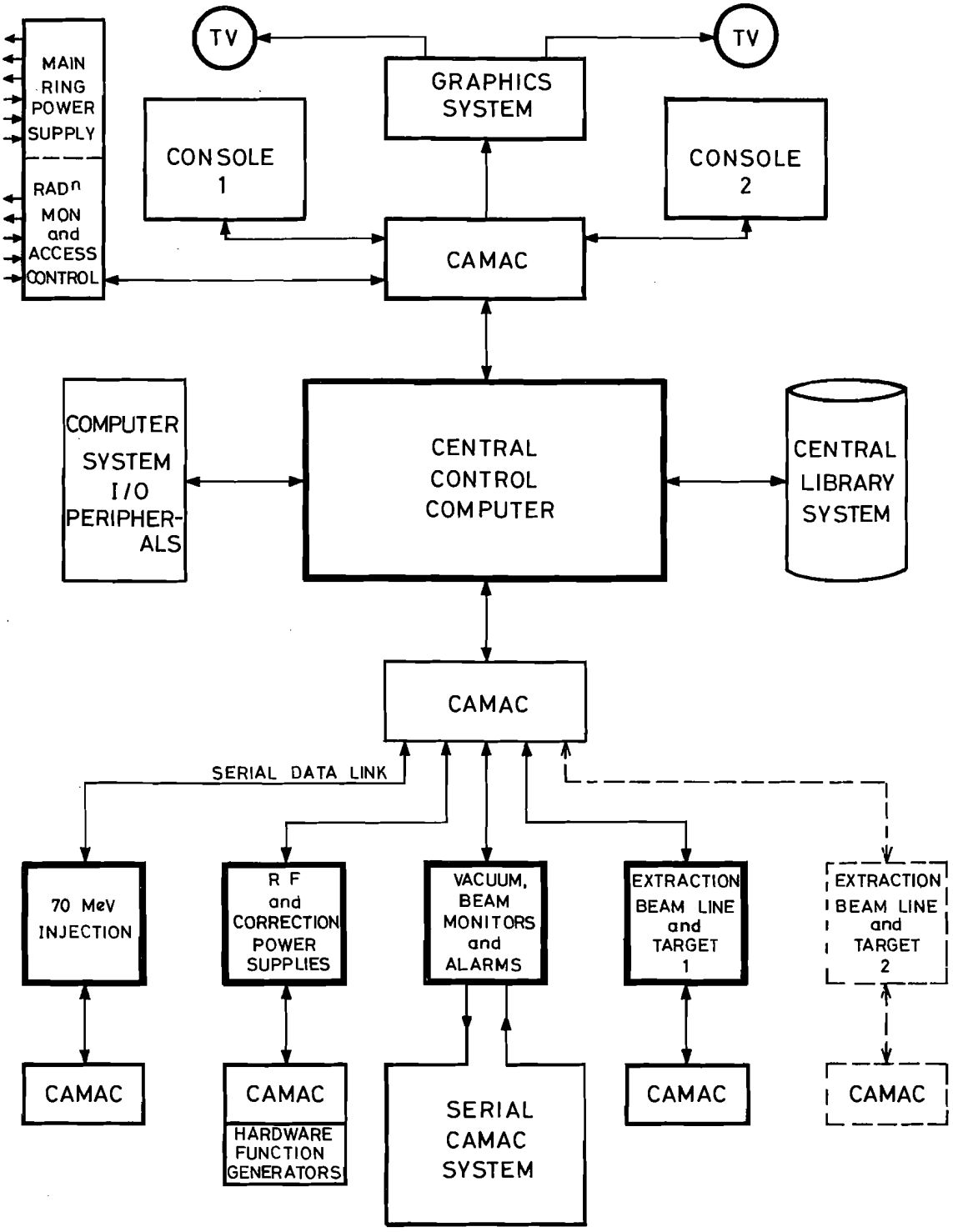

FIG.1.12 SCHEMATIC LAYOUT OF S N S CONTROL SYSTEM

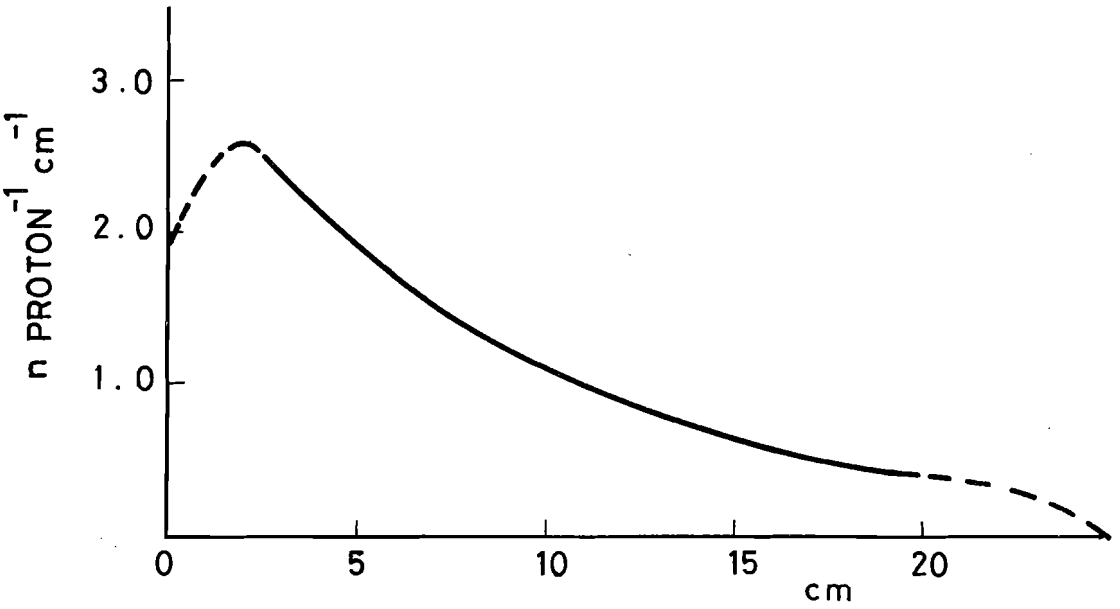

FIG. 2.1(a) YIELD OF NEUTRONS WITH AXIAL DISTANCE IN THE TARGET FOR AN INC. 800MeV PROTON

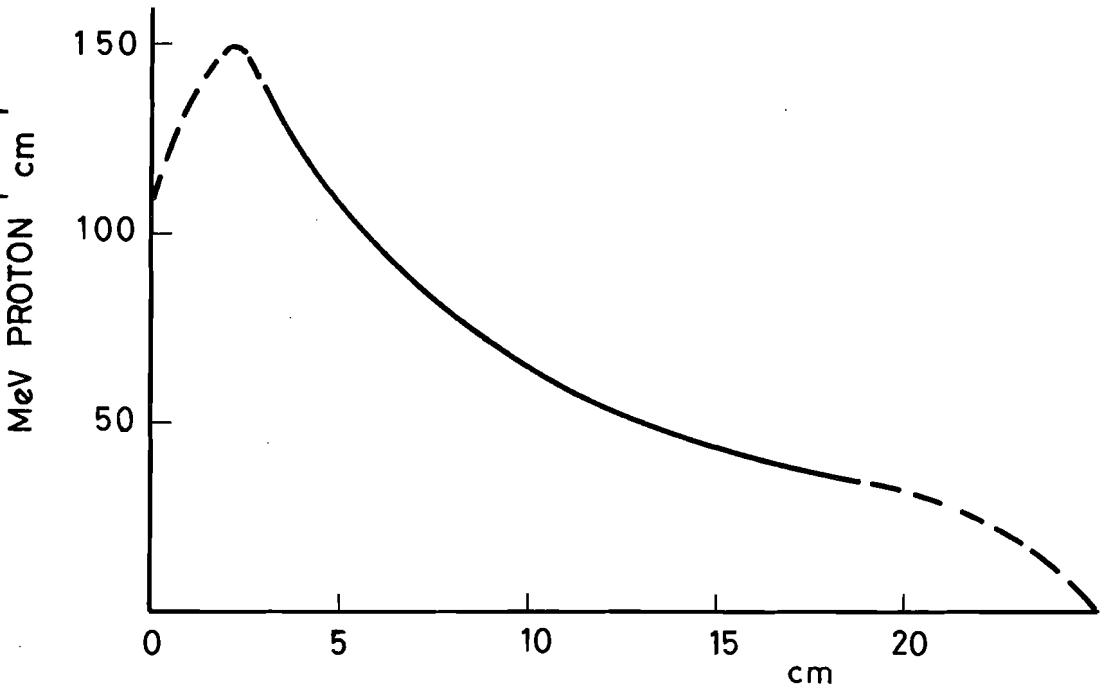

FIG. 2.1(b) HEAT DEPOSITION WITH AXIAL DISTANCE IN THE TARGET FOR AN INC. 800MeV PROTON

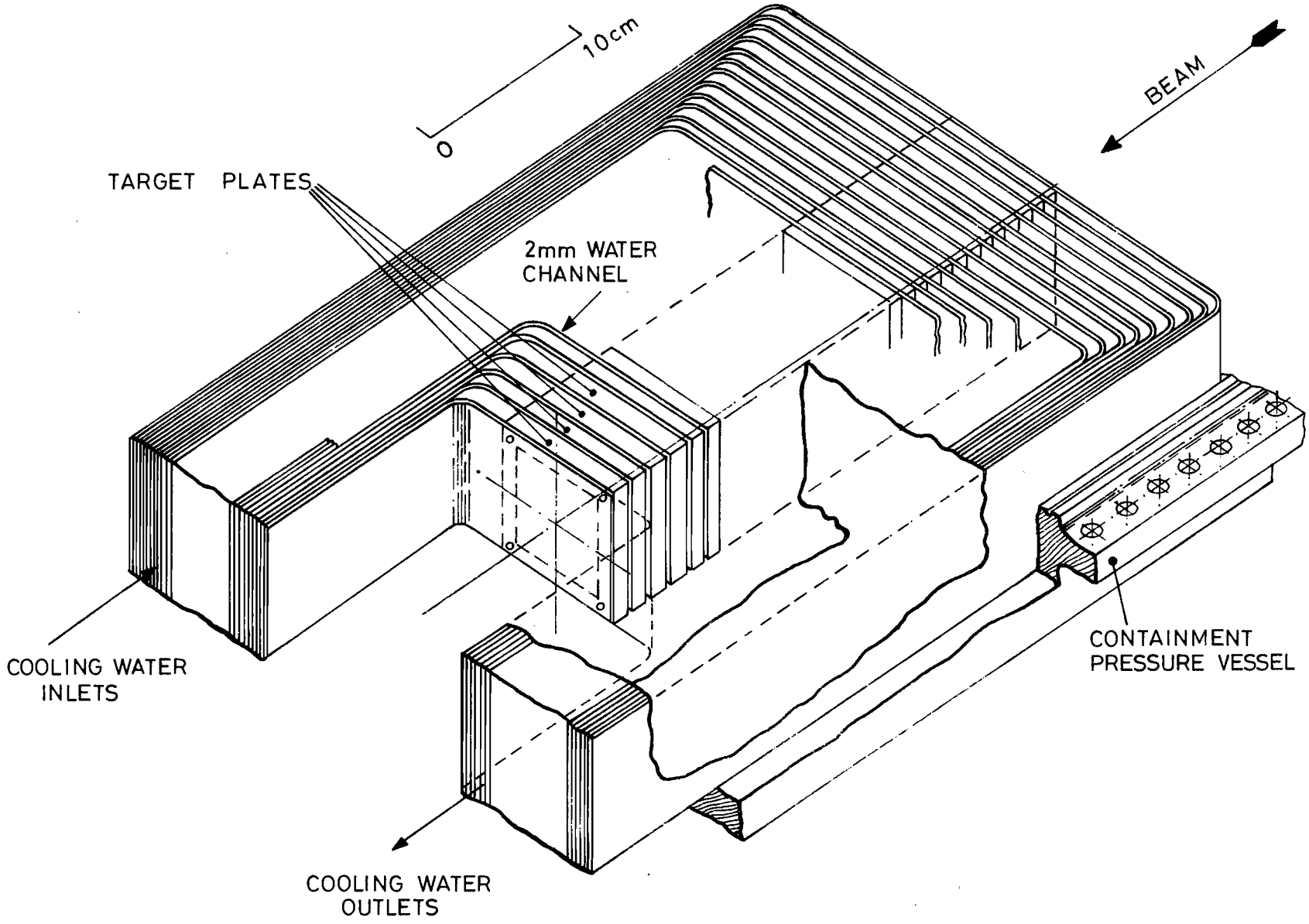

FIG. 2.2 ISOMETRIC VIEW OF TARGET

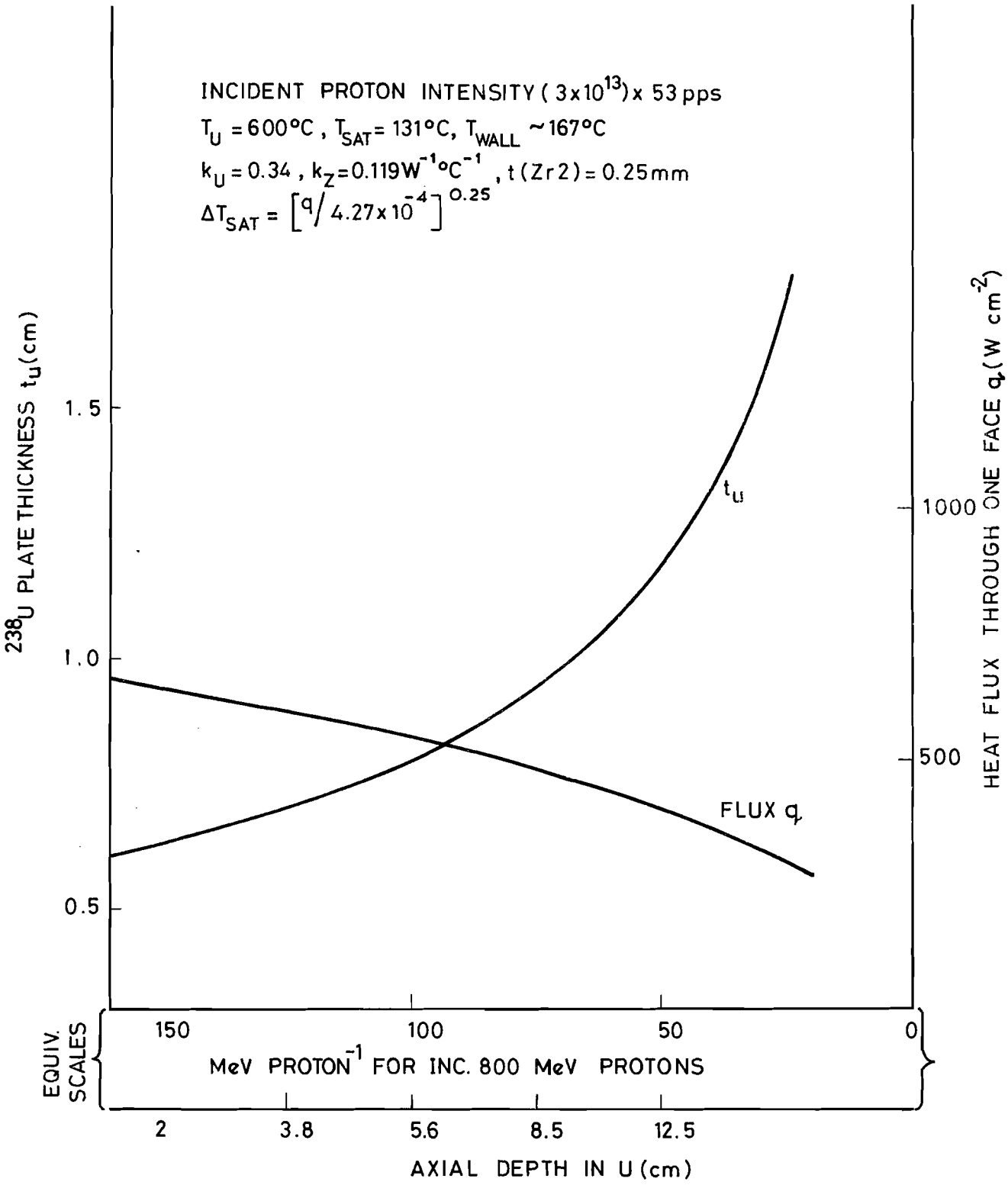

FIG. 2.3 URANIUM PLATE THICKNESS AND HEAT FLUX IN TARGET

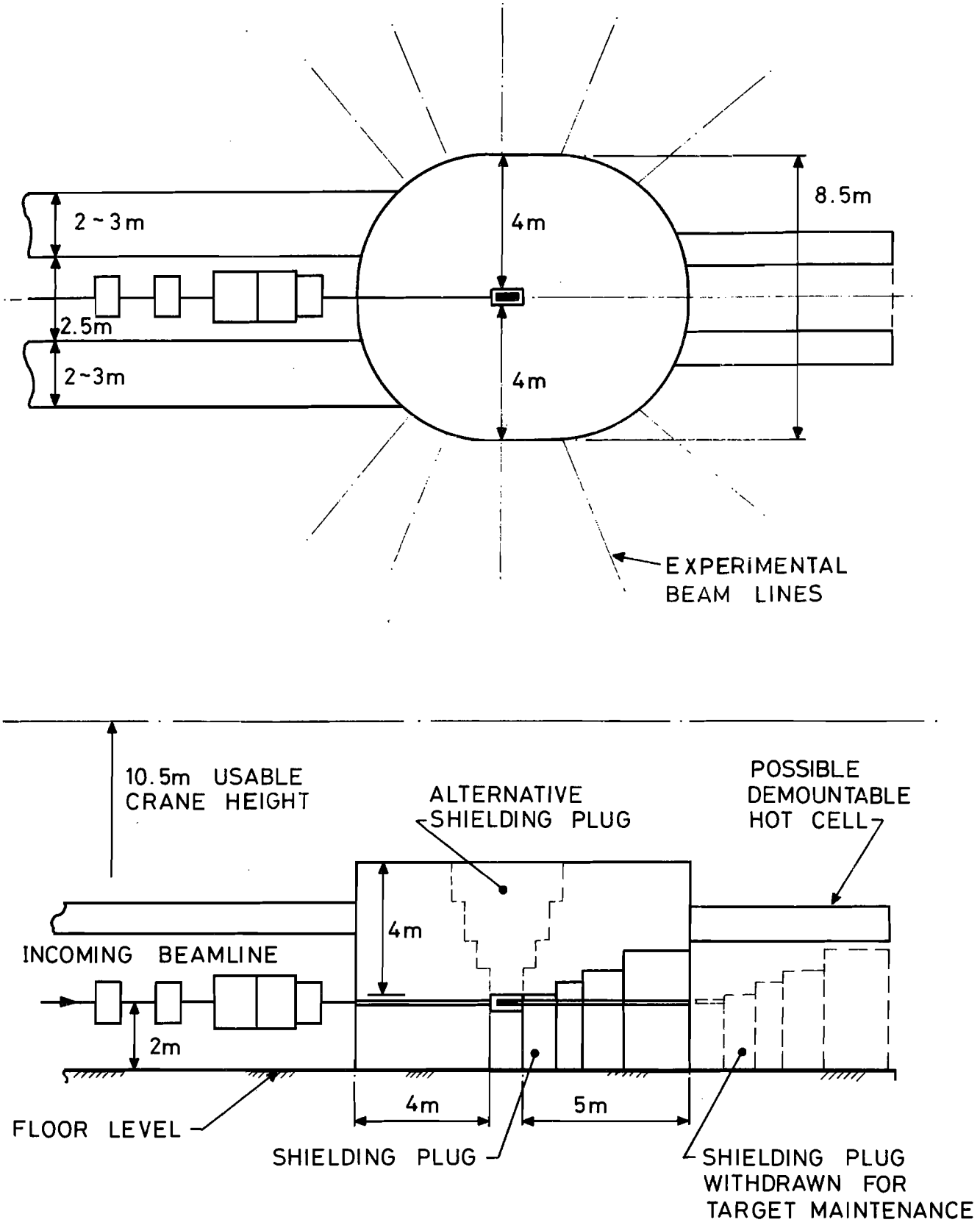

FIG. 2.4 SCHEMATIC OF HORIZONTAL TARGET & SHIELDING

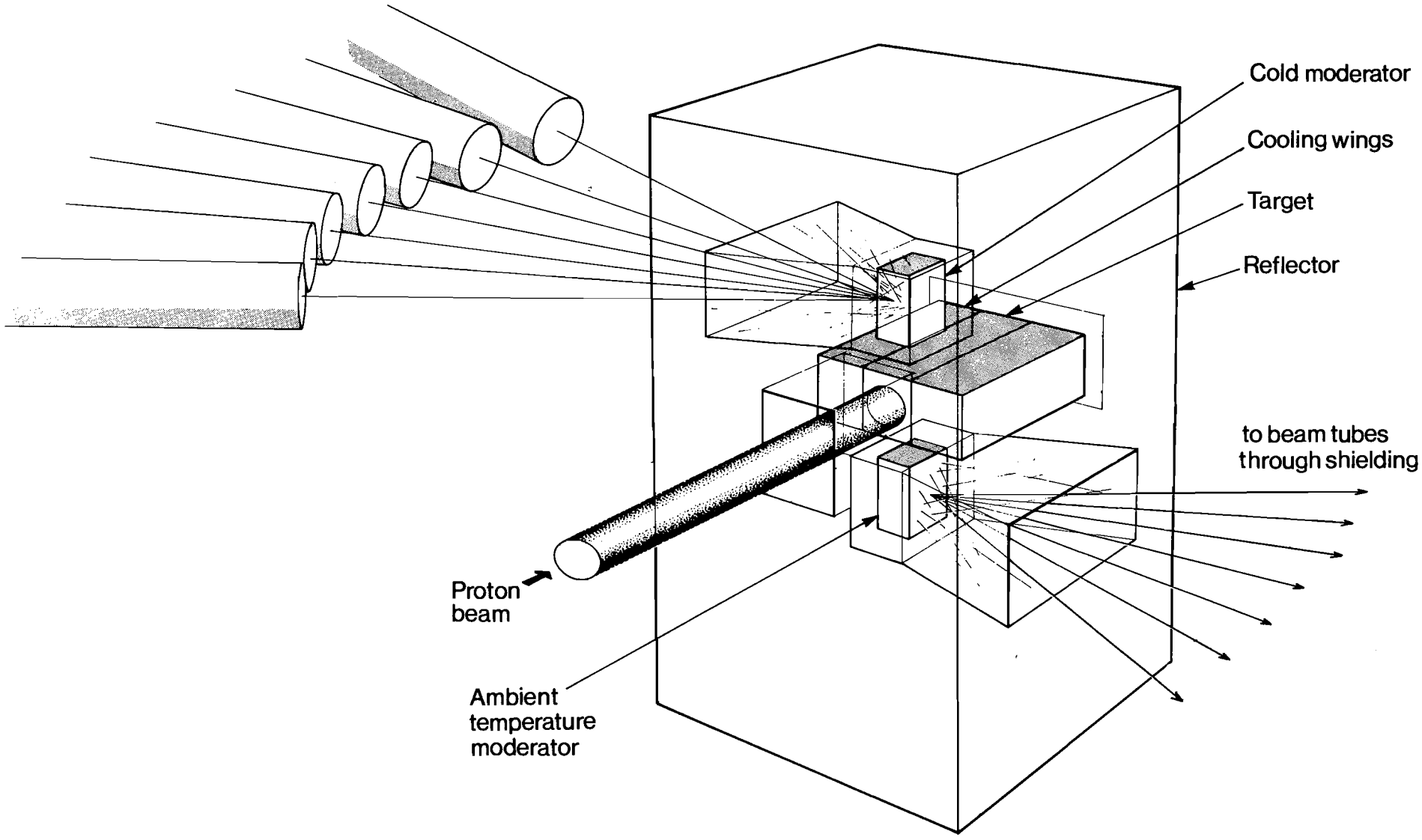

FIG. 4.1 SKETCH SHOWING POSSIBLE BEAM CONFIGURATION